ICES International Council for the Exploration of the Sea
CIEM Conseil International pour l'Exploration de la Mer

ICES COOPERATIVE RESEARCH REPORT
NO. 292
OCTOBER 2008
ICES Zooplankton Status Report 2006/2007

ICES International Council for the Exploration of the Sea
CIEM Conseil International pour l'Exploration de la Mer

ICES COOPERATIVE RESEARCH REPORT
RAPPORT DES RECHERCHES COLLECTIVES

NO. 292 SPECIAL ISSUE
OCTOBER 2008

ICES Zooplankton Status Report 2006/2007

Editors:

Todd D. O'Brien
Angel López-Urrutia
Peter H. Wiebe
Steve Hay

International Council for the Exploration of the Sea
Conseil International pour l'Exploration de la Mer

H. C. Andersens Boulevard 44–46
DK-1553 Copenhagen V
Denmark
Telephone (+45) 33 38 67 00
Telefax (+45) 33 93 42 15
www.ices.dk
info@ices.dk

Recommended format for purposes of citation:
O'Brien, T. D., López-Urrutia, A., Wiebe, P. H., and Hay, S. (Eds). 2008.
ICES Zooplankton Status Report 2006/2007.
ICES Cooperative Research Report No. 292. 168 pp.

For permission to reproduce material from this publication, please apply to the General Secretary.

This document is a report of an Expert Group under the auspices of the International Council for the Exploration of the Sea and does not necessarily represent the view of the Council.

ISBN 978-87-7482-037-6
ISSN 1017–6195

© 2008 International Council for the Exploration of the Sea

Above.
Calanus finmarchicus is a key North Atlantic species. Photo courtesy of Ecosystem Research Division, Bedford Institute of Oceanography.

Cover image.
Zooplankton. Photo courtesy of Ecosystem Research Division, Bedford Institute of Oceanography.

TABLE OF CONTENTS

Photo courtesy of Larissa Litvinchuk

Jesús Alberto Cabal Naves
1962–2008

Our colleague Dr Jesús Cabal passed away on 25 June 2008 at the early age of 45. Jesús was a prominent zooplankton taxonomist and ecologist. His friendly personality and profound knowledge and love of nature earned him the deep esteem of everybody who met him. Jesús Cabal was heavily involved in many activities of the ICES Working Group on Zooplankton Ecology (WGZE). A few days before his sudden death, Jesús contributed the summary text for the Santander and Coruña transects in this report.

For his years of friendship and contributions to WGZE and its members, we dedicate this year's report to Jesús Cabal. We, along with his family and colleagues at the Instituto Español de Oceanografía, will truly miss him.

1. BACKGROUND

In its strategic plan, ICES recognized its role in making scientific information accessible to the public as well as to fisheries and environmental assessment groups. During the 1999 Annual Science Conference, ICES requested the Oceanography Committee working groups to develop data products and summaries that could be routinely provided to the ICES community via the ICES website. The Working Group on Zooplankton Ecology (WGZE) has given priority to producing a summary report on zooplankton activities in the ICES Area based on the time-series obtained from national monitoring programmes.

This is the seventh summary of zooplankton monitoring in the ICES Area and expands on previous reports with improved analysis, data, and presentation. This year's report includes eight new monitoring sites: five from the western North Atlantic, two from the northern Baltic, and one from the northern Skagerrak. For each of the 37 zooplankton monitoring sites (Figure 1), WGZE has continued to seek out and include co-sampled temperature and chlorophyll data, as well as any available phytoplankton and nutrient data.

Although this report follows the structure of previous reports, it now features a new "standardized" graphical visualization for each site. This new presentation quickly summarizes the seasonal cycle and interannual variability of the zooplankton at each site and offers a quick overview of zooplankton interactions and/or synchrony with other co-sampled biological and hydrographic variables at the site. Each site also includes a long-term assessment of the monitoring area through comparison with a 100-year record of sea surface temperature (SST) data and up to 60 years of continuous plankton recorder (CPR) zooplankton data (when available near that site). Finally, this report concludes with a basin-wide overview of SST, phytoplankton, and zooplankton across the entire North Atlantic, using data from the CPR surveys (Figure 2).

This year's report also includes a brief introduction to six Mediterranean zooplankton monitoring sites (Figure 1, yellow stars), a tribute to our Mediterranean colleagues, as ICES and the Mediterranean Science Commission (CIESM) prepare for the October 2008 "Joint ICES/CIESM Workshop to Compare Zooplankton Ecology and Methodologies Between the Mediterranean and the North Atlantic" (WKZEM; www.wkzem.net).

This report benefits from contributions by members of WGZE and colleagues in ICES Member Countries who lead zooplankton time-series programmes. A list of contributors to this report can be found at the end of the report.

The report was compiled and edited by Todd D. O'Brien, Angel López-Urrutia, Peter H. Wiebe, and Steve Hay. The editors thank all those who contributed data and/or material to this report for their invaluable contributions.

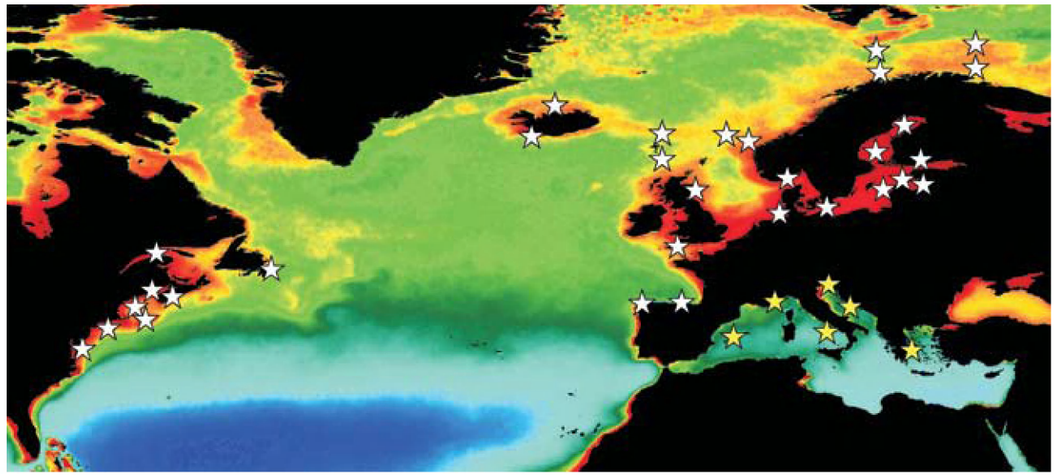

Figure 1.
Zooplankton monitoring sites within the ICES Area (white stars) and from colleagues in the Mediterranean Science Commission (CIESM; yellow stars). Only programmes summarized in this report are indicated on this map.

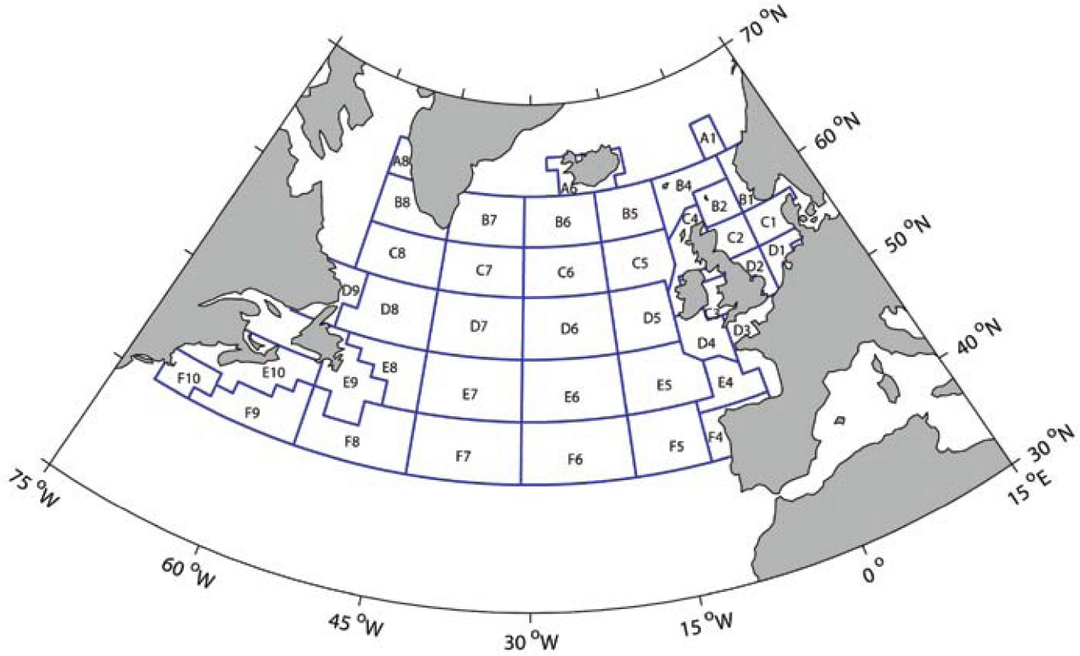

Figure 2.
Map of Continuous Plankton Recorder (CPR) "standard areas". Designated by general hydrographic and geospatial boundaries, all CPR data within each respective area are compiled into a single representative time-series for that area.

2. STANDARD ANALYSIS AND VISUALIZATION

Todd D. O'Brien

The data preparation methods, analyses, and graphical visualizations used in this report were developed in collaboration with the Coastal & Oceanic Plankton Ecology, Production, & Observation Database (COPEPOD; www.st.nmfs.noaa.gov/plankton) and the Scientific Committee on Oceanic Research (SCOR) Working Group 125 (WG125: Global Comparisons of Zooplankton Time-series; http://wg125.net). These analyses and visualizations are designed to allow for easy comparison of zooplankton (and other hydrographic variables) of different types, measures, and sampling frequencies (e.g. "biomass sampled three times per year" vs. "copepod abundance sampled weekly"). This is accomplished by looking at changes in the data values, relative to the long-term average of those data, as a unit-less ratio (or "anomaly").

A zooplankton time-series $Z(t)$ can be presented as a series of log-scale anomalies $z'(t)$ relative to the long-term average $\overline{Z}$ (climatology) of these data:

$$z'(t) = \log[\, Z(t)\,] - \log[\,\overline{Z}\,] = \log[\,\overline{Z}(t)/\overline{Z}\,]$$

Between the various WGZE zooplankton monitoring sites, differences in sampling and processing methods introduce a variety of biases into the data (see Perry *et al.*, 2004, for an extensive discussion). Although the zooplankton sites in this report do not share a common methodology, the data are collected consistently and uniformly internally at each site for the duration of the dataset. The anomalies will remain constant (unbiased) as long as all the samples in the dataset share a common method or sampling bias (b). Because this bias and the measurement units of the data are present in both the numerator and denominator of the calculation, they are cancelled out during the calculation:

$$z'(t) = \log[\, b \times Z(t)\,] - \log[\, bxZ\,] = \log[\, b\overline{Z}(t)/b\overline{Z}\,] = \log[\, Z(t)/\overline{Z}\,]$$

By using these unit-less anomalies, WGZE can make comparisons in the form "at Site A, copepod biomass doubled during the same time interval that total zooplankton biomass decreased by half at Site B".

A plot of these log-scale anomalies will quickly reveal interannual variability and trends in the time-series (Figure 3). In this example, there was an extended period of below-average abundance (blue bars) for 1975–1980, 1991–1995, and 1998–2006, with 1976 and 2006 having especially low abundance values. In contrast, 1983–1990 and 1996–1997 were years of above-average (red bars) abundance, with 1985 and 1990 having especially high values. Within these log-scale anomalies, an anomaly of 1.0 indicates a value ten times larger than the long-term average, whereas an anomaly of –1.0 indicates a value ten times smaller than the long-term average. In Figure 3, the positive 1990 log-scale anomaly of 0.4 indicates that the average abundance in that year was two and a half times larger than the long-term average, whereas the negative log-scale anomaly of –0.48 in 2006 indicates abundance three times lower than the long-term average.

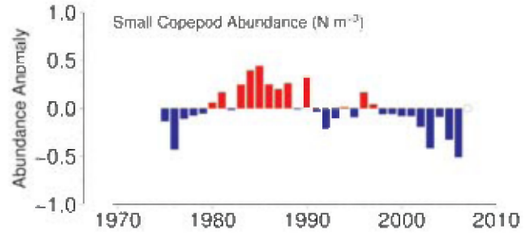

Figure 3.
An example of log-scale anomalies of annual copepod abundance. Red bars indicate positive anomalies (years with copepod abundance above the long-term average of the entire time-series). Blue bars indicate negative anomalies (years with copepod abundance below the long-term average).

In most regions of the North Atlantic, zooplankton have a strong seasonal cycle, with periods of high (usually in summer) and low (usually in winter) abundance and/or biomass. Calculation of an annual average of zooplankton abundance from low-frequency and/or irregular sampling (e.g. once per season, once per year) can be greatly influenced by when the sampling occurs (e.g. during, before, or after the summer peak). This problem is further compounded by missing months between sampling years. One solution to this problem is summarized in Mackas *et al.* (2001), in which the annual anomaly is calculated as an average of individual monthly anomalies. This method was used for the analysis in this report because it reduces many of the issues of low-frequency and/or irregular sampling and also removes the seasonal signal from the year-to-year analysis.

2.1 Standardized WGZE time-series summary plot

Each zooplankton time-series features a standardized summary plot of a primary zooplankton measurement, typically total zooplankton/copepod abundance or total biomass. If additional variables are present in a time-series, they are shown in the co-sampled variables plot (discussed in Section 2.2). The standard WGZE summary plot briefly presents the sampling frequency and coverage of the dataset, along with its seasonal cycle and monthly and interannual trends (see examples in Figures 4 and 5).

Subplot A. This shows the distribution of log-transformed zooplankton data values (i.e. total copepod abundance), binned by month, for the entire time-series illustrated in subplot B. The green dots show the range of individual values for each month (from all years in the time-series), whereas the red circles show the long-term average (climatology) for that month.

Subplot B. This shows the monthly averages of the zooplankton data values over the duration of the time-series. The colours in this plot show "an equal-n ranking of the monthly means", not the actual values. To create this ranking, the values of all the monthly means are sorted numerically and then divided into 20 equal *(n)* member groups. The rankings are then assigned a colour: dark to light blue = lowest value grouping; green to yellow = middle value grouping; orange to red = highest value grouping. The purpose of this plotting approach is to show clearly the transition between high- and low-value states over the duration of the time-series. If the actual mean values were plotted, the resulting figures would tend to be dominated by a single colour (e.g. 99% green with a few squares of red or blue). Months with no data are shown as empty (white) grid cells in this plot. For example, in Figure 5, sampling data for February were not available until the late 1990s, and data from June were never available.

Subplot C. This shows the monthly anomalies of the zooplankton data values (a comparison of the anomalies for the month with the long-term average for that month) for the duration of the time-series. The colours in this plot show a four-category ranking of the monthly anomaly values: red = strong positive; pink = weak positive; light blue = weak negative; dark blue = strong negative. A "strong positive anomaly" ranking is assigned to an anomaly greater than the mean of all other positive-anomaly values in the time-series. A "strong negative anomaly" ranking is assigned to an anomaly less than the mean of all other negative-anomaly values.

Subplot D. This shows the annual anomalies of the zooplankton data values by year for the duration of the time-series. Each annual anomaly is calculated as an average of all the monthly anomalies for that year. Positive anomalies are assigned a red bar and negative anomalies a blue bar.

Years with no data (from the start of the time-series to 2007) are indicated by an open circle. For example, no data were available for the years 1990, 1996, or 2007 in Figure 5.

Subplot E. This shows Reynolds sea surface temperature (SST) values and averages by month in the sampling region. The red dots show the individual temperature value range for that month, whereas the open (white) circles show the long-term average (climatology) for that month. (The Reynolds SST is discussed in Section 2.4.)

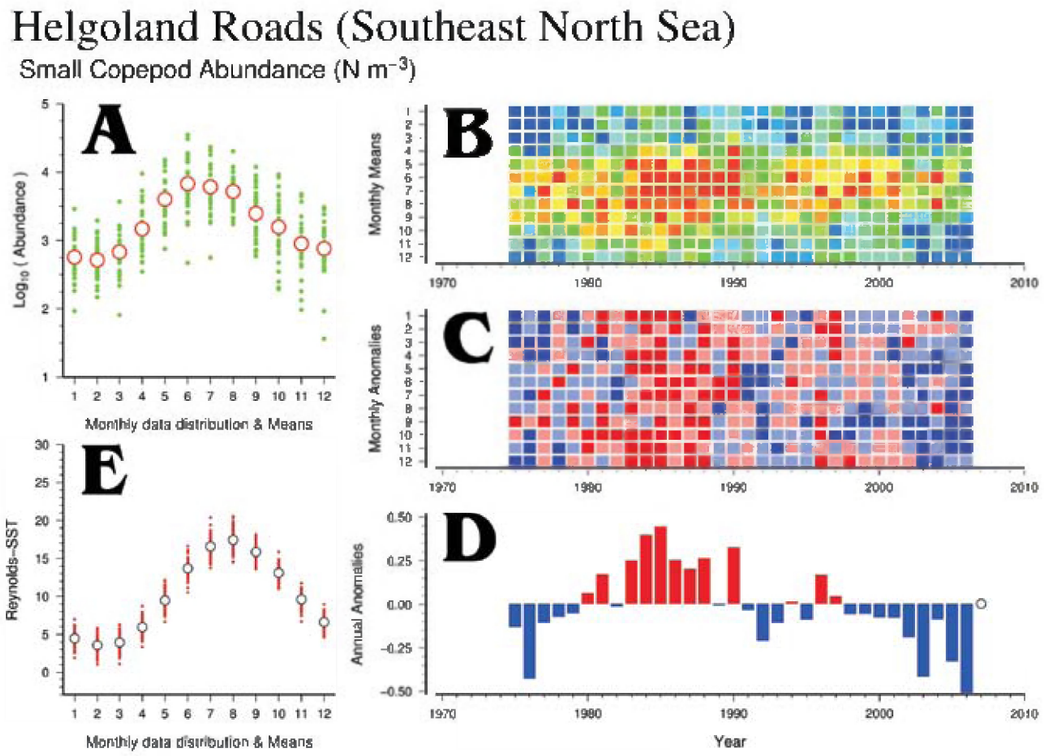

Figure 4
Example of a high-frequency time-series (see also Section 3.5, Site 27, Helgoland Roads), plotted in the standardized WGZE.

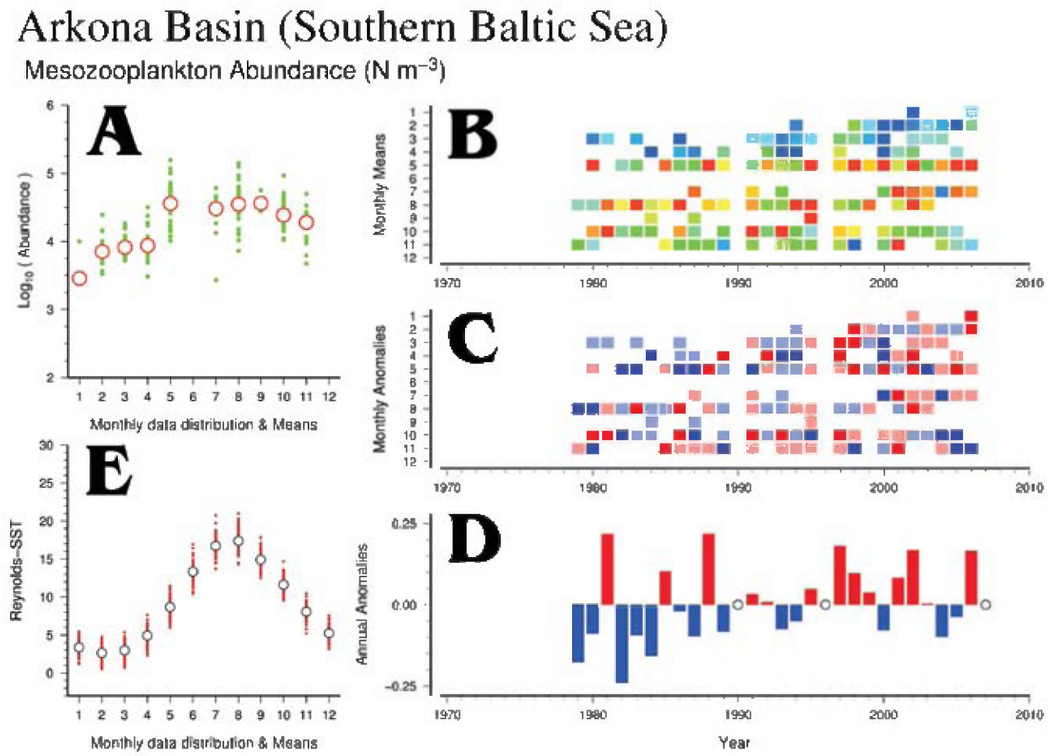

Figure 5.
Example of a data-sparse standardized WGZE time-series summary plot (see also Section 34, Site 25, Arkona Basin). Data were sampled in most months, except June, from 1979 to 2007. Data were not available for the years 1990, 1996, and 2007.

2.2 Co-sampled variables plot

The co-sampled variables plot shows the "Subplot A" and "Subplot D" portions of the standard WGZE summary plot and other variables sampled at the time-series site. This section starts with the primary zooplankton variable, includes up to five co-sampled covariables, and ends with the Reynolds SST for the site. For example, the Stonehaven co-sampled variables plot (Figure 6) begins with the primary zooplankton variable (total copepod abundance), continues with co-sampled chlorophyll, nitrate, salinity, and at-site temperature, and ends with the Reynolds SST series for that site.

When covariables are available at a zooplankton time-series site, the co-sampled variables plot can provide considerable information about the environmental history and seasonal cycles within a site. (See Section 3.5, Site 28, Stonehaven site summary, for a discussion of the data in this plot.)

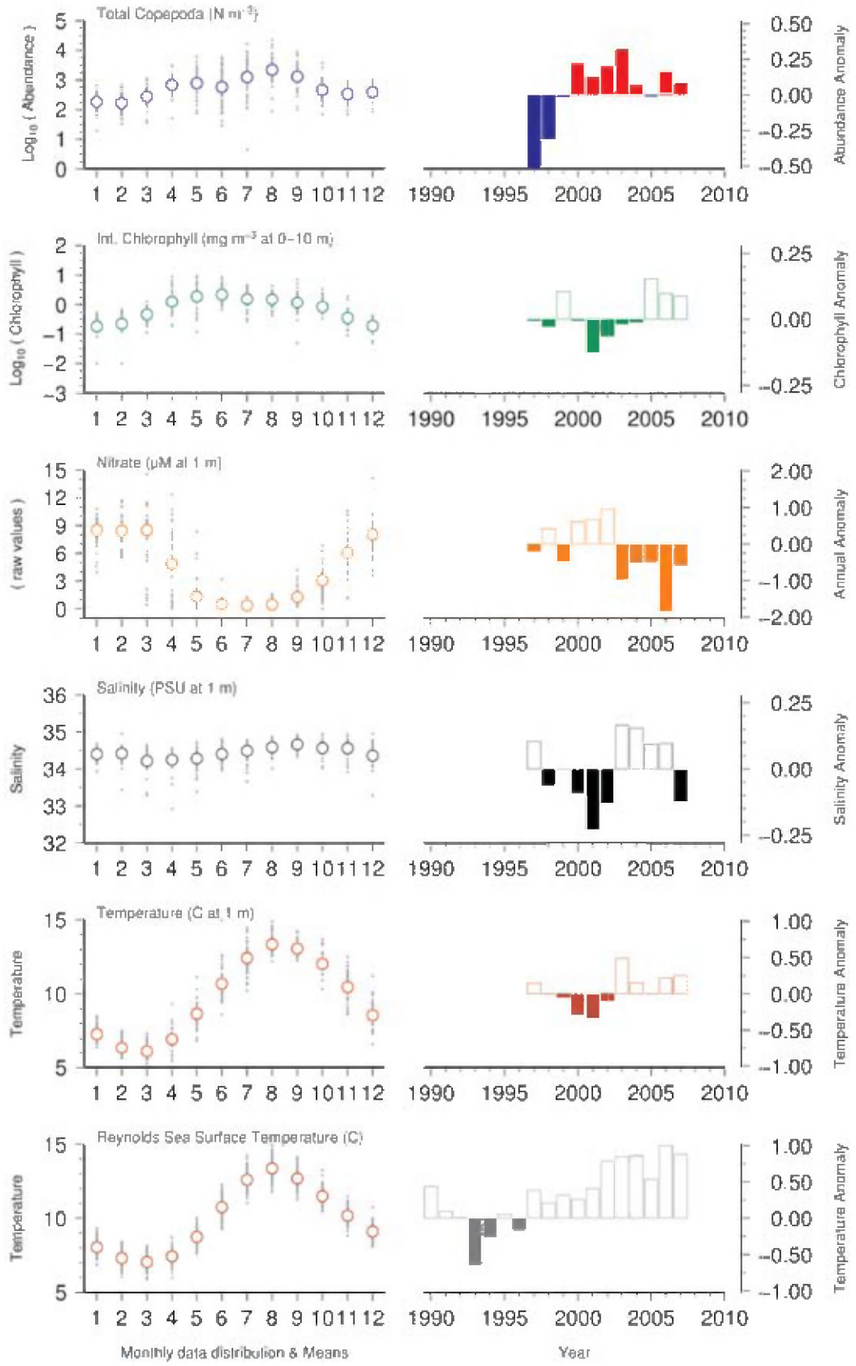

Figure 6.
Example of a co-sampled variables plot (see also Section 3.5, Site 28, Stonehaven).

2.3 Long-term comparison plot

The long-term comparison plot displays the primary zooplankton variable on a 100-year time-scale (1900–2007), together with Reynolds SST and continuous plankton recorder (CPR) data from the nearest CPR standard area (if available). The Reynolds SST and CPR data represent a larger temporal and spatial view of zooplankton and temperature conditions in the general area of each sampling site. Although they may not necessarily capture the exact conditions at the sampling site, they do represent the general physical and biological conditions that surround, and probably influence, the sampling site.

Figure 7 shows annual anomalies of Helgoland Roads small copepod abundance, CPR copepod abundance (from standard area "D1", the nearest to the Helgoland site), and Reynolds SST values plotted on an axis from 1900 to 2010. In the small copepod abundance and CPR subplots, positive annual anomalies are shown by red bars and negative annual anomalies by blue bars. In the Reynolds SST subplot, positive annual anomalies are shown by open (white) bars and negative annual anomalies by filled (grey) bars. The Reynolds SST subplot also features a dashed red line, which indicates the maximum temperature recorded during the period 1900–2000, also referred to as the "100-year maximum". As an example, the subplot in Figure 7 shows that water temperatures in the Helgoland Roads area have been at, or above, this 100-year maximum since 2000. Prior to 2000, the highest water temperatures were seen in the 1930s and early 1990s, but from 2007, water temperatures were 0.5°C warmer than this maximum and over 1.25°C warmer than the 100-year average temperature for this region.

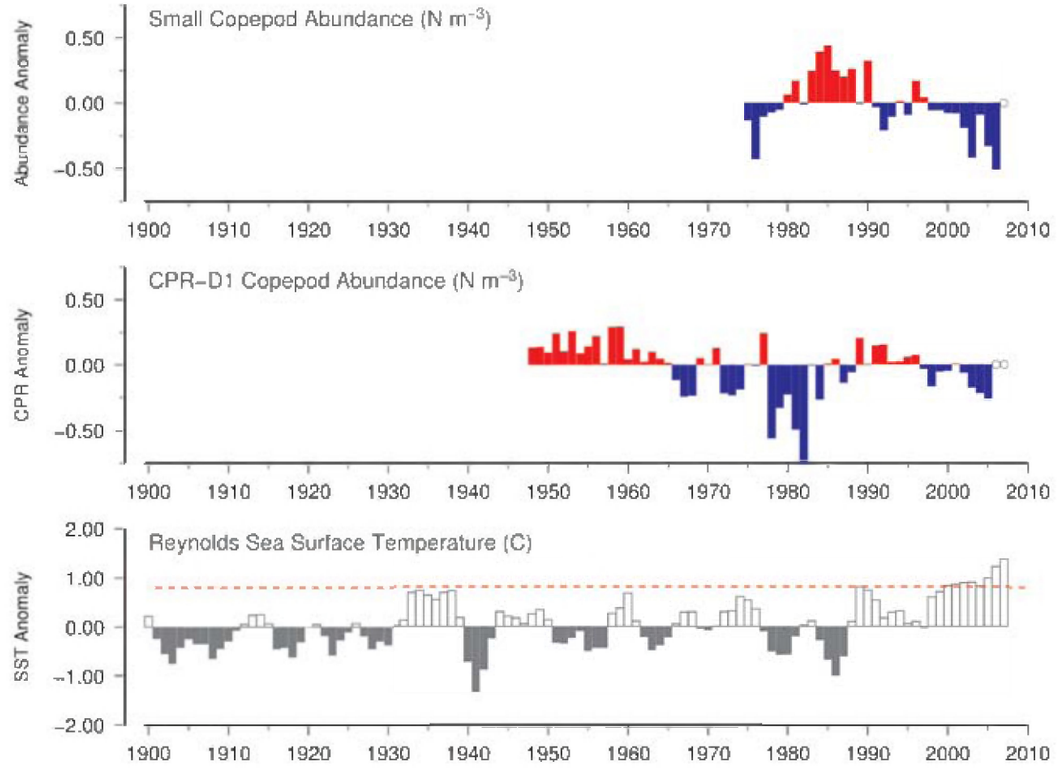

Figure 7.
Example of a long-term comparison plot (see also Section 3.5, Site 27, Helgoland Roads).

2.4 The "Reynolds SST"

Water temperature is an excellent indicator of the physical and physiological environment in which zooplankton are living and developing. Unfortunately, co-sampled temperature data were not available at every site, and when available, they often existed only for the period and duration of sampling (i.e. the same months, same years of coverage). This lack of data made it very difficult to examine long-term temperature trends within sites and across the North Atlantic.

In order to provide a common, long-term dataset of water temperatures for every site in the North Atlantic study area, the Reynolds Extended Reconstructed Sea Surface Temperatures, version 3 (ERSST.v3), dataset was used to add standard temperature data to each site. The ERSST.v3 (referred to as "Reynolds SST" in this report) is a global dataset of monthly SST values from 2007 back to 1854. This uses *in situ* data from the International Comprehensive Ocean-Atmosphere Data Set (ICOADS), along with statistical reconstruction (in data-sparse time periods and/or regions) and satellite validation, to create a continuous global time-series at a 2° spatial resolution (roughly 200 km × 200 km). The Reynolds SST/ERSST data are not intended to represent the exact temperatures in which the zooplankton were sampled, but they do provide a 100-year, or greater, average of general water temperatures in and around the sampling area.

For each zooplankton time-series, the immediately overlying ERSST.v3 2°-grid cell was selected. For single-point zooplankton sampling sites (e.g. Stonehaven and Plymouth L4), this 2°-grid cell would cover a ~200 km × 200 km area around and including the sampling site. For transects and region-based surveys (e.g. Iceland, Norway, Gulf of Maine), the centre point of the transect or region was used to select a single 2°-grid cell to represent the general conditions of the entire sampling area. (Comparisons with multicell averages revealed no significant differences.) Once a 2°-grid cell was selected, all ERSST.v3 temperature data were extracted from that cell for the period 1900–2007 and used to calculate annual anomalies.

The Extended Reconstructed Sea Surface Temperatures – version 3 (ERSST.v3) is available online at www.ncdc.noaa.gov/oa/climate/research/sst/ersstv3.php.

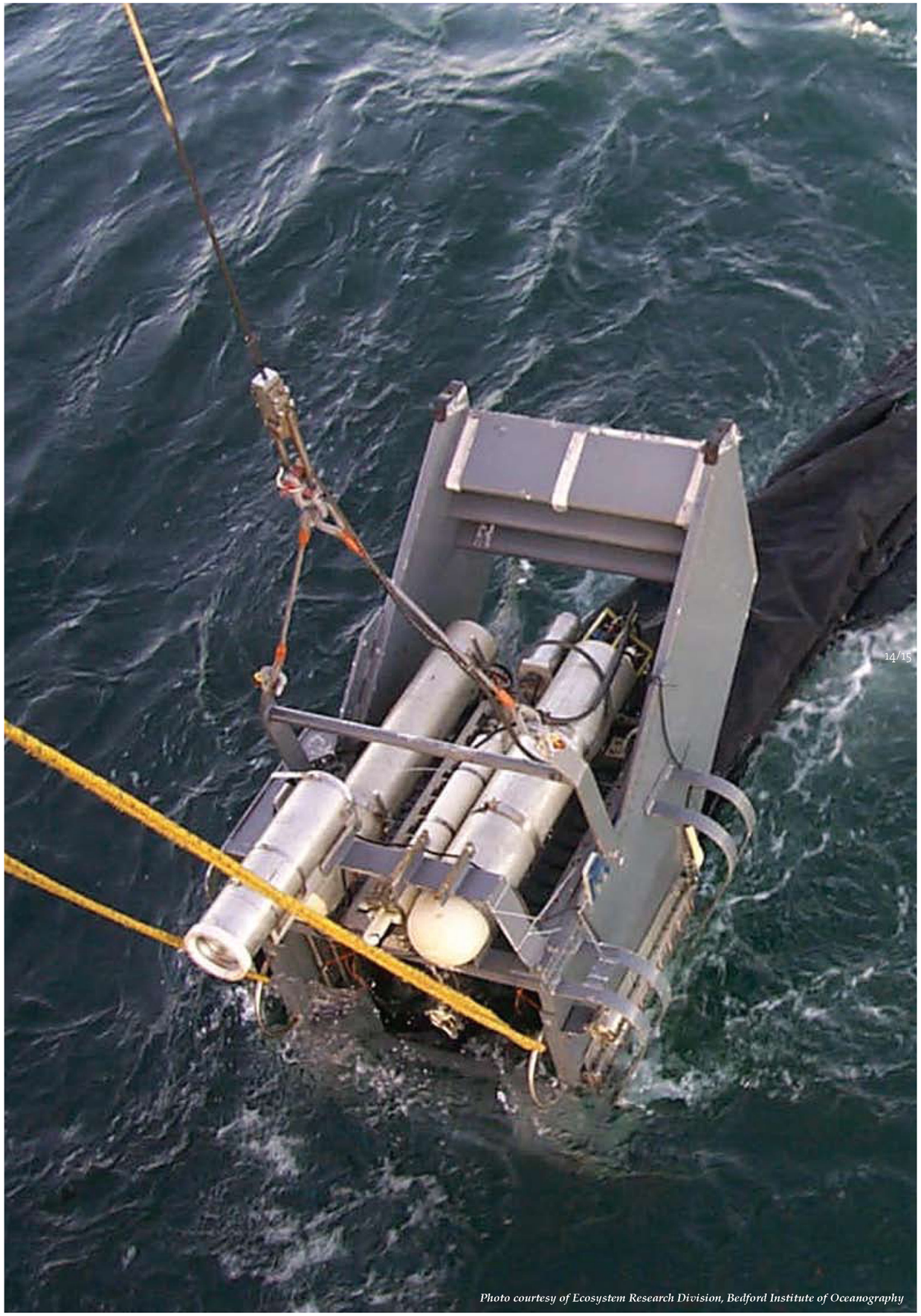

Photo courtesy of Ecosystem Research Division, Bedford Institute of Oceanography

3. NORTH ATLANTIC ZOOPLANKTON MONITORING

The information collated in this report is derived from more than 37 zooplankton sampling sites within the ICES Area (Figure 1, white stars) and from six additional sites in the Mediterranean (Figure 1, yellow stars). These sites have been grouped into the following geographic regions:

3.1 Western North Atlantic
3.2 Icelandic–Norwegian Basin
3.3 Barents Sea
3.4 Baltic Sea
3.5 North Sea and English Channel
3.6 Bay of Biscay and Iberian Coast
3.7 Mediterranean Sea

Together, these sites represent a broad range of hydrographic environments, from the temperate latitudes south of Portugal to the colder regions north of Norway, Iceland, and Canada, and from the lower salinity waters of the Baltic to the higher salinity waters of the Mediterranean. Across this broad range of physical conditions, abundance and biomass of zooplankton varies substantially between years, with clear cyclical patterns ranging from a few years to decades in duration and being apparent at all sites. Regional water temperatures can greatly influence the community structure and production of zooplankton, causing large seasonal, annual, and decadal changes in zooplankton population size and species composition, and in distribution. Included in this year's analysis is a 100-year record of sea surface temperatures (SST) for every site, in which we find some recent and disturbing trends in many of the eastern North Atlantic sites.

This report concludes with an overview of the North Atlantic (Section 4), featuring a coast-to-coast, basin-wide analysis using over 60 years of continuous plankton recorder (CPR) sampling. In addition to zooplankton abundance, this CPR study includes data from the CPR phytoplankton colour index (PCI), SST, and SeaWiFS (Sea-viewing Wide Field-of-view Sensor).

A map-based, interactive version of the materials and zooplankton time-series summarized in this report is available online at http://wgze.net/.

3.1 Western North Atlantic

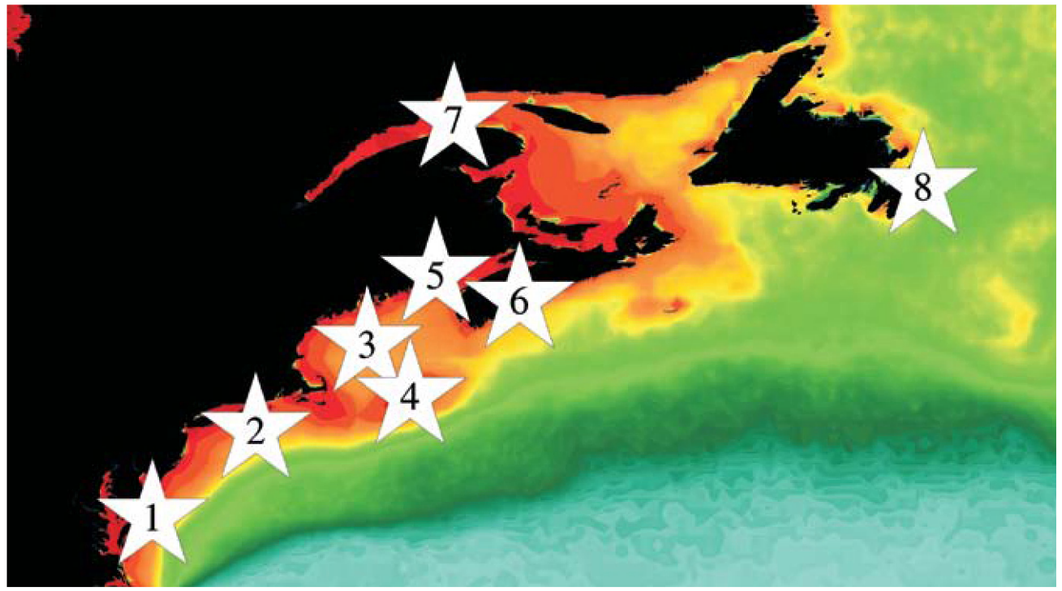

Figure 8.
Locations of western North Atlantic zooplankton time-series (Sites 1–8), plotted on a map of SeaWiFS average chlorophyll concentrations. Red/orange = high (productive), green/yellow = medium (moderate), blue = low (oligotrophic).

The Northwest Atlantic shelf regions where these zooplankton time-series samples are collected (see Figure 8) are influenced by water flowing towards the equator from the Labrador Sea and points to the north extending into the Arctic Ocean. Cold, relatively fresh Arctic/Boreal Labrador Current water flows into the Gulf of St Lawrence through the Strait of Belle Isle and around the southern end of Newfoundland. Outflow from the Gulf of St Lawrence Seaway joins the flow from southern Newfoundland and travels along the Scotian Shelf south of Nova Scotia, into the Gulf of Maine, and then around Georges Bank and along the Mid-Atlantic Bight to Cape Hatteras. The Arctic/Boreal waters are moderated during their passage to the southwest, and the species composition varies, with boreal species dominant in the north and more temperate species dominant in the south. The Gulf of Maine/Georges Bank region represents a southern boundary for many boreal species and a northern limit for some temperate and subtropical coastal species, although this is changing with the warming trend that is becoming evident in the area.

Sites 1–4: NMFS Ecosystem Monitoring (Northeast US continental shelf)

Jon Hare, Jack Jossi, and Joe Kane

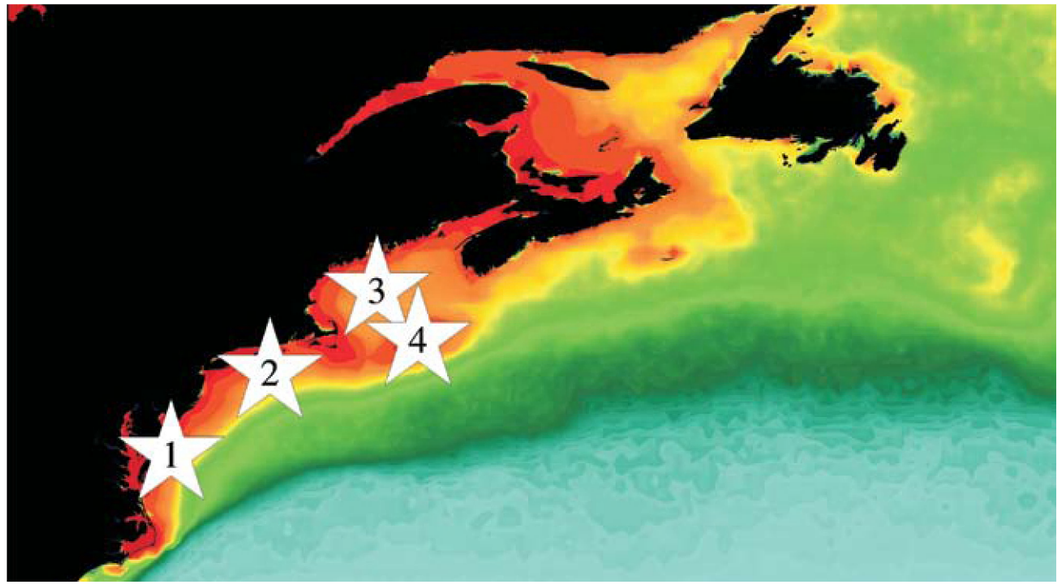

Figure 9.
Centre points of NMFS Ecosystem Monitoring regions on the northeast US continental shelf: Mid-Atlantic Bight (Site 1), Southern New England (Site 2), Gulf of Maine (Site 3), and Georges Bank (Site 4) survey areas, plotted on a map of SeaWiFS chlorophyll concentration. Red/orange = high (productive), green/yellow = medium (moderate), blue = low (oligotrophic).

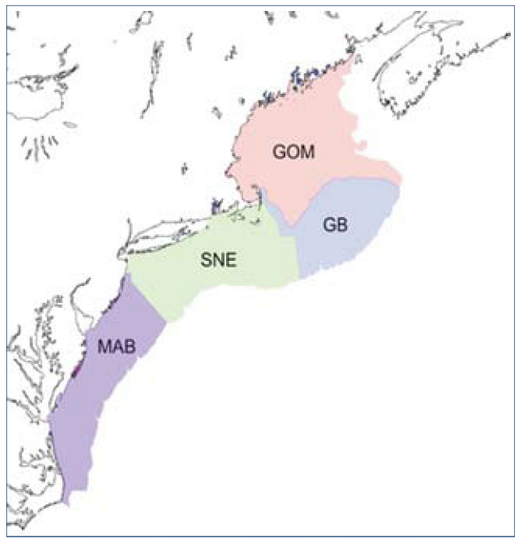

Figure 10.
Biophysical regions of the northeast US continental shelf: Mid-Atlantic Bight (MAB), Southern New England (SNE), Georges Bank (GB), and Gulf of Maine (GOM).

The Northeast Fisheries Science Center (NEFSC) of the National Marine Fisheries Service (NMFS) has a longstanding monitoring programme covering most of the northeast US continental shelf (Figure 9). The NEFSC sampling protocol divides the continental shelf into four regions, based on their different physical and biological characteristics (Figure 10), and collects hydrographic and tow data using a randomized spatial sampling technique that samples ~30 stations per region per 2-month period. During these surveys, zooplankton are collected using a bongo net (60 cm diameter, 333 µm mesh) towed obliquely from 200 m (or the bottom) to the surface.

Along the northeast US continental shelf, primary production is highest near the shore of each region and in the upwelling area of Georges Bank (Figure 9, Site 4). Lowest primary production is found in the deep-water areas of the Gulf of Maine (Figure 9, Site 3). The distribution of zooplankton biomass is similar to that of primary production, with the highest levels also found in the nearshore regions and along Georges Bank, whereas the lowest levels are found in the Gulf of Maine.

Changes in the northeast US continental shelf zooplankton community have been observed in all regions. All regions in the northeast US continental shelf demonstrate a general increasing trend in total annual zooplankton biomass since the early 1980s (Figures 11–14). Changes in species composition over this period have also been observed (Kane, 2007), with smaller-bodied taxa increasing in abundance in the 1990s. There is also some evidence of a shift in seasonality for some zooplankton species (e.g. *Calanus finmarchicus*), with the peak abundance period beginning earlier in the season and lasting longer.

Long-term SST trends at all four sites (Figures 15–18) demonstrate that, although temperatures are currently higher than the 100-year average for each region, they are lower than the 100-year maximum (Figures 15–18, bottom, red dashed line) seen in the 1950s. Since 1960, water temperatures in the Mid-Atlantic Bight (Figure 15) and Southern New England (Figure 16) have remained cooler than the 1950 maximum, but water temperatures have been slowly increasing towards this maximum in the Gulf of Maine (Figure 17) and on Georges Bank (Figure 18). Water temperature is influenced by the influx of cooler, fresher water from the north, and the occurrence of low-salinity events has also increased since the early 1990s (Mountain, 2004).

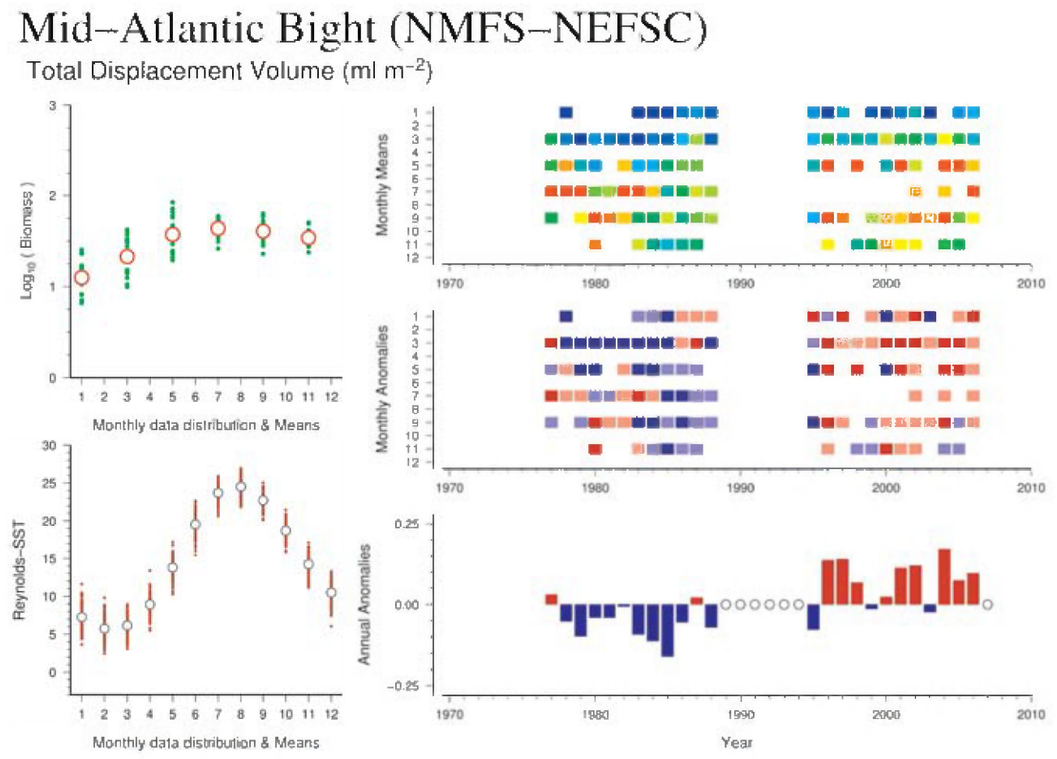

Figure 11.
Standardized WGZE time-series summary plot for total zooplankton displacement volumes in the Mid-Atlantic Bight. (See Section 2.1 for an explanation of the subplots in this figure.)

Southern New England (NMFS–NEFSC)

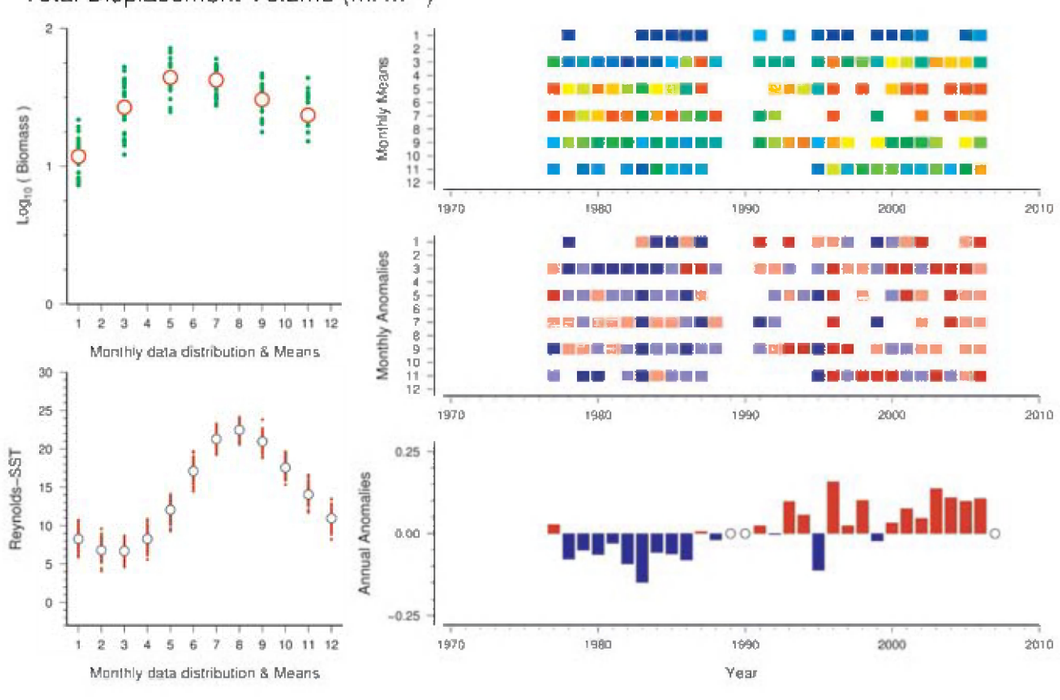

Figure 12.
Standardized WGZE time-series summary plot for total zooplankton displacement volumes in the Southern New England region. (See Section 2.1 for an explanation of the subplots in this figure.)

Gulf of Maine (NMFS–NEFSC)

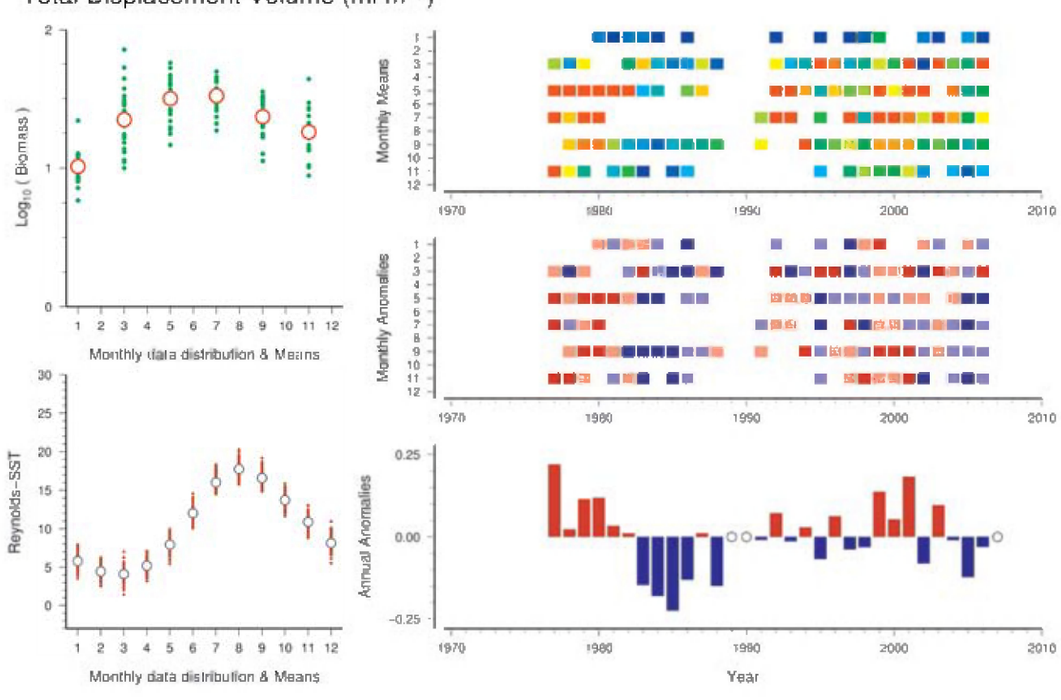

Figure 13.
Standardized WGZE time-series summary plot for total zooplankton displacement volumes in the Gulf of Maine. (See Section 2.1 for an explanation of the subplots in this figure.)

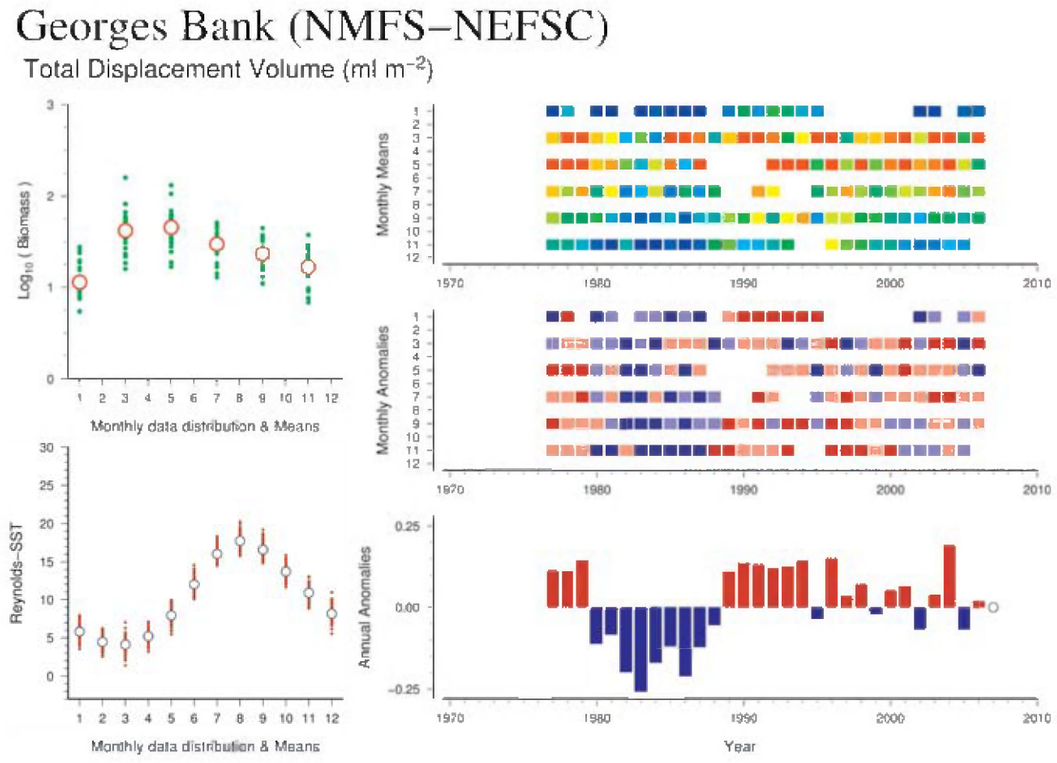

Figure 14.
Standardized WGZE time-series summary plot for total zooplankton displacement volumes on Georges Bank. (See Section 2.1 for an explanation of the subplots in this figure.)

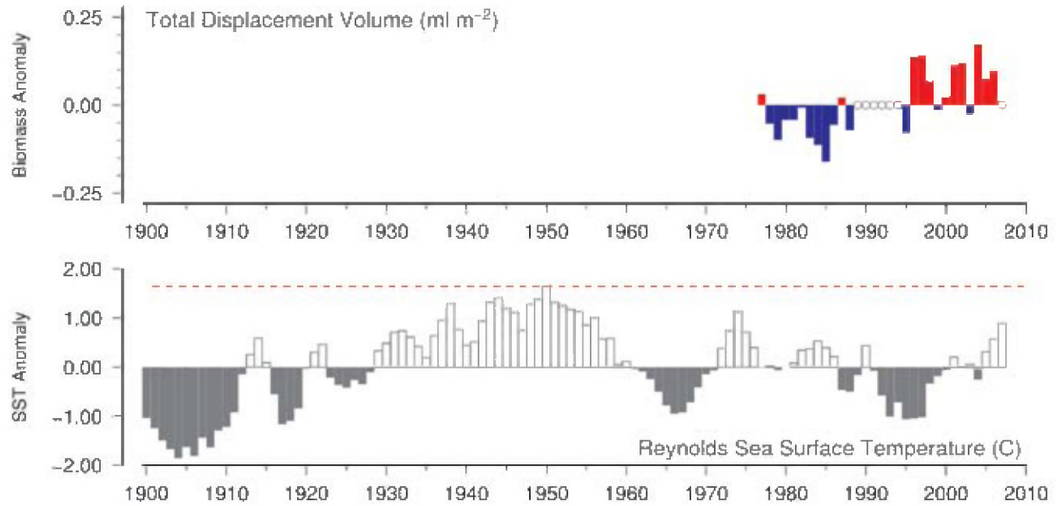

Figure 15.
Long-term comparison of Mid-Atlantic Bight total zooplankton displacement volumes with Reynolds sea surface temperatures for the region. CPR data were not available for this region. (See Section 2.3 for an explanation of the subplots in this figure.)

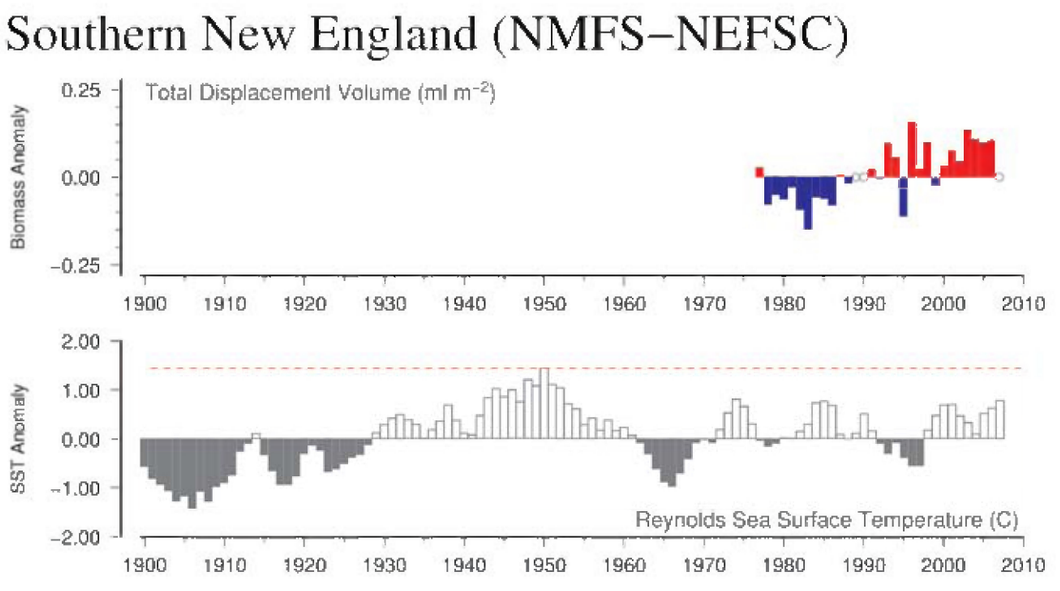

Figure 16.
Long-term comparison of Southern New England total zooplankton displacement volumes with Reynolds sea surface temperatures for the region. CPR data were not available for this region. (See Section 2.3 for an explanation of the subplots in this figure.)

Gulf of Maine (NMFS–NEFSC)

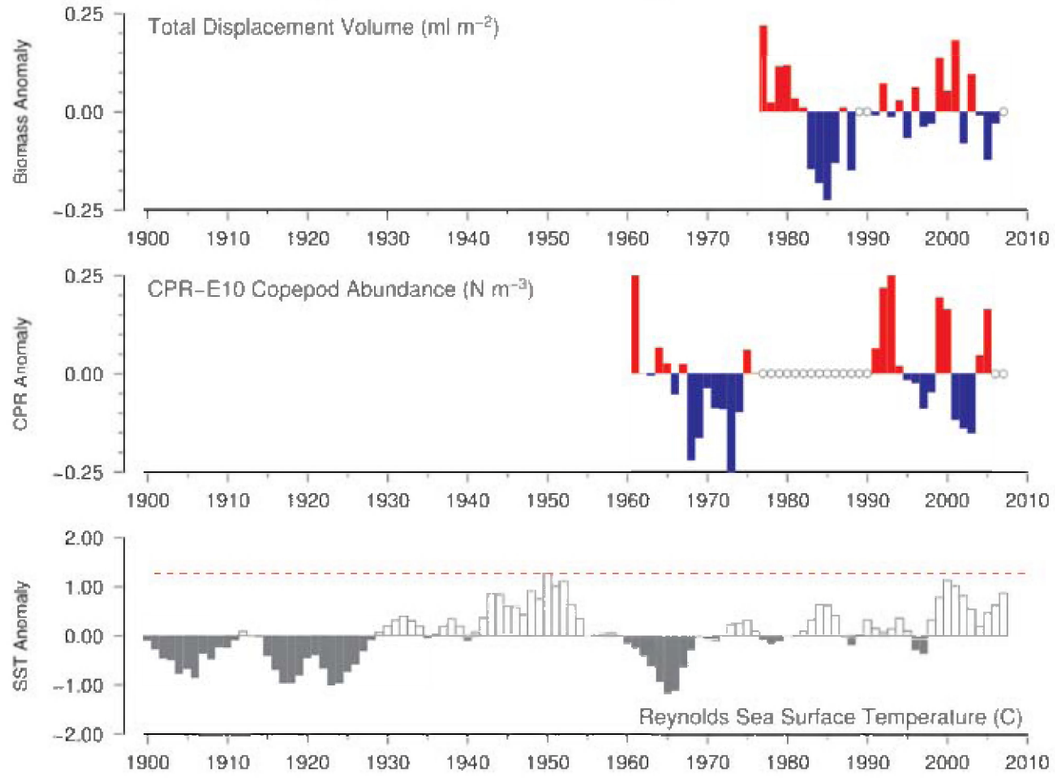

Figure 17.
Long-term comparison of Gulf of Maine total zooplankton displacement volumes with copepod abundance in CPR standard area "E10" and Reynolds sea surface temperatures for the region. (See Section 2.3 for an explanation of the subplots in this figure.)

Georges Bank (NMFS–NEFSC)

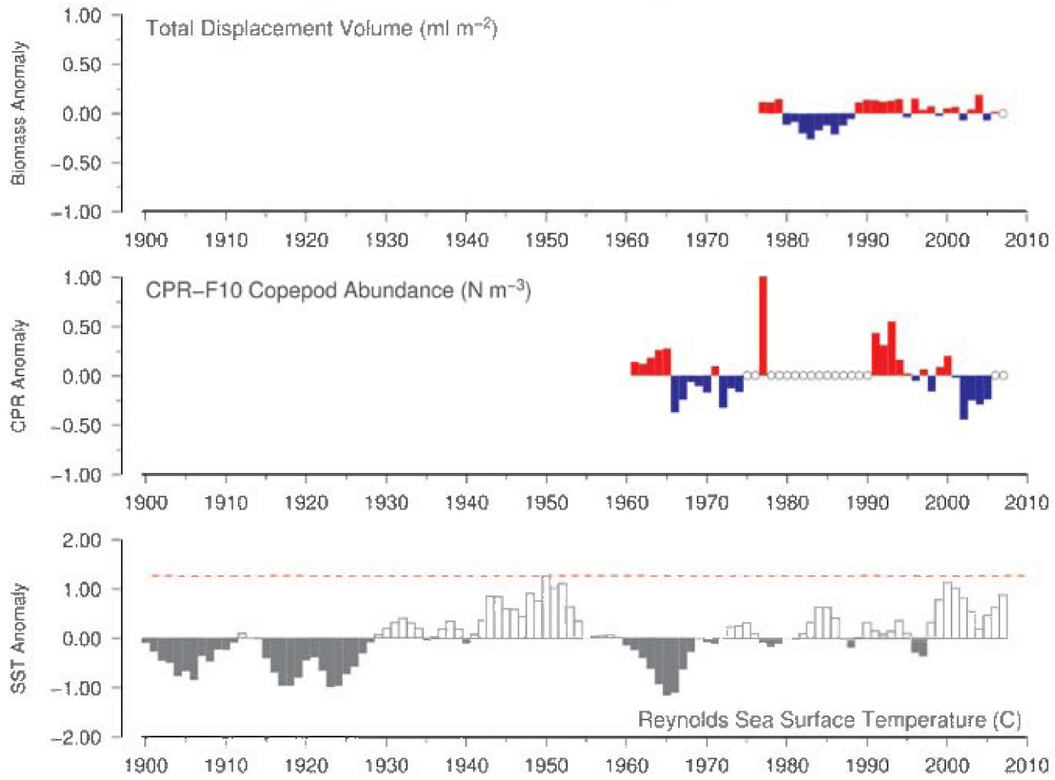

Figure 18.
Long-term comparison of Georges Bank total zooplankton displacement volumes with copepod abundance in CPR standard area "F10" and Reynolds sea surface temperatures for the region. (See Section 2.3 for an explanation of the subplots in this figure.)

Site 5: Prince 5 (Bay of Fundy)

Erica Head

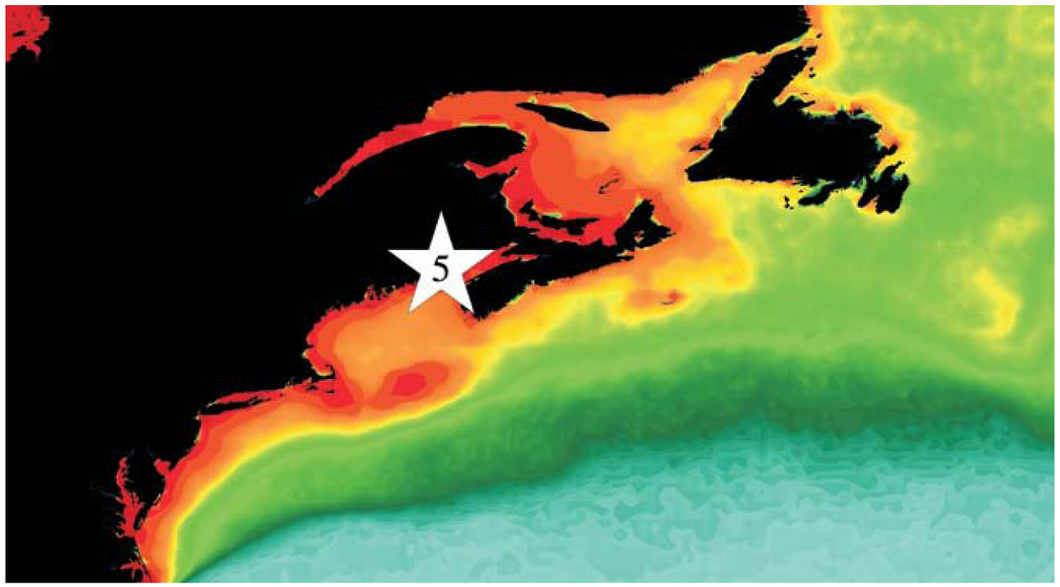

Figure 19.
Location of the Prince 5 survey area (Site 5), plotted on a map of SeaWiFS chlorophyll concentration. Red/orange = high (productive), green/yellow = medium (moderate), blue = low (oligotrophic).

Zooplankton are sampled every 2–4 weeks at Prince 5, which is a 100 m deep station located just off Campobello Island in the northwest of the Bay of Fundy, approximately 6 km offshore from St Andrews, New Brunswick (Figure 19). Vertical tows are made from near-bottom to surface using a ringnet (0.75 m diameter, 200 µm mesh). A small vessel is used as the sampling platform. Conductivity, temperature, and depth (CTD) profiles are recorded, and water samples are collected in Niskin bottles for measuring phytoplankton, nutrients, and extracted chlorophyll. Zooplankton samples are split, and one-half is used for wet–dry weight determination. The other half is subsampled for taxonomic identification and enumeration. Biomass of the dominant groups is also calculated using individually determined dry weights and abundance data for the dominant species groups (*Calanus, Oithona, Pseudocalanus*, and *Metridia*). The data are entered into the "BioChem" database at the Canadian Department of Fisheries and Oceans (DFO). An ecosystem status report on the state of phytoplankton and zooplankton in Canadian Atlantic waters is prepared every year. This report is available online at www.dfo-mpo.gc.ca/csas/Csas/English/Status/general.htm.

Monthly average abundance of total copepods is variable, but values are generally lowest during winter (January–April) and highest in late summer/autumn (August–October). Annual average copepod abundance anomalies were highest in 2001 and 2006, and lowest in 2002 and 2005 (Figure 20). In years of low abundance, i.e. years with negative annual abundance anomalies, the summer/autumn high abundance period was often weaker and/or of shorter duration.

In addition to copepod abundance, co-sampled time-series of total zooplankton wet weight, integrated chlorophyll, and integrated temperature data were available for the site (Figure 21). Although the seasonal cycles of copepod abundance and total wet weight are similar, the annual anomalies of total wet weight differ slightly as a result of the influence of phytoplankton blooms contaminating the measurement. Chlorophyll concentrations demonstrate a seasonal cycle similar to that of the copepods, but preceding it by one month, and the annual chlorophyll concentrations have demonstrated a slight downward trend over time. At-site sampled integrated temperature and Reynolds SST show similar interannual increases and decreases, but differ slightly in seasonal cycle, most probably caused by the larger spatial region represented by the Reynolds data.

The SST values are at the high end of an approximately 50-year multidecadal trend (Figure 22). Within this region, water temperatures are often correlated with the state of the North Atlantic Oscillation (NAO). At this time, any relationship between water temperature and zooplankton abundance is inconclusive.

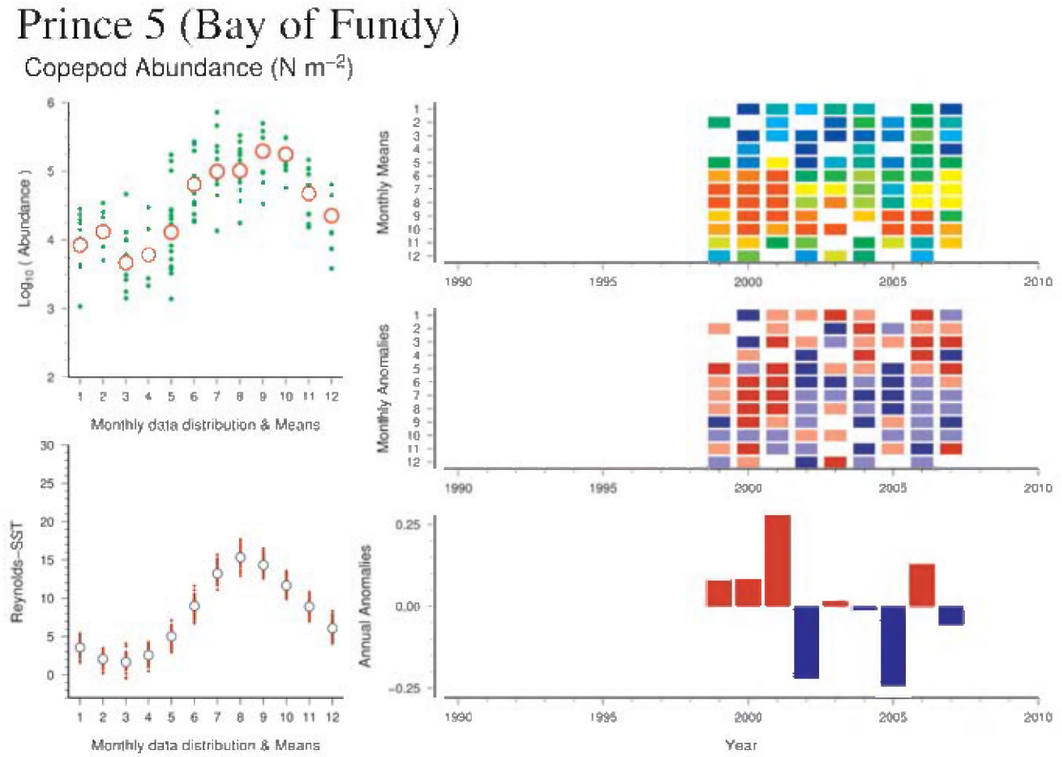

Figure 20.
Standardized WGZE time-series summary plot for copepod abundance at Prince 5. (See Section 2.1 for an explanation of the subplots in this figure.)

Prince 5 (Bay of Fundy)

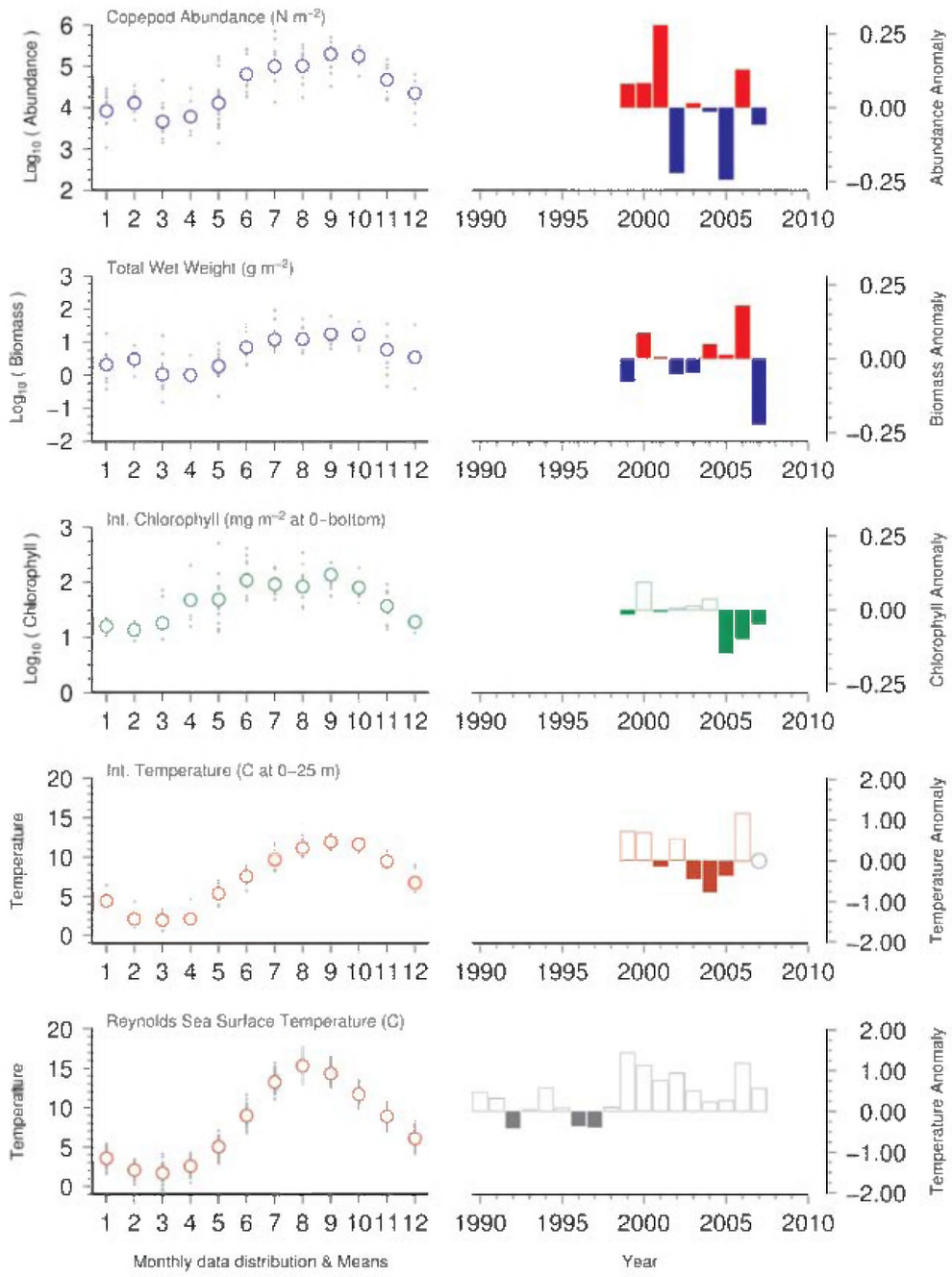

Figure 21.
Seasonal and interannual comparison of co-sampled variables at Prince 5. (See Section 2.2 for an explanation of the subplots in this figure.)

Prince 5 (Bay of Fundy)

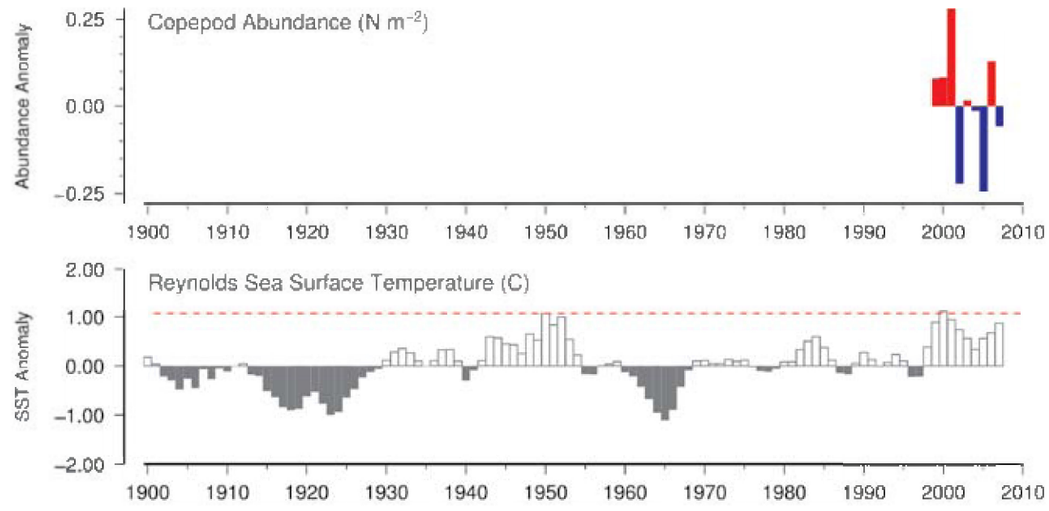

Figure 22.
Long-term comparison of Prince 5 copepod abundance with Reynolds sea surface temperatures for the region. CPR data were not available for this region. (See Section 2.3 for an explanation of the subplots in this figure.)

Site 6: Halifax Line 2 (Scotian Shelf)

Erica Head

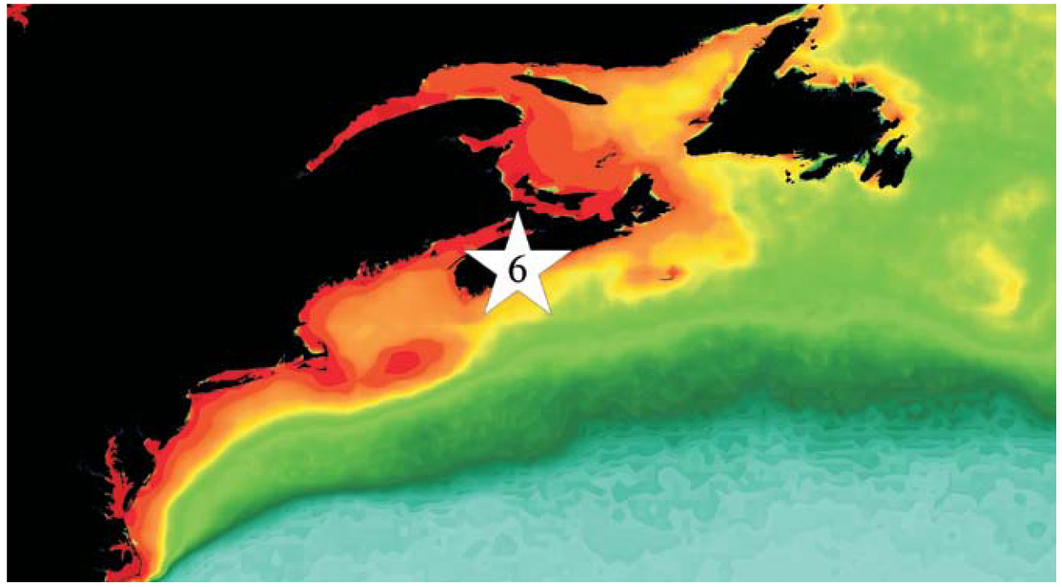

***Figure* 23.**
Location of the Halifax Line 2 survey area (Site 6), plotted on a map of SeaWiFS chlorophyll concentrations. Red/orange = high (productive), green/yellow = medium (moderate), blue = low (oligotrophic).

Zooplankton are sampled every 2–4 weeks at Station 2 of the Halifax Line (HL2), which is 150 m deep and located approximately 12 kilometres offshore from Halifax on the inshore edge of Emerald Basin (Figure 23). Vertical tows are made from near-bottom to surface using a ringnet (0.75 m diameter, 200 µm mesh). Research ships, trawlers, and small vessels are used as sampling platforms. CTD profiles are recorded, and water samples are collected in Niskin bottles for the measurement of phytoplankton, nutrients, and extracted chlorophyll. Chlorophyll and nutrient concentrations are measured for individual depths, whereas subsamples from each depth are combined to give an integrated sample for phytoplankton cell counting. Zooplankton samples are split, and one-half is used for wet–dry weight determination. The other half is subsampled for taxonomic identification and enumeration. Biomass of the dominant groups is calculated using dry weights and abundance data for various groupings (*Calanus* – by species and stage, *Oithona*, *Pseudocalanus*, and *Metridia*). The data are entered into the "BioChem" database at the DFO. An ecosystem status report on the state of phytoplankton and zooplankton in Canadian Atlantic waters is prepared every year. This report is available online at www.dfo-mpo.gc.ca/csas/csas/Publications/Pub_Index_e.htm.

Monthly average abundance of total copepods is very variable at HL2, but shows minima in February and September. Annual average abundance anomalies were highest in 1999 and 2000, and lowest in 2002 and 2007 (Figure 24), suggesting an overall downward trend. In addition to copepod abundance, co-sampled time-series of total zooplankton wet weight, integrated chlorophyll, and integrated temperature data were available for the site (Figure 25), together with Reynolds SST. Although the seasonal cycles of copepod abundance and total wet weight are similar, the annual anomalies of total wet weight differ slightly as a result of the influence of phytoplankton blooms in the measurement. Chlorophyll concentrations demonstrate a seasonal cycle similar to that of the copepods. Like Prince 5, the annual chlorophyll concentrations demonstrate a slight downward trend over time, thought to be caused by a decline in diatom abundance (Li *et al.*, 2006). At-site sampled integrated temperature and Reynolds SST demonstrate similar interannual increases and decreases, but differ slightly in their seasonal cycles, most probably attributable to the larger spatial region represented by the Reynolds data.

The CPR standard area closest to HL2 is "E10" (Figure 2). Copepod abundance from the CPR corresponds neatly with the HL2 copepod abundance (Figure 26), whereas differences between CPR copepod abundance and HL2 wet weight are probably caused by contamination with phytoplankton in the wet mass measurement.

The SST values are at the high end of an approximately 50-year, multidecadal trend (Figure 26). In general, water temperature is often correlated with the state of the North Atlantic Oscillation (NAO). At this time, any relationship between water temperature and zooplankton abundance is inconclusive.

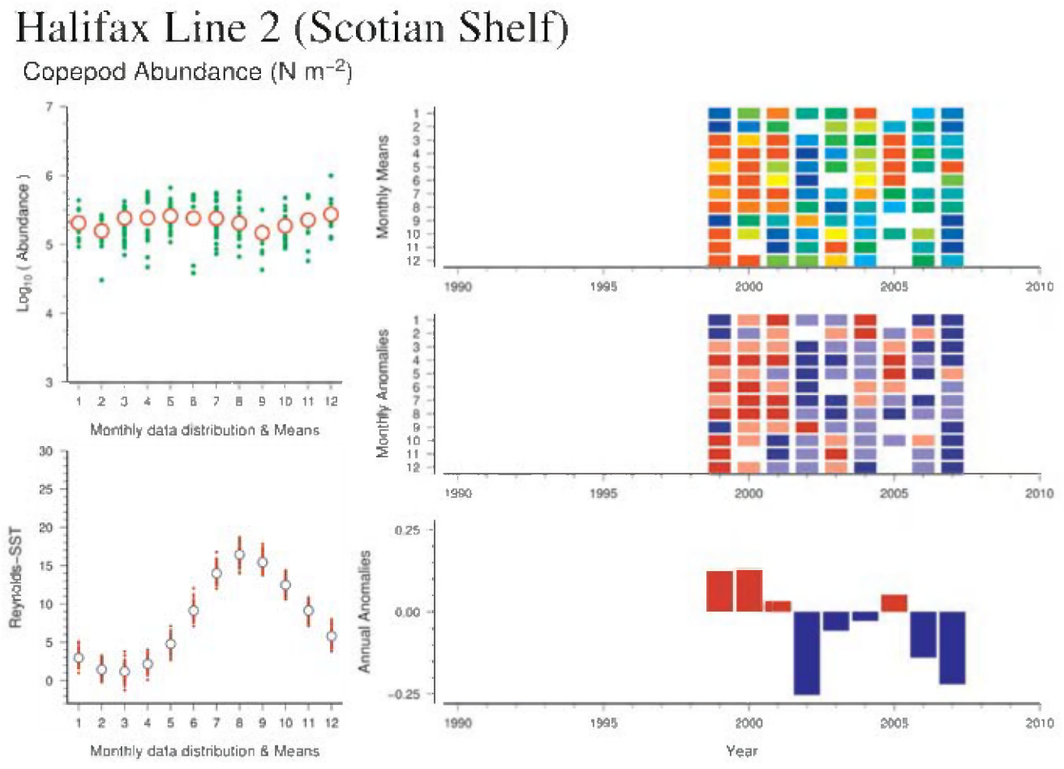

***Figure* 24.**
Standardized WGZE time-series summary plot for copepod abundance at Halifax Line 2. (See Section 2.1 for an explanation of the subplots in this figure.)

Halifax Line 2 (Scotian Shelf)

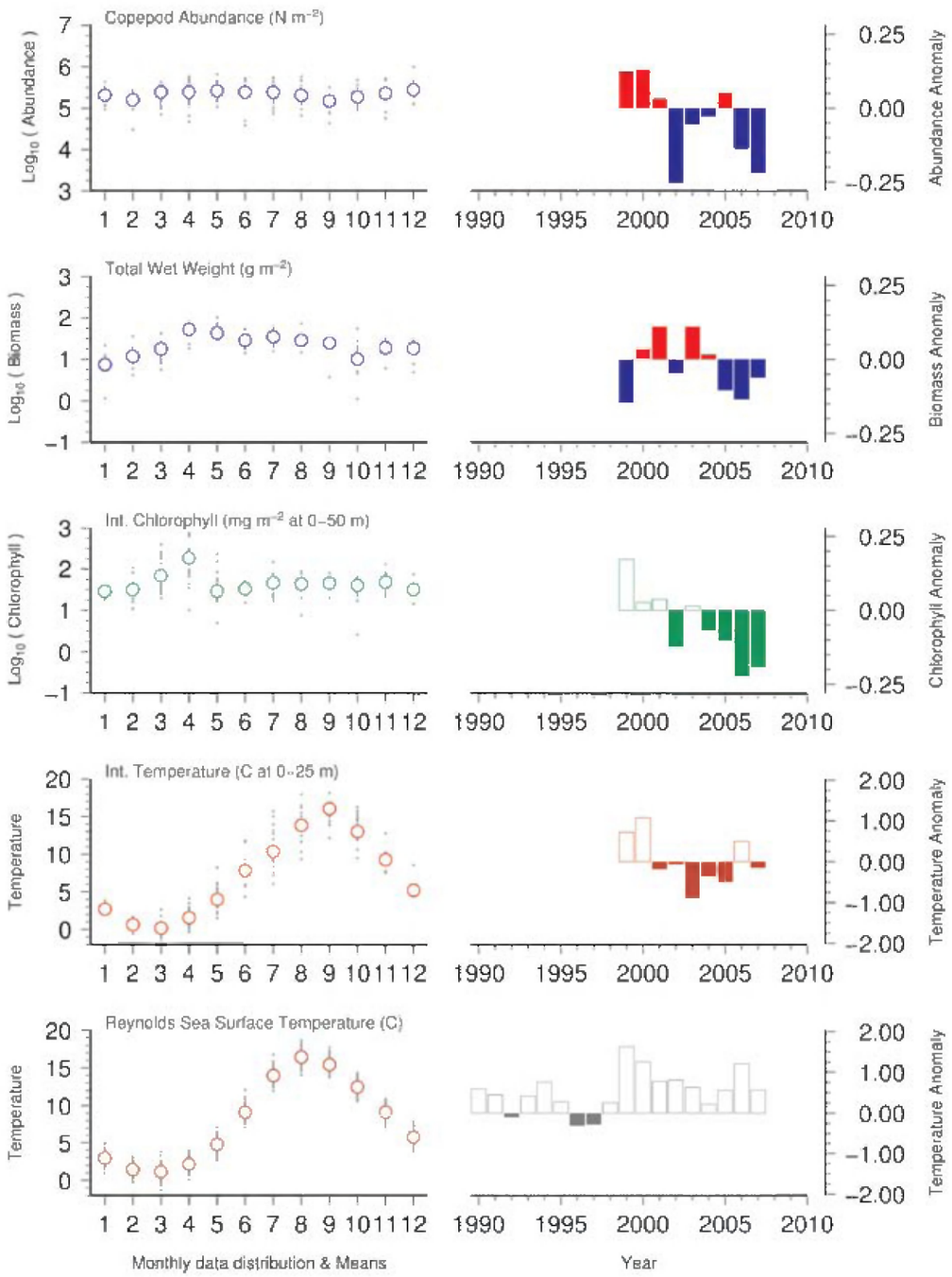

Figure 25.
Seasonal and interannual comparison of co-sampled variables at Halifax Line 2. (See Section 2.2 for an explanation of the subplots in this figure.)

Halifax Line 2 (Scotian Shelf)

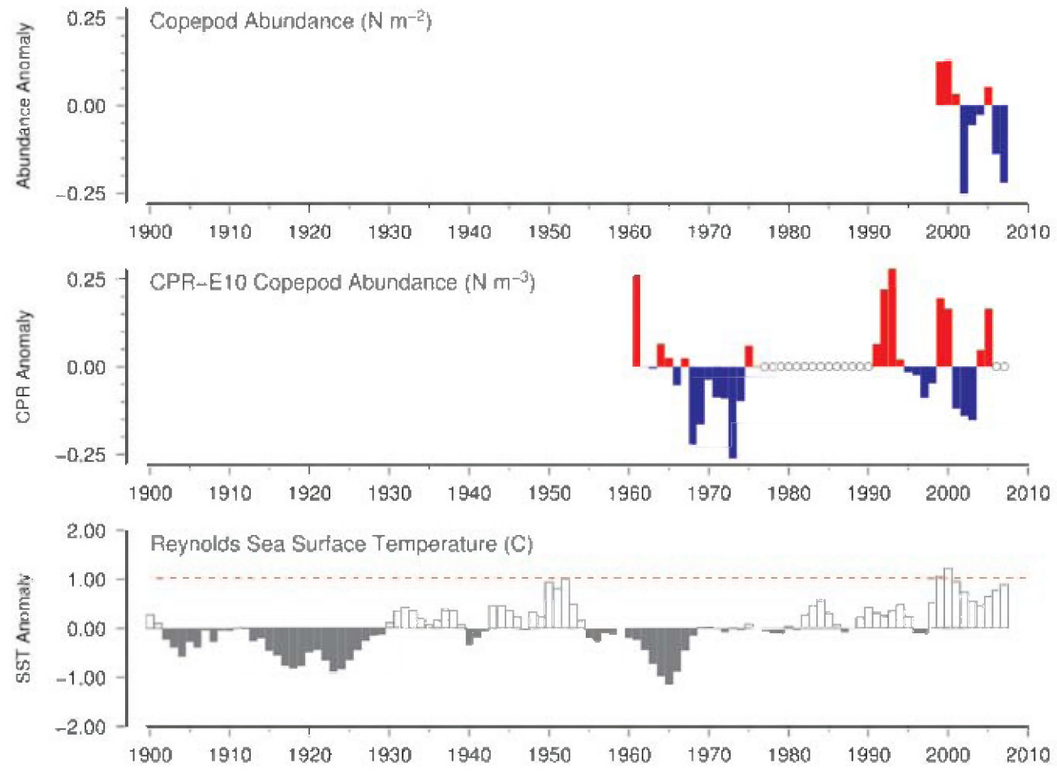

Figure 26.
Long-term comparison of Halifax Line 2 copepod abundance with copepod abundance in CPR standard area "E10" and Reynolds sea surface temperatures for the region. (See Section 2.3 for an explanation of the subplots in this figure.)

Site 7: Gaspé Current and Anticosti Gyre (Gulf of St Lawrence)

Michel Harvey

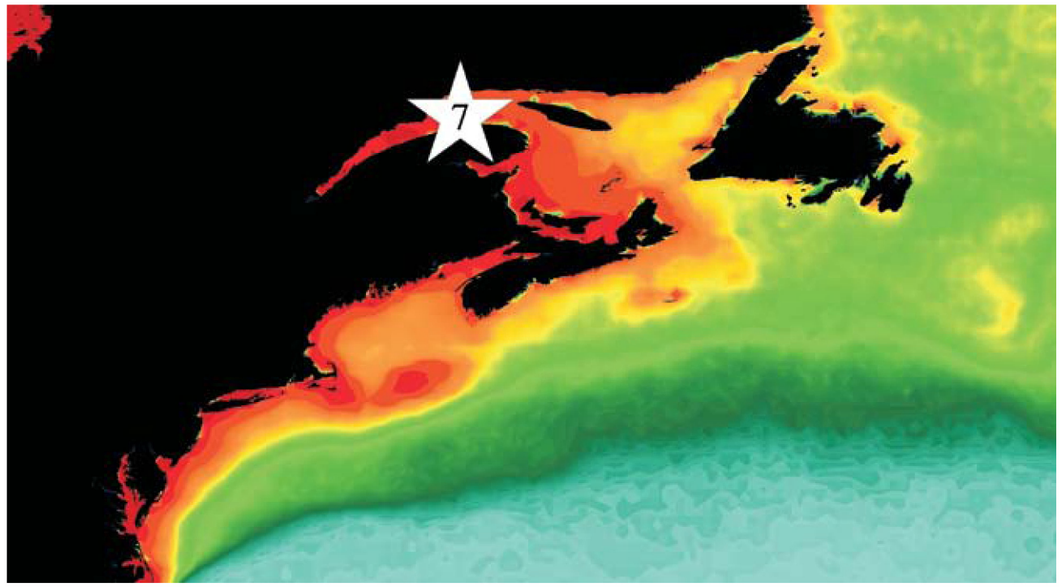

Figure 27.
Location of the Gulf of St Lawrence survey area (Site 7), plotted on a map of SeaWiFS chlorophyll concentration. Red/orange = high (productive), green/yellow = medium (moderate), blue = low (oligotrophic).

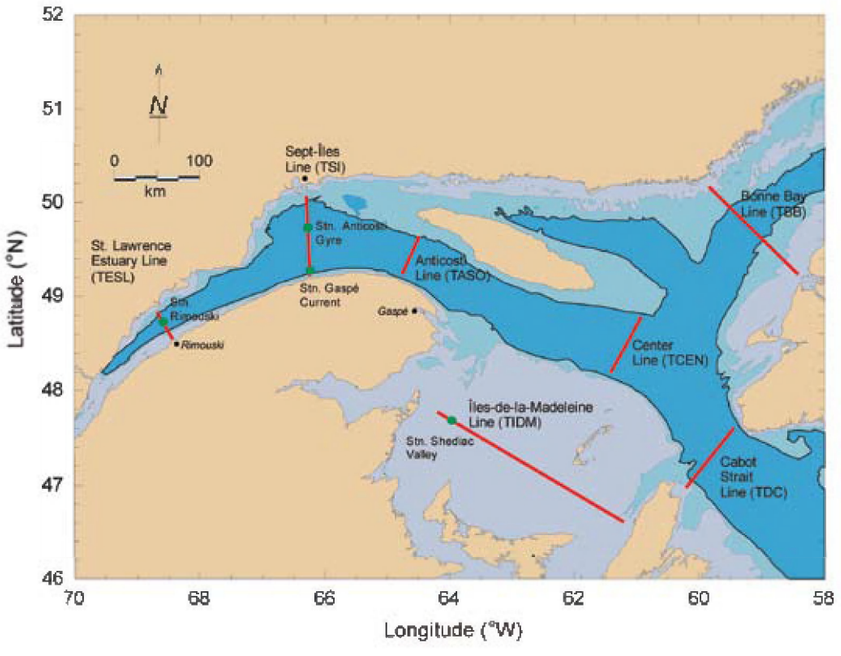

Figure 28.
Sections (red lines) and fixed stations (green dots) sampled in the Québec region.

The Atlantic Zone Monitoring Programme (AZMP) was implemented in 1998 with the aim of collecting and analysing the biological, chemical, and physical field data that are necessary to: (i) characterize and understand the causes of oceanic variability at the seasonal, interannual, and decadal scales; (ii) provide multidisciplinary datasets that can be used to establish relationships among the biological, chemical, and physical variables; and (iii) provide adequate data to support the sound development of ocean activities. The key element of AZMP sampling strategy is the oceanographic sampling at fixed stations and along sections. The fixed stations are occupied about every two weeks, conditions permitting, and the sections are sampled in June and November. Zooplankton are sampled from the bottom to the surface with a ringnet (0.75 m diameter, 200 µm mesh). CTD profiles are recorded, and samples for phytoplankton, nutrients, and extracted chlorophyll are collected using Niskin bottles at fixed depths. Samples are combined to give an integrated sample. An ecosystem status report on the state of phytoplankton and zooplankton is prepared every year and available online at www.dfo-mpo.gc.ca/csas/csas/Publications/Pub_Index_e.htm.

Data presented in this report are from two sampling stations in the northwest Gulf of St Lawrence (GSL, Figure 27): the Anticosti Gyre (AG) and the Gaspé Current (GC; Figure 28). The GSL is a coastal marine environment with a particularly high zooplankton biomass relative to other coastal areas, dominated by *Calanus* species (de Lafontaine *et al.*, 1991). Annual anomalies of zooplankton biomass and abundance at GC (Figure 29) and AG (Figure 30) indicate that, in 2007, biomass was slightly lower than normal and abundance was above normal at both sites. Hierarchical community analysis revealed that copepods continue to numerically dominate the zooplankton year-round at both fixed stations in 2007, with the exception of a pulse of appendicularians that was observed during summer at AG and GC. There was no apparent change in copepod community structure in 2007 at either station.

Zooplankton abundance and biomass do not follow the same pattern as the concentration of chlorophyll *a*. For example, the zooplankton peak observed at GC in 2003 corresponded to a chlorophyll *a* minimum (Figure 31), whereas the chlorophyll *a* peak at AG in 2001 corresponded to a zooplankton minimum (Figure 32). This absence of correlation between zooplankton and algal biomass has been observed in the GSL (de Lafontaine *et al.*, 1991; Roy *et al.*, 2000) and was attributed to the complex estuarine circulation pattern observed at GC and AG. Annual cycles of SST in both cases are similar, with values below 0°C in winter and peaks above 14°C during summer. Long-term SST values in the region (1900–2007) reveal that temperatures are currently at the high end of an approximately 50-year multidecadal trend and have been at, or above, the 100-year maximum (Figures 33 and 34, bottom, red dashed line) since 1998. The exact effects of these high temperatures are not fully understood, although total zooplankton abundance at both regions is currently increasing with the increasing temperature at GC (Figure 33) and AC (Figure 34).

The abundance and percentage of the ten most abundant taxa at AG and GC are shown in Tables 1, 2, 3, and 4. In 2007, some major changes were observed in the zooplankton composition within the top ten taxa over the time-series. In addition to some changes in the rank order of the top ten species, some new groups appeared in 2007 as dominant species for the first time at both stations. The most important new group is the Larvacea, which made up 6% of the total zooplankton abundance at AG in 2007. In addition, the dominant species at both stations is the small copepod *Oithona* spp.

Table 1.

Rank	Taxa	% of total abundance 1999–2006	% of total zooplankton 2007	(Δ)	Mean abundance (N m^{-3}) 1999–2006	Abundance (N m^{-3}) 2007	(Δ%)
1	*Oithona* spp.	42.5	36.1	(–6.4)	373.9	408.1	(9)
2	*Calanus finmarchicus*	13.5	16.7	(3.2)	118.9	189.4	(59)
3	Copepod nauplii (N3–N6)	12.8	13.7	(0.9)	112.3	154.5	(38)
4	Copepod eggs (> 202 mm)	8.6	2.0	(–6.6)	75.7	22.7	(-70)
5	*Pseudocalanus* spp.	4.3	7.4	(3.0)	38.2	83.4	(118)
6	*Euphausiacea* (eggs, nau, juv.)	4.0	2.9	(–1.2)	35.6	32.7	(–8)
7	*Calanus hyperboreus*	1.9	1.2	(–0.8)	17.1	13.0	(–24)
8	*Metridia* spp.	1.8	1.0	(–0.8)	15.6	10.9	(–31)
9	*Microcalanus* spp.	1.6	1.4	(–0.3)	14.2	15.4	(8)
10	Larvacea	1.6	9.4	(7.8)	13.8	106.1	(665)
	"Top ten" totals	**92.6**	**91.6**	**(–1.1)**	**815.4**	**1 036.4**	**(27)**
	Total abundance of all zooplankton (N m^{-3})				**880.1**	**1 131.8**	**(29)**

Table 1.
Average abundance and relative dominance (percentage of the total zooplankton collected) of the top ten most abundant zooplankton taxa collected at the Gaspé Current site in previous years (1999–2006) compared with that collected in 2007. Colours in the "Δ" and "Δ%" columns indicate either an increase (red) or decrease (blue) in relative dominance compared with previous years.

Table 2.

Rank	Taxa	% of total abundance 2007	Abundance (N m^{-3}) 2007
1	*Oithona* spp.	36.1	408.1
2	*Calanus finmarchicus*	16.7	189.4
3	Copepod nauplii (N3–N6)	13.7	154.5
4	Appendicularia	9.4	106.1
5	*Pseudocalanus* spp.	7.4	83.4
6	Euphausiids (eggs, nau, juv.)	2.9	32.7
7	Copepod eggs (> 202 mm)	2.0	22.7
8	**Echinoderm larvae**	**1.8**	**20.7**
9	*Microcalanus* spp.	1.4	15.4
10	**Bivalve larvae**	**1.2**	**13.5**
	"Top ten" totals	**92.5**	**1 046.8**
	Total abundance of all zooplankton (N m^{-3})		**1 131.8**

Table 2.
Abundance and relative dominance (percentage of the total zooplankton collected) of the top ten most abundant zooplankton taxa collected at the Gaspé Current site in 2007. Bold entries indicate new taxa dominant in 2007, but not previously dominant in the 1999–2006 time-series (see Table 1).

Table 3.

Rank	Taxa	% of total abundance 1999–2006	% of total zooplankton 2007	(Δ)	Mean abundance (N m^{-3}) 1999–2006	Abundance (N m^{-3}) 2007	(Δ%)
1	*Oithona* spp.	24.3	29.2	(4.9)	134.5	150.2	(12)
2	Copepod nauplii (N3–N6)	15.4	1.7	(-13.7)	85.3	8.9	(-90)
3	*Calanus finmarchicus*	12.2	13.3	(1.0)	67.8	68.5	(1)
4	*Calanus hyperboreus*	10.5	11.4	(0.8)	58.4	58.6	(0)
5	Copepod eggs *(>202 mm)*	9.3	0.8	(-8.4)	51.2	4.3	(-92)
6	*Microcalanus* spp.	4.5	9.0	(4.4)	25.1	46.1	(84)
7	Ostracoda	4.0	6.6	(2.6)	22.3	34.1	(53)
8	Echinoderm larvae	3.9	0.7	(–3.2)	21.7	3.7	(–83)
9	*Metridia* spp.	3.7	3.3	(–0.5)	20.7	16.8	(-19)
10	*Pseudocalanus* spp.	2.5	4.1	(1.6)	13.8	21.3	(54)
	"Top ten" totals	**90.5**	**80.1**	**(–10.4)**	**501.0**	**412.6**	**(-18)**
	Total abundance of all zooplankton (N m^{-3})				**553.8**	**515.3**	**(-7)**

Table 3.
Average abundance and relative dominance (percentage of the total zooplankton collected) of the top ten most abundant zooplankton taxa collected at the Anticosti Gyre site in previous years (1999–2006) compared with that collected in 2007. Colours in the "Δ" and "Δ%" columns indicate either an increase (red) or decrease (blue) in relative dominance compared with previous years.

Table 4.

Rank	Taxa	% of total abundance 2007	Abundance (N m^{-3}) 2007
1	*Oithona* spp.	31.1	150.2
2	*Calanus finmarchicus*	14.2	68.5
3	*Calanus hyperboreus*	12.1	58.6
4	*Microcalanus* spp.	9.5	46.1
5	Ostracoda	7.1	34.1
6	**Larvacea**	**5.8**	**28.2**
7	*Pseudocalanus* spp.	4.4	21.3
8	*Metridia* spp.	3.5	16.8
9	**Oncea spp.**	**2.1**	**9.9**
10	Copepod nauplii (N3–N6)	1.8	8.9
	"Top ten" totals	**91.6**	**442.6**
	Total abundance of all zooplankton (N m^{-3})		**515.3**

Table 4.
Abundance and relative dominance (percentage of the total zooplankton collected) of the top ten most abundant zooplankton taxa collected at the Anticosti Gyre site in 2007. Bold entries indicate new taxa dominant in 2007, but not previously dominant in the 1999–2006 time-series (see Table 3).

Gaspé Current (Gulf of St Lawrence)

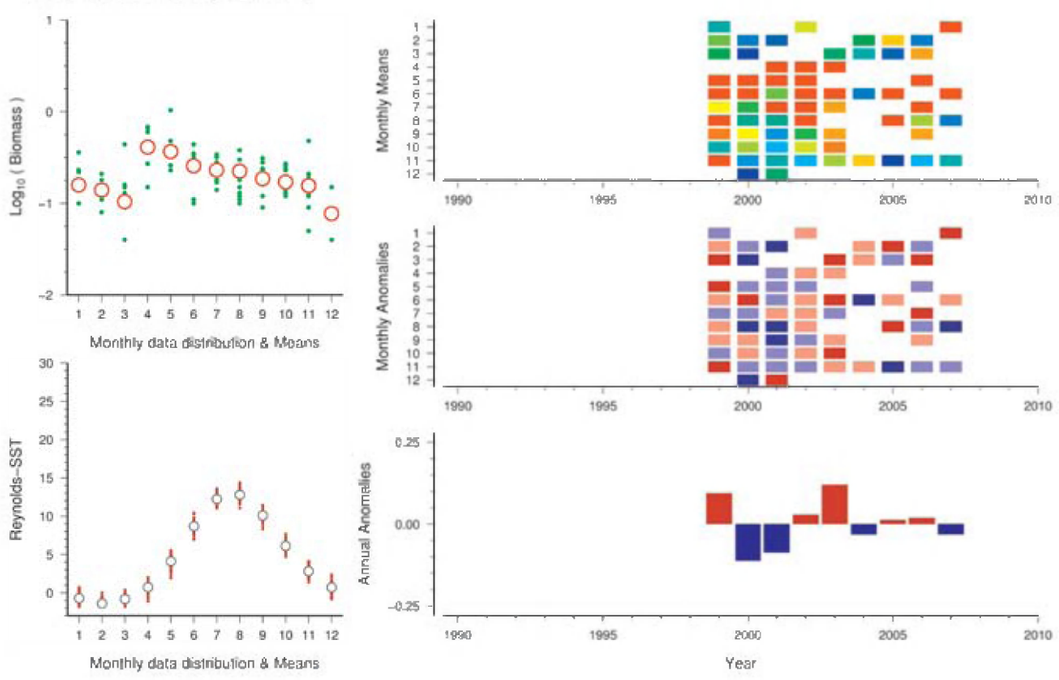

Figure 29.
Standardized WGZE time-series summary plot for total zooplankton wet mass at the Gaspé Current site. (See Section 2.1 for an explanation of the subplots in this figure.)

Anticosti Gyre (Gulf of St Lawrence)

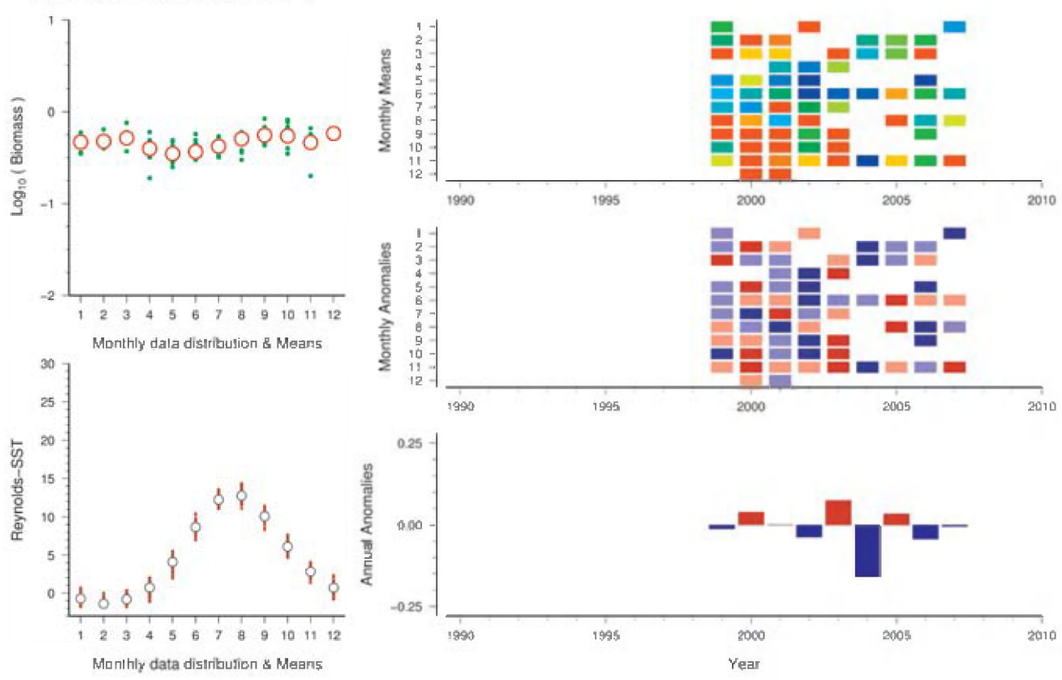

Figure 30.
Standardized WGZE time-series summary plot for total zooplankton wet mass at the Anticosti Gyre site. (See Section 2.1 for an explanation of the subplots in this figure.)

Gaspé Current (Gulf of St Lawrence)

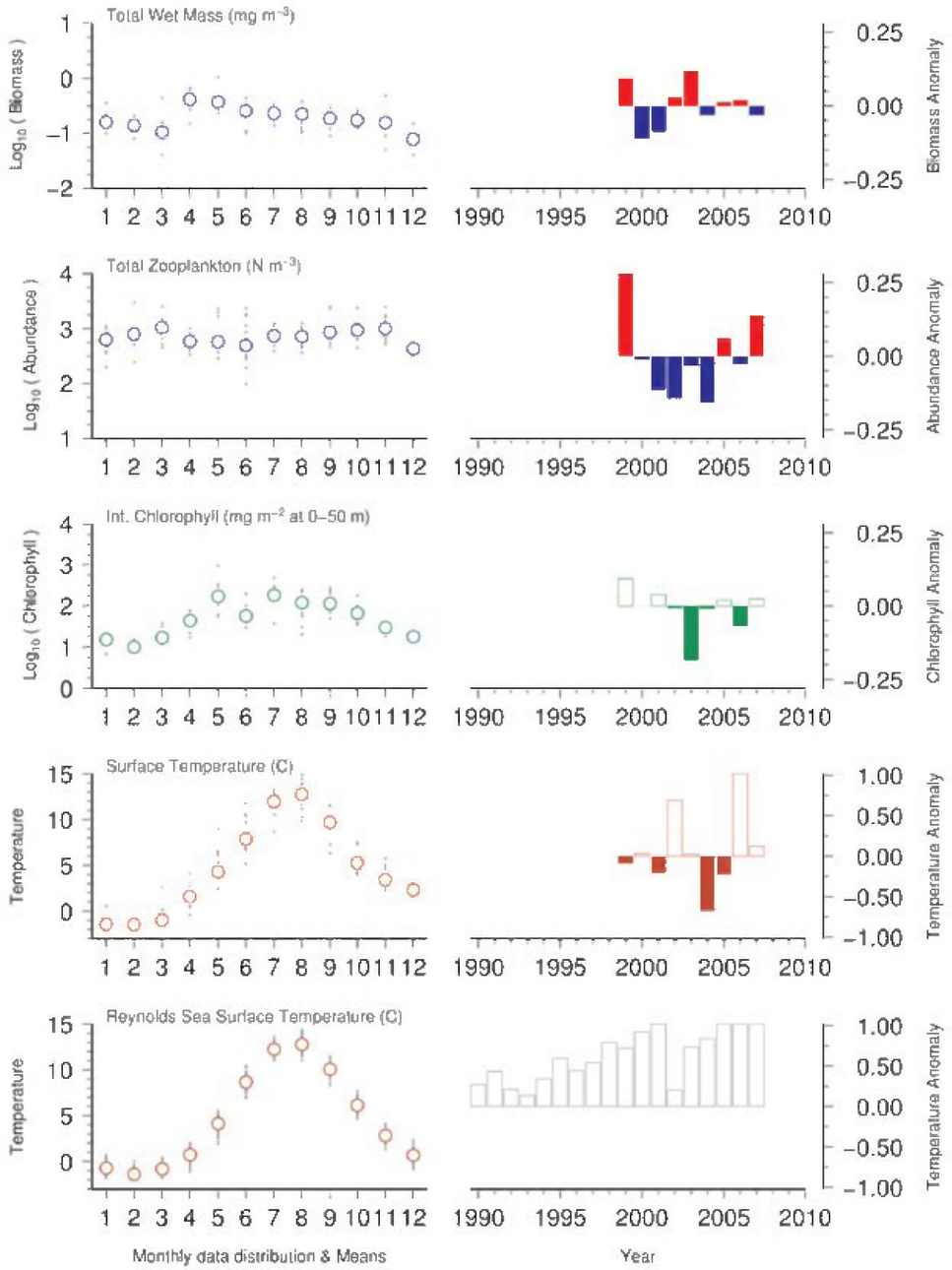

Figure 31.
Seasonal and interannual comparison of co-sampled variables at the Gaspé Current site. (See Section 2.2 for an explanation of the subplots in this figure.)

Anticosti Gyre (Gulf of St Lawrence)

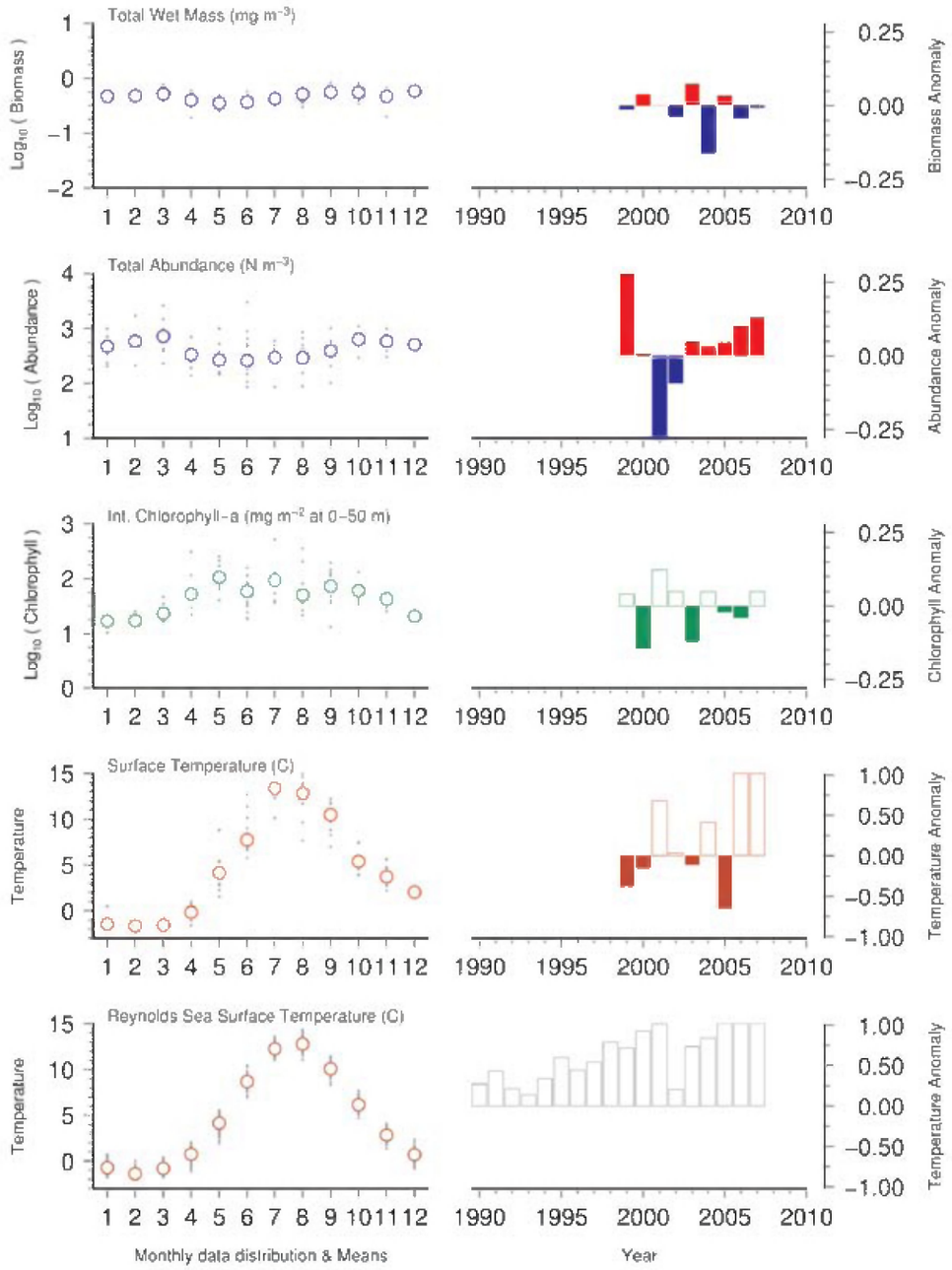

Figure 32.
Seasonal and interannual comparison of co-sampled variables at the Anticosti Gyre site. (See Section 2.2 for an explanation of the subplots in this figure.)

Gaspé Current (Gulf of St Lawrence)

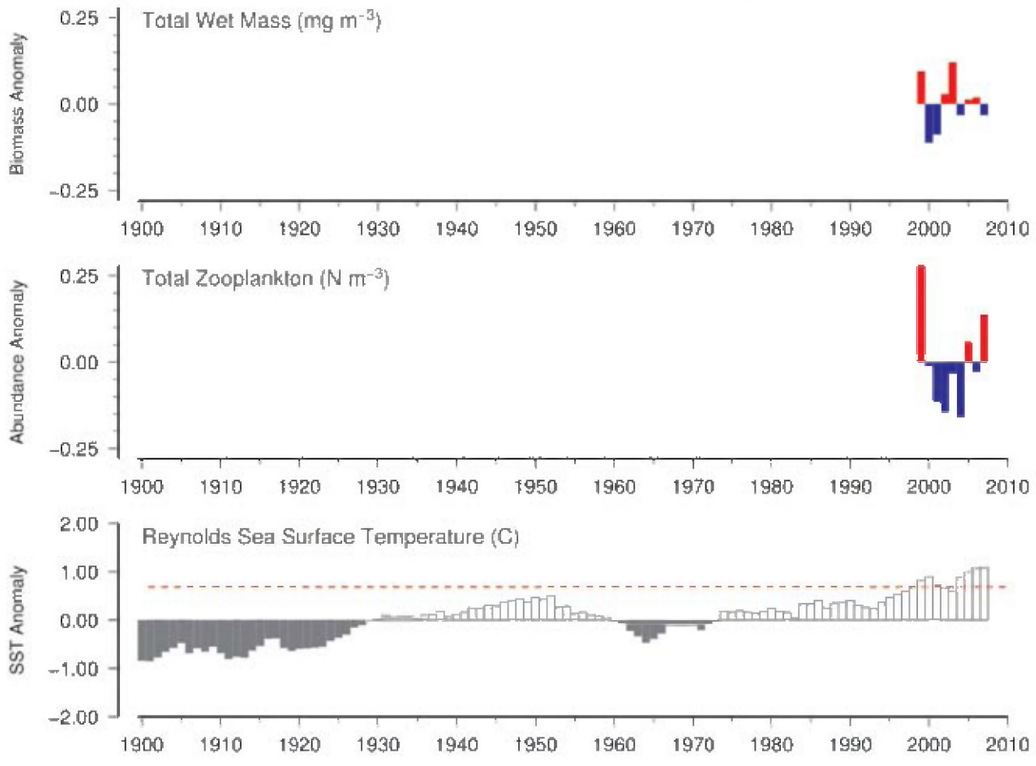

Figure 33.
Long-term comparison of Gaspé Current total zooplankton wet mass and total zooplankton abundance with Reynolds sea surface temperatures for the region. CPR data were not available for this region. (See Section 2.3 for an explanation of the subplots in this figure.)

Anticosti Gyre (Gulf of St Lawrence)

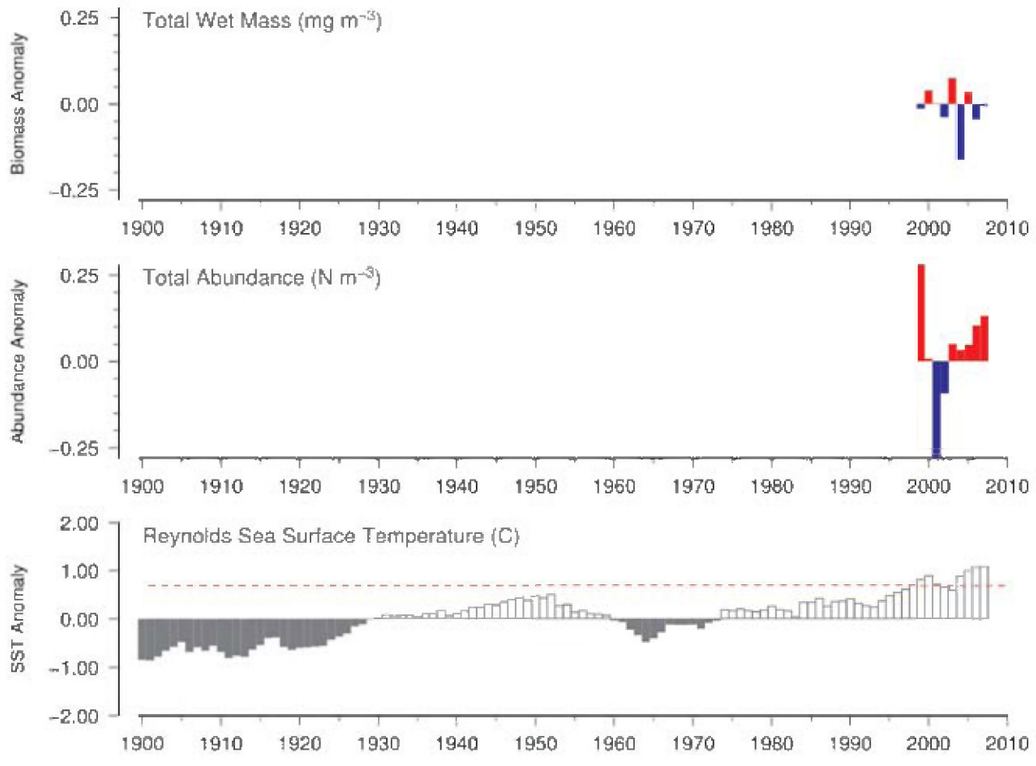

Figure 34.
Long-term comparison of Anticosti Gyre total zooplankton wet mass and total zooplankton abundance with Reynolds sea surface temperatures for the region. CPR data were not available for this region. (See Section 2.3 for an explanation of the subplots in this figure.)

Site 8: Station 27 (Newfoundland Shelf)

Pierre Pepin

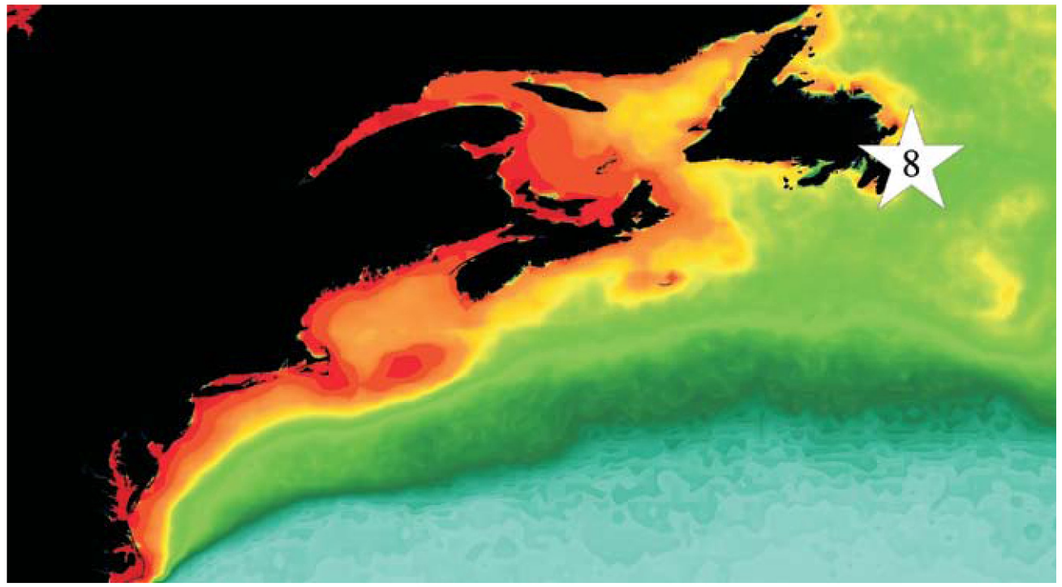

Figure 35.
Location of the Station 27 survey area (Site 8), plotted on a map of SeaWiFS chlorophyll concentration. Red/orange = high (productive), green/yellow = medium (moderate), blue = low (oligotrophic).

Zooplankton are sampled every 2–4 weeks (if possible) from research vessels using a ringnet (0.75 m diameter, 200 µm mesh). Sampling is carried out at a number of stations on a series of transects running perpendicular to the coast of Newfoundland across the Newfoundland and Labrador Shelves and the Grand Banks. The most frequently sampled station, Station 27, is located five nautical miles east of St John's harbour (Figure 35), on the northwestern edge of the Grand Banks and has a 170 m water depth. CTD profiles are recorded, and samples for phytoplankton, nutrients, and extracted chlorophyll are collected using Niskin bottles at fixed depths. Subsamples are combined to give an integrated sample.

Zooplankton samples are split, and one-half is used for wet–dry weight determination. The other half is subsampled to give at least 200 organisms, which are identified to genus or species and counted. Another subsample is taken containing at least 100 *Calanus* spp., which are identified to species and stage and counted. Biomasses of the dominant groups are calculated using dry weights of various groupings (*Calanus*, *Oithona*, *Pseudocalanus*, and *Metridia*) and abundance data.

A more detailed ecosystem status report on the state of chemical and biological oceanographic conditions in the Newfoundland and Labrador region (Canadian Atlantic waters) is prepared every year as a Science Advisory Report. It is available online at www.dfo-mpo.gc.ca/csas/csas/Publications/Pub_Index_e.htm.

There is limited seasonal variability in total copepod biomass, but overall, it tends to be higher in autumn than in winter or spring (Figure 36). Interannual variations in total copepod biomass tend to mirror that of large copepods (Figure 37), which dominate the community in weight but not in numbers. Large copepods are most abundant following a spring phytoplankton bloom, reflecting the production cycle of nauplii and copepodites of the dominant *Calanus* species, whereas the biomass of small copepods peaks in late autumn as a result of large numbers of *Oithona* spp. (Figure 37). Overall, there are greater interannual variations in the biomass of large copepods relative to smaller species.

The seasonal cycle in local temperatures differs markedly from the Reynolds SST, although the general pattern in interannual variability is similar (Figure 37). The differences reflect the wide area of the continental shelf represented in the Reynolds estimates relative to the more local measurements taken at Station 27, which is located in the inshore arm of the Labrador Current. Similarities in interannual variations are the result of large decorrelation scales for SST anomalies in the region (Ouellet *et al.*, 2003).

Interannual variations in the abundance of large copepods correspond well with the nearest CPR standard area ("E9"), but the long-term pattern in variation demonstrates no clear relationship with temperature anomalies in the region (Figure 38). Overall, the abundance of copepods at Station 27 increased in 2007, following 3–4 years with low abundance indices.

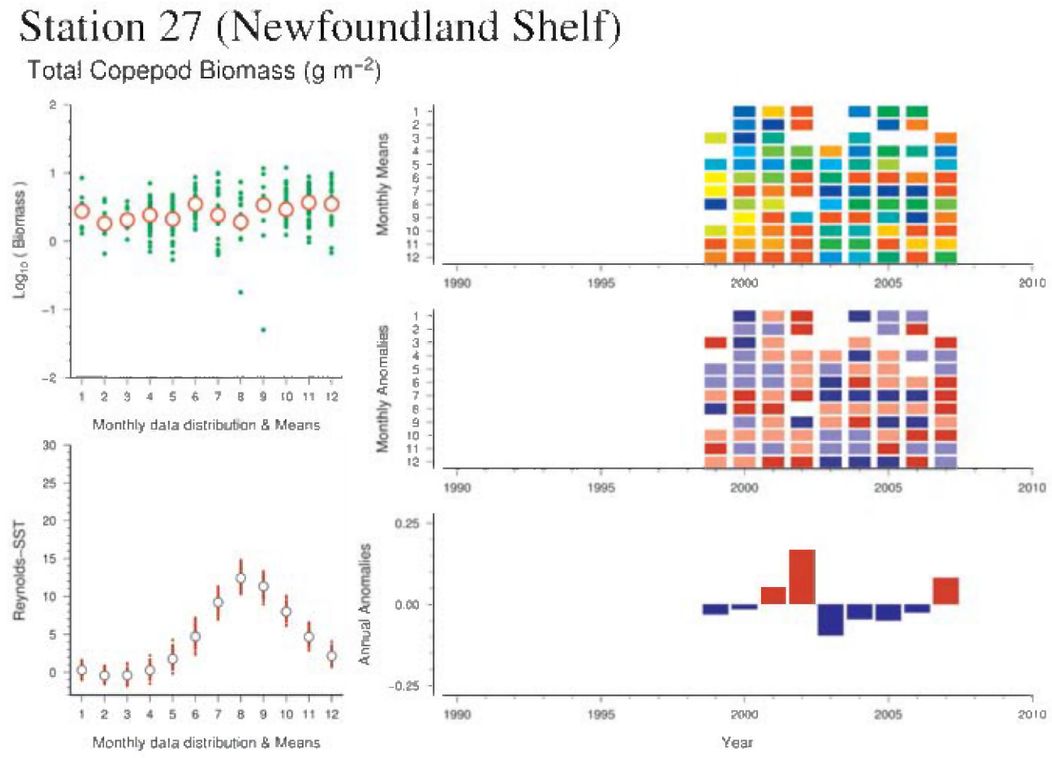

Figure 36.
Standardized WGZE time-series summary plot for copepod biomass at Station 27. (See Section 2.1 for an explanation of the subplots in this figure.)

Station 27 (Newfoundland Shelf)

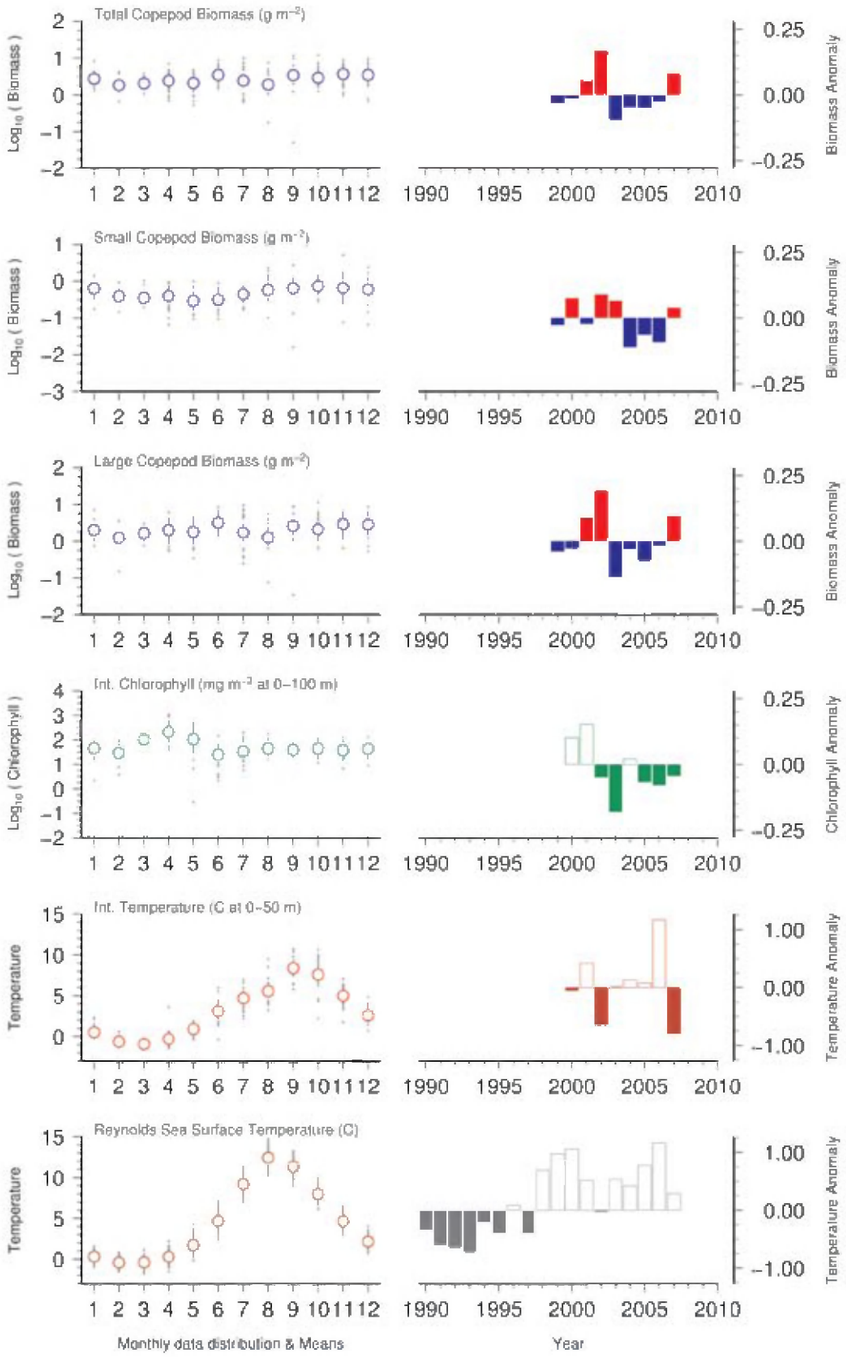

Figure 37.
Seasonal and interannual comparison of co-sampled variables at Station 27. (See Section 2.2 for an explanation of the subplots in this figure.)

Station 27 (Newfoundland Shelf)

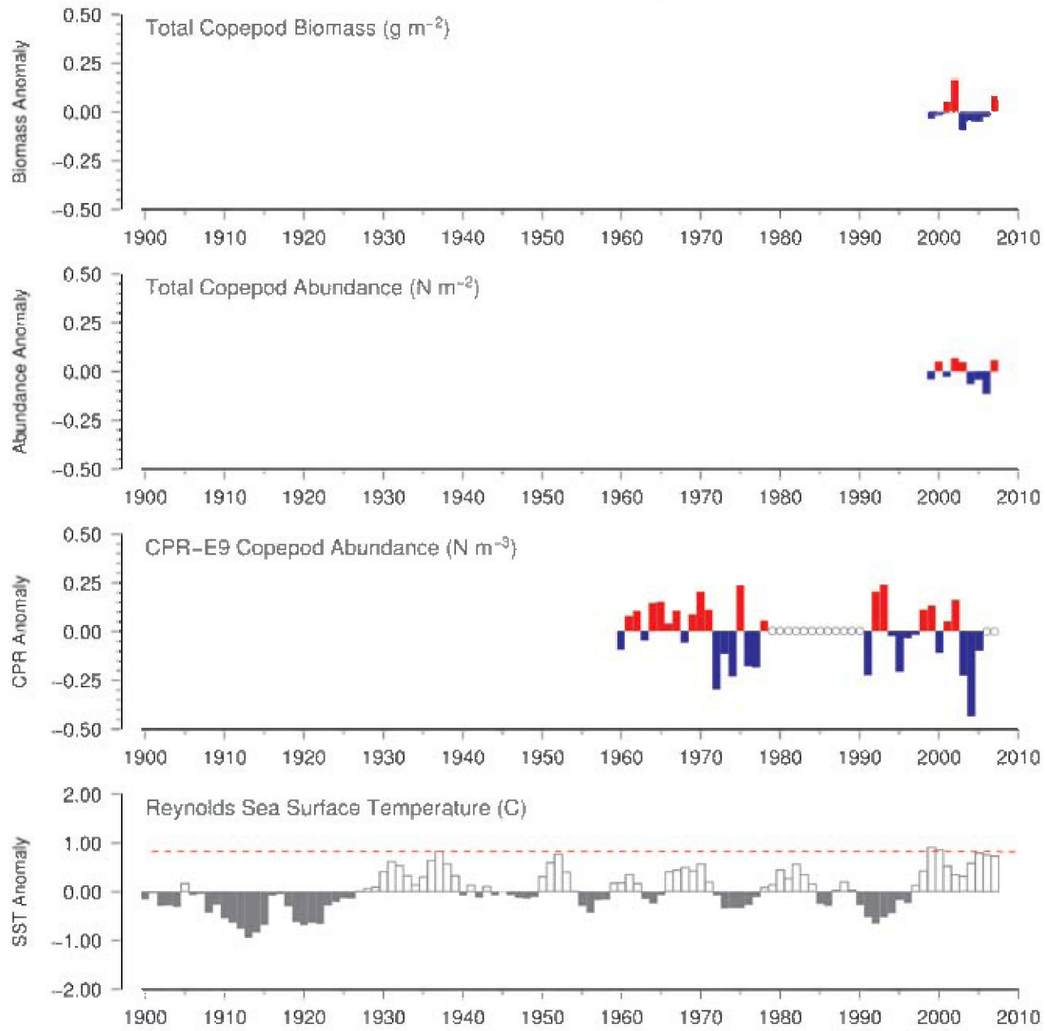

Figure 38.
Long-term comparison of Station 27 total copepod biomass and abundance with copepod abundance in CPR standard area "E9" and Reynolds sea surface temperatures for the region. (See Section 2.3 for an explanation of the subplots in this figure.)

3.2 Icelandic–Norwegian Basin

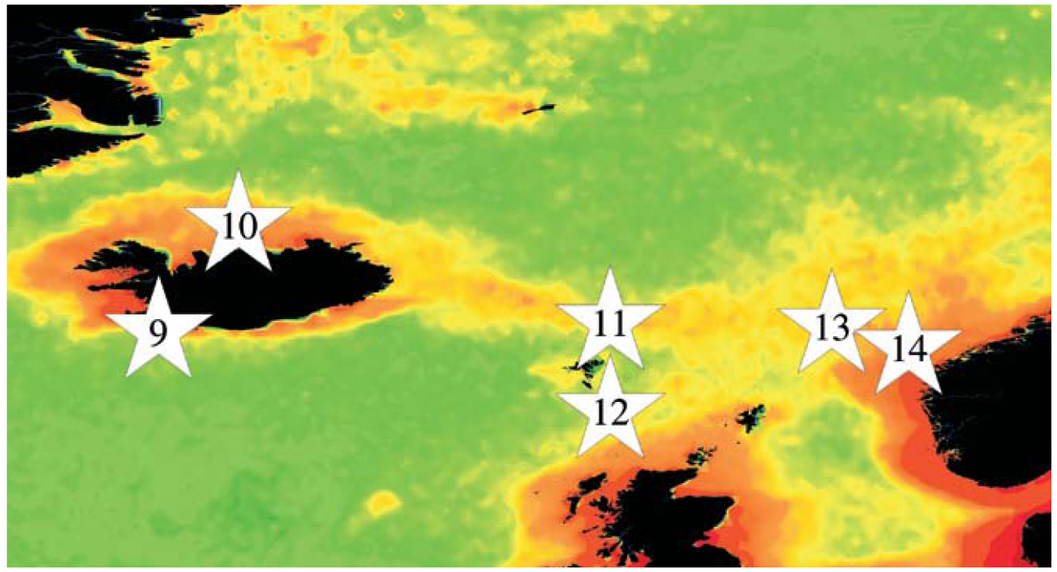

Figure 39.
Locations (Sites 9–14) of Icelandic–Norwegian Basin zooplankton time-series plotted on a map of SeaWiFS average chlorophyll concentrations. Red/orange = high (productive), green/yellow = medium (moderate), blue = low (oligotrophic).

The cold, Arctic waters of the Icelandic–Norwegian Basin (Figure 39) are regularly influenced by warm saline Atlantic seawater flowing from the south. One branch flows west along the south coast of Iceland and then clockwise to the north of Iceland. A second branch flows north between the Faroe Islands and northern Scotland, through the Faroe–Shetland Channel, and up the west coast of Norway. The deep ocean basins adjoining the coastal areas are subject to intense winter cooling and deep convection. The populations of zooplankton are dominated by Arctic/Boreal species, and there is a typical seasonal cycle of primary and secondary production, beginning with a spring bloom triggered by water column stratification, and, in some places, a secondary autumn peak in production accompanying the onset of the breakdown in summer stratification.

Site 9–10: Selvogsbanki and Siglunes (Iceland)

Astthor Gislason

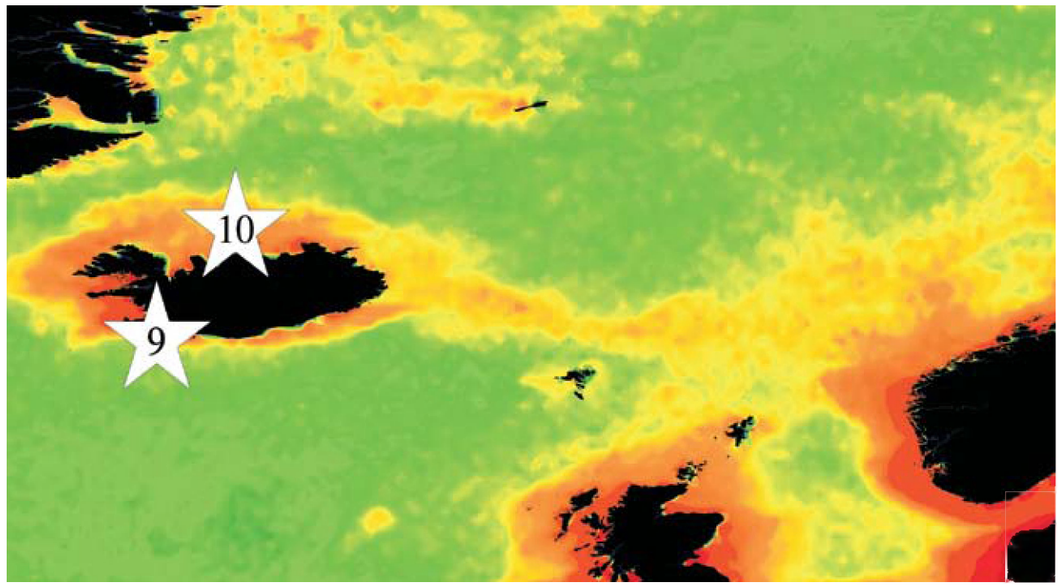

Figure 40.
Locations of the Selvogsbanki (Site 9) and Siglunes (Site 10) survey areas, plotted on a map of SeaWiFS chlorophyll concentration. Red/orange = high (productive), green/yellow = medium (moderate), blue = low (oligotrophic).

The Icelandic monitoring programme for zooplankton consists of a series of transects perpendicular to the coastline. Sampling at stations along the transects north and east of Iceland was started in the 1960s. Additional section lines south and west were added in the 1970s. Currently, there are approximately 90 stations. Zooplankton investigations are carried out at these stations every year in May and June. In this summary, long-term changes in zooplankton biomass are examined at the Selvogsbanki transect (south Iceland; Figure 40, Site 9) and the Siglunes transect (north Iceland; Figure 40, Site 10). Values from Siglunes are an average from eight stations, while values from Selvogsbanki are an average from five stations.

At Selvogsbanki, zooplankton biomass demonstrated a maximum during the mid-1990s, while a low was observed during the late 1980s (Figure 41). The period between zooplankton peaks at Selvogsbanki is between five and ten years. The values for dominant zooplankton taxa along the Selvogsbanki transect show that *Calanus finmarchicus* is generally the most abundant species (~32% of the total zooplankton), followed by *Oithona* spp. (*O. similis* and *O. spinirostris*, ~20%) and *Temora longicornis* (~9%; Table 5). In 2006, the abundance of *C. finmarchicus* was unusually high (~43%), with *Evadne nordmanni* and *Oithona* spp. ranking second and third (~23% and ~10%, respectively; Table 6).
In the waters off northern Iceland, the high values of zooplankton at the beginning of the Siglunes time-series dropped drastically with the onset of the Great Salinity Anomaly (GSA) of the 1960s. Since then, zooplankton biomass has varied with highs at approximately 7- to 10-year intervals (Figure 42). North of Iceland (Siglunes transect), *C. finmarchicus* is, on average, the most important species (~30%) of the total zooplankton, followed by copepod nauplii (mainly *C. finmarchicus* ~21%) and *Oithona* spp. (*O. similis* and *O. spinirostris* ~15%; Tables 7 and 8). These three taxonomic groups were also the most abundant in 2006.

Long-term data from the CPR programme were only available for the region off Selvogsbanki (CPR standard area "A6", Figures 2 and 40). As seen in the Siglunes time-series, a dramatic drop in biomass occurred in the mid-1960s (Figure 43), also attributed to the GSA. These decreases also correspond to a clearly visible shift in average SST values in both regions. Currently, SST values at both Siglunes and Selvogsbanki are higher than the 100-year averages for each region, presenting the upper end of a ~50-year cycle in temperatures (Figures 43 and 44). However, water temperatures at both sites are still below the 100-year maximum (Figures 43 and 44, bottom, red dashed line).

Zooplankton biomass north of Iceland is influenced by the inflow to the area of warm Atlantic water. Thus, in warm years, when the flow of higher salinity Atlantic water on to the northern shelf is high (Figure 44), the zooplankton biomass can be almost twice as high as in cold years, when this inflow is not as evident (Astthorsson and Gislason, 1998; Astthorsson and Vilhjalmsson, 2002). The reasons for this may include better feeding conditions for zooplankton, resulting from increased primary production in warm years; advection of zooplankton with Atlantic water from the south; and more rapid, temperature-dependent growth of zooplankton in warm years. During both 2000 and 2001, when the biomass of zooplankton north of Iceland was particularly high, the inflow of warm Atlantic water on to the northern shelf was also high. South of Iceland, the links between climate and zooplankton biomass are not as evident as the links north of Iceland. Most probably, the variability off the south and west coasts is related to the timing and magnitude of the primary productivity on the banks, which, in turn, are influenced by fresh water from rivers and by wind force and direction.

Table 5.

Rank	Taxa	% of total abundance 1990–2005	% of total zooplankton 2006	(Δ)	Mean abundance (N m^{-3}) 1999–2005	Abundance (N m^{-3}) 2006	(Δ%)
1	*Calanus finmarchicus*	31.7	42.8	(11.1)	1 041	1 805	(73)
2	*Oithona* spp.	20.4	10.2	(-10.2)	669	430	(-36)
3	*Temora longicornis*	8.6	7.6	(-1.1)	283	319	(13)
4	*Evadne nordmanni*	8.6	22.6	(14.0)	281	954	(240)
5	Euphausiacea (eggs + juv.)	7.4	4.9	(-2.5)	242	205	(-15)
6	Copepoda nauplii	7.3	1.1	(–6.2)	241	48	(–80)
7	Cirripedia indet.	3.2	5.7	(2.5)	106	240	(126)
8	Larvacea indet.	2.5	0.0	(–2.5)	82	1	(–99)
9	*Podon leuckarti*	1.9	2.9	(1.0)	61	122	(100)
10	Echinodermata	1.7	0.0	(–1.7)	55	0	(-100)
	"Top ten" totals	**93.2**	**97.7**	**(4.5)**	**3 061**	**4 124**	**(35)**
	Total abundance of all zooplankton (N m^{-3})				**3 284**	**4 221**	**(29)**

Table 5.
Average abundance and relative dominance (percentage of the total zooplankton collected) of the top ten most abundant zooplankton taxa collected along the Selvogsbanki transect in previous years (1990–2005) compared with that collected in 2006. Colours in the "Δ" and "Δ%" columns indicate either an increase (red) or decrease (blue) in relative dominance from previous years.

Table 6.

Rank	Taxa	% of total abundance 2007	Abundance (N m^{-3}) 2007
1	*Calanus finmarchicus*	42.8	1 805
2	*Evadne nordmanni*	22.6	954
3	*Oithona* spp.	10.2	430
4	*Temora longicornis*	7.6	319
5	Cirripedia indet.	5.7	240
6	Euphausiacea (eggs + juv.)	4.9	205
7	*Podon leuckarti*	2.9	122
8	*Copepoda nauplii*	1.1	48
9	**Foraminifera indet.**	**0.7**	**30**
10	***Pseudocalanus* spp.**	**0.4**	**18**
	"Top ten" totals	**98.8**	**4 171**
	Total abundance of all zooplankton (N m^{-3})		**4 221**

Table 6.
Abundance and relative dominance (percentage of the total zooplankton collected) of the top ten most abundant zooplankton taxa collected along the Selvogsbanki transect in 2006. Bold entries indicate new taxa dominant in 2006, but not previously dominant in the 1990–2005 time-series (see Table 5).

Table 7.

Rank	Taxa	% of total abundance 1990–2005	% of total zooplankton 2006	(Δ)	Mean abundance (N m^{-3}) 1999–2005	Abundance (N m^{-3}) 2006	(Δ%)
1	*Calanus finmarchicus*	30.0	30.6	(0.6)	738	580	(-21)
2	Copepoda nauplii	21.1	24.9	(3.8)	520	472	(-9)
3	*Oithona* spp.	14.8	23.0	(8.2)	364	436	(20)
4	Echinodermata	13.5	1.2	(-12.3)	332	22	(-93)
5	Euphausiacea (eggs + juv.)	10.4	4.5	(-5.9)	256	86	(-66)
6	*Pseudocalanus* spp.	2.7	4.8	(2.1)	67	91	(36)
7	Larvacea indet	2.2	2.8	(0.6)	54	52	(-4)
8	*Calanus hyperboreus*	1.3	2.5	(1.2)	33	48	(45)
9	*Oncaea* spp.	1.0	0.8	(-0.1)	24	16	(-33)
10	*Acartia* spp.	0.5	0.1	(-0.4)	11	1	(-91)
	"Top ten" totals	**97.5**	**95.2**	**(-2.3)**	**2 399**	**1 804**	**(-25)**
	Total abundance of all zooplankton (N m^{-3})				**2 460**	**1 894**	**(-23)**

Table 7.
Average abundance and relative dominance (percentage of the total zooplankton collected) of the top ten most abundant zooplankton taxa collected along the Siglunes transect in previous years (1990–2005) compared with that collected in 2006. Colours in the "Δ" and "Δ%" columns indicate either an increase (red) or decrease (blue) in relative dominance from previous years.

Table 8.

Rank	Taxa	% of total abundance 2006	Abundance (N m^{-3}) 2006
1	*Calanus finmarchicus*	30.6	580
2	*Copepod nauplii*	24.9	472
3	*Oithona* spp.	23.0	436
4	*Pseudocalanus* spp.	4.8	91
5	Euphausiacea (eggs + juv.)	4.5	86
6	Larvacea indet	2.8	52
7	*Calanus hyperboreus*	2.5	48
8	Echinodermata	1.2	22
9	***Para/Pseudocalanus***	**1.0**	**19**
10	**Foraminifera indet.**	**0.9**	**17**
	"Top ten" totals	**96.2**	**1 823**
	Total abundance of all zooplankton (N m^{-3})		**1 894**

Table 8.
Abundance and relative dominance (percentage of the total zooplankton collected) of the top ten most abundant zooplankton taxa collected along the Siglunes transect in 2006. Bold entries indicate new taxa dominant in 2006, but not previously dominant in the 1990–2005 time-series (see Table 7).

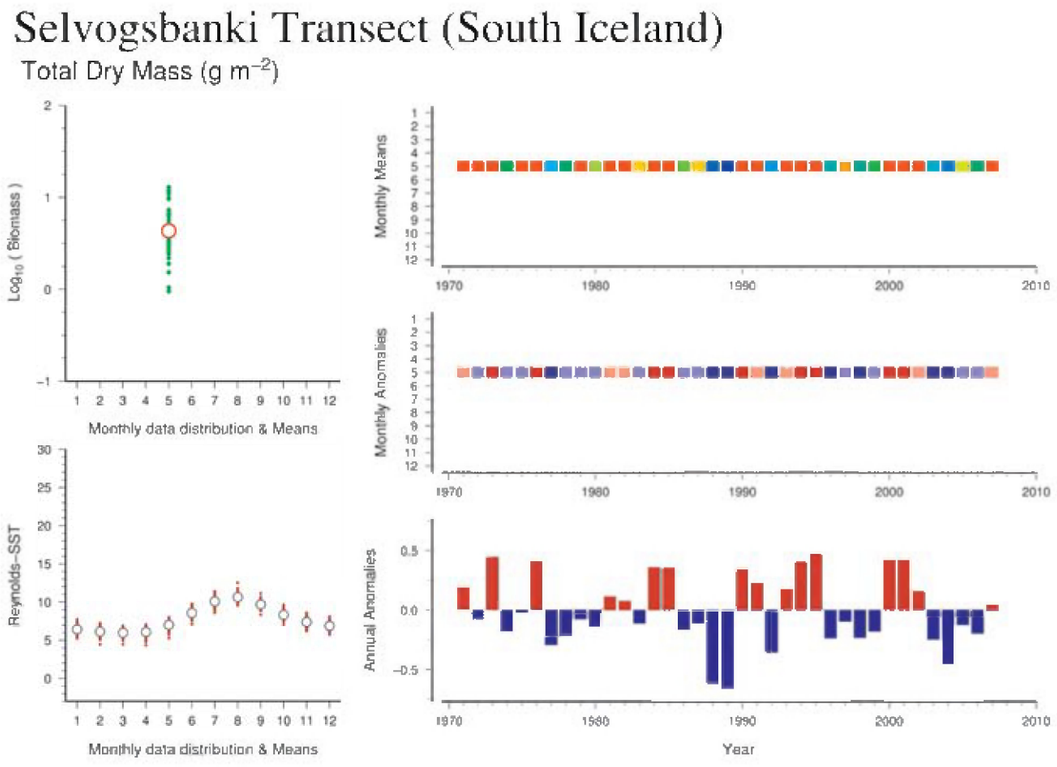

Figure 41.
Standardized WGZE time-series summary plot for total zooplankton dry mass at Selvogsbanki. (See Section 2.1 for an explanation of the subplots in this figure.)

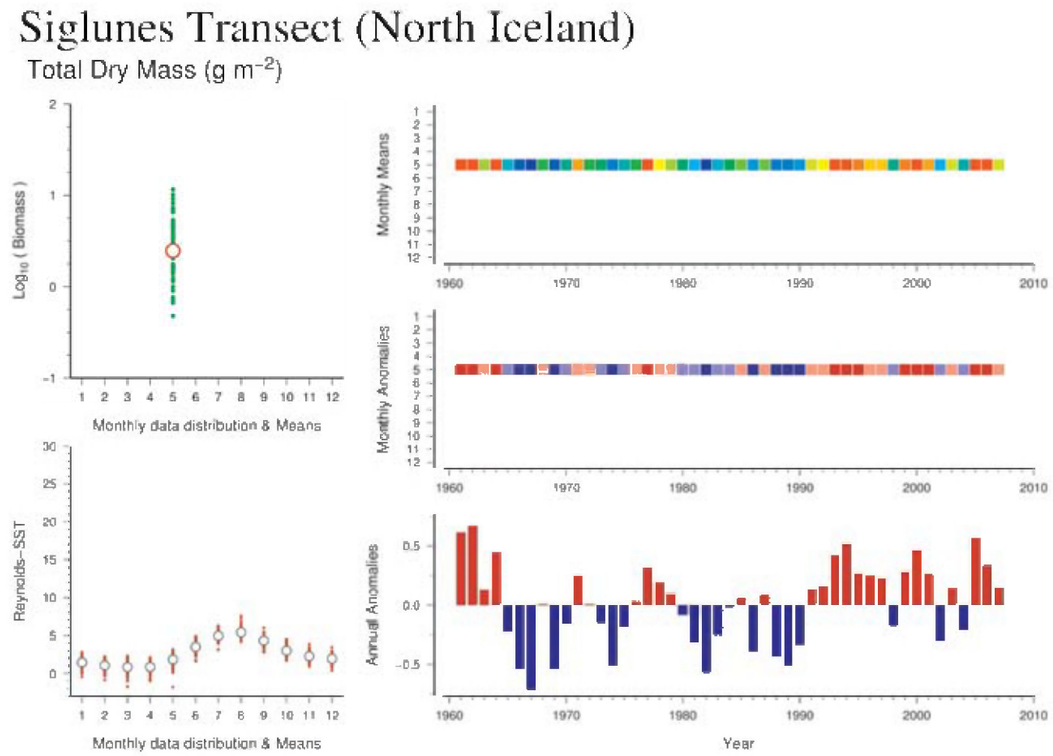

Figure 42.
Standardized WGZE time-series summary plot for total zooplankton dry mass at Siglunes. (See Section 2.1 for an explanation of the subplots in this figure.)

Selvogsbanki Transect (South Iceland)

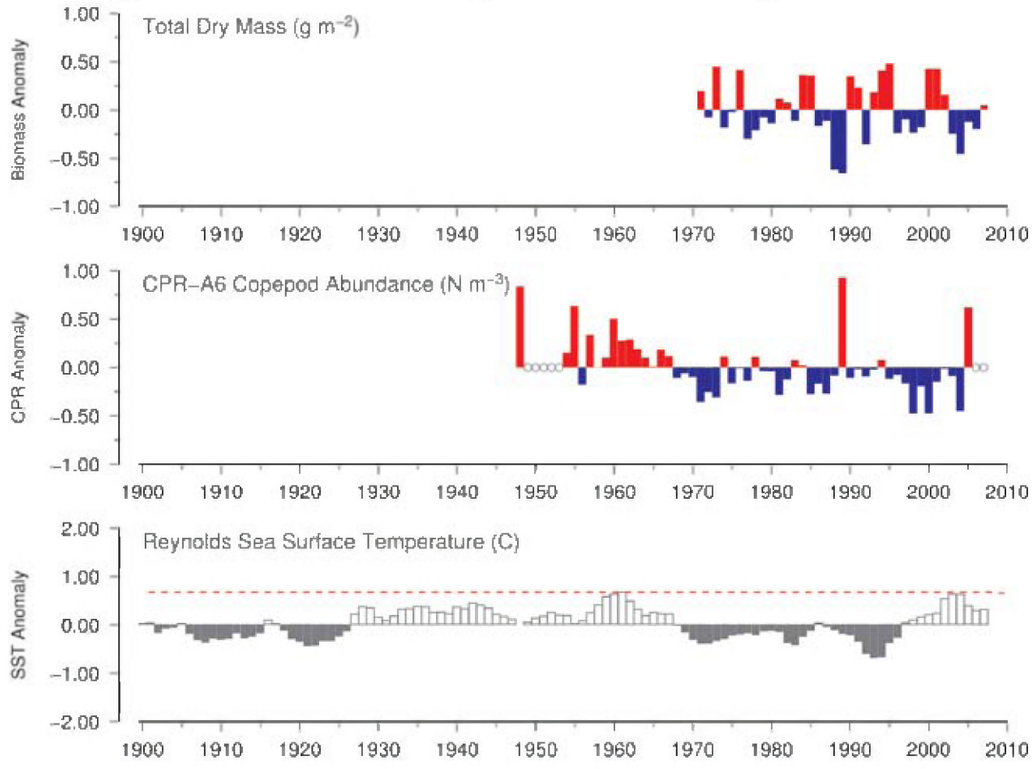

Figure 43.
Long-term comparison of Selvogsbanki total zooplankton dry mass with copepod abundance in CPR standard area "A6" and Reynolds sea surface temperatures for the region. (See Section 2.3 for an explanation of the subplots in this figure.)

Siglunes Transect (North Iceland)

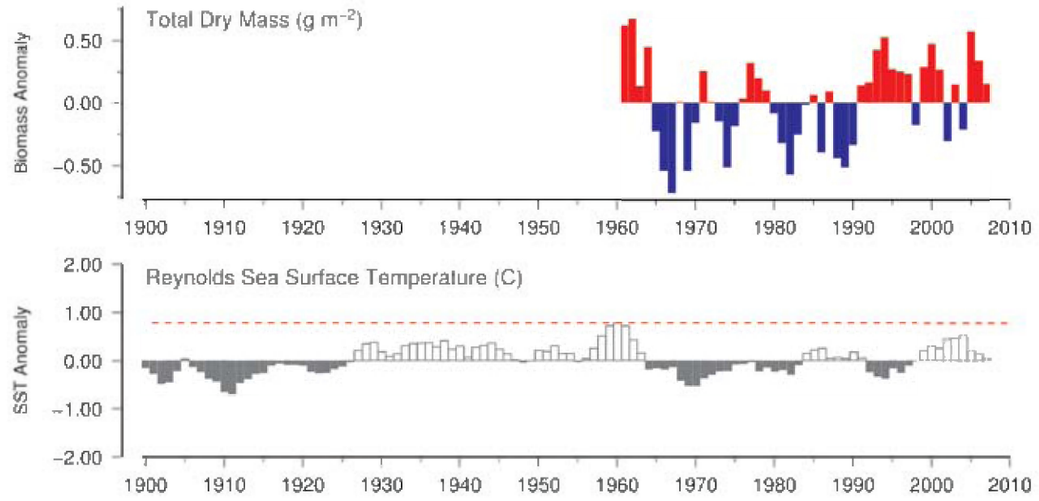

Figure 44.
Long-term comparison of Siglunes total zooplankton dry mass with Reynolds sea surface temperatures for the region. CPR data were not available for this region. (See Section 2.3 for an explanation of the subplots in this figure.)

Sites 11–12: Faroe Islands (Northern Transect/North Faroe Islands and Faroe Shelf/South Faroe Islands)

Eilif Gaard

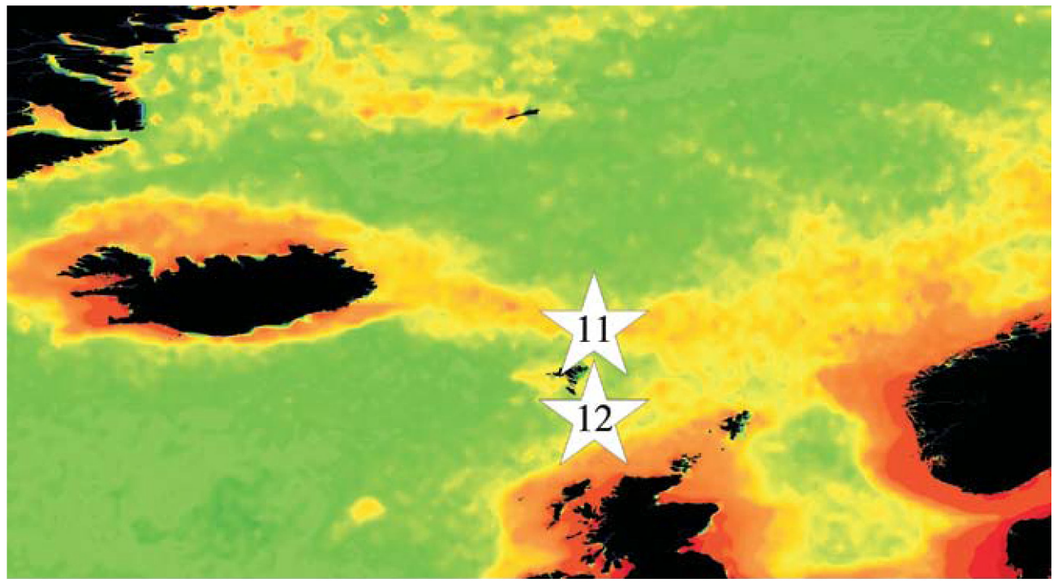

Figure 45.
Locations of the Faroe Islands survey areas (North Faroe Islands, Site 11; Faroe Shelf/South Faroe Islands, Site 12), plotted on a map of SeaWiFS chlorophyll concentration. Red/orange = high (productive), green/yellow = medium (moderate), blue = low (oligotrophic).

The Faroese Fisheries Laboratory operates four standard transects radiating north, west, east, and south from the Faroe Islands. This report summarizes results from the northern transect (North Faroe Islands; Figure 45, Site 11), which runs northwards into the southern Norwegian Sea, and the southern transect (Faroe Shelf/South Faroe Islands; Figure 45, Site 12), which covers the southern waters of the Faroe Shelf. Along each transect, zooplankton were collected once a year in May, with vertical hauls from 50 m depth to the surface using a WP2-net (56 cm diameter, 200 µm mesh).

The northern transect is dominated by cold East Icelandic water (EIW) flowing from the northwest, with an average May water temperature of 4.4°C (Figure 46, bottom). The southern transect is dominated by warmer Atlantic water (AW) in the Faroe Current, which flows from the southwest and has an average May water temperature of 7.8°C (Figure 47, bottom). The May sampling period corresponds to the spring phytoplankton bloom in both areas. In general, chlorophyll *a* concentrations are slightly higher in the northern transect (Figure 46, centre), but are generally more variable from year to year along the southern transect (Figure 47, centre). The northern transect also has a higher zooplankton biomass (Figure 48), caused by higher abundance of overwintered *Calanus finmarchicus* (CV and adults) and *Calanus hyperboreus* in the northern transect waters. In contrast, the southern transect has a high abundance of smaller life stages, but fewer large individuals, creating a higher copepod abundance, but a lower total biomass than in the northern transect (Figures 46 and 47).

Since 2003, the May abundance of young *C. finmarchicus* copepodite stages in the northern transect has increased significantly, whereas *C. hyperboreus* has not been seen in northern transect samples since 2003. As *C. hyperboreus* was a significant proportion of the biomass, the differences between the northern and southern transect biomass values have decreased significantly since 2003 (Figure 48).

Changes in the timing of *C. finmarchicus* development and the distribution of *C. hyperboreus* in the northern transect may be due, in part, to water temperature changes and/or weakening of the East Icelandic Current. Long-term SST values in both the northern and southern transect areas are currently above a 100-year average for each region (Figures 49 and 50). Water temperatures since 2002 have also been near or above the previous 100-year maximum temperatures seen in each region (Figures 49 and 50, bottom, red dashed line).

Sixty years of CPR data are available for the region surrounding the Faroe Islands (CPR standard area "B4", Figure 2). Copepod abundance data from CPR and the Faroe Island transects do not demonstrate much synchrony where the sampling years overlap (Figures 49 and 50). This is most probably caused by the large differences in the spatial sampling areas of the two programmes. The CPR data suggest that the larger area around the Faroe Islands may be in a recovery period (an upward trend in copepod abundance) after a 40-year period (1950–1990) of steady decrease (Figures 49 and 50). A comparison of the CPR data with the SST record also suggests that there is a positive relationship between copepod abundance and SST at the interdecadal scale.

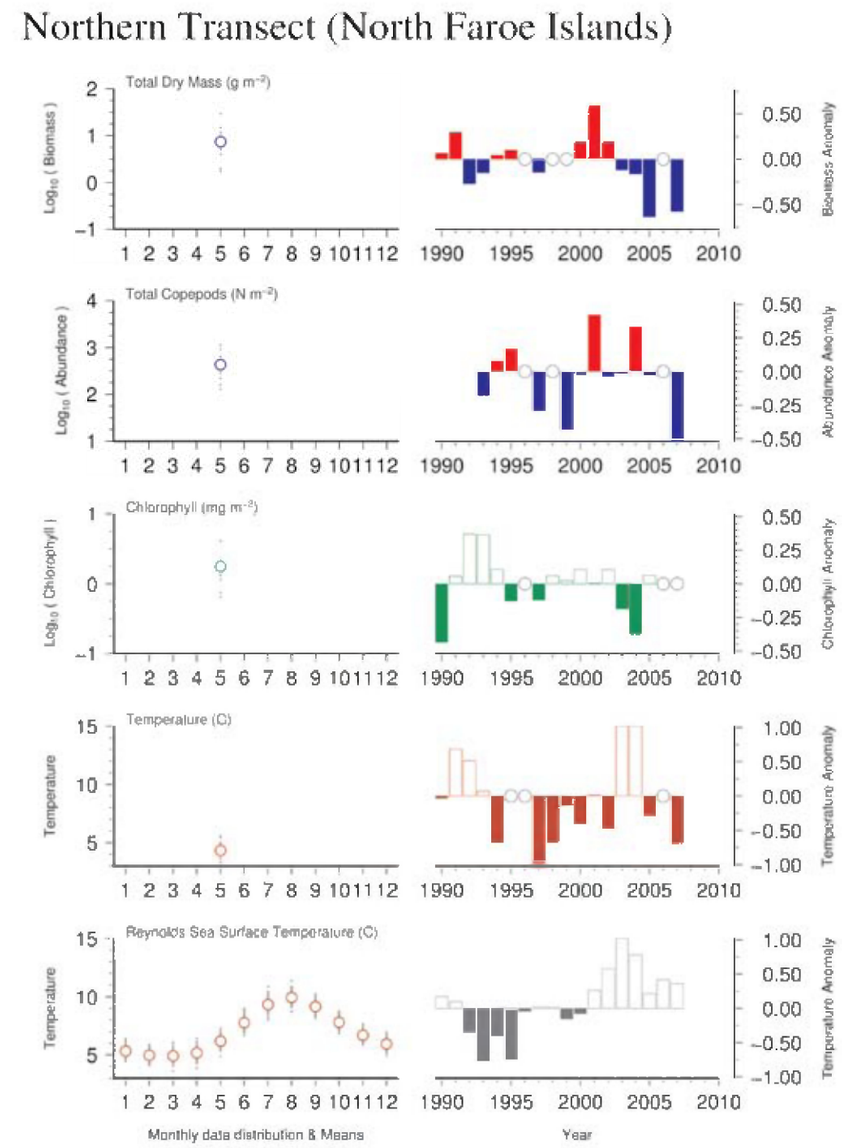

Figure 46.
Seasonal and interannual comparison of co-sampled variables along the northern (North Faroe Islands) transect. (See Section 2.2 for an explanation of the subplots in this figure.)

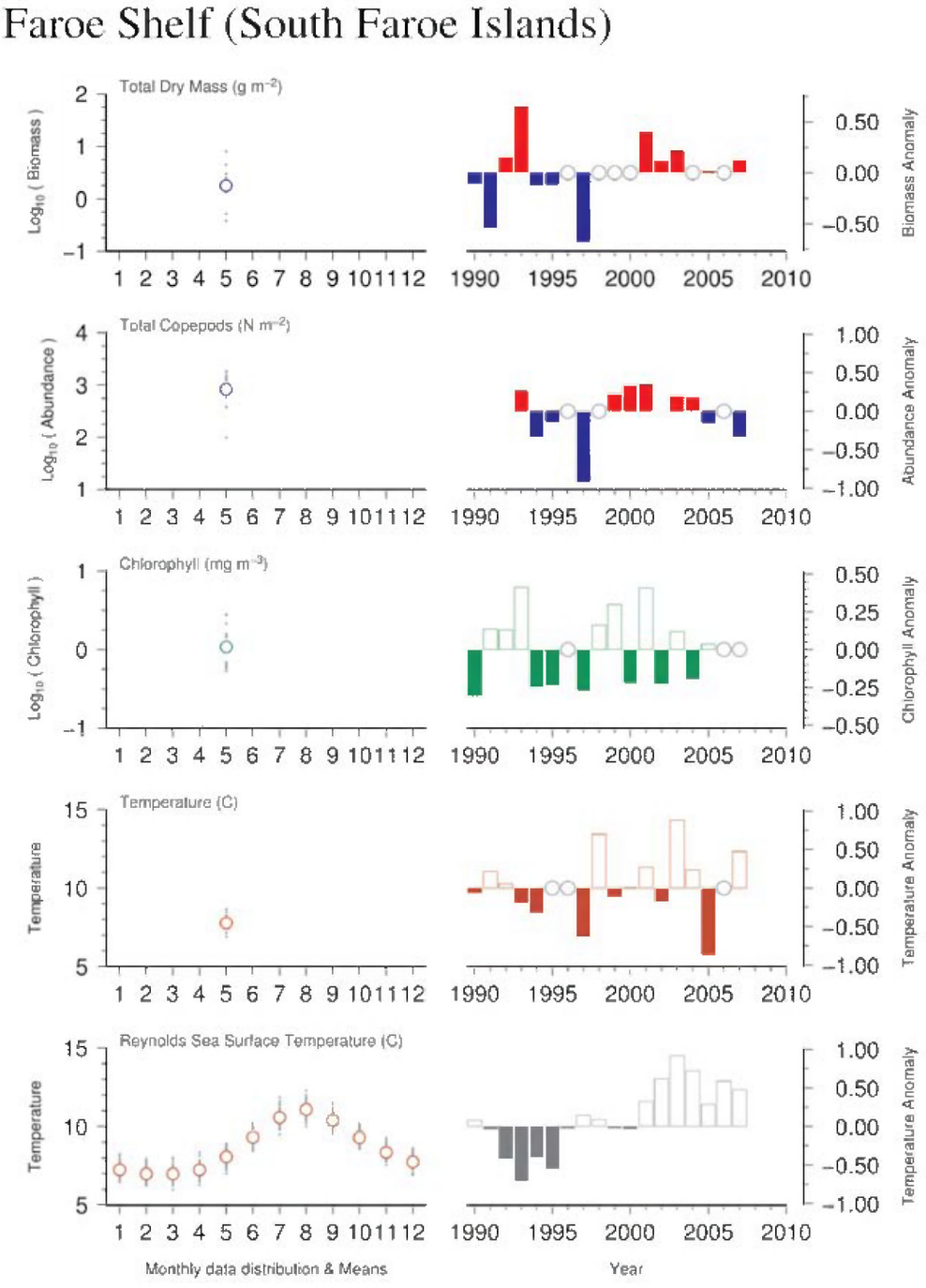

Figure 47.
Seasonal and interannual comparison of co-sampled variables along the southern (Faroe Shelf) transect. (See Section 2.2 for an explanation of the subplots in this figure.)

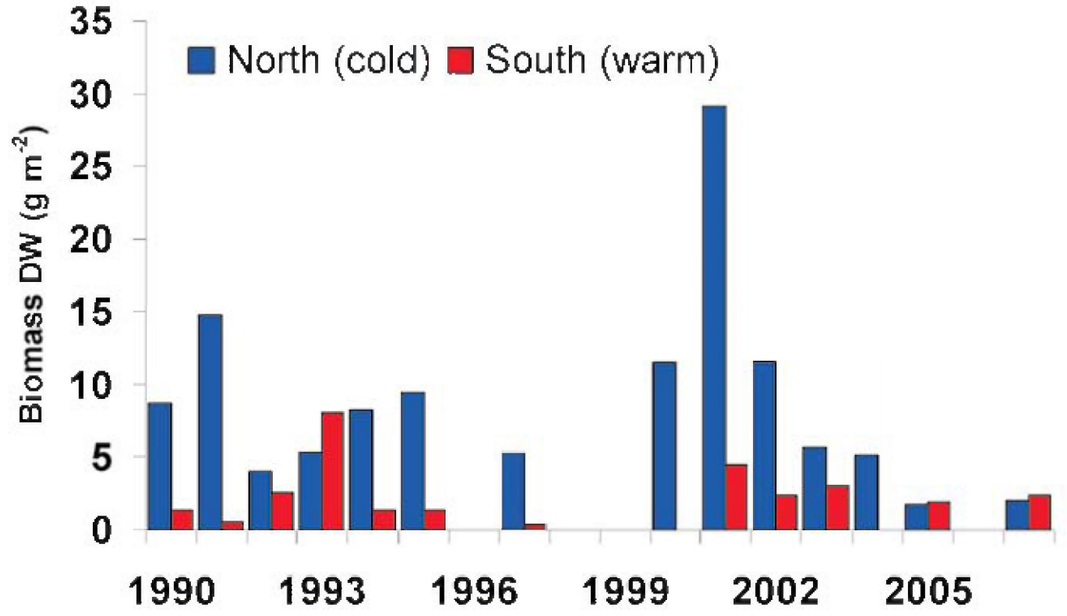

Figure 48.
Zooplankton biomass from the northern (cold East Icelandic Water) and southern (warmer Atlantic Water) transects. Zooplankton data were not available for 1996, 1998, 1999, and 2006.

Northern Transect (North Faroe Islands)

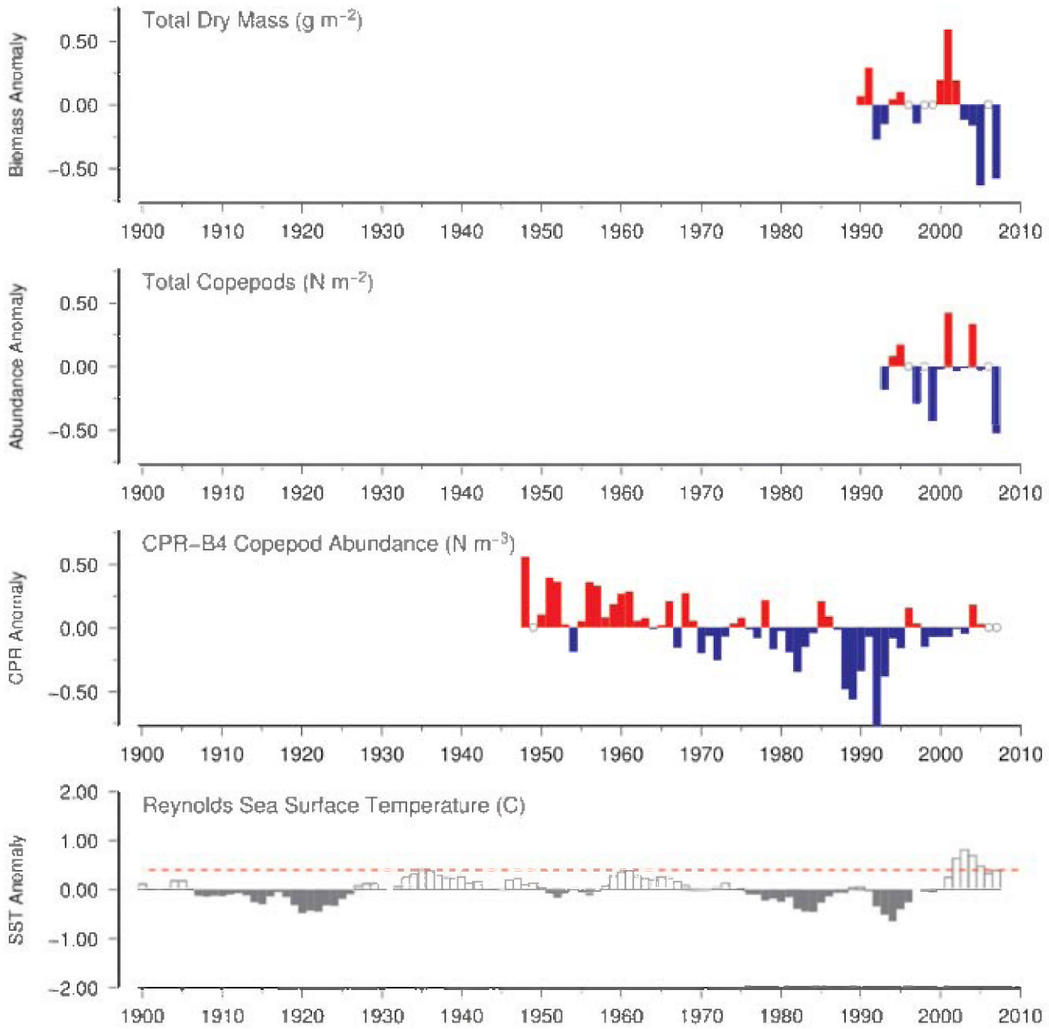

Figure 49.
Long-term comparison of northern (North Faroe Islands) transect total zooplankton dry mass and copepod abundance with copepod abundance in CPR standard area "B4" and Reynolds sea surface temperatures for the region. (See Section 2.3 for an explanation of the subplots in this figure.)

Faroe Shelf (South Faroe Islands)

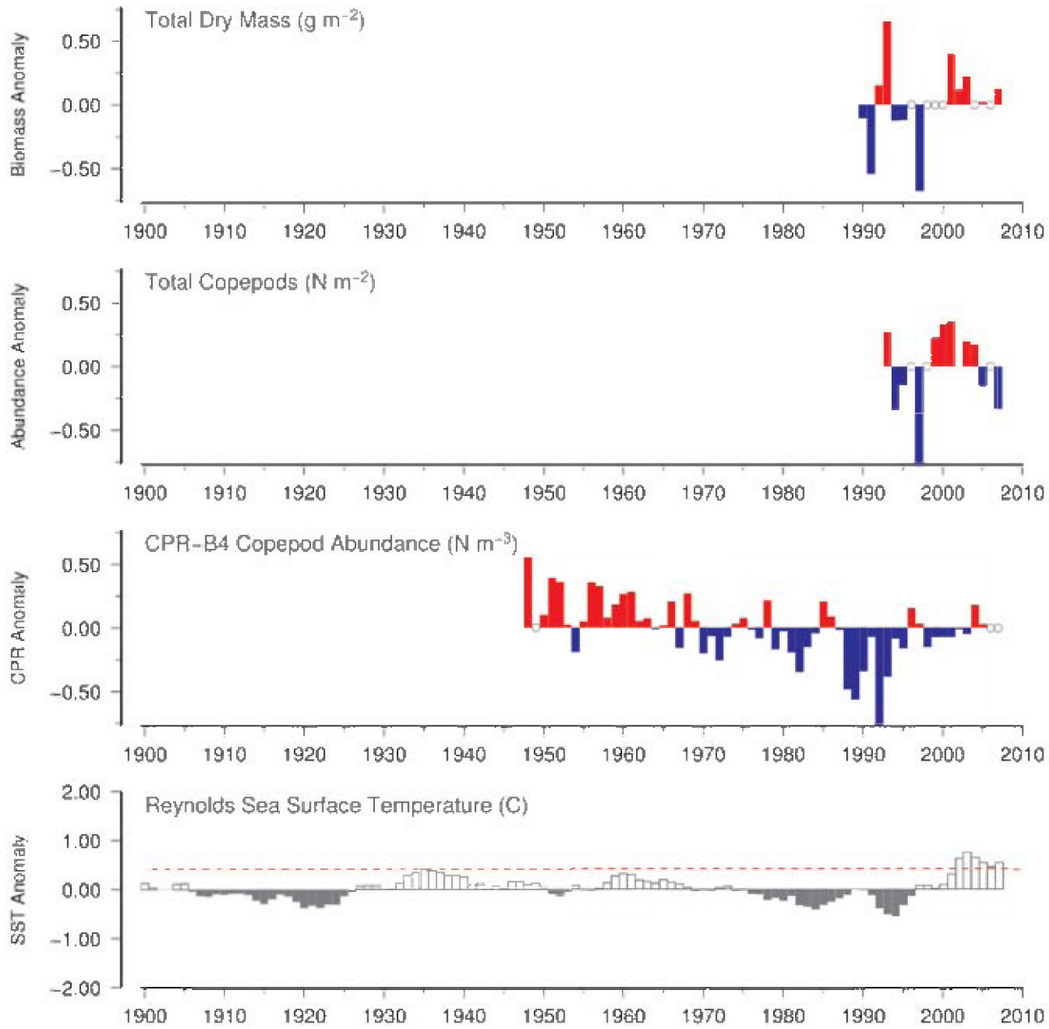

Figure 50.
Long-term comparison of southern (Faroe Shelf) transect total zooplankton dry mass and copepod abundance with copepod abundance in CPR standard area "B4" and Reynolds sea surface temperatures for the region. (See Section 2.3 for an explanation of the subplots in this figure.)

Sites 13–14: Svinøy transect (Norwegian Sea)

Webjørn Melle and Cecilie Broms

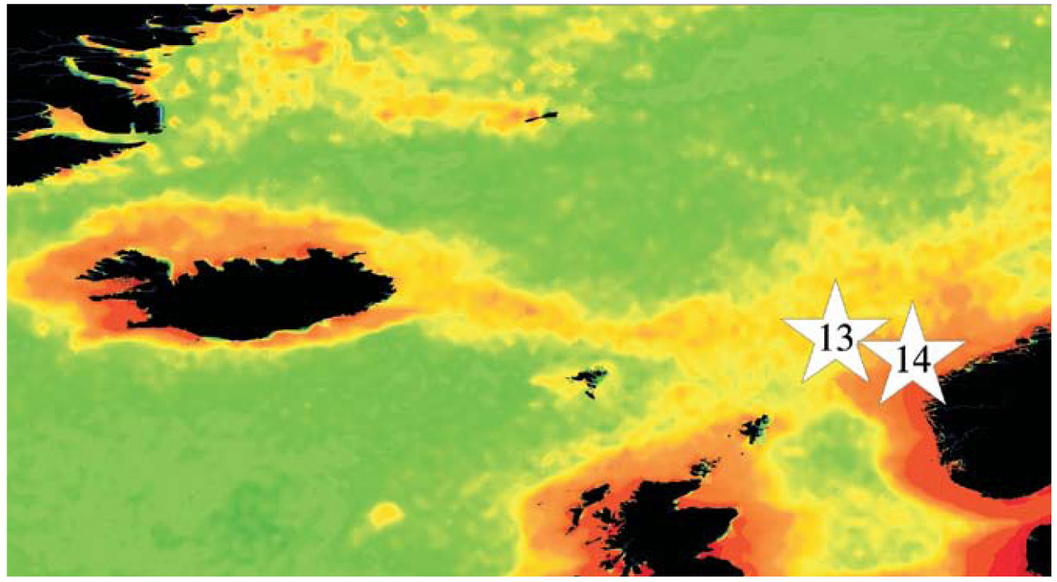

Figure 51.
Locations of the Svinøy Transect (West, Site 13; East, Site 14) survey areas, plotted on a map of SeaWiFS chlorophyll concentration. Red/orange = high (productive), green/yellow = medium (moderate), blue = low (oligotrophic).

The Institute of Marine Research (IMR) Monitoring Programme samples two fixed transects in the Norwegian Sea: the Svinøy transect (15 stations) and the Gimsøy transect (ten stations). Additionally, the Norwegian Sea is surveyed in May and July/August, both surveys covering approximately 50–100 stations. Data are stored at the TINDOR database at IMR, with annual reports made to the Ministry of Fisheries and in the IMR Annual Report on Marine Ecosystems. The Svinøy transect is split into two sections: West (Figure 51, Site 13) and East (Figure 51, Site 14). Each section is sampled four to ten times each year with a WP-2 net (56 cm diameter, 180 µm mesh) from 200 m depth to the surface.

Along the Svinøy transect, zooplankton biomass starts to increase in March/April in the western section (Figure 52) and slightly earlier, in February, in the eastern section (Figure 53). The development (timing) of zooplankton biomass in spring at the Svinøy transect does not otherwise indicate any shifts in seasonality over the sampling period 1997–2007. Although the seasonal cycle of biomass at both sites is almost identical, annual anomalies between sites reveal a lagged synchrony. Both sites are currently in a period of lower-than-average biomass, a trend coherent with other zooplankton biomass data from the Norwegian Sea.

Water temperatures along the Svinøy transect range from 5°C to 15°C, with the seasonal high in August and the seasonal low in February/March (Figures 54 and 55, bottom). A chlorophyll bloom occurs in late April and early May (Figures 54 and 55, middle), with a slightly stronger bloom in May along the eastern side of the transect. A protracted post-bloom period persists throughout summer and early autumn along the transect, which is typical for the southern Norwegian Sea. For the duration of the time-series, chlorophyll concentrations at both sides of the transect demonstrate a downward trend, whereas water temperatures have been increasing during the same period. Zooplankton biomass appears to be positively correlated with chlorophyll and negatively correlated with temperature during this period.

The nearest CPR standard area is "B1". Interannual trends within CPR copepod abundance correspond fairly well with zooplankton biomass in both the western (Figure 56) and eastern (Figure 57) sections of the Svinøy transect. Long-term SST values along the transect demonstrate that water temperatures since 2000 have been higher than any seen in the previous 100 years.

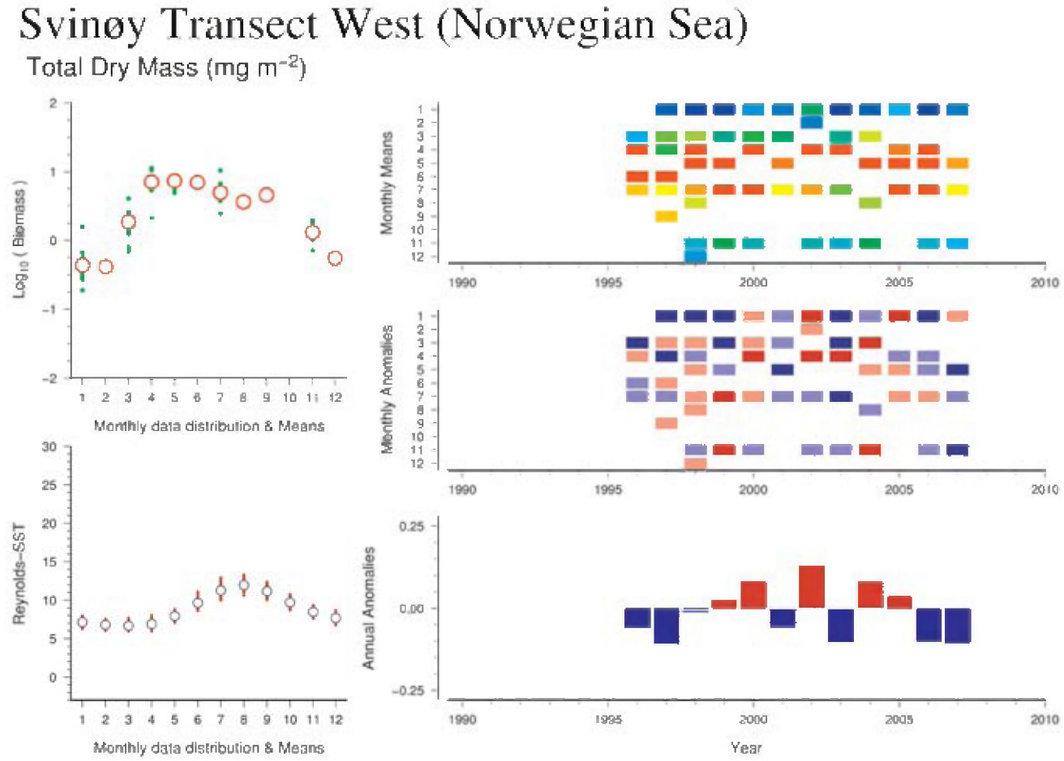

Figure 52.
Standardized WGZE time-series summary plot for total zooplankton dry mass at Svinøy Transect (West). (See Section 2.1 for an explanation of the subplots in this figure.)

Svinøy Transect East (Norwegian Sea)

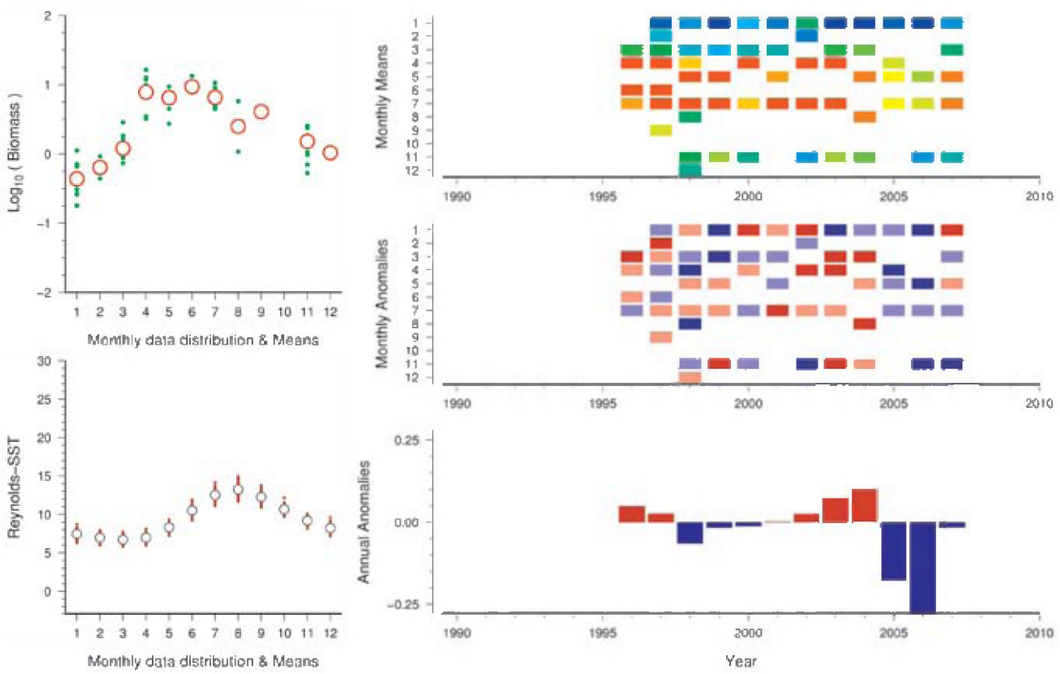

Figure 53.
Standardized WGZE time-series summary plot for total zooplankton dry mass at Svinøy Transect (East). (See Section 2.1 for an explanation of the subplots in this figure.)

Svinøy Transect West (Norwegian Sea)

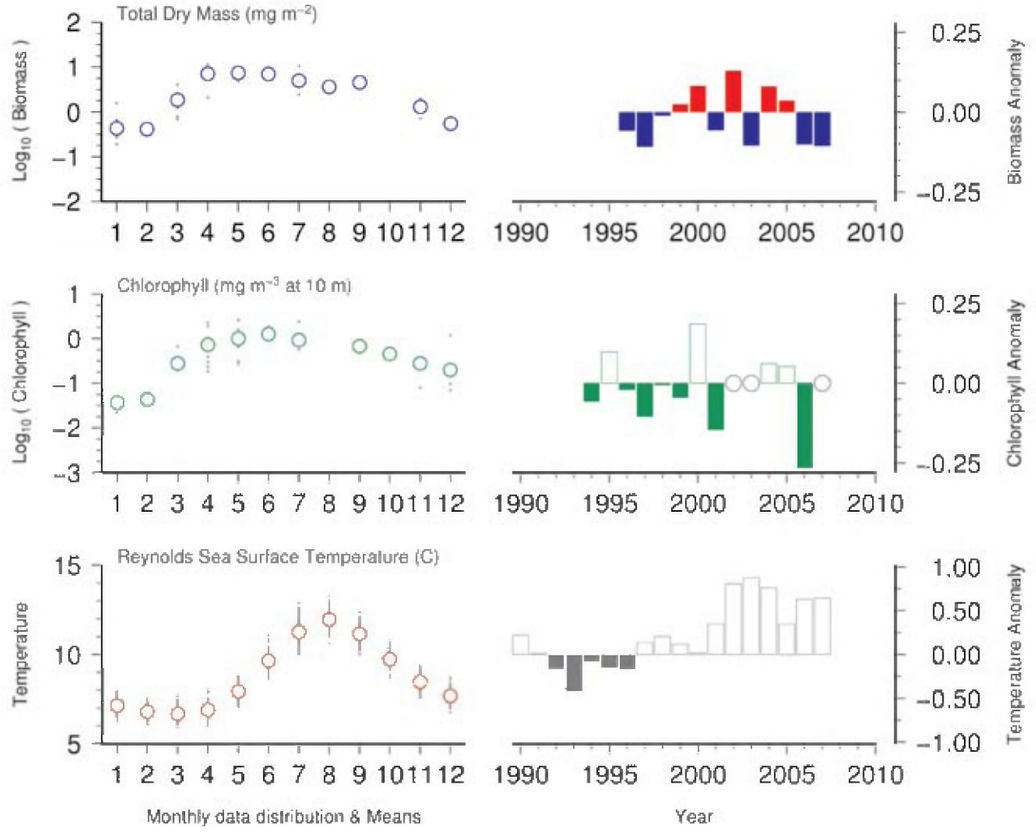

Figure 54.
Seasonal and interannual comparison of co-sampled variables at Svinøy Transect (West). (See Section 2.2 for an explanation of the subplots in this figure.)

Svinøy Transect East (Norwegian Sea)

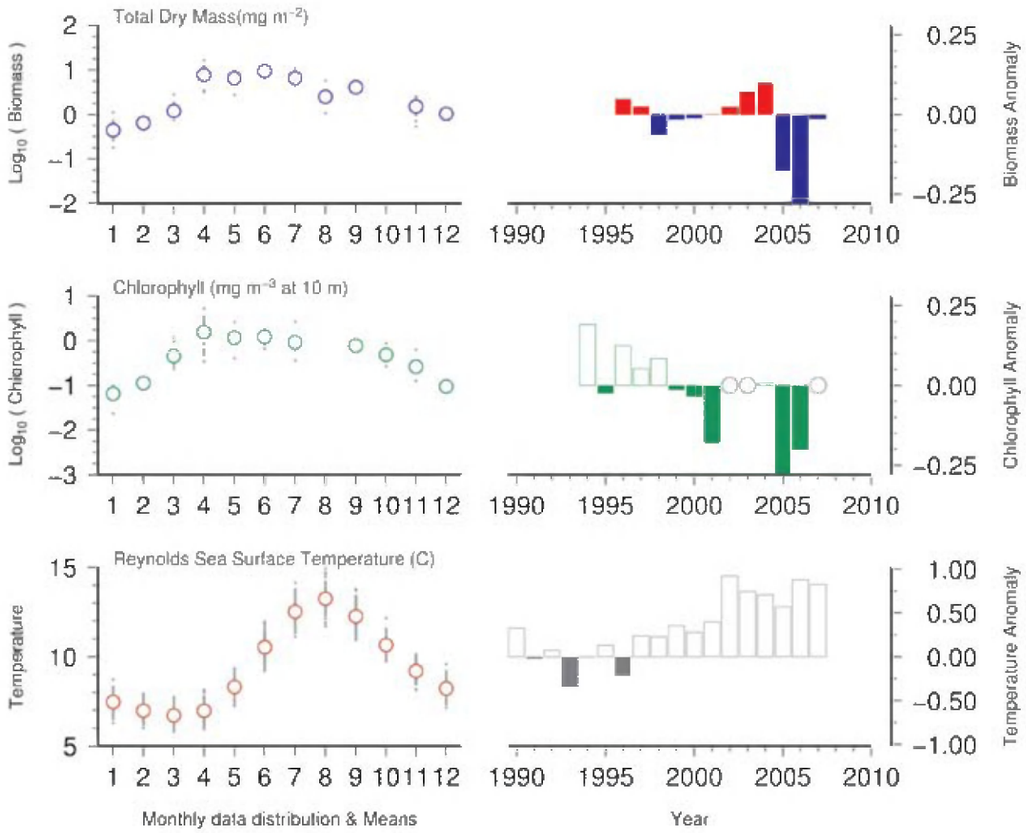

Figure 55.
Seasonal and interannual comparison of co-sampled variables at Svinøy Transect (East). (See Section 2.2 for an explanation of the subplots in this figure.)

Svinøy Transect West (Norwegian Sea)

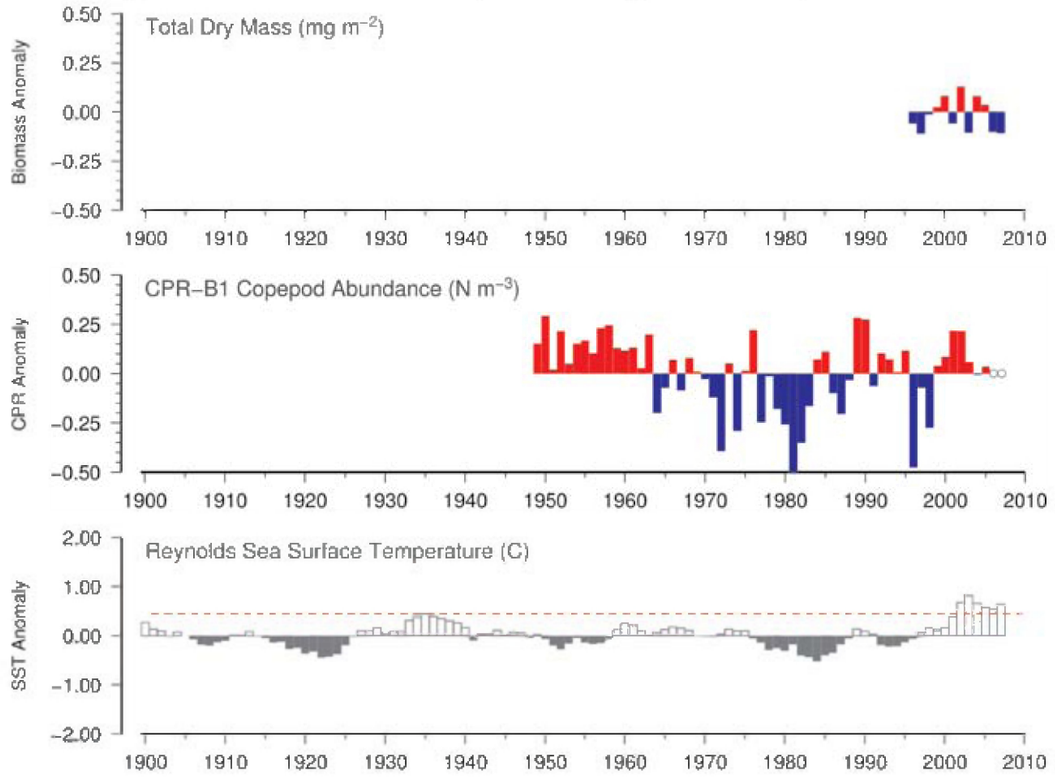

Figure 56.
Long-term comparison of Svinøy Transect (West) total zooplankton dry mass with copepod abundance in CPR standard area "B1" and Reynolds sea surface temperatures for the region. (See Section 2.3 for an explanation of the subplots in this figure.)

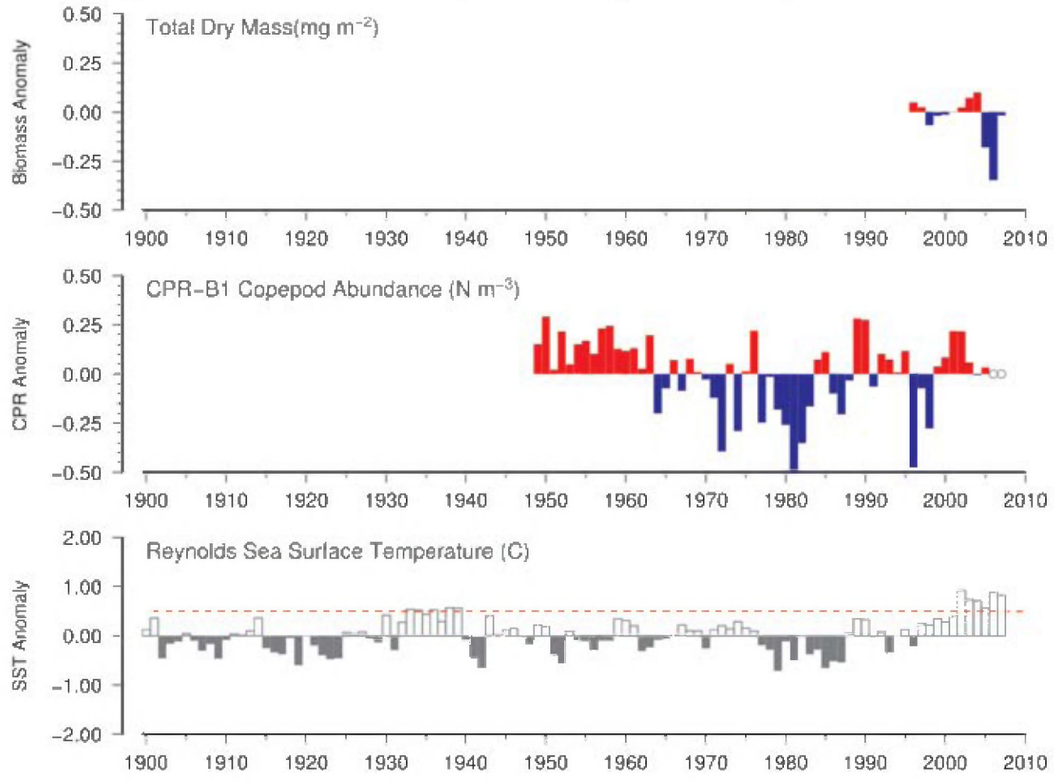

Figure 57.
Long-term comparison of Svinøy Transect (East) total zooplankton dry mass with copepod abundance in CPR standard area "B1" and Reynolds sea surface temperatures for the region. (See Section 2.3 for an explanation of the subplots in this figure.)

3.3 Barents Sea

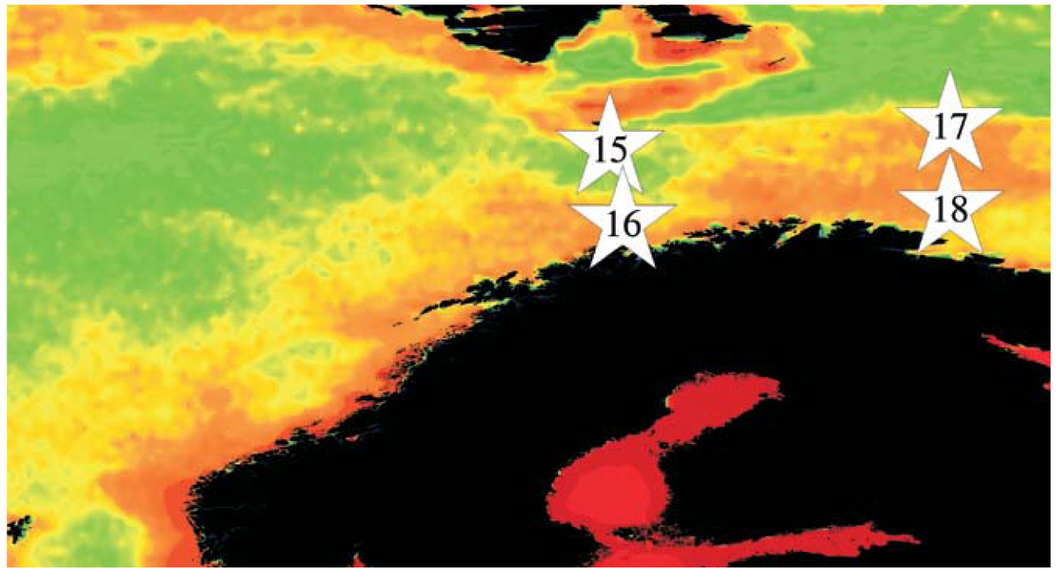

Figure 58.
Locations (Sites 15–18) of Barents Sea zooplankton time-series, plotted on a map of SeaWiFS average chlorophyll concentrations. Red/orange = high (productive), green/yellow = medium (moderate), blue = low (oligotrophic).

The Barents Sea (Figure 58) is a deep shelf region of the Arctic Ocean bordered by Norway and Russia. Remnants of the North Atlantic Drift, the northward continuation of the Gulf Stream, bring warm Atlantic waters up along the shoreline. These warm waters keep the shoreline and ports ice-free for the entire year and lead to an earlier spring phytoplankton bloom. Within this region, the Polar Front separates warm, higher salinity Atlantic waters from cold, lower salinity Arctic waters. The western half of the Polar Front, influenced by bottom topography, is strong and relatively stable from year to year, whereas the eastern half is variable in strength and location. The complex hydrography and currents in the Barents Sea make it one of the most highly productive regions of the world.

Sites 15–16: Fugløya–Bjørnøya transect (Western Barents Sea)

Webjørn Melle and Cecilie Broms

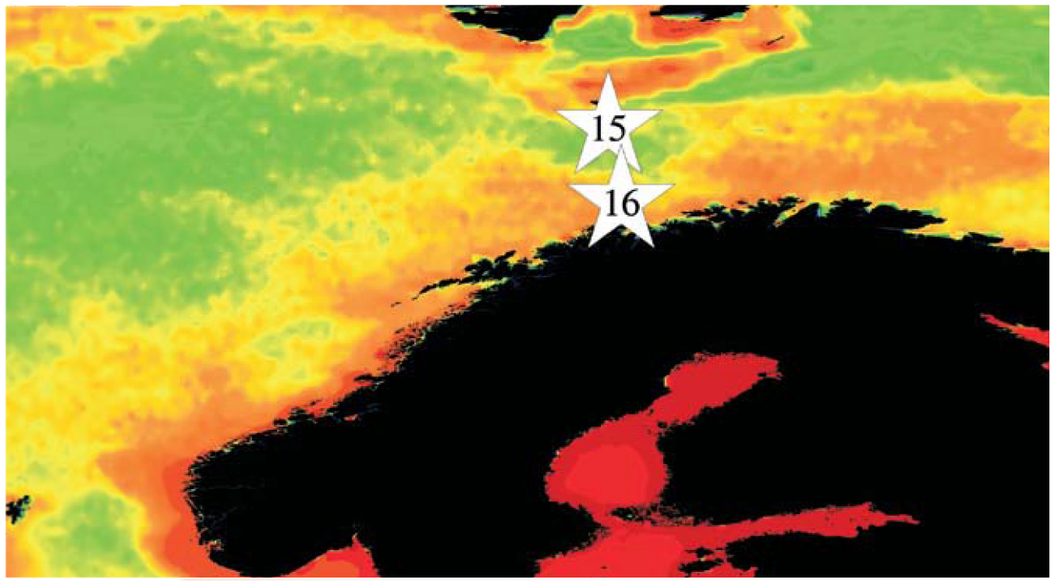

Figure 59.
Locations of the Fugløya–Bjørnøya Transect (North, Site 15; South, Site 16), survey areas, plotted on a map of SeaWiFS chlorophyll concentration. Red/orange = high (productive), green/yellow = medium (moderate), blue = low (oligotrophic).

The Institute of Marine Research (IMR) Monitoring Programme samples two standard transects in the Barents Sea: the Fugløya–Bjørnøya transect (seven stations) and the Vardø Nord transect (eight stations). The Fugløya–Bjørnøya transect is split into two sections: North (Figure 59, Site 15) and South (Figure 59, Site 16), which are each sampled three to six times a year with WP-2 nets (56 cm diameter, 180 µm mesh) from 100 m and/or bottom to the surface. The data in this report are from bottom-to-surface hauls (100–0 m).

Water temperatures along the Fugløya–Bjørnøya transect range from 4°C to 9°C, with the seasonal high in August and the seasonal low in February (Figures 60 and 61, bottom left). Peak zooplankton biomass is found from June to August in the northern section (Figure 60) and from May to July in the southern section (Figure 61). Zooplankton biomass has been steadily decreasing over the duration of the time-series, most noticeably in the northern section. This is also seen in the weakening (reduced magnitude) of the peak biomass period in the northern section (Figure 60, top right) and to a lesser extent in the southern section (Figure 61, top right).

Although water temperatures have been increasing since 1975 in both sections (Figures 62 and 63), long-term water temperatures along the transect reveal that these temperatures are currently at, or very slightly above, the 100-year maximum observed in the 1960s (Figures 62 and 63, red dashed line).

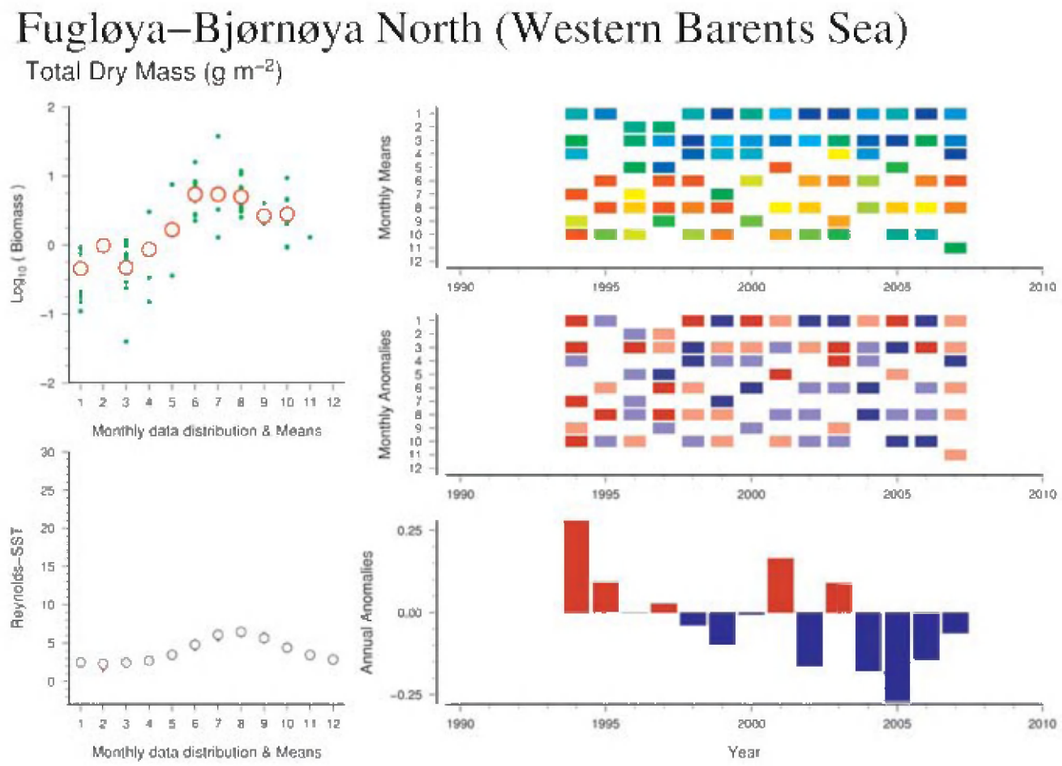

Figure 60.
Standardized WGZE time-series summary plot for total zooplankton dry mass at Fugløya–Bjørnøya (North). (See Section 2.1 for an explanation of the subplots in this figure.)

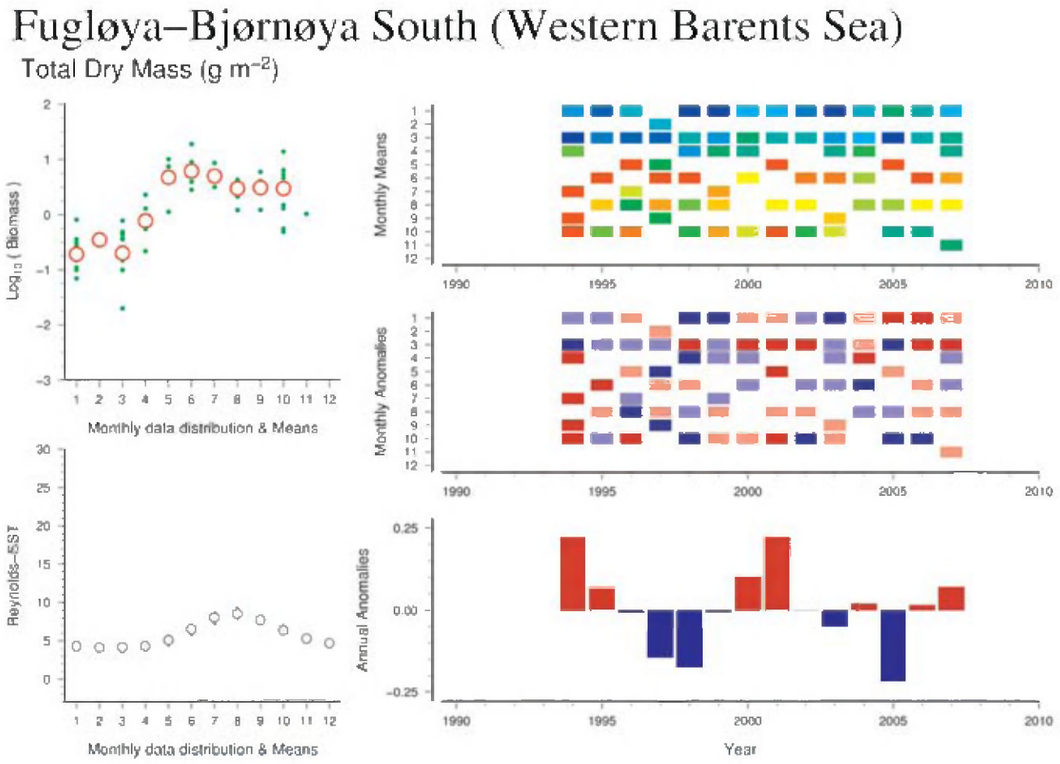

Figure 61.
Standardized WGZE time-series summary plot for total zooplankton dry mass at Fugløya–Bjørnøya (South). (See Section 2.1 for an explanation of the subplots in this figure.)

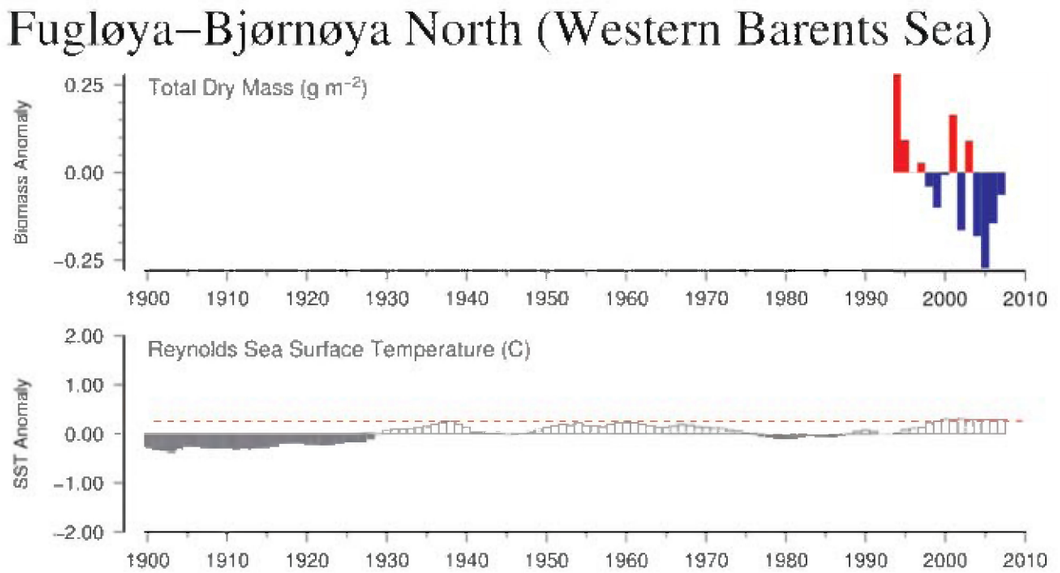

Figure 62.
Long-term comparison of Fugløya–Bjørnøya (North) total zooplankton dry mass with Reynolds sea surface temperatures for the region. CPR data were not available for this region. (See Section 2.3 for an explanation of the subplots in this figure.)

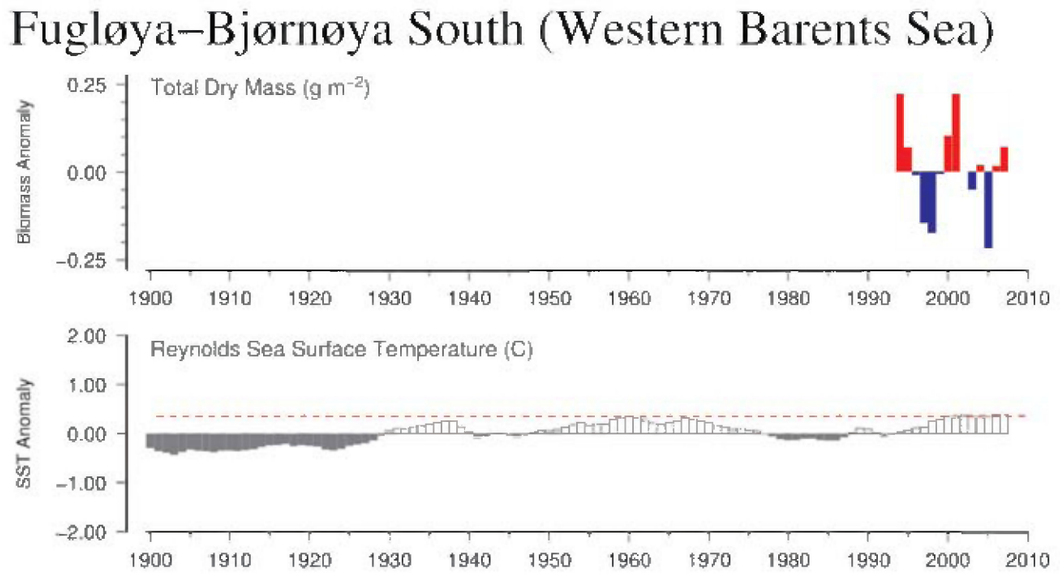

Figure 63.
Long-term comparison of Fugløya–Bjørnøya (South) total zooplankton dry mass with Reynolds sea surface temperatures for the region. CPR data were not available for this region. (See Section 2.3 for an explanation of the subplots in this figure.)

Sites 17–18: Vardø Nord transect (Eastern Barents Sea)

Webjørn Melle and Cecilie Broms

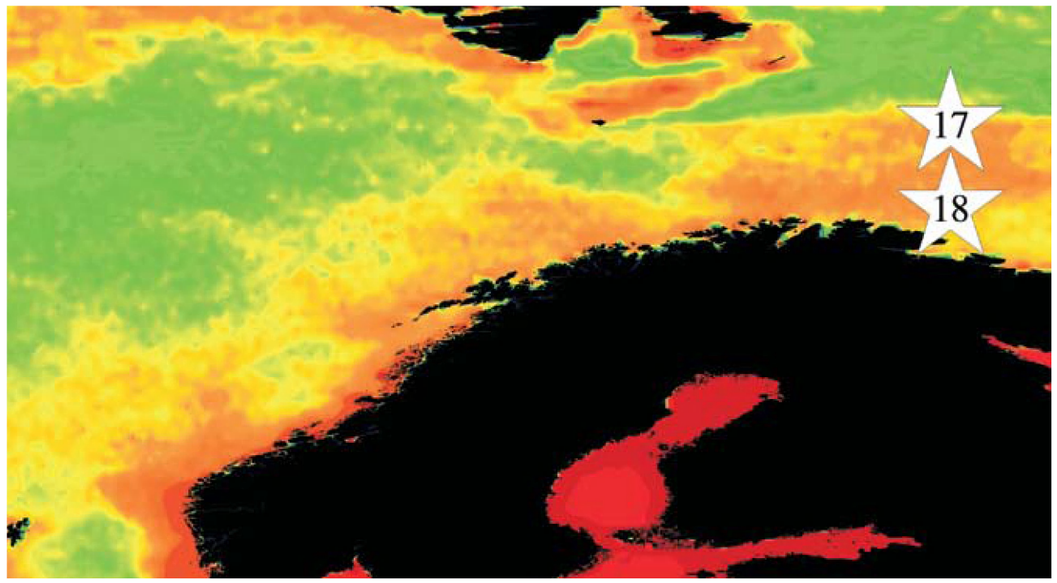

Figure 64.
Locations of the Vardø Nord Transect (North, Site 17; South, Site 18) survey areas, plotted on a map of SeaWiFS chlorophyll concentration. Red/orange = high (productive), green/yellow = medium (moderate), blue = low (oligotrophic).

The Institute of Marine Research (IMR) Monitoring Programme samples two standard sections in the Barents Sea: the Fugløya–Bjørnøya (seven stations) and the Vardø Nord transect (eight stations). The Vardø Nord transect is split into two sections: North (Figure 64, Site 17) and South (Figure 64, Site 18), which are each sampled three to four times a year with a WP-2 net (56 cm diameter, 180 µm mesh) from 100 m and/or bottom to the surface. The data presented in this report are based on bottom-to-surface hauls.

Water temperatures along the Vardø Nord transect range from 3°C to 8°C, with the seasonal high in August and the seasonal low in March (Figures 65 and 66, bottom left). Zooplankton biomass starts to increase sometime between April and June, and peaks in July (Figures 65 and 66). Zooplankton biomass has been steadily decreasing over the duration of the time-series, most noticeably in the southern section (Figure 66, bottom right). Lower biomass (during the last four years of sampling) and an overall decreasing trend are common among all sampling sites in the Norwegian and Barents Seas. Water temperatures are currently above the 100-year average for this region and have been increasing since 1980 in both the northern (Figure 67) and southern (Figure 68) sections. Looking further back, however, the current water temperatures are actually significantly lower than the 100-year maximum reached in 1960 (Figures 67 and 68, red dashed line).

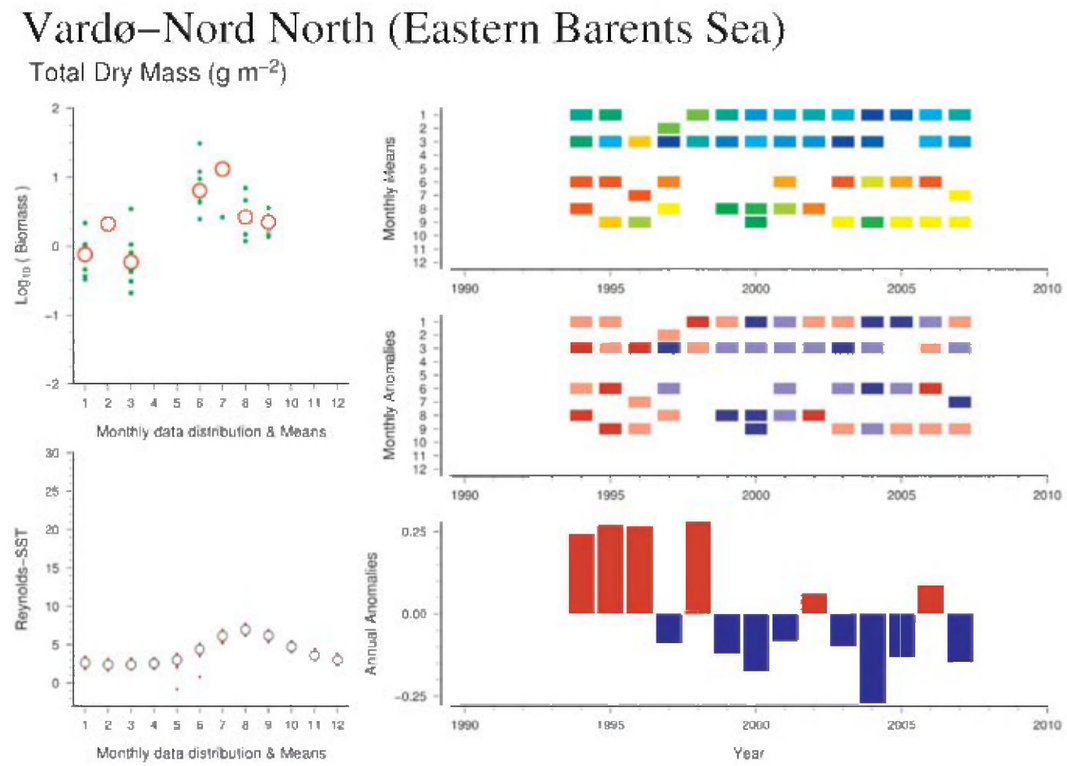

Figure 65.
Standardized WGZE time-series summary plot for total zooplankton dry mass at Vardø Nord (North). (See Section 2.1 for an explanation of the subplots in this figure.)

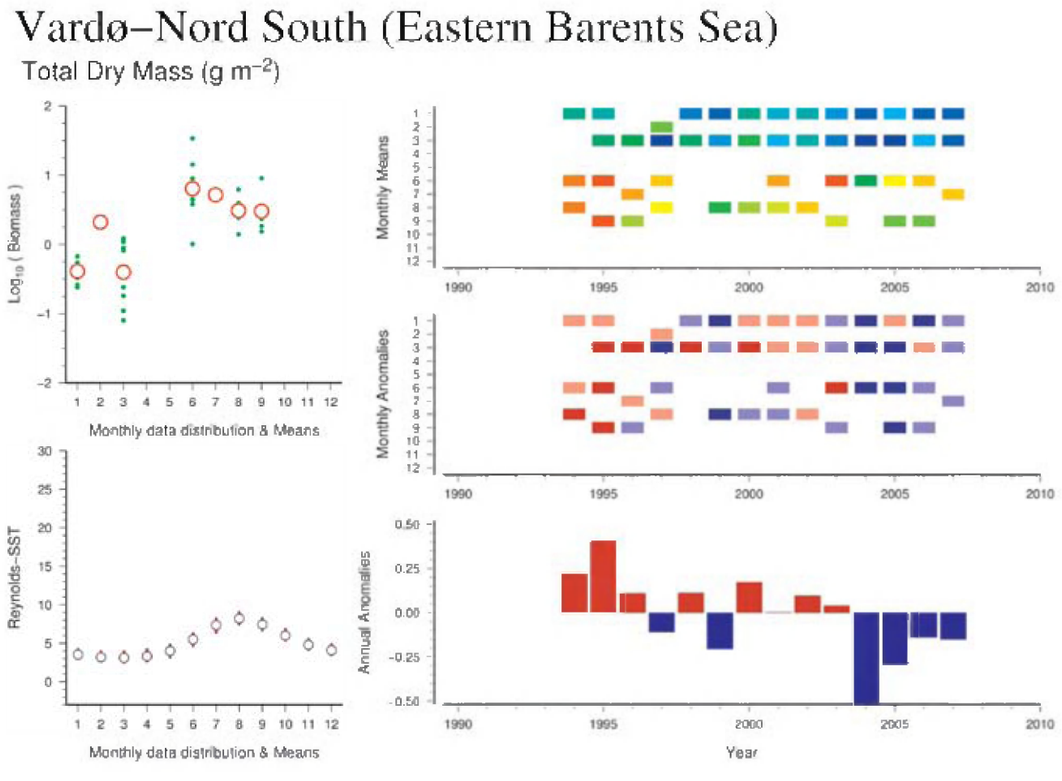

Figure 66.
Standardized WGZE time-series summary plot for total zooplankton dry mass at Vardø Nord (South). (See Section 2.1 for an explanation of the subplots in this figure.)

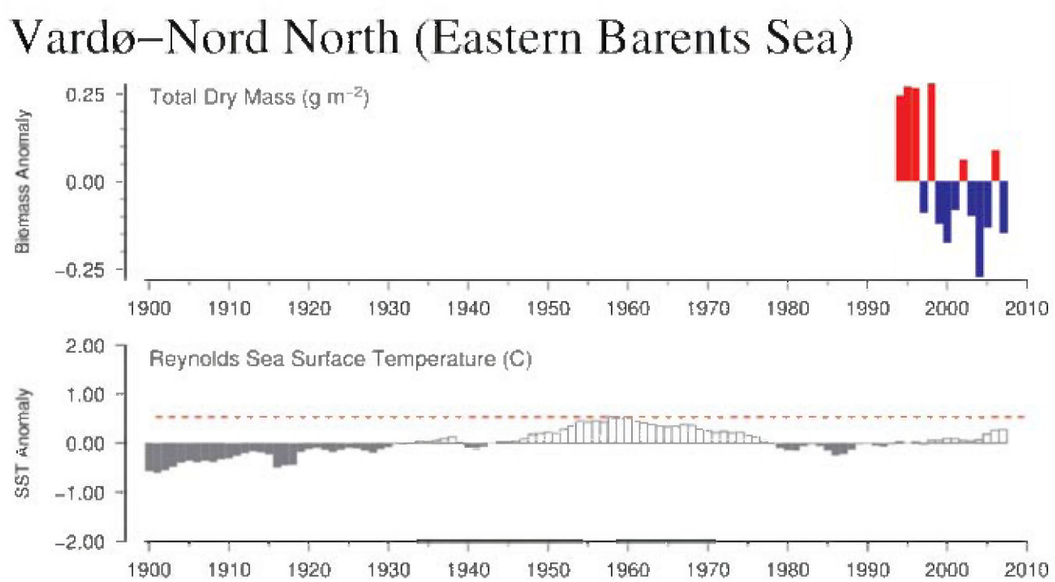

Figure 67.
Long-term comparison of Vardø Nord (North) total zooplankton dry mass with Reynolds sea surface temperatures for the region. CPR data were not available for this region. (See Section 2.3 for an explanation of the subplots in this figure.)

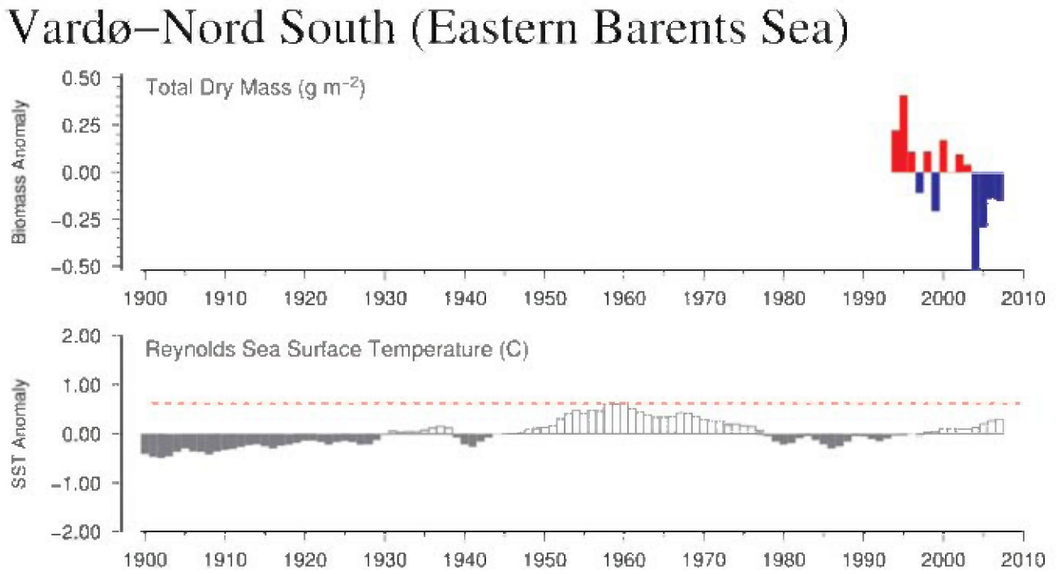

Figure 68.
Long-term comparison of Vardø Nord (South) total zooplankton dry mass with Reynolds sea surface temperatures for the region. CPR data were not available for this region. (See Section 2.3 for an explanation of the subplots in this figure.)

3.4 Baltic Sea

Figure 69.
Locations (Sites 19–25) of Baltic Sea zooplankton time-series, plotted on a map of SeaWiFS average chlorophyll concentrations. Red/orange = high (productive), green/yellow = medium (moderate), blue = low (oligotrophic).

The Baltic Sea (Figure 69) is a brackish inland sea bounded by the Scandinavian peninsula, mainland Europe, and the Danish islands. Average salinity in the Baltic Sea is much lower than that of the North Atlantic as a result of fresh-water run-off from the surrounding land. In general, the surface waters, flowing out of the Baltic into the North Sea, are brackish, while the deep water has higher salinity as a result of the deep waters flowing in from the North Sea. These salinity differences lead to strong stratification in the water column, which, combined with eutrophication and pollution, lead to low oxygen levels in much of the Baltic Sea deep water. The zooplankton of the Baltic Sea range from fresh-water/brackish species to North Sea neritic and occasional oceanic species, depending mainly on the distance from the Baltic Sea–North Sea interface.

Sites 19–20: Bothnian Bay and Bothnian Sea (Northern Baltic Sea)

Juha Flinkman

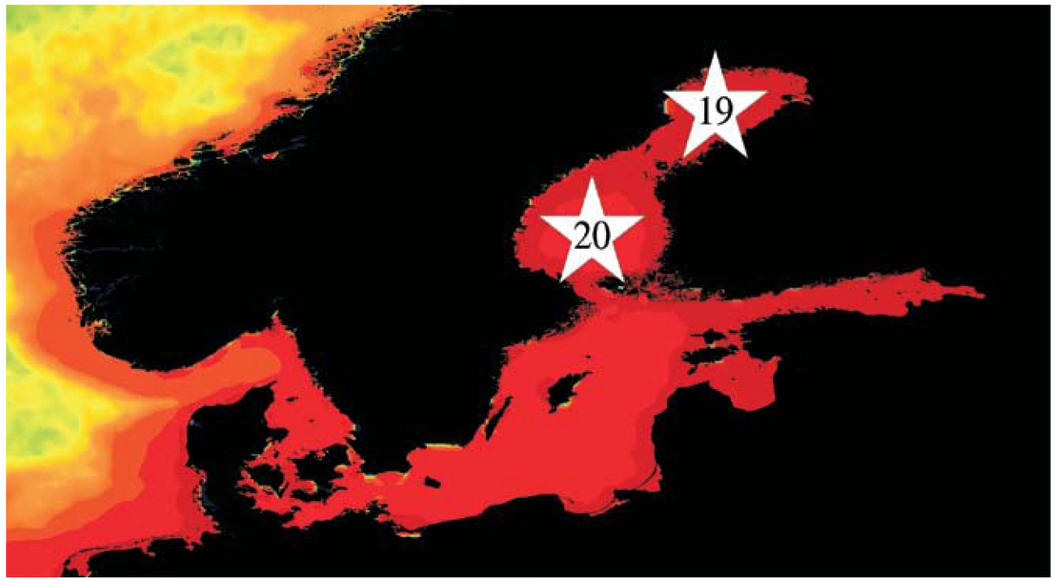

Figure 70.
Locations of the Bothnian Bay (Site 19) and Bothnian Sea (Site 20) survey areas, plotted on a map of SeaWiFS chlorophyll concentration. Red/orange = high (productive), green/yellow = medium (moderate), blue = low (oligotrophic).

Zooplankton monitoring by the Finnish Institute of Marine Science began in 1979 after the Helsinki Convention (HELCOM) initiated cooperative environmental monitoring of the Baltic Sea. Monitoring was divided into four subareas based on differing hydrographic environments, including the Baltic Proper, Gulf of Finland, Bothnian Sea, and Bothnian Bay. For the purposes of this report, only the Bothnian Bay and Bothnian Sea regions are summarized (Figure 70). Zooplankton were collected in August, the peak abundance period, using a WP-2 net (56 cm diameter, 100 µm mesh). Zooplankton data for Bothnian Bay are an average of two stations, whereas data from the Bothnian Sea are an average of three stations.

Water temperature in the Bothnian Bay is 1–2°C colder than in the Bothnian Sea. At both sites, water temperatures are lowest in February/March and warmest in August (Figures 71 and 72). Both regions have relatively low salinities, with Bothnian Sea surface salinity ranging from 4.5 psu to 6 psu, and Bothnian Bay salinity ranging from 2.5 psu to 4 psu. These differences in salinity influence the zooplankton community structure in each region, with taxa preferring higher salinity (e.g. *Acartia* spp.) being fairly abundant in the Bothnian Sea and nearly absent in the Bothnian Bay. This is changing, however, as surface salinity in both areas has been decreasing since the 1960s. In the late 1970s, the Bothnian Sea zooplankton biomass was dominated by *Eurytemora* spp., *Acartia* spp., and *Limnocalanus macrurus*. Since 1979, the biomass of *Acartia* has

been steadily decreasing, whereas the other two taxa and total biomass in the region have been increasing (Figure 72). This increase in *L. macrurus* or in total biomass is not evident in the Bothnian Bay (Figure 71), perhaps because a salinity threshold has already been reached in this community.

The general Baltic-wide decrease in salinity is the result of warmer temperatures and increased precipitation/river run-off in the Baltic. The SST values in both regions (Figures 73 and 74) have been above the 100-year average since the 1990s. Those in the Bothnian Sea have also been above the 100-year maximum since 2000 (Figure 74, bottom, red dashed line), as have those in the Bothnian Bay since 2005 (Figure 73, red dashed line).

Bothnian Bay (Northern Baltic)

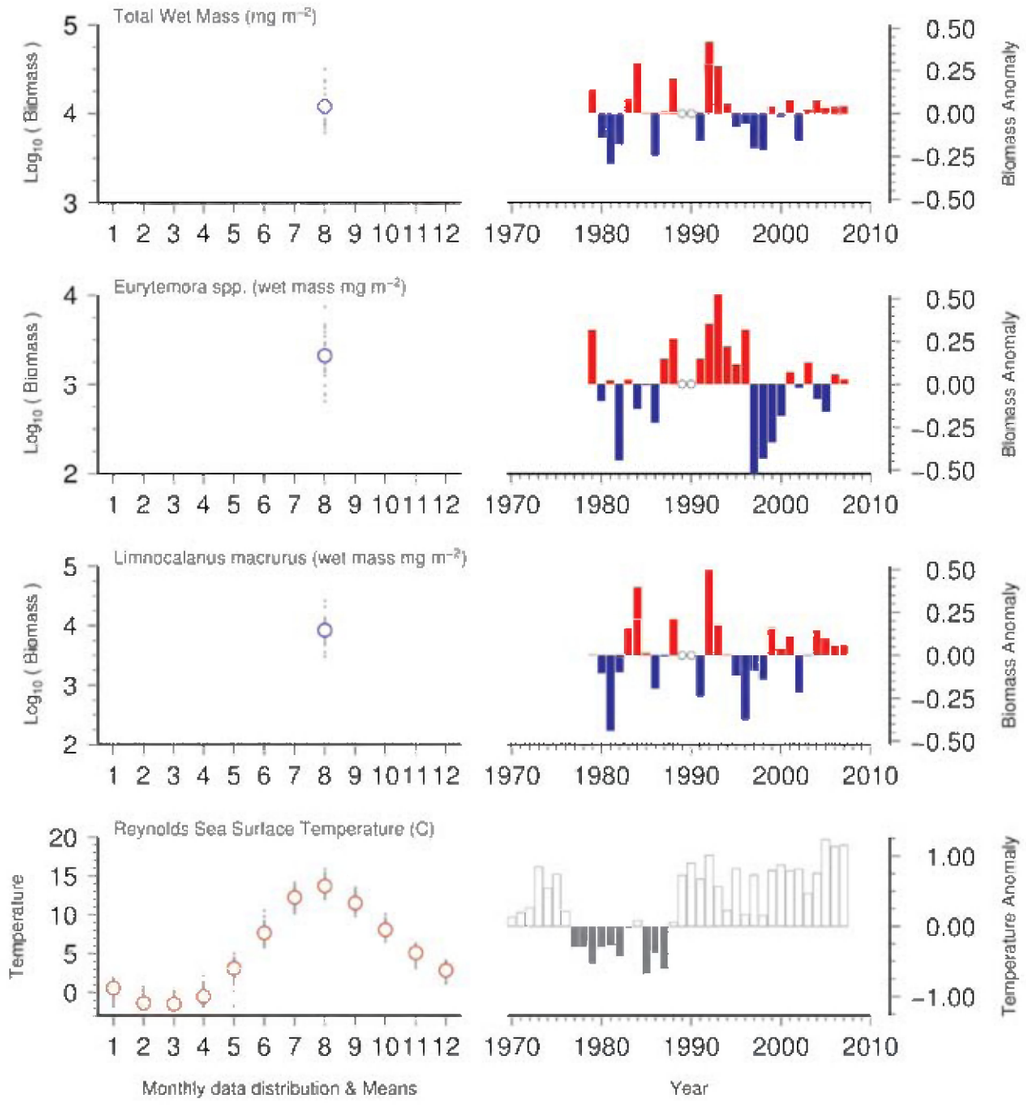

Figure 71.
Seasonal and interannual comparison of zooplankton wet mass and co-sampled variables in the Bothnian Bay. (See Section 2.2 for an explanation of the subplots in this figure.)

Bothnian Sea (Northern Baltic)

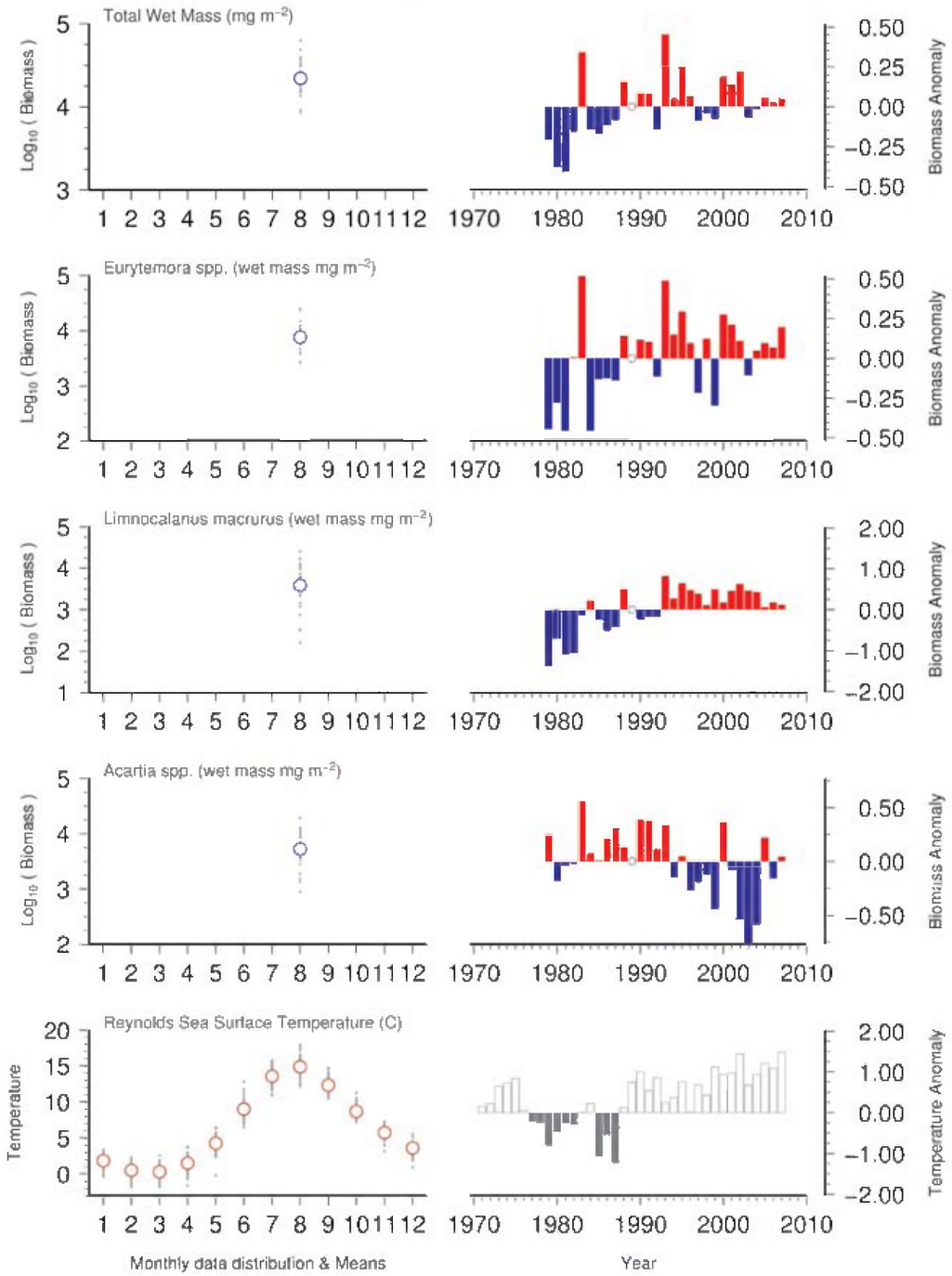

Figure 72.
Seasonal and interannual comparison zooplankton wet mass and co-sampled variables in the Bothnian Sea. (See Section 2.2 for an explanation of the subplots in this figure.)

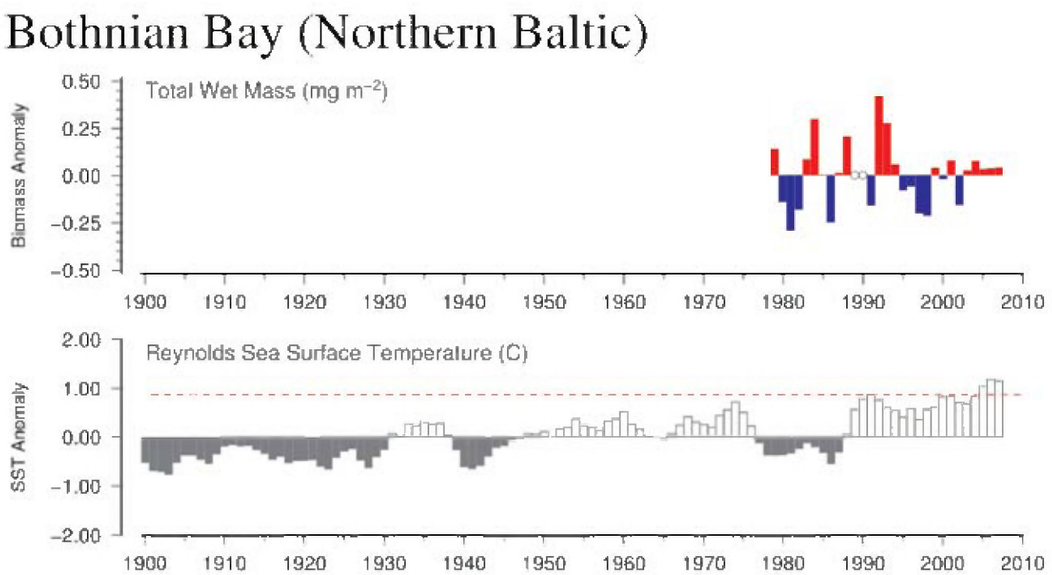

Figure 73.
Long-term comparison of Bothnian Bay zooplankton wet mass with Reynolds sea surface temperatures for the region. CPR data were not available for this region. (See Section 2.3 for an explanation of the subplots in this figure.)

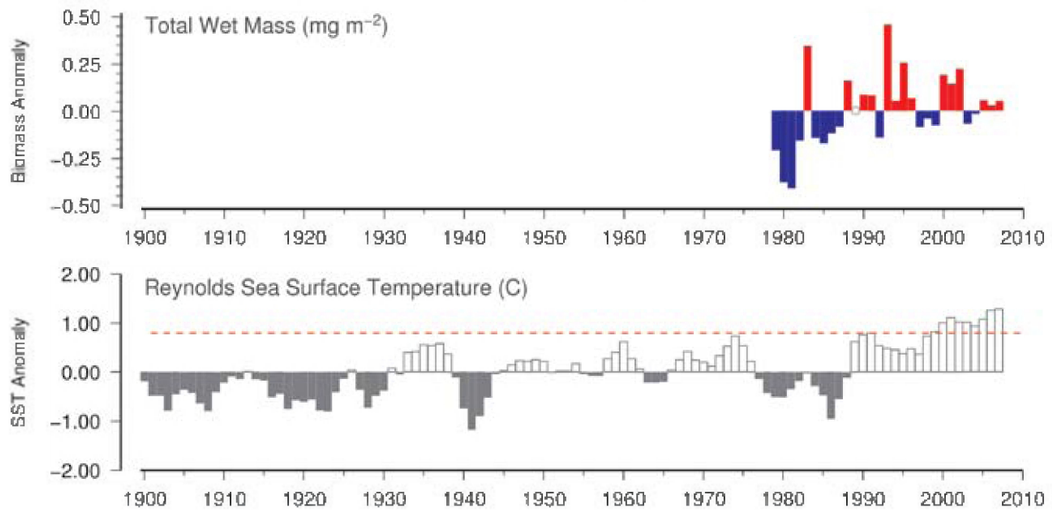

Figure 74.
Long-term comparison of Bothnian Sea zooplankton wet mass with Reynolds sea surface temperatures for the region. CPR data were not available for this region. (See Section 2.3 for an explanation of the subplots in this figure.)

Site 21: Tallinn Bay (Gulf of Finland)

Arno Põllumäe

Figure 75.
Location of the Tallinn Bay survey area (Site 21), plotted on a map of SeaWiFS chlorophyll concentration. Red/orange = high (productive), green/yellow = medium (moderate), blue = low (oligotrophic).

The Gulf of Finland is represented by one HELCOM sampling station located in the middle of Tallinn Bay at 59°32.2′N 24°41.3′E (Figure 75). Zooplankton were collected using vertical hauls of a Juday plankton net (0.38 m mouth opening, 90 µm mesh) up to ten times a year.

Zooplankton in the Baltic Sea are typically smaller than elsewhere. The dominant copepod species in Estonian waters are *Eurytemora affinis* and *Acartia bifilosa*, the most abundant cladoceran is *Bosmina coregoni*, and rotifers also constitute a large proportion of the total zooplankton abundance. The maximum zooplankton biomass is usually observed in late summer, corresponding to the warmest water temperatures (Figure 76). In years with warmer winters, high abundance may be observed in spring, when a shorter period of ice cover causes more mixing and phosphorus release from the bottom, resulting in higher chlorophyll concentrations in spring and summer. This mechanism may also explain the corresponding increase in chlorophyll with temperature over time (Figure 77) and the slight increase in copepod abundance during the same period. In the long term, water temperatures at the sampling site have been warmer than the 100-year average since 1989 (Figure 78) and are currently warmer than the 100-year maximum (Figure 78, bottom, red dashed line).

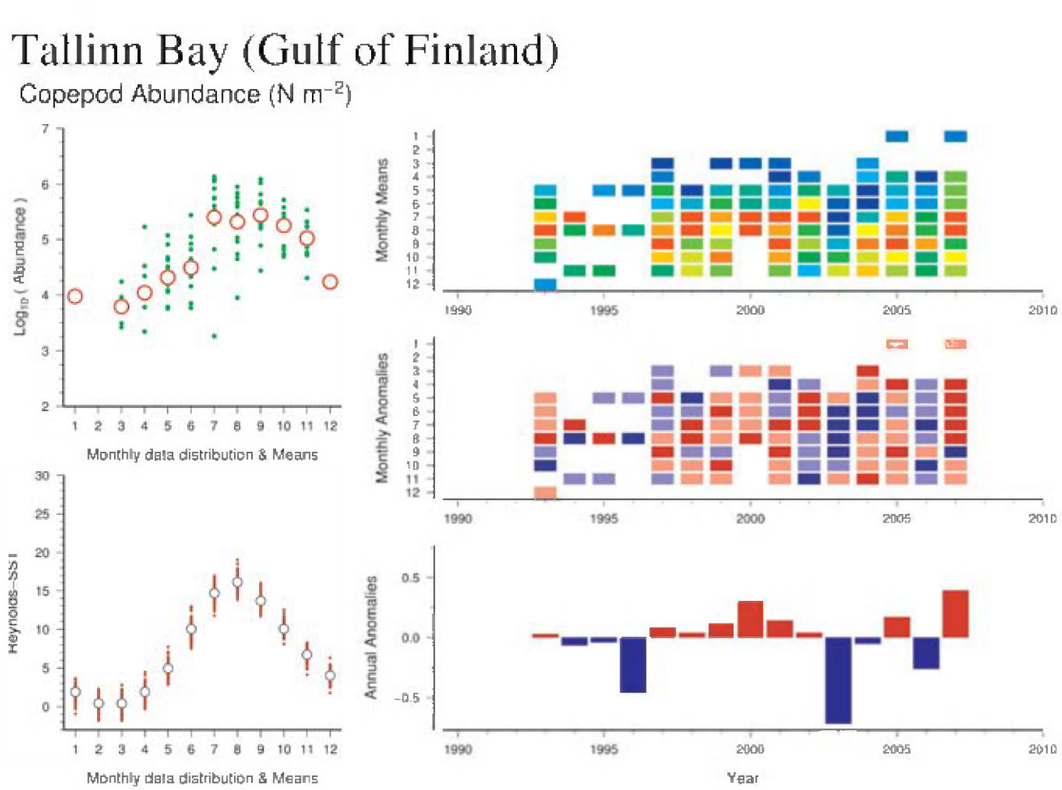

Figure 76.
Standardized WGZE time-series summary plot for copepod abundance in Tallinn Bay. (See Section 2.1 for an explanation of the subplots in this figure.)

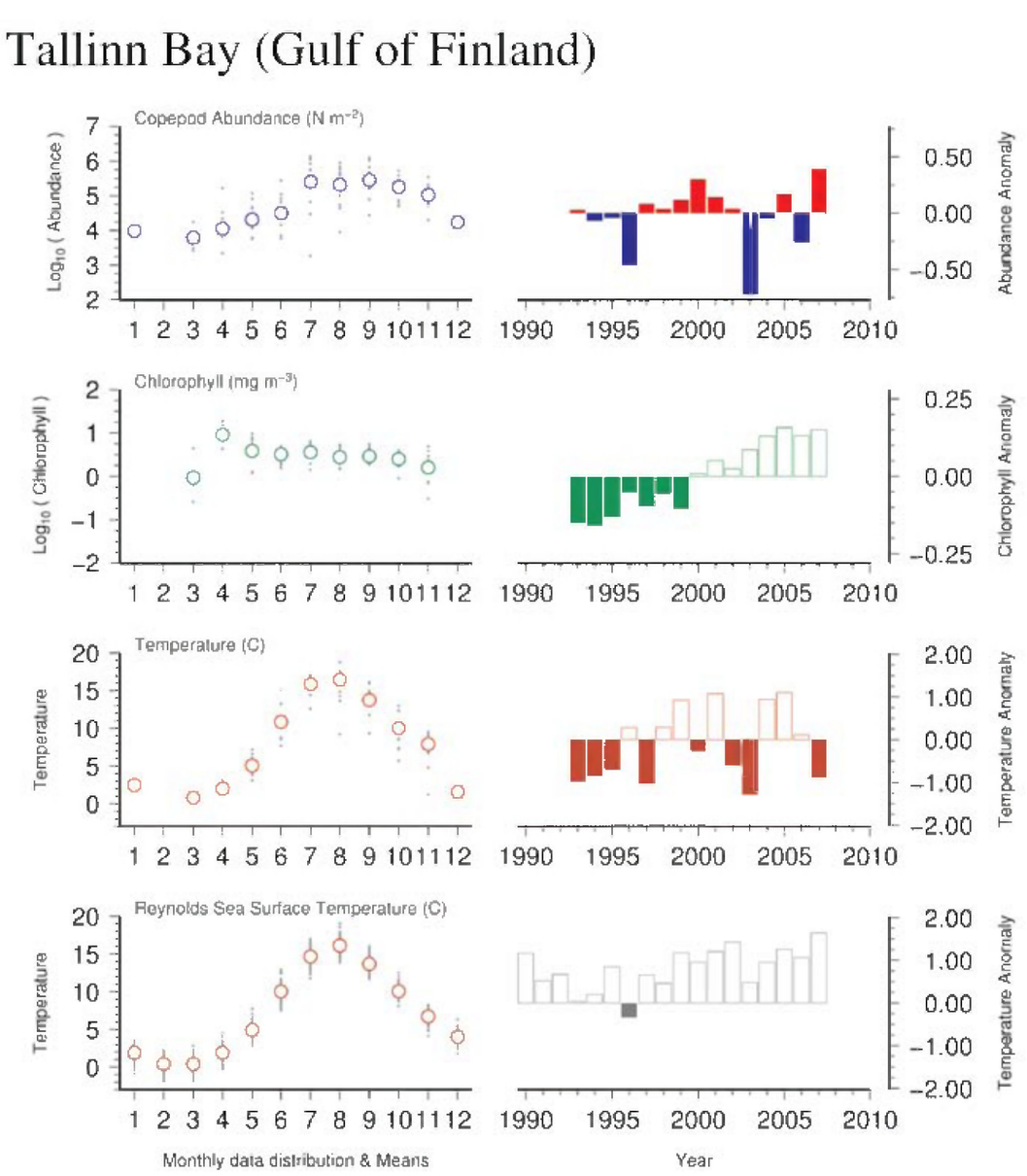

Figure 77.
Seasonal and interannual comparison of co-sampled variables in Tallinn Bay. (See Section 2.2 for an explanation of the subplots in this figure.)

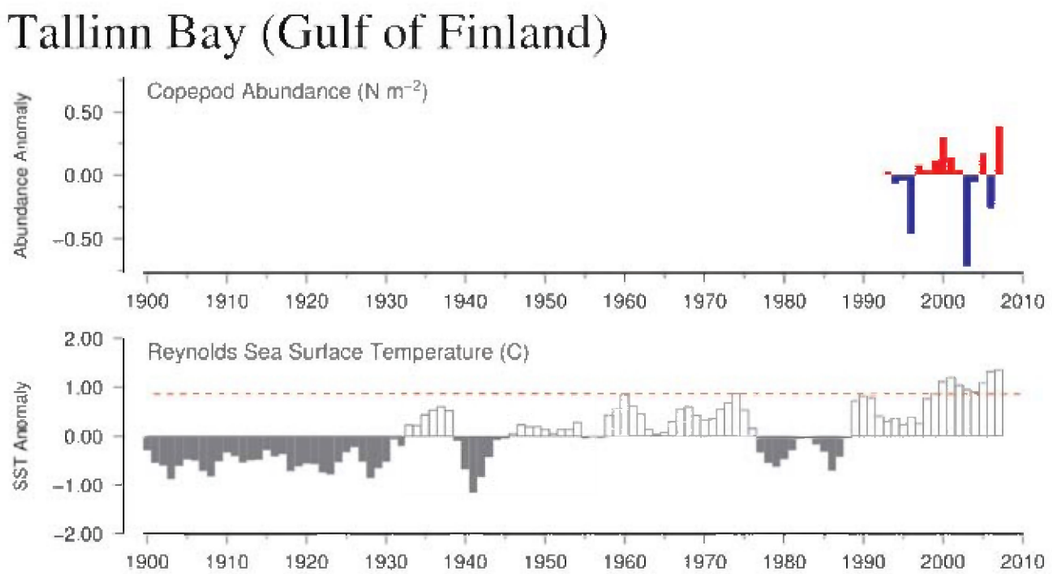

Figure 78.
Long-term comparison of Tallinn Bay copepod abundance with Reynolds sea surface temperatures for the region. CPR data were not available for this region. (See Section 2.3 for an explanation of the subplots in this figure.)

Site 22: Pärnu Bay (Gulf of Riga)

Arno Põllumäe and Maria Põllupiüü

Figure 79.
Location of the Pärnu Bay survey area (Site 22), plotted on a map of SeaWiFS chlorophyll concentration. Red/orange = high (productive), green/yellow = medium (moderate), blue = low (oligotrophic).

Pärnu Bay is a shallow, semi-enclosed water basin in the northeast Gulf of Riga in the Baltic Sea (Figure 79). Its maximum depth gradually increases from 7.5 m in the inner part to 23 m in the southwestern part. The hydrological conditions of the bay are influenced by meteorological processes, river discharge, and water exchange with the open part of the Gulf of Riga. The salinity of Pärnu Bay is slightly lower than in the Gulf of Riga, with an average salinity of 5 psu. Pärnu Bay also suffers from heavy anthropogenic eutrophication, with nitrate and phosphate coming into the bay from the town of Pärnu and the Pärnu River.

Zooplankton samples are collected in the middle part of the bay, where water depth is 10 m, using a Juday plankton net (0.1 m^2 mouth opening, 90 µm mesh). The frequency of sampling has varied over the years, from at least once a month to several times a week during summer in some years. Peak copepod abundance occurs in the warmer summer months (Figure 80), after the spring chlorophyll peak and just before the summer temperature increase (Figure 81).

The diversity of zooplankton in Pärnu Bay is low; two species, *Eurytemora affinis* and *Acartia bifilosa*, constitute 99% of the total copepod abundance, and *Bosmina coregoni maritima* is the prevailing cladoceran. Although copepod abundance has been increasing slightly for the duration of the time-series, cladoceran abundance went from an increasing to a decreasing trend around 1989 (Figure 81). The 1989 period corresponds with a rise in both copepod abundance and water temperature from below-average to above-average levels (Figure 81). One reason for the decreased cladoceran abundance in the 1990s may be the introduced predatory cladoceran *Cercopagis pengoi*, which occurs in large numbers in Pärnu Bay during periods of warm water. Water temperatures in Pärnu Bay have been warmer than the 100-year average since 1989 and are currently warmer than the 100-year maximum (Figure 82, bottom, red dashed line).

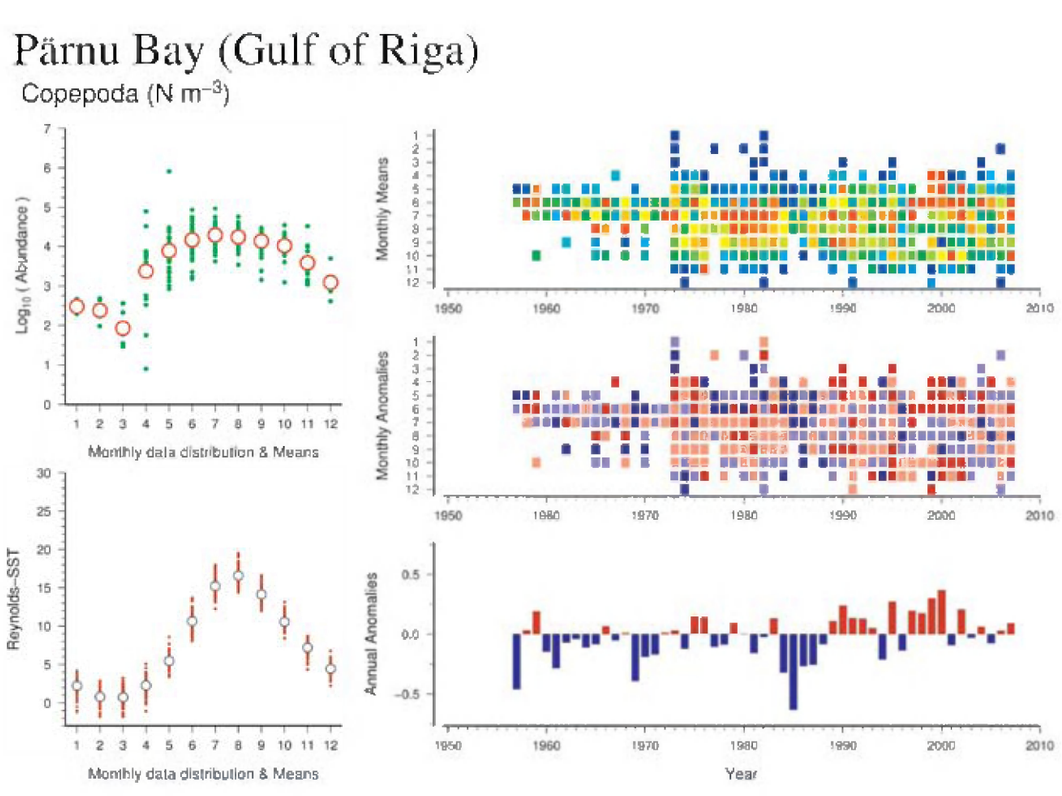

Figure 80.
Standardized WGZE time-series summary plot for copepod abundance in Pärnu Bay. (See Section 2.1 for an explanation of the subplots in this figure.)

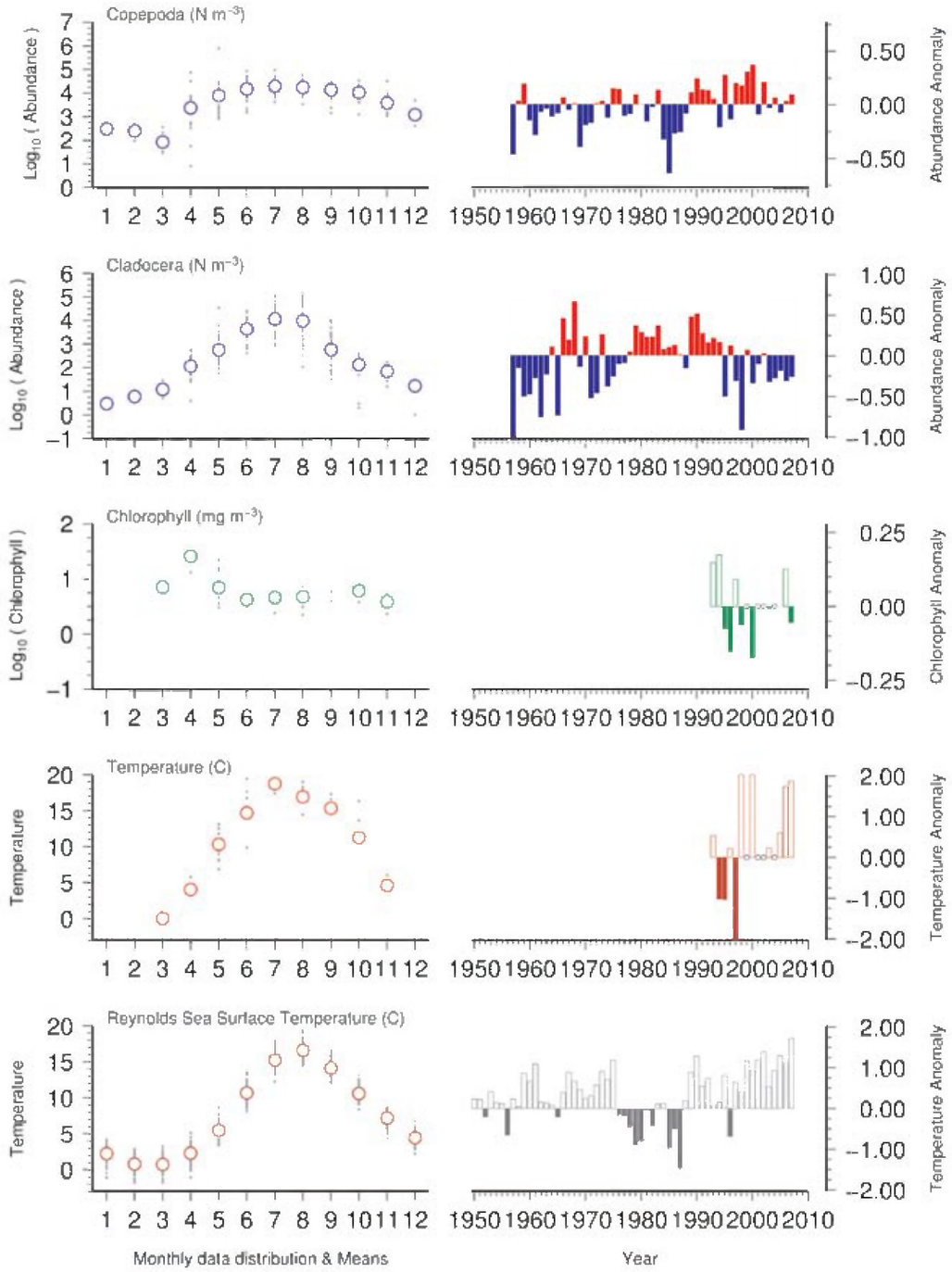

Figure 81.
Seasonal and interannual comparison of co-sampled variables in Pärnu Bay. (See Section 2.2 for an explanation of the subplots in this figure.)

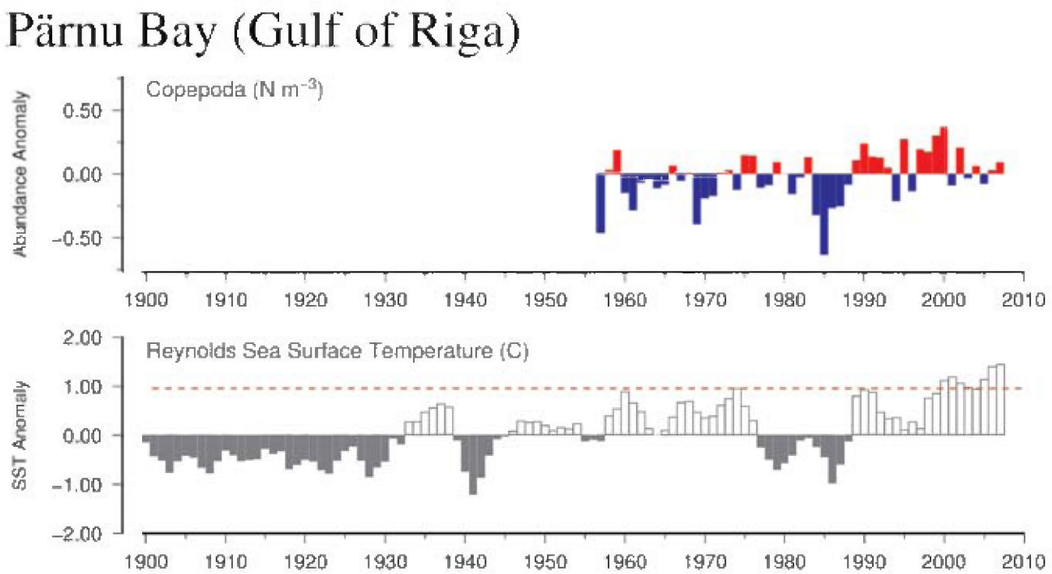

Figure 82.
Long-term comparison of Pärnu Bay copepod abundance with Reynolds sea surface temperatures for the region. CPR data were not available for this region. (See Section 2.3 for an explanation of the subplots in this figure.)

Site 23: Station 121 (Gulf of Riga)

Anda Ikauniece

Figure 83.
Location of the Station 121 survey area (Site 23), plotted on a map of SeaWiFS chlorophyll concentration. Red/orange = high (productive), green/yellow = medium (moderate), blue = low (oligotrophic).

Sampling Station 121 is located in the central part of the Gulf of Riga (Figure 83), approximately 50 km offshore, at a water depth of 55 m. Zooplankton samples for determination of abundance and wet-weight biomass were collected by vertical hauls from a depth of 50 m to the surface using a WP-2 net (56 cm diameter, 100 µm mesh). Sampling was carried out at least three times a year, representing the most productive seasons, i.e. spring (May), summer (August), and autumn (October–November).

For the first half of the year, water temperature in the Gulf of Riga is the main determinant of zooplankton abundance and biomass. Minimum copepod abundance and biomass values are found from January until the beginning of March, and correspond to the coldest water temperatures (Figure 84). In May, the spring zooplankton community is dominated by copepods and rotifers (*Synchaeta* spp.). From the end of May to the beginning of June, as water temperatures rise, thermophilic species, such as cladocerans and rotifers (*Keratella* spp.), begin to appear, reaching maximum abundance and biomass in August. When water temperatures fall in autumn, the thermophilic species disappear, reducing copepod abundance and biomass (Figure 85).

Water temperatures in the Gulf of Riga have been above the 100-year average for the duration of the time-series, and they have been above the 100-year maximum since 2000 (Figure 86, bottom, red dashed line). There has been an overall decreasing trend in zooplankton abundance since the beginning of the time-series. In recent years, biomass and abundance maxima have been observed more frequently in July than in August, due in part to this overall warming in the region and a subsequent shift in the timing of community development. Other possible reasons for the observed decline in zooplankton are: August predation pressure on copepods by herring, which have been increasing over the past ten years, and the increasing presence of the invasive cladoceran *Cercopagis pengoi* since the late 1990s.

Station 121 (Gulf of Riga)

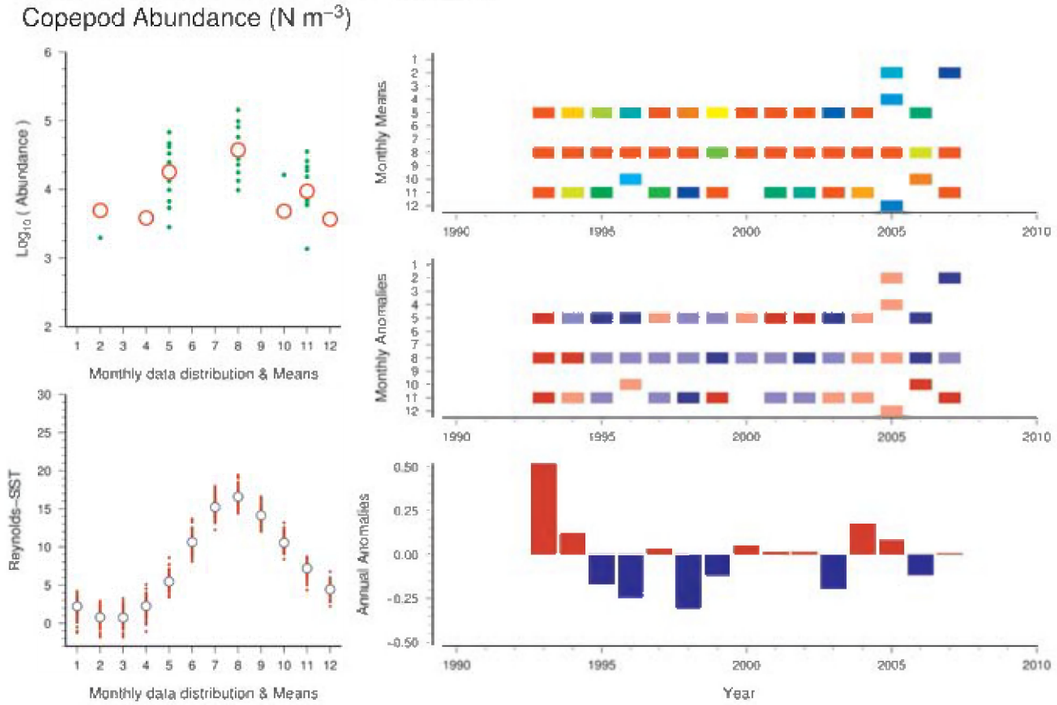

Figure 84.
Standardized WGZE time-series summary plot for copepod abundance at Station 121. (See Section 2.1 for an explanation of the subplots in this figure.)

Station 121 (Gulf of Riga)

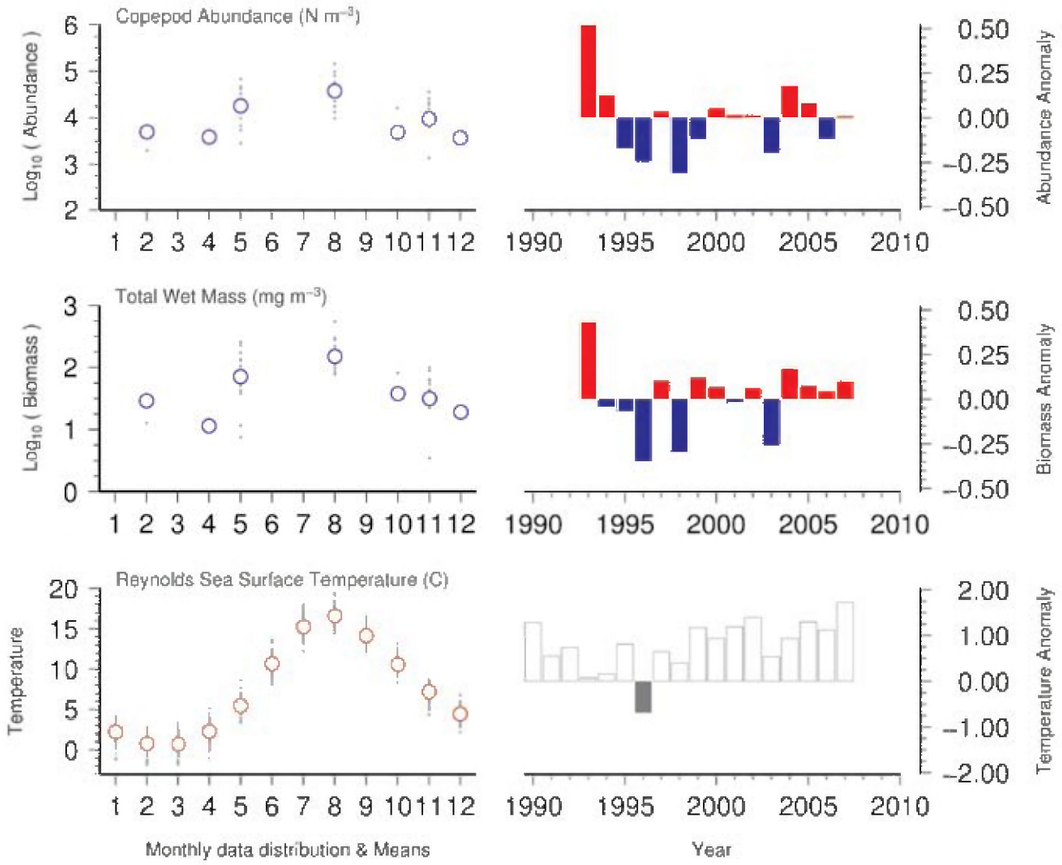

Figure 85.
Seasonal and interannual comparison of co-sampled variables at Station 121. (See Section 2.2 for an explanation of the subplots in this figure.)

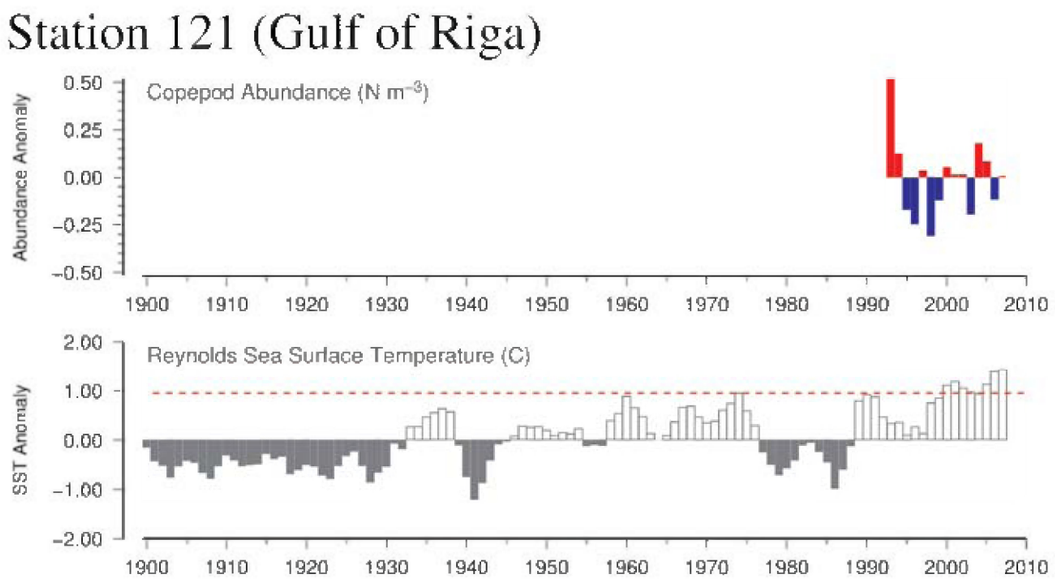

Figure 86.
Long-term comparison of Station 121 copepod abundance with Reynolds sea surface temperatures for the region. CPR data were not available for this region. (See Section 2.3 for an explanation of the subplots in this figure.)

Site 24: Eastern Gotland Basin (Central Baltic)

Solvita Strake and Georgs Kornilovs

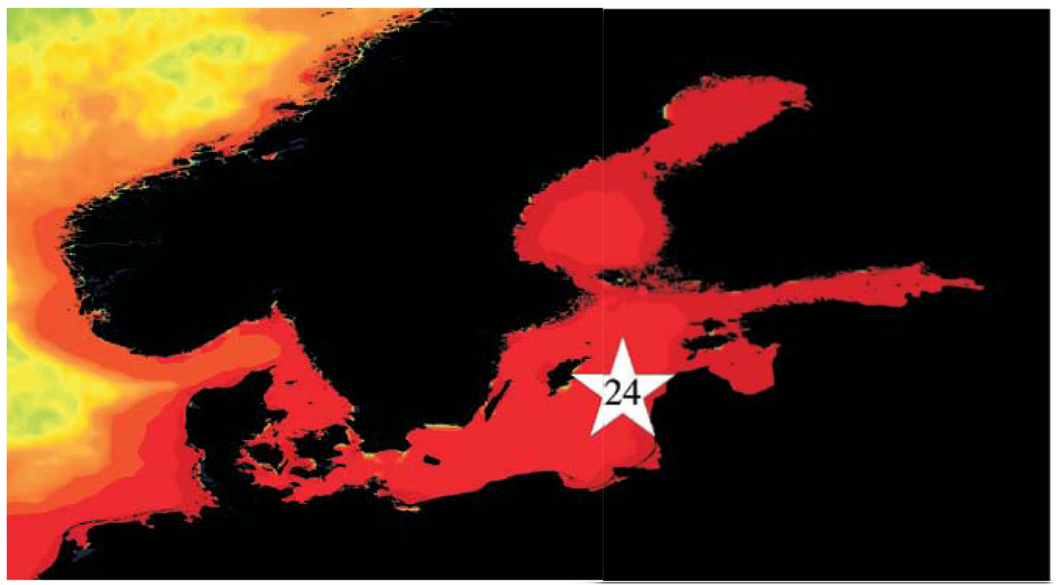

Figure 87.
Location of the Eastern Gotland Basin survey area (Site 24), plotted on a map of SeaWiFS chlorophyll concentration. Red/orange = high (productive), green/yellow = medium (moderate), blue = low (oligotrophic).

The Eastern Gotland Basin sampling site is located in the central Baltic Sea, ICES Subdivision 28 (Figure 87). Zooplankton biomass (wet weight) was sampled using a Juday net (0.36 m opening diameter, 160 µm mesh). Individual hauls were carried out in vertical steps, resulting in full coverage of the water column to a maximum depth of 100 m. Sampling has been conducted in spring (May), summer (August), and autumn (October/November) since 1959 (Figure 88).

The dominant zooplankton species in the central Baltic Sea are the copepods *Acartia* spp., *Temora longicornis*, and *Pseudocalanus acuspes*. Since the early 1970s, high positive biomass anomalies were observed for *P. acuspes*, followed by a drastic decline after 1990 (Figure 89). At the same time, an opposite trend was observed for *T. longicornis*. Changes in temperature (increasing) and salinity (decreasing) are considered to be the reason for the shift in zooplankton species composition from *P. acuspes* to *T. longicornis*. Similarly, the species composition of the central Baltic fish community shifted from cod (*Gadus morhua*), which was dominant during the 1980s, to sprat (*Sprattus sprattus*), which became dominant during the 1990s (Möllmann *et al.*, 2003, 2005). Water temperatures in the survey area have been increasing since the 1900s, with some variability, and are currently warmer than any measured during the past century (Figure 90). Increased precipitation and river run-off have accompanied the warmer temperatures. This affects the Baltic and its zooplankton communities by directly freshening surface waters and preventing inflows of saline and oxygenated water from the Kattegat and North Sea (Matthäus and Schinke, 1999).

Eastern Gotland Basin (Central Baltic)

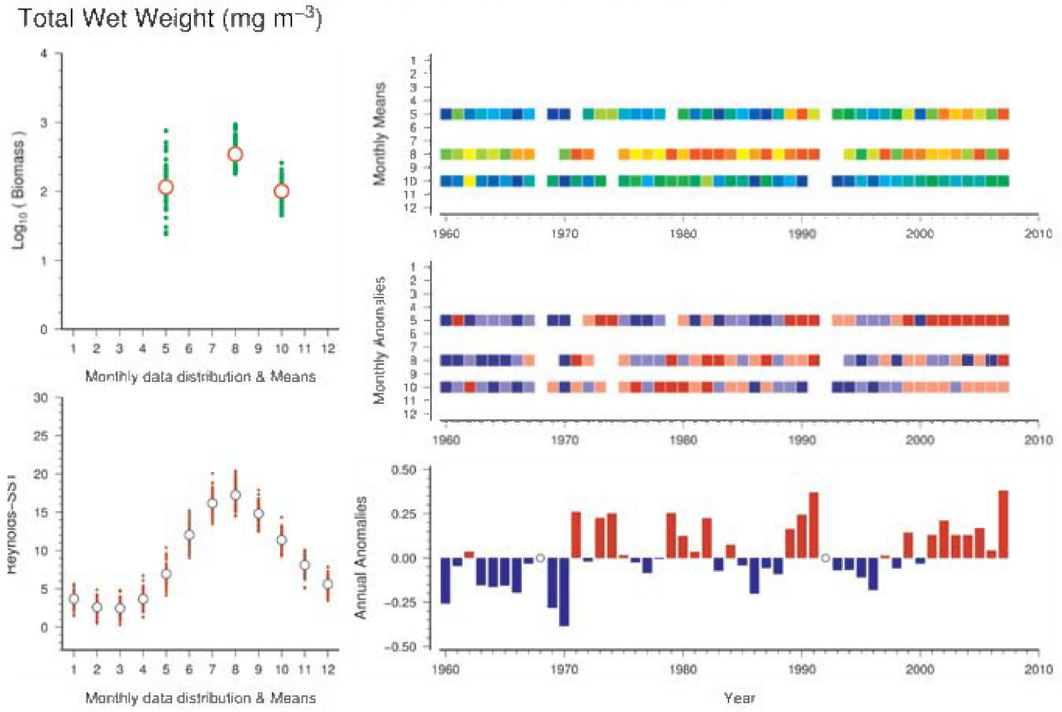

Figure 88.
Standardized WGZE time-series summary plot for total zooplankton wet weight in the eastern Gotland Basin. (See Section 2.1 for an explanation of the subplots in this figure.)

Eastern Gotland Basin (Central Baltic)

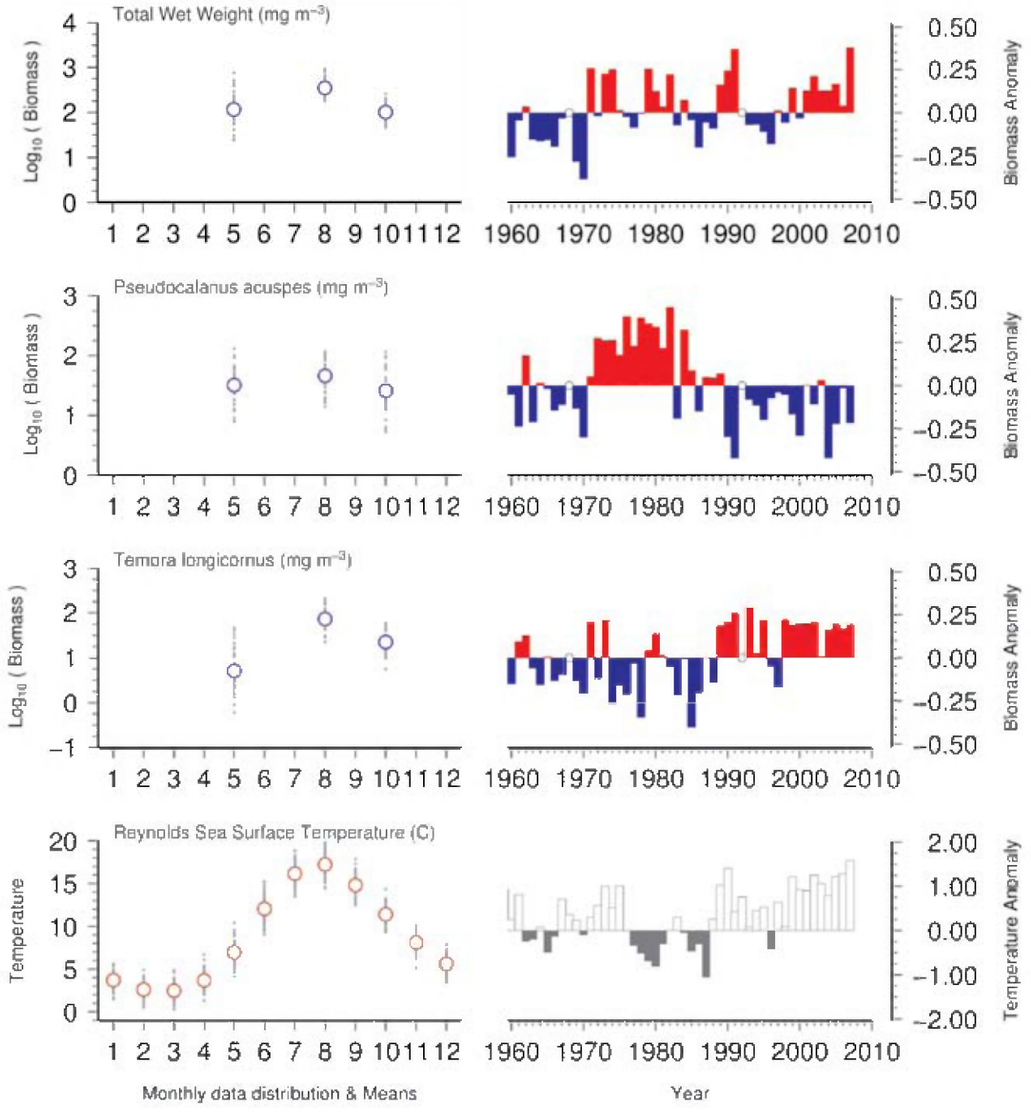

Figure 89.
Seasonal and interannual comparison of co-sampled variables in the eastern Gotland Basin. (See Section 2.2 for an explanation of the subplots in this figure.)

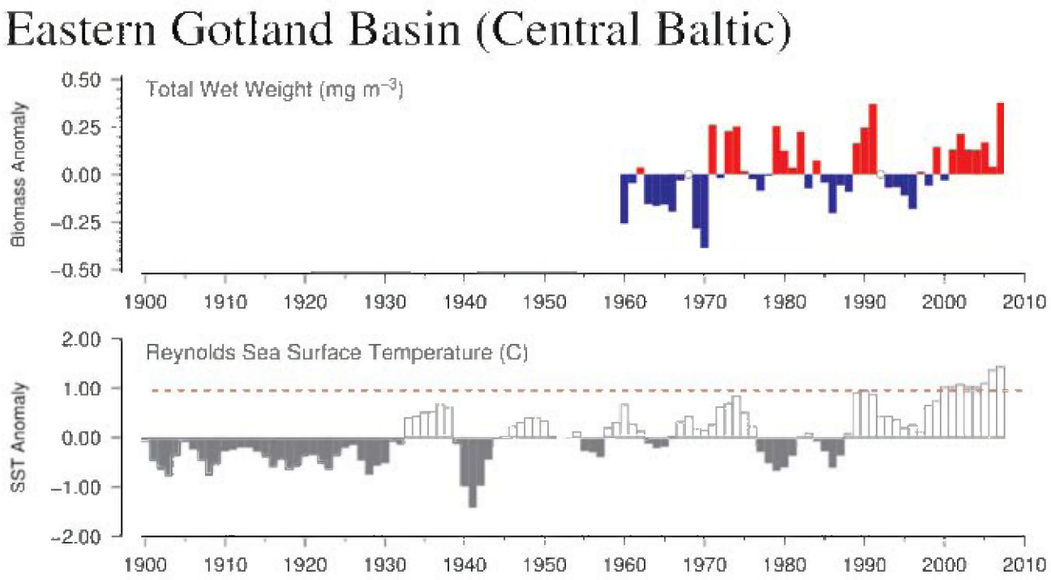

Figure 90.
Long-term comparison of eastern Gotland Basin total zooplankton wet weight with Reynolds sea surface temperatures for the region. CPR data were not available for this region (See Section 2.3 for an explanation of the subplots in this figure.)

Site 25: Arkona Basin (Southern Baltic Sea)

Lutz Postel

Figure 91.
Location of the Arkona Basin survey area (Site 25), plotted on a map of SeaWiFS chlorophyll concentration. Red/orange = high (productive), green/yellow = medium (moderate), blue = low (oligotrophic).

The Arkona Basin site (54°55'N 13°30'E, Figure 91) is one of six German monitoring stations in the Baltic, running from the Kiel Bight to the Eastern Gotland Basin. At the Arkona Basin site, zooplankton are collected five times a year, using a WP-2 net (56 cm diameter, 100 µm mesh) and sampling from the surface to a depth of 15–36 m (25 m average). Although sampling began in 1973, some years have been poorly sampled (e.g. 1995 and 1996). Maximum zooplankton abundance occurs during midsummer (Figure 92). The mesozooplankton community is dominated by *Acartia* spp. and *Pseudocalanus* spp. nauplii in early spring, followed by meroplanctonic larvae (polychaetes) in March. *Temora longicornis* nauplii and rotifers then dominate during early May, while the summer communities are dominated by bivalve larvae.

Mass development of rotifer populations are responsible for the peaks in total zooplankton abundance during spring of some years (Figure 92, top right, years 1980, 1985, 1988, 1995, 1998, 2000, 2002, and 2005–2006), particularly those that had especially mild conditions during the previous winter. During summer, when the water temperature reaches 16°C (HELCOM, 1996), the cladoceran *Bosmina coregonii* becomes the dominant species.

Chlorophyll was collected at standard depths and averaged for the 0–10 m layer at three locations surrounding the zooplankton sampling station. Chlorophyll concentration at the Arkona Basin site is usually high, with concentrations of over 2 µg l^{-1} during most of the year, reaching 6 µg l^{-1} during the spring bloom.

Water temperature, zooplankton abundance, and chlorophyll show a positive trend since the beginning of the time-series in 1979 (Figure 93). The long-term record in regional SST values (Figure 94) reveals that, since 1999, this region has experienced a particularly warm period, with temperatures higher than the 100-year maximum observed during 1900–2000 (Figure 94, bottom, red dashed line).

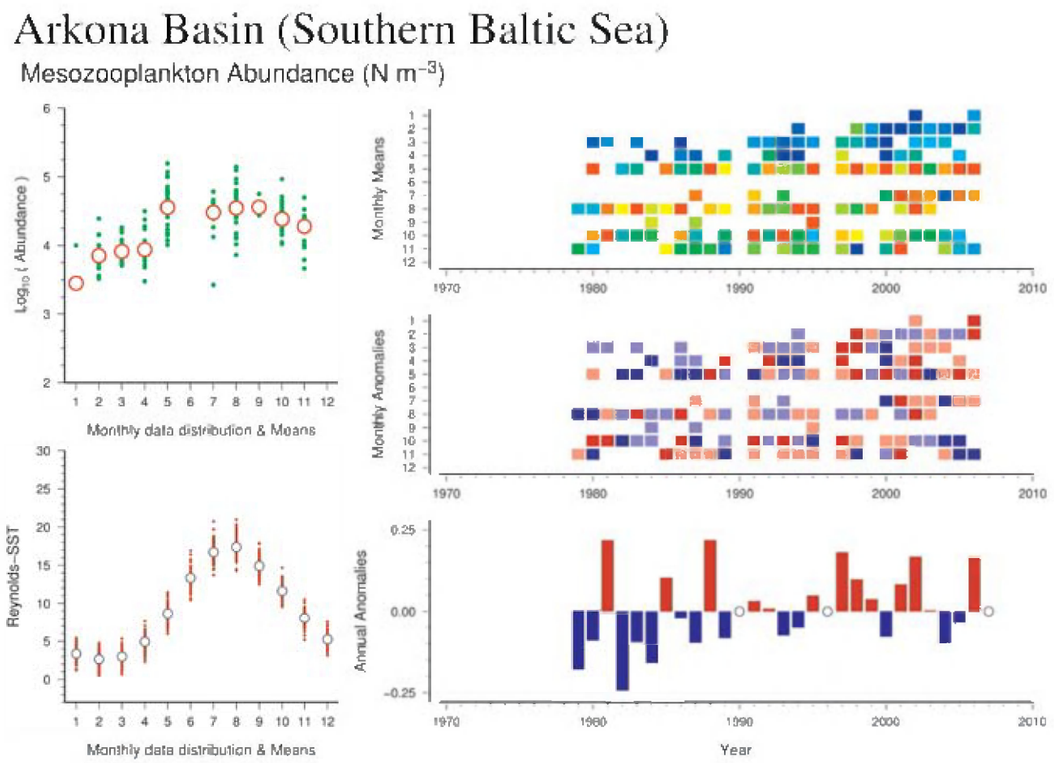

Figure 92.
Standardized WGZE time-series summary plot for mesozooplankton abundance at the Arkona Basin site. (See Section 2.1 for an explanation of the subplots in this figure.)

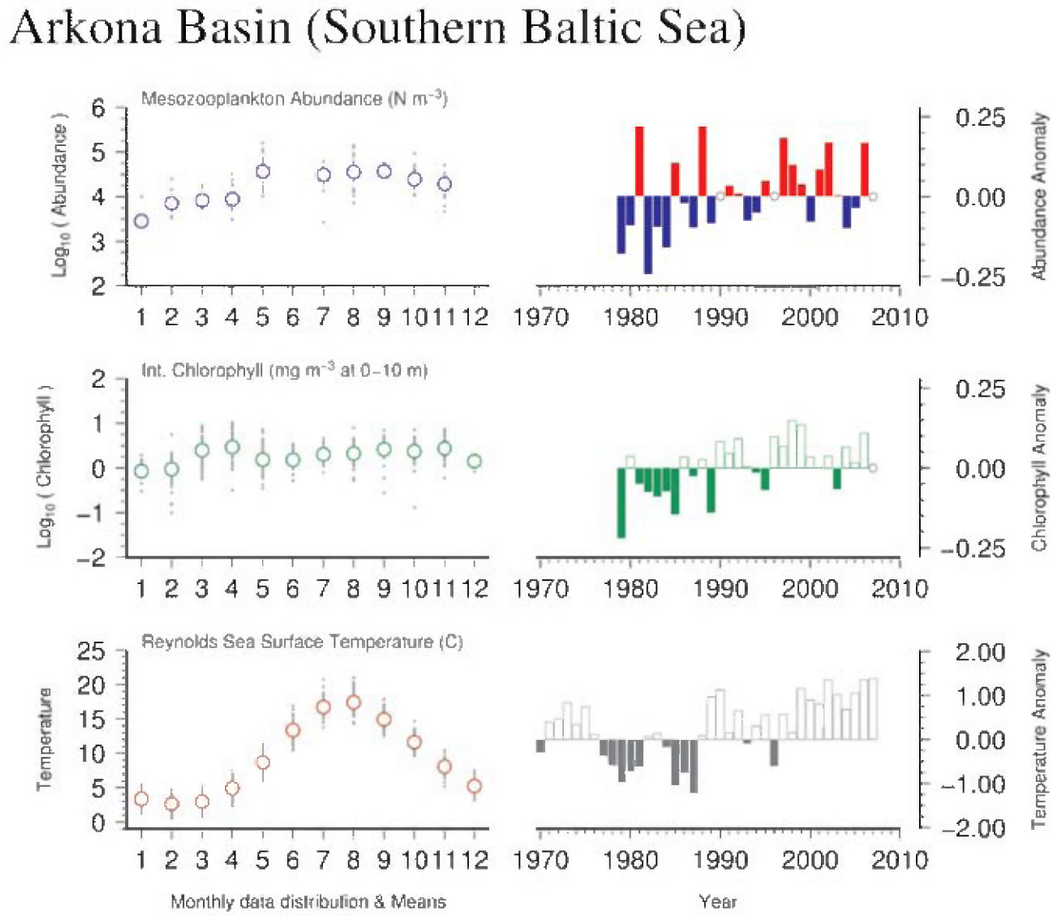

Figure 93.
Seasonal and interannual comparison of co-sampled variables at the Arkona Basin site. (See Section 2.2 for an explanation of the subplots in this figure.)

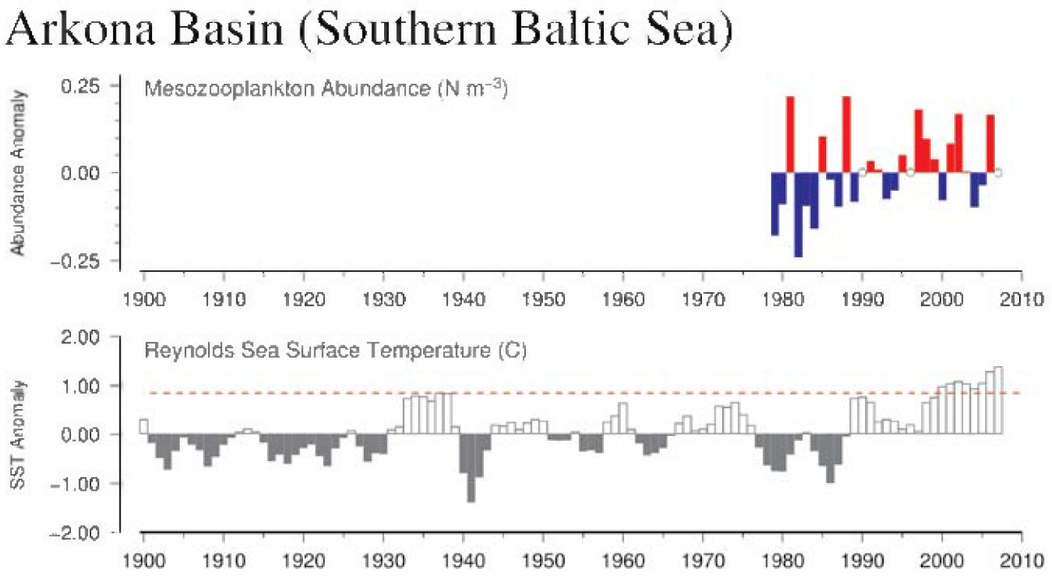

Figure 94.
Long-term comparison of Arkona Basin mesozooplankton abundance with Reynolds sea surface temperatures for the region. CPR data were not available for this region. (See Section 2.3 for an explanation of the subplots in this figure.)

Photo courtesy of Nancy J. Copley

3.5 North Sea and English Channel

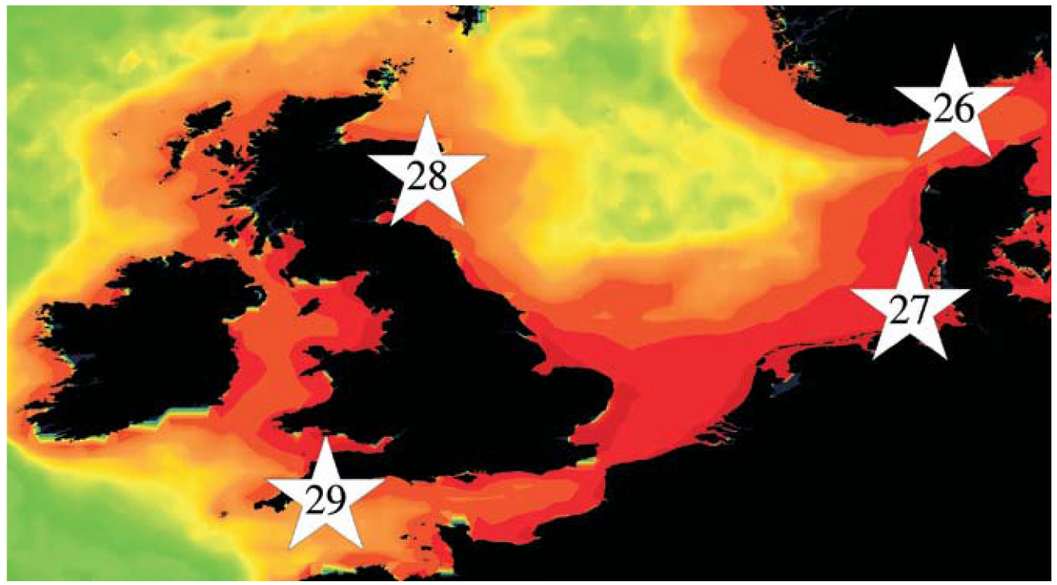

Figure 95.
Locations of North Sea and English Channel zooplankton time-series (Sites 26–29), plotted on a map of SeaWiFS average chlorophyll concentrations. Red/orange = high (productive), green/yellow = medium (moderate), blue = low (oligotrophic).

The North Sea and English Channel (Figure 95) are classified by Longhurst (1998) as part of the Northeast Atlantic Shelf Province (NASP). This province extends from northern Spain to Denmark and is separated from the Atlantic Subarctic Region by the Faroe–Shetland Channel and the Norwegian Trench. The NASP follows the classic plankton calendar for temperate regions: mixed conditions and light limitation in winter, a strong spring bloom that leads to nutrient limitation during the stratified summer (often broken up by tidal and shelf fronts), and a secondary bloom during autumn when mixing conditions break down the thermocline. The zooplankton in this region are characterized by a mixture of neritic and coastal species (Beaugrand *et al.*, 2002), with occasional and temporary influxes of oceanic species into shelf waters.

Site 26: Arendal Station 2 (Northern Skagerrak)

Tone Falkenhaug and Lena Omli

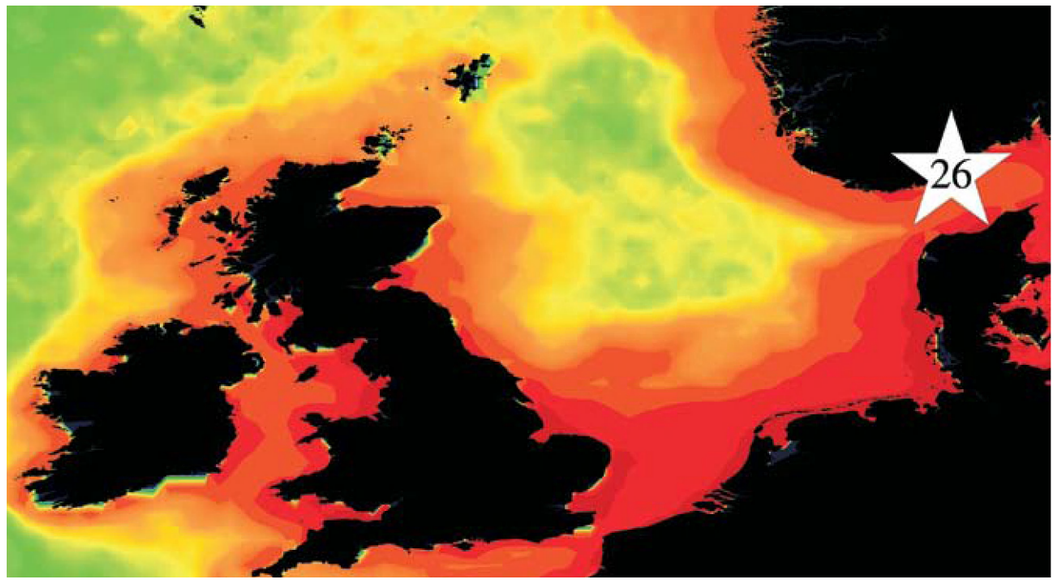

Figure 96.
Location of the Arendal survey area (Site 26), plotted on a map of SeaWiFS chlorophyll concentration. Red/orange = high (productive), green/yellow = medium (moderate), blue = low (oligotrophic).

The Arendal sampling site (northern Skagerrak) is located at 58°23′N 8°49′E, approximately one nautical mile offshore from the Flødevigen Research Station (Institute of Marine Research, IMR) off southern Norway (Figure 96). The water depth at the site is 105 m. Sampling for hydrographic parameters and abundance of phytoplankton and zooplankton (biomass and species) has been carried out twice a month since January 1994. Zooplankton is sampled fortnightly with a WP-2 net (56 cm diameter, 180 µm mesh) towed vertically from a depth of 50 m to the surface. Each sample is split in half, providing data on both species composition/abundance and biomass.

The seasonal maximum in zooplankton biomass generally occurs in April/May (Figure 97), with a secondary, smaller peak in the zooplankton occurring in July/August. Large differences can be seen between years in the observed biomass of zooplankton, with maximum values in 2003 and minimum values in 1998. A general increase in biomass and abundance was observed from 1998 to 2003, but a lower abundance overall was observed in 2004–2007 (Figure 97). The observed lower abundance in recent years is especially pronounced in the autumn peak (July/August). This is mainly caused by the reduced abundances of the copepods *Oithona* spp. and *Pseudocalanus* spp. in the period 2004–2007 (Figure 98).

The seasonal maximum in zooplankton biomass (April/May) is dominated by *Calanus finmarchicus* (Figure 98), whereas the secondary peak (July/August) is dominated by smaller copepods (*Pseudocalanus, Oithona, Acartia, Temora*). The important common copepod genus, *Calanus*, is represented

by three species at the Arendal sampling site: *C. finmarchicus*, *C. helgolandicus*, and *C. hyperboreus*. *C. finmarchicus* is the most abundant species during spring. This species overwinters in the Norwegian Deep (20 nautical miles farther offshore from this station), and interannual variability in overwinter survival is likely to affect the population dynamics. *C. helgolandicus* generally occurs in smaller numbers than *C. finmarchicus*, although the proportion of *C. helgolandicus* increases from spring (<10%) to autumn (>80%). *C. hyperboreus* is rarely observed in spring (March/April) and is associated with the influx of Atlantic water from the Norwegian Sea. The abundance and percentage of the top ten most abundant taxa at Station 2 are shown in Tables 9 and 10.

The Arendal sampling site is influenced by relatively fresh coastal waters (25–32 psu) in the upper 30 m and by saltier Skagerrak water (32–35 psu) in the greater depths. Water movement is generally westerly and is caused by the coastal current bringing low-salinity water from the Baltic Sea and Kattegat. The site is also influenced by Atlantic water (>35 psu) advected from the Norwegian Sea into the Skagerrak Deep during winter. Together, these influxes create a relatively large seasonal cycle in salinity (Figure 99).

The seasonal minimum temperature in the surface layer generally occurs in February (2°C) and the maximum in August (>20°C). At 75 m, the variation is less pronounced (minimum 4°C in February/March to maximum 14°C in August/September). Although the water column is mixed throughout the winter, increased fresh-water run-off causes a strong halocline to appear from February/March to June (Figure 99). A spring bloom usually occurs in April/March, dominated by diatoms. The chlorophyll values are generally low during summer (May–August), followed by an autumn bloom of dinoflagellates in August/September. In summer, the water remains stratified because of surface heating.

During the past 20 years, a trend towards higher temperatures has been observed in Skagerrak, both in surface and deeper layers. Since 2001, water temperatures in the region have been higher than previously seen in the past 100 years (Figure 100).

Table 9.

Rank	Taxa	% of total abundance 1994–2007	% of total zooplankton 2007	(Δ)	Mean abundance (N m^{-3}) 1994–2007	Abundance (N m^{-3}) 2007	(Δ%)
1	*Oithona* spp.	42.7	35.3	(–7.3)	65 586	32 165	(-51)
2	Mollusca	22.0	25.4	(3.4)	33 883	23 173	(-32)
3	*Pseudocalanus* sp.	13.5	21.2	(7.7)	20 819	19 328	(-7)
4	*Calanus* spp.	8.1	3.1	(–5.0)	12 512	2 819	(–77)
5	*Temora longicornis*	4.5	7.0	(2.5)	6 851	6 345	(–7)
6	Calanoid copepod nauplii	3.7	4.9	(1.2)	5 625	4 452	(–21)
7	*Centropages* spp.	2.0	1.1	(–0.9)	3 070	1 002	(–67)
8	*Acartia longicornis*	0.9	0.0	(–0.9)	1 433	9	(–99)
9	Cladocera	0.9	0.8	(–0.1)	1 379	766	(–44)
10	*Microcalanus pusillus*	0.5	0.3	(–0.1)	740	308	(–58)
	"Top ten" totals	**98.8**	**99.2**	**(0.4)**	**151 897**	**90 367**	**(–41)**
	Total abundance of all zooplankton (N m^{-3})				**880.1**	**1 131.8**	**(–40)**

Table 9.
Average abundance and relative dominance (percentage of the total zooplankton collected) of the top ten most abundant zooplankton taxa collected at Arendal Station 2 in previous years (1994–2007) compared with that collected in 2007. Colours in the "Δ" and "Δ%" columns indicate either an increase (red) or decrease (blue) in relative dominance from previous years.

Table 10.

Rank	Taxa	% of total abundance 2007	Abundance (N m^{-3}) 2007
1	Calanoid copepods (except *Calanus*)	25.0	23 117
2	**Cyclopoid copepods**	**20.9**	**19 328**
3	Mollusca	20.3	18 823
4	Cladocera	6.9	6 345
5	*Calanus* spp.	6.2	5 721
6	Calanoid copepod nauplii	4.8	4 452
7	**Echinoderm larvae**	**4.7**	**4 365**
8	**Ostracoda**	**3.4**	**3 108**
9	**Cirripede larvae**	**3.0**	**2 819**
10	**Euphausiacea nauplii**	**1.3**	**1 196**
	"Top ten" totals	**92.5**	**89 273**
	Total abundance of all zooplankton (N m^{-3})		**92 607**

Table 10
Abundance and relative dominance (percentage of the total zooplankton collected) of the top ten most abundant zooplankton taxa collected at Arendal Station 2 in 2007. Bold entries indicate new taxa dominant in 2007, but not previously dominant in the 1994–2007 time-series (see Table 9).

Arendal Station 2 (Northern Skagerrak)

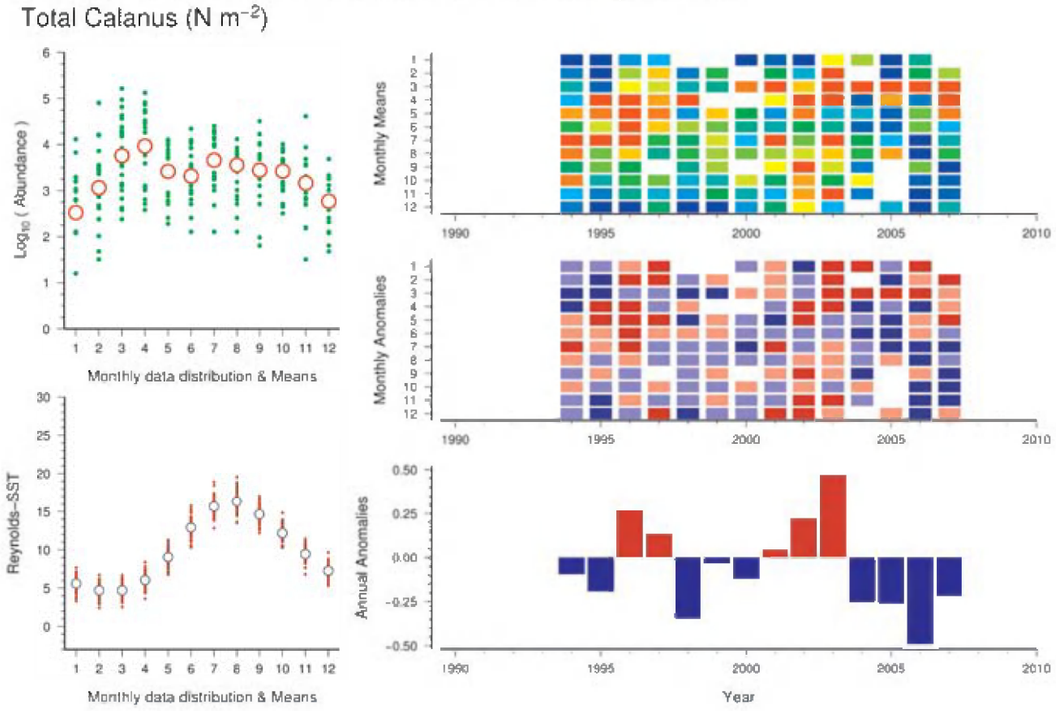

Figure 97.
Standardized WGZE time-series summary plot for Calanus *abundance at Arendal Station 2. (See Section 2.1 for an explanation of the subplots in this figure.)*

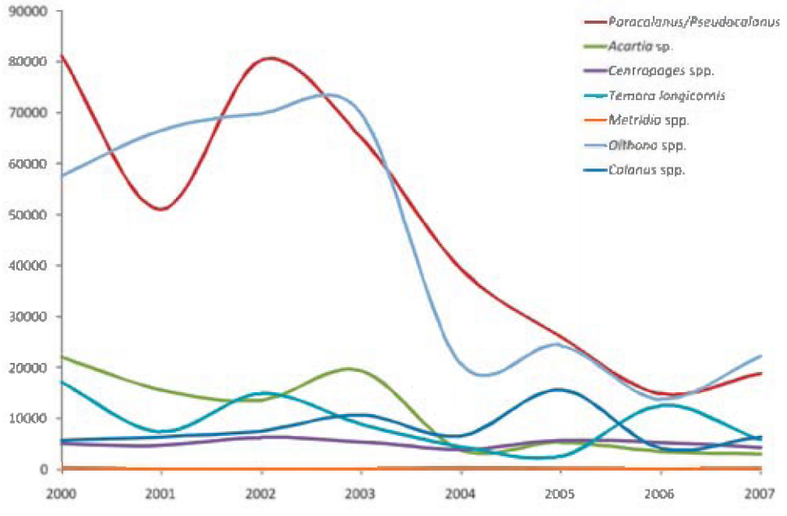

Figure 98.
Yearly averages of selected copepod species (N m⁻³) at Arendal Station 2.

Arendal Station 2 (Northern Skagerrak)

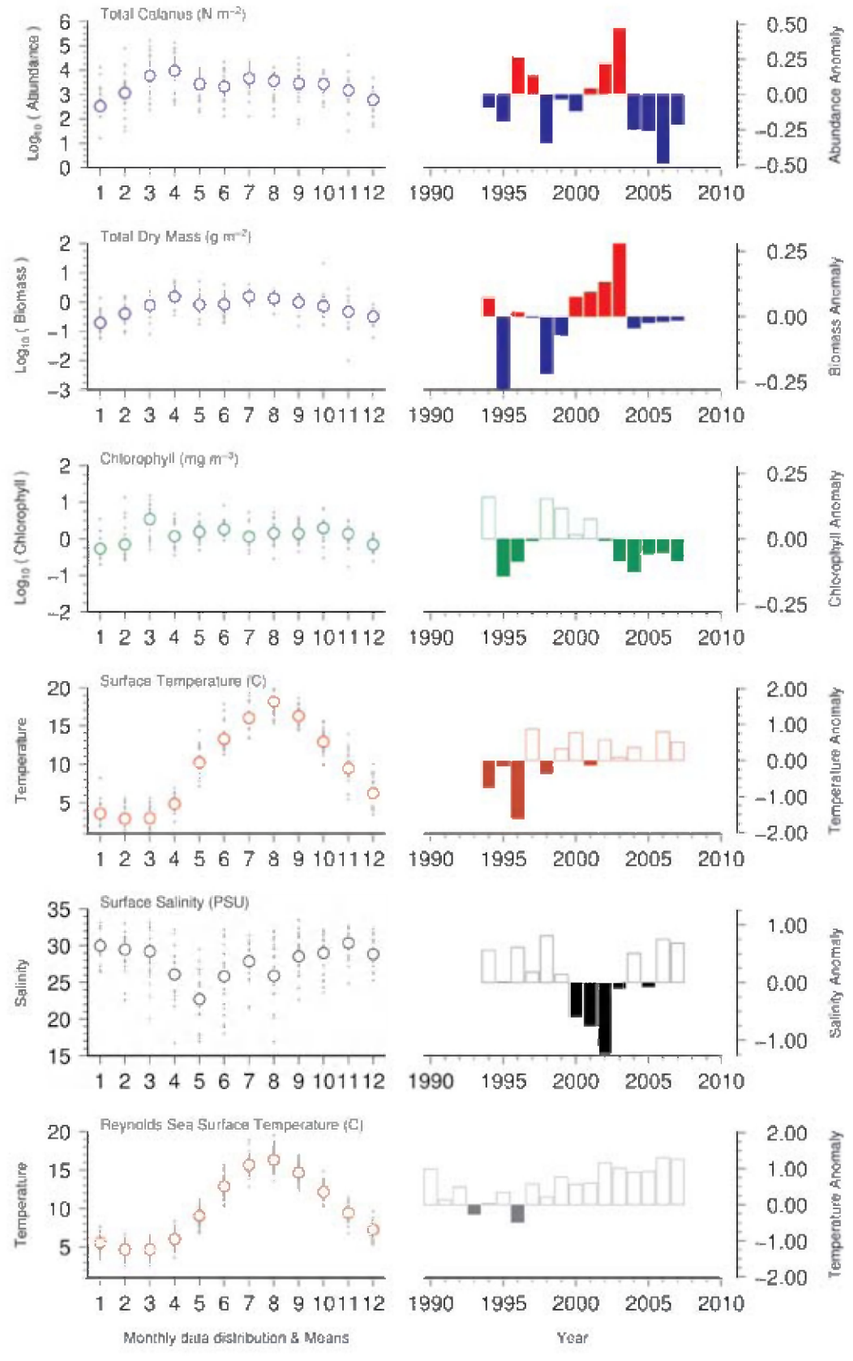

Figure 99.
Seasonal and interannual comparison of co-sampled variables at Arendal Station 2. (See Section 2.2 for an explanation of the subplots in this figure.)

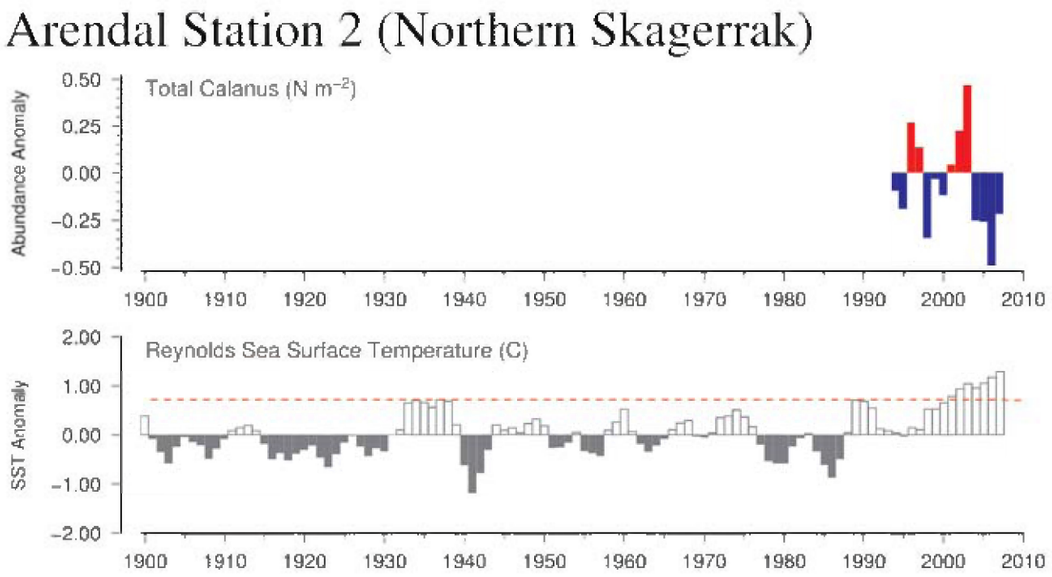

Figure 100.
Long-term comparison of Arendal Calanus *abundance with Reynolds sea surface temperatures for the region. CPR data were not available for this region. (See Section 2.3 for an explanation of the subplots in this figure.)*

Site 27: Helgoland Roads (Southeastern North Sea)

Maarten Boersma

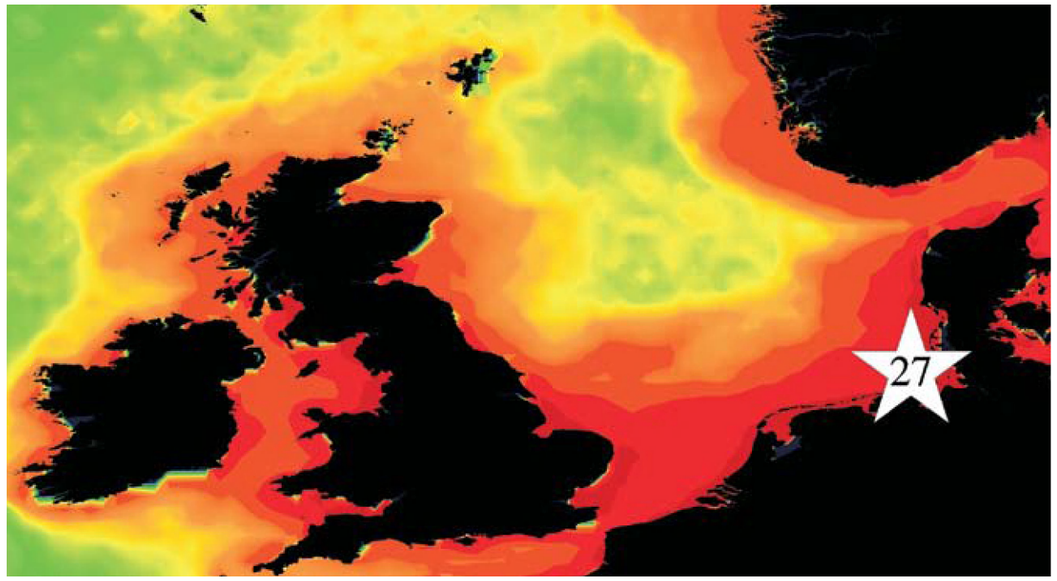

Figure 101.
Location of the Helgoland Roads survey area (Site 27), plotted on a map of SeaWiFS chlorophyll concentration. Red/orange = high (productive), green/yellow = medium (moderate), blue = low (oligotrophic).

The Helgoland Roads time-series was started in 1975 by Wulf Greve, initially at the Biologische Anstalt Helgoland Institute and later continued in cooperation with the German Centre for Marine Biodiversity and the Federal Maritime and Hydrographic Agency. Every Monday, Wednesday, and Friday, two oblique plankton net samples (150 µm and 500 µm mesh) are collected from the monitoring site, which is located at 54°11′18″N 7°4′E (Figure 101). From each sample, almost 400 taxonomic entities of holoplankton and meroplankton (e.g. benthic and fish larvae) are identified and counted for abundance, making the Helgoland Roads time-series one of the finest WGZE sites in both taxonomic and sampling resolution.

The purpose of the Helgoland Roads programme is to monitor and document high-frequency plankton population dynamics for the recognition of variances and irregularities in distributions, such as changes in biodiversity caused by external factors. The wealth of publications and materials available from the site cover the use of several analytical techniques, the types of information extracted from the data, and models on prognosis for zooplankton dynamics on several time-scales (e.g. Greve *et al.*, 2001, 2004; Heyen *et al.*, 1998; Johannsen *et al.*, 1999; Wiltshire *et al.*, 2008).

At the Helgoland Roads sampling site, small copepods, mostly *Acartia clausi*, *Temora longicornis*, and *Pseudocalanus* spp., represent a significant fraction of the total zooplankton population. Seasonal and interannual variations in the numbers of small copepods are large, both in timing and magnitude. In most years, maximum density occurs in midsummer (Figure 102, top left), and the 30-year time-series reveals clear decadal variability (Figure 102, bottom right). Starting with a negative phase at the beginning of the time-series (1975), copepod abundance increased steadily and was consistently higher than average during much of the 1980s. After a period of transition (1990–1997), copepod density decreased and has remained in a negative phase, where abundance is consistently low.

Values for the monthly mean copepod abundance by year (Figure 102, top right) reveal that years with a strong positive annual anomaly (e.g. 1983–1988) are characterized by an extended period of high maximum abundance in midsummer, whereas years with a strong negative annual anomaly (e.g. 2003–2006) have a shorter period of lower maximum abundance during midsummer. Values for monthly anomalies (Figure 102, middle right) reveal that, in years with a strong positive annual anomaly, all the monthly anomalies

are positive, whereas, in years with a strong negative annual anomaly, the opposite is true (i.e. the monthly anomalies are generally negative). The extent of peak abundance each year is therefore most greatly influenced by the copepod population density during the winter months, leading up to the summer peak.

Average SST anomalies in the Helgoland Roads over the past 100 years reveal that the average water temperatures at the site have been at or above the 100-year maximum (Figure 103, bottom, red dashed line) since 2000. Anomalies in SST values and small copepod abundance seem to be inversely related, with the lowest copepod abundance occurring during the past few years of highest water temperatures. Further research is needed to determine whether this is due to a direct causal relationship (i.e. biophysical factors within the copepod organisms) or the effect of temperature on food availability or predator pressure.

The CPR standard area nearest to Helgoland Roads is "D1" (Figures 2 and 101). The relationship between water temperature and CPR copepod abundance (Figure 103) has been variable, switching from positive to negative throughout periods in the time-series. Like the Helgoland Roads data, the CPR data clearly show that copepod abundance has entered a phase of negative and decreasing annual anomalies since 1988. A comparison of the Helgoland Roads and CPR data suggests a time-lagged synchrony in copepod abundance, with the Helgoland Roads abundance anomalies being ahead of the CPR anomalies by 3–5 years. Increases in water temperature around the shallow Helgoland Roads site have been more dramatic than those in the North Sea as a whole, which may account for the changes in the copepod population occurring more rapidly than in those sampled in the larger water body within the CPR standard area.

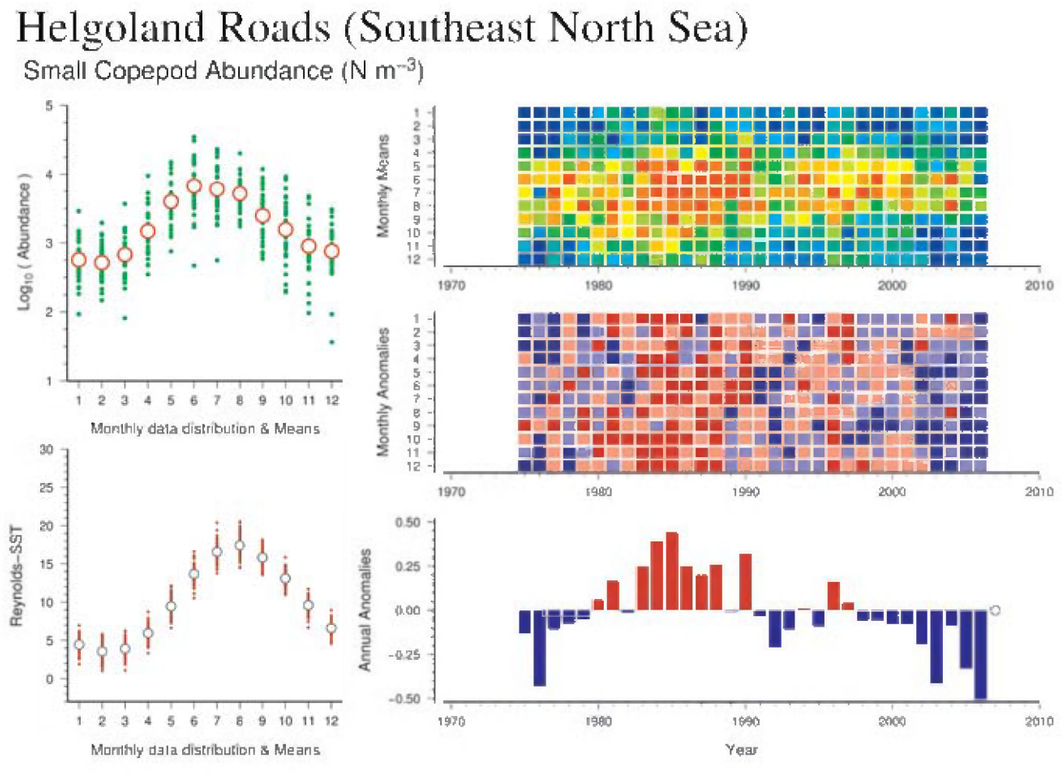

Figure 102.
Standardized WGZE time-series summary plot for small copepod abundance at the Helgoland Roads site. (See Section 2.1 for an explanation of the subplots in this figure.)

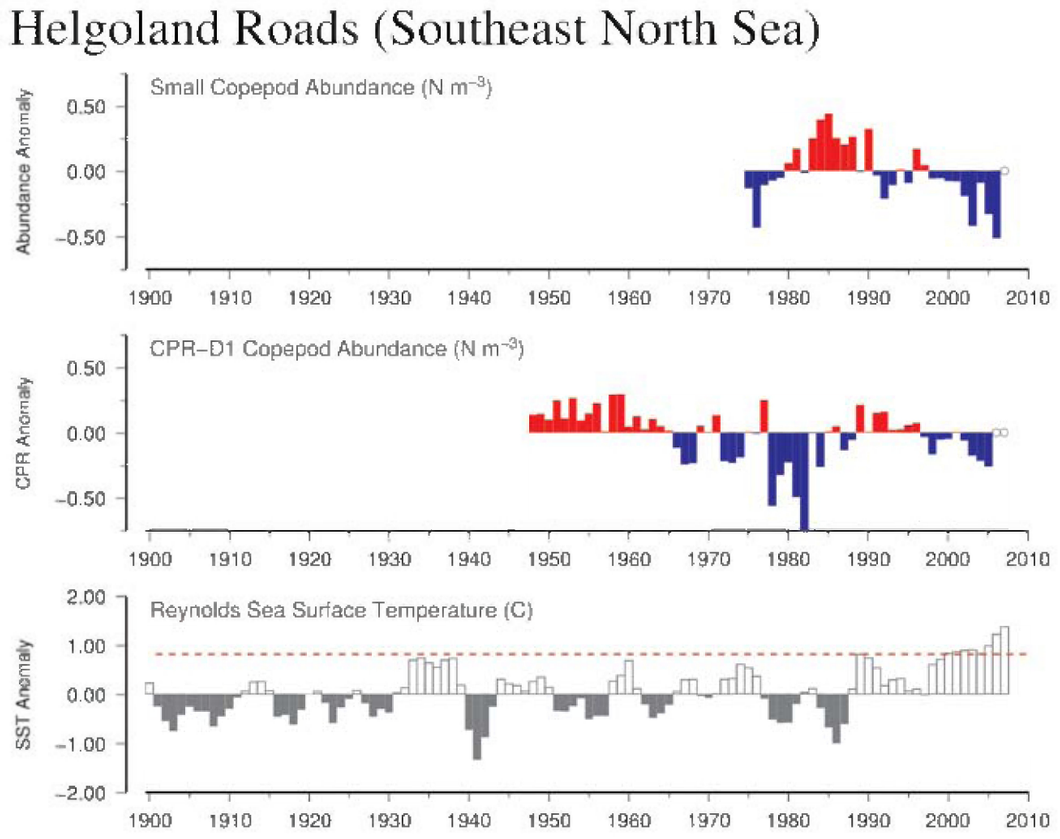

Figure 103.
Long-term comparison of Helgoland Roads small copepod abundance with copepod abundance in CPR standard area "D1" and Reynolds sea surface temperatures for the region. (See Section 2.3 for an explanation of the subplots in this figure.)

Site 28: Stonehaven (Northwestern North Sea)

Steve Hay

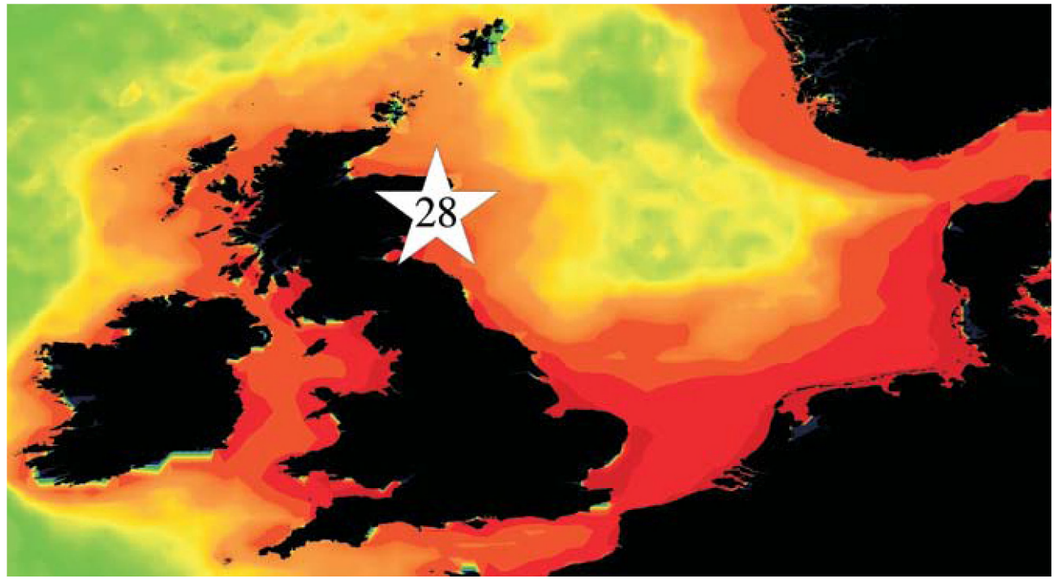

Figure 104.
Location of the Stonehaven survey area (Site 28), plotted on a map of SeaWiFS chlorophyll concentration. Red/orange = high (productive), green/yellow = medium (moderate), blue = low (oligotrophic).

The Stonehaven sampling site is located at 56°57.80′N 02°06.20′W (Figure 104), approximately 5 km offshore from Stonehaven, a small town 28 km south of Aberdeen, in a water depth of 50 m. Sampling for hydrographic parameters, concentrations of inorganic chemical nutrients, and the abundance of phytoplankton and zooplankton species has been carried out weekly off Stonehaven since January 1997. Zooplankton are collected using a bongo net (40 cm diameter, 200 µm mesh) and flow meter, and, since 1999, detailed taxonomic analysis has been carried out on the mesozooplankton and phytoplankton samples. The objective of the sampled time-series is to establish a monitoring base for assessing the status of the Scottish coastal ecosystem and to gauge responses to climate change. Comparison of the results with archive regional data on temperature, salinity, nutrients, and phytoplankton biomass (chlorophyll *a*) indicates that the site provides a reliable index of the state of the coastal waters. The biological data illustrate the consistencies and variability in seasonal succession of plankton species and their abundance. It is evident that there are significant differences among seasons and years.

The water column at the sampling site remains well mixed throughout much of the year, with the exceptions of summer and autumn, when surface heating and settled weather often cause temporary thermoclines to appear. The seasonal minimum temperature of around 6°C generally occurs in late February/early March and rises to ~12–14°C in August (Figure 105, bottom left). Water movement is generally southerly, with quite strong tidal currents and a local tidal excursion of around 10 km. The origins of the water passing down the Scottish east coast lie to the north and west of Scotland and are a variable mix of coastal and oceanic Atlantic waters. Throughout late summer and autumn, the sampled salinity and species indicate a variable, but often significant, increase in the proportion of Atlantic Ocean water passing the site. The wider northern North Sea has demonstrated a slight warming trend over the past 50 years, with temperatures in the past six years being higher than those seen over the past 100 years (Figure 107, bottom, red dashed line). From hydrographic data measured directly at the Stonehaven site, temperature tends to vary smoothly and is correlated with salinity, but the salinity pattern shows considerably more annual variation.

The Stonehaven time-series samples are collected consistently and at a relatively high frequency, affording an insight into the seasonal dynamics and succession of zooplankton species throughout the annual cycle. This time-series dataset provides an excellent background and context both for experimental work and for more intense or focused studies of individual species groups, ecosystem dynamics, and rates and processes. Strong support is provided for model development and validation, although comparisons with other monitoring sites provide assessments of local variability and consideration of the local effects of broader patterns of ocean climate change.
At the temperate UK Stonehaven site, the annual cycles are evident in all the measured variables (Figure 106). The concentration of nitrate, a vital nutrient, rises as it is replenished during winter, when both light levels and temperature are low. The nitrate concentration then falls, often abruptly, with the growth of the spring phytoplankton bloom. This growth uses up nitrate and other nutrients, and accelerates as sea temperature increases. Throughout summer, these plants, which are nitrogen-dependent, rely on the regenerated nitrate supplied by microbial action and from the ammonia excreted by zooplankton.

Zooplankton, in turn, feed on phytoplankton and each other, and increase in abundance after the spring bloom. Later, after a summer peak that coincides with peak temperature, zooplankton abundance declines as winter approaches and food again becomes scarce. In order to survive winter, some species build up oil reserves, whereas others rely on eggs. Some common neritic copepods, such as *Temora longicornis* and *Acartia clausi*, lay eggs that lie dormant on the seabed during winter. Other species, such as the copepod *Centropages typicus* and the planktonic mollusc *Spiratella retroversa*, are not resident throughout winter, but are reseeded each year, carried by the circulation and influx of mixed coastal and oceanic waters from the north and from areas south and west of Scotland. Although the patterns are broadly consistent, the dynamics of seasonal population cycles vary between years for both the environmental and species components of the ecosystem.

Several zooplankton species are of particular interest because they may be biomass dominants or indicators of changing conditions. Several demonstrate wide variations in their annual abundance patterns. Overall copepod abundance was lower than average in 1997 and 1998 and higher in 2002 and 2003. An example of this variation is the important copepod genus *Calanus*, which is represented by two species in Scottish seas: *C. finmarchicus* and *C. helgolandicus*. Historically most abundant in spring and summer, the arctic boreal *C. finmarchicus* is an important species with a large spring influx, arising from the winter diapause in deeper waters off the edge of the continental shelf. This species provides food for many fish larvae in spring. However, there has been a decline in the abundance of *C. finmarchicus*, whereas *C. helgolandicus*, a more southerly species, generally most productive in summer and autumn, has shown evidence of increased abundance and productivity in this region, and has become approximately ten times more abundant. Indeed, *C. helgolandicus* had become one of the top ten most numerically abundant species by 2007 (Tables 11 and 12).

Another example is the copepod species *Eucalanus crassus*, which has been seen regularly in small numbers at Stonehaven since 2003, mainly in autumn. A fairly common species southwest of the UK, it was very rare east of Scotland. This indicates an environmental change that now permits its survival in the area, most probably an increased influx and persistence of warmer waters throughout late summer. Copepod abundance at Stonehaven has increased fairly steadily over the past ten years. Comparison with CPR data from the same region (Figure 107) suggests that this may reflect part of a positive phase in a multiyear (~10-year) cycle of variation.

Data from the Stonehaven site are regularly processed in the database of the Fishery Research Services Marine Laboratory at Aberdeen (FRS MLA), and some of these data are displayed on the MLA website, www.frs-scotland.gov.uk/Delivery/standalone.aspx?contentid=1144.

Table 11.

Rank	Taxa	% of total abundance 1999–2007	% of total zooplankton 2007	(Δ)	Mean abundance (N m^{-3}) 1999–2007	Abundance (N m^{-3}) 2007	(Δ%)
1	*Acartia clausi*	30.8	30.3	(–0.5)	703.3	632.1	(-10)
2	*Pseudocalanus elongatus*	11.6	13.0	(1.4)	251.8	271.9	(8)
3	*Oithona* spp.	9.7	11.8	(2.0)	242.1	245.7	(1)
4	Appendicularia	7.4	4.1	(–3.3)	144.6	85.3	(–41)
5	*Temora longicornis*	6.4	3.7	(-2.6)	140.0	78.1	(–44)
6	Lamellibranch larvae	4.7	0.5	(-4.2)	84.4	9.7	(–88)
7	Polychaete larvae	3.2	2.8	(–0.5)	64.7	57.9	(–10)
8	*Paracalanus parvus*	2.4	3.6	(1.2)	55.4	75.1	(35)
9	Cyphonautes larvae (Bryozoa)	2.4	2.5	(0.1)	49.1	51.5	(5)
10	Echinoderm larvae	2.3	0.9	(–1.5)	49.1	17.7	(–64)
	"Top ten" totals	**81.0**	**73.1**	**(-7.9)**	**1 784.6**	**1 525.0**	**(–15)**
	Total abundance of all zooplankton (N m^{-3})				**2 217.8**	**2 088.0**	**(-6)**

Table 11.
Average abundance and relative dominance (percentage of the total zooplankton collected) of the top ten most abundant zooplankton taxa collected at Stonehaven in previous years (1999–2007) compared with that collected in 2007. Colours in the "Δ" and "Δ%" columns indicate either an increase (red) or decrease (blue) in relative dominance from previous years.

Table 12.

Rank	Taxa	% of total abundance 2007	Abundance (N m^{-3}) 2007
1	*Acartia clausi*	30.3	632.1
2	*Pseudocalanus elongatus*	13.0	271.9
3	*Oithona* spp.	11.8	245.7
4	Appendicularia	4.1	85.3
5	*Temora longicornis*	3.7	78.1
6	*Paracalanus parvus*	3.6	75.1
7	*Calanus* spp. (C1–4)	3.6	74.2
8	Polychaete larvae	2.8	57.9
9	*Calanus helgolandicus* (C5–6)	2.5	52.7
10	Cyphonautes larvae (Bryozoa)	2.5	51.5
	"Top ten" totals	**77.8**	**1 624.4**
	Total abundance of all zooplankton (N m^{-3})		**2 088.0**

Table 12.
Abundance and relative dominance (percentage of the total zooplankton collected) of the top ten most abundant zooplankton taxa collected at Stonehaven in 2007. Bold entries indicate new taxa dominant in 2007, but not previously dominant in the 1999–2007 time-series (Table 11).

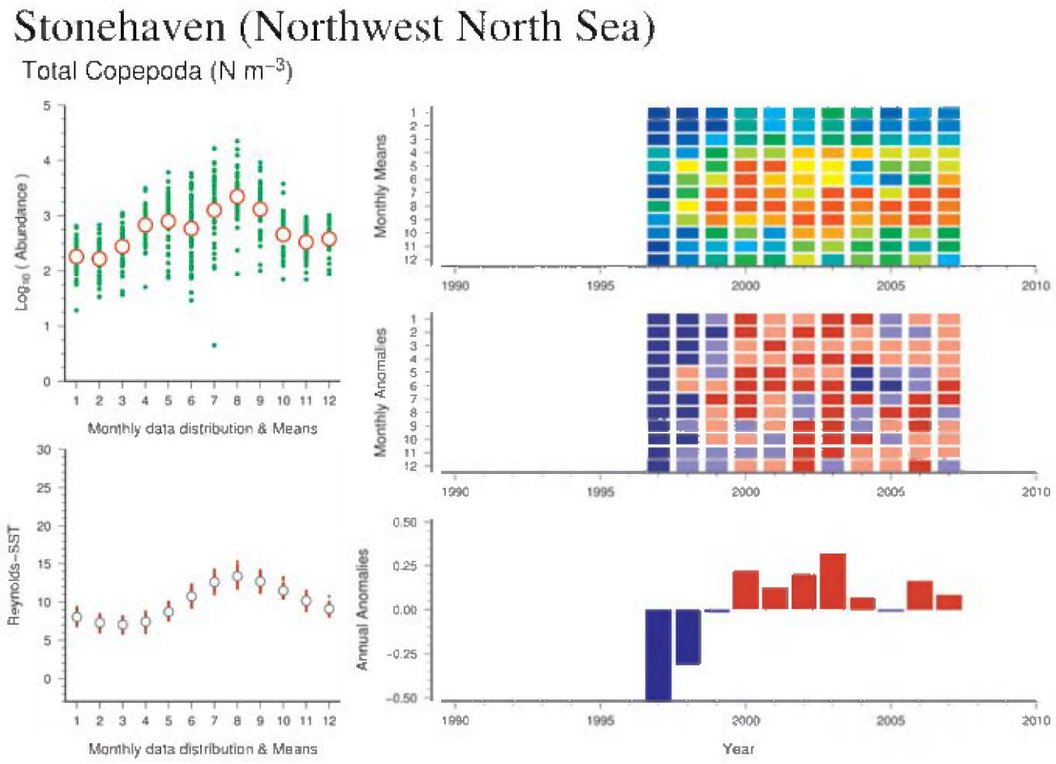

Figure 105.
Standardized WGZE time-series summary plot for copepod abundance at the Stonehaven site. (See Section 2.1 for an explanation of the subplots in this figure.)

Stonehaven (Northwest North Sea)

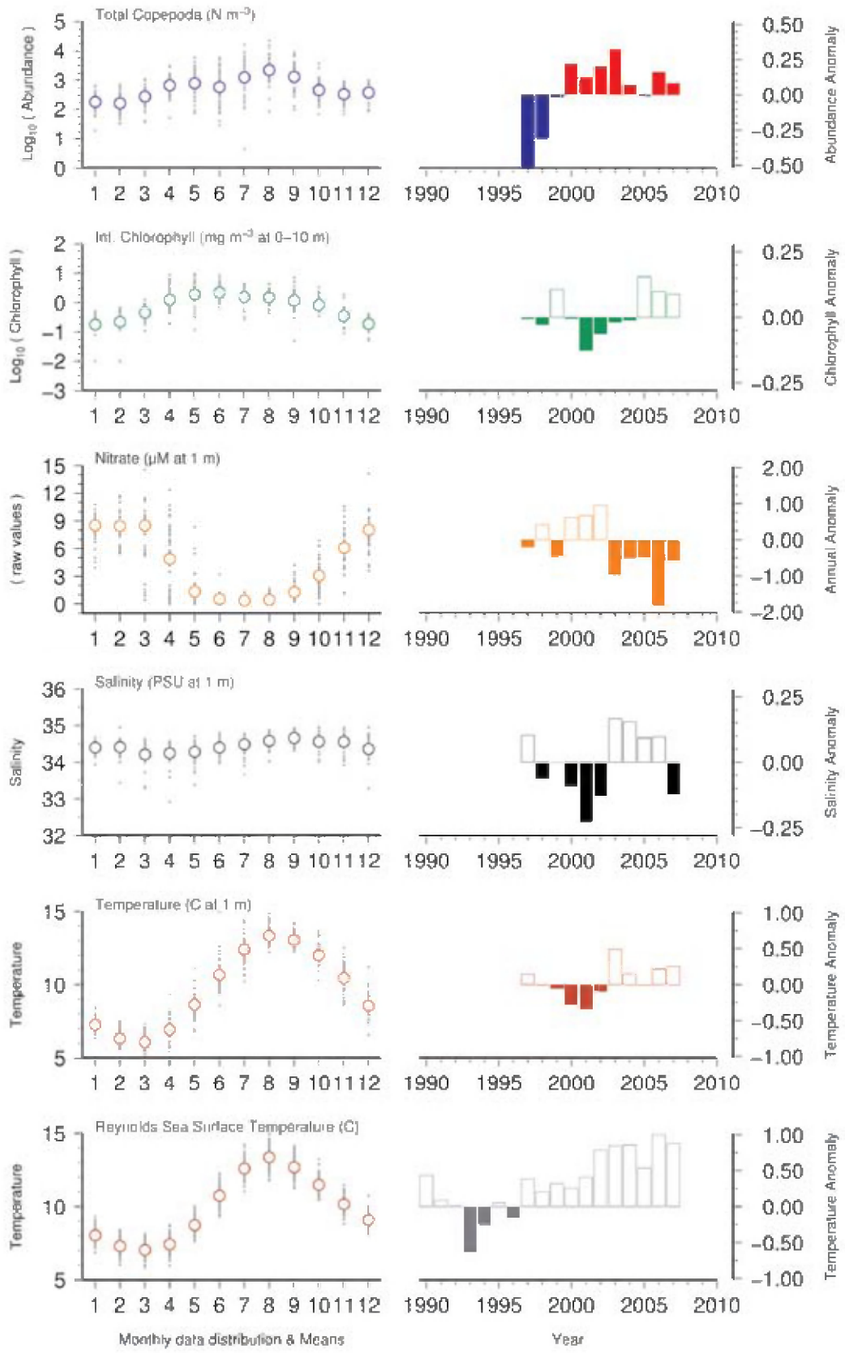

Figure 106.
Seasonal and interannual comparison of co-sampled variables at the Stonehaven site. (See Section 2.2 for an explanation of the subplots in this figure.)

Stonehaven (Northwest North Sea)

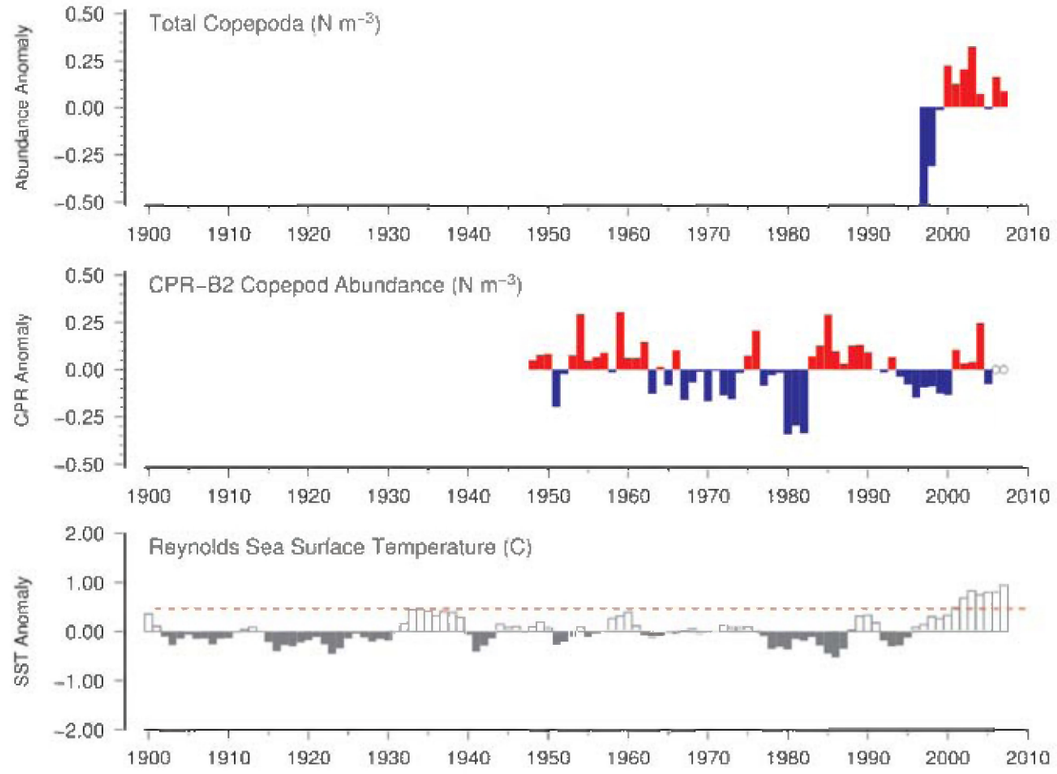

Figure 107.
Long-term comparison of Stonehaven copepod abundance with copepod abundance in CPR standard area "B2" and Reynolds sea surface temperatures for the region. (See Section 2.3 for an explanation of the subplots in this figure.)

Site 29: Plymouth L4 (English Channel)

Roger Harris

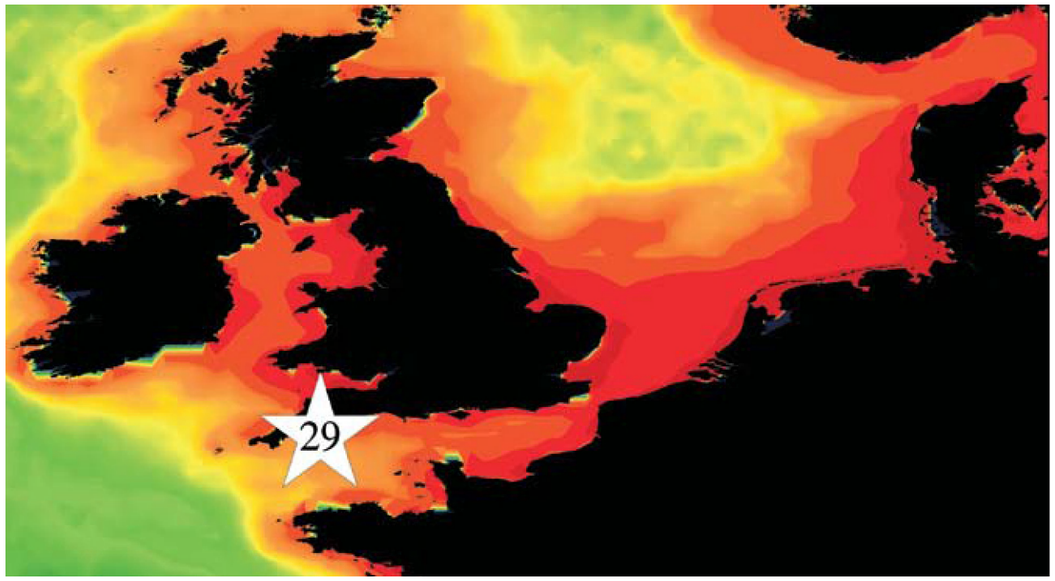

Figure 108.
Location of the Plymouth L4 survey area (Site 29), plotted on a map of SeaWiFS chlorophyll concentration. Red/orange = high (productive), green/yellow = medium (moderate), blue = low (oligotrophic).

Plymouth Station L4 (4°13′W 50°15′N) is located about 16 km southwest of Plymouth in the western English Channel (Figure 108). The station is about 50 m deep and is influenced by seasonally stratified and transitional mixed–stratified waters (Pingree and Griffiths, 1978). Since 1988, zooplankton have been collected on a weekly basis using a WP-2 net (56 cm diameter, 200 µm mesh) towed vertically from the seabed (~54 m depth) to the surface. Samples are split, and organisms are counted and identified to major taxonomic groups and families. For some groups, particularly copepods, organisms are identified at species level; sex and life stages are determined for some targeted species (e.g. *Calanus helgolandicus*). The SST has been measured since the beginning of the time-series, using a mercury-in-glass thermometer immersed in an aluminium bucket of water collected at the surface. Since 1992, water samples collected from a depth of 10 m with a Niskin bottle have been analysed to determine abundance and estimate carbon biomass of phytoplankton and microzooplankton. Organisms are counted and identified at genus or species level using inverted microscopy. At the same time, chlorophyll *a* triplicate measurements are made using a Turner fluorometer after filtering of sea surface water samples and extraction. Additionally, since 2002, water column profiles of CTD measurements have also been available for temperature, salinity, and fluorescence. The L4 data are maintained at the Plymouth Marine Laboratory and are available online at the Western Channel Observatory website, www.pml.ac.uk/.

The seasonal cycle of SST is characterized by strong seasonality, with a winter minimum of 9±1°C in March and a summer maximum of 17±1.5°C in August (Figure 109). The water column is subject to a weak seasonal stratification, with a thermocline temperature difference of 2–3°C in summer. The seasonal cycle of chlorophyll *a* and phytoplankton are both characterized by two peaks. The first occurs during late April/early May, with an intense, short period corresponding to the spring diatom bloom, followed by a second peak in late summer/early autumn, with a lower magnitude, but a longer period (~2 months), corresponding to the late summer dinoflagellate bloom (Figure 109). The seasonal cycle of zooplankton is characterized by a maximum peak in abundance in April, followed by a slight decrease until August, when the summer phytoplankton bloom leads to a second increase in zooplankton abundance (Figure 110). Zooplankton abundance remains variable until October, followed by a decrease in November/December, with the lowest abundance in January/February, which also corresponds to the lowest values in chlorophyll *a* and phytoplankton abundance (Figure 109).

The mesozooplankton community at L4 is dominated by copepods, which represent 69–74% of the total zooplankton abundance and are the most abundant species in the top ten species ranking (Table 13). Each year, the ten species listed in this table (out of more than 70 different species and groups identified at the site) have represented more than 80% of the total zooplankton population, and their relative composition has remained fairly constant over the 20 years of the time-series. In contrast, the major phytoplankton groups show clearly visible trends in their composition, with diatom abundance decreasing and coccolithophores abundance increasing (Figure 109). It is possible that copepod abundance may be following phytoplankton abundance (with a 1–2 year lag) and this should be investigated further.

Although the community composition seems to be stable, the interannual variation in zooplankton abundance is important, but does not demonstrate any long-term trend. Nevertheless, periods with high abundance are observable (e.g. 2000/2004, see Figure 110), but do not seem to be related to temperature or phytoplankton variations (Figure 109). Furthermore, zooplankton abundance observed at L4 is not synchronized with the CPR abundances observed for the corresponding area (Figure 111), suggesting that station L4 may be influenced by the nearshore and currents.

The values for average SST in the Plymouth L4 area over the past 100 years (Figure 111) show that water temperatures have been rising steadily over the past 100 years. The past three years (2005–2007) have been especially warm, with temperatures higher than any recorded in the past 100 years (Figure 111, bottom, red dashed line). These high-temperature years correspond to below-average copepod abundance since 2005, but the trend is too short to establish any clear relationship. Local CPR copepod abundance has also been decreasing with increasing water temperatures over the past 50 years (Figure 111), so this may be a trend to watch for as sampling continues.

Table 13.

Rank	Taxa	% of total abundance 1984–2007	% of total zooplankton 2007	(Δ)	Mean abundance (N m^{-3}) 1984–2007	Abundance (N m^{-3}) 2007	(Δ%)
1	*Pseudocalanus* spp.	13.2	12.3	(–0.9)	411.4	369.9	(-10)
2	*Oncaea* spp.	11.5	12.2	(0.7)	358.9	366.5	(2)
3	*Oithona* spp.	11.1	11.3	(0.2)	346.5	339.8	(-2)
4	*Paracalanus* spp.	10.4	10.7	(0.3)	322.8	319	(–1)
5	Cirripede larvae	9.8	10.3	(0.6)	304.0	309.3	(2)
6	*Temora* spp.	8.8	8.6	(-0.1)	272.9	257.9	(–5)
7	Acartia spp.	5.8	5.4	(–0.5)	182.2	160.9	(–12)
8	*Paracalanus parvus*	5.2	4.8	(–0.4)	163.2	144.7	(–11)
9	*Corycaeus spp.*	2.7	2.8	(0.2)	82.6	84.1	(2)
10	Appendicularia	2.5	2.4	(–1.0)	78.1	71.0	(–9)
	"Top ten" totals	**80.9**	**80.9**	**(-0.0)**	**2 522.5**	**2 422.9**	**(–4)**
	Total abundance of all zooplankton (N m^{-3})				**3 119.0**	**2 996.5**	**(-4)**

Table 13.
Average abundance and relative dominance (percentage of the total zooplankton collected) of the top ten most abundant zooplankton taxa collected at the Plymouth L4 site in previous years (1984–2007) compared with that collected in 2007. Colours in the "Δ" and "Δ%" columns indicate either an increase (red) or decrease (blue) in relative dominance from previous years.

Plymouth L4 (English Channel)

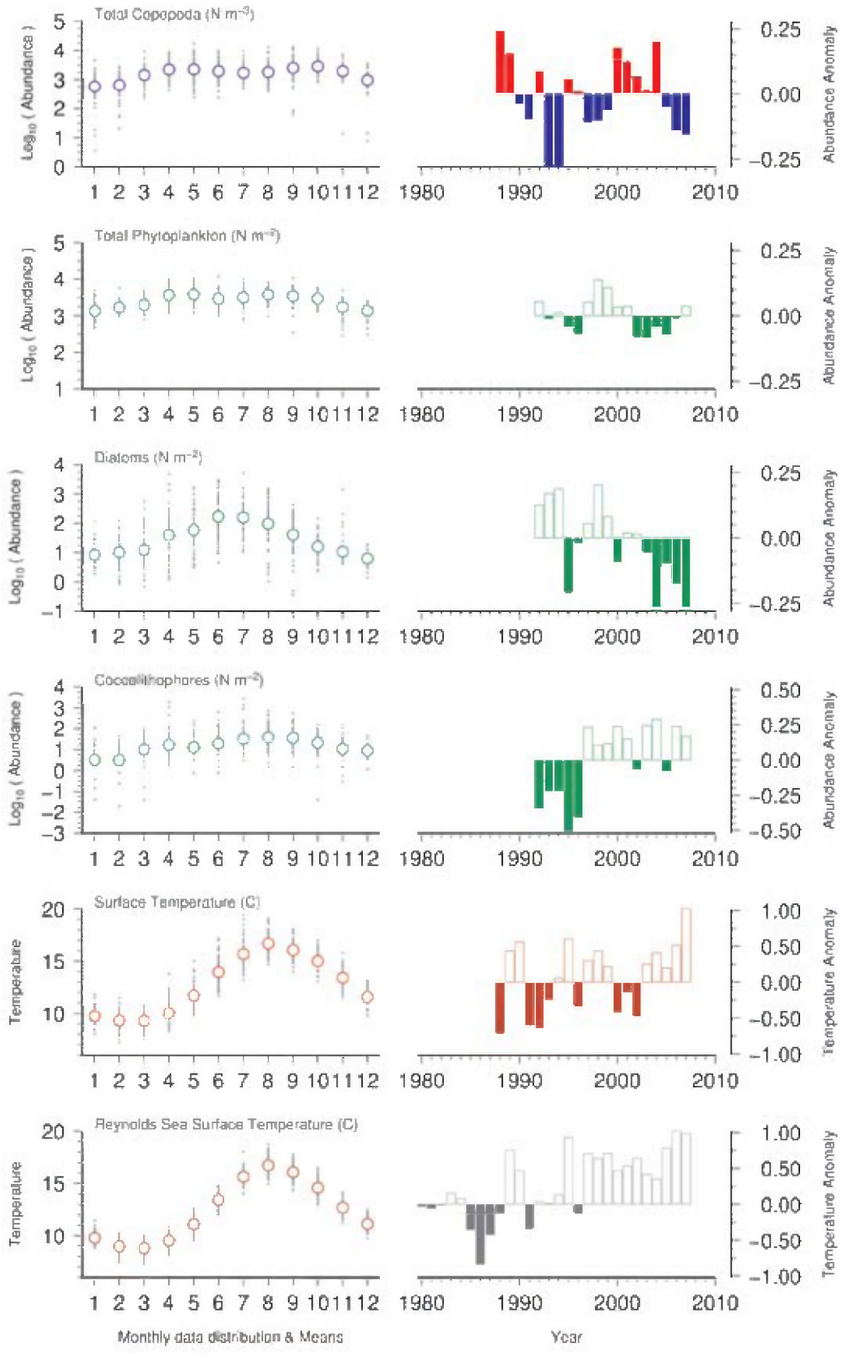

Figure 109.
Seasonal and interannual comparison of co-sampled variables at Plymouth L4. (See Section 2.2 for an explanation of the subplots in this figure.)

Plymouth L4 (English Channel)

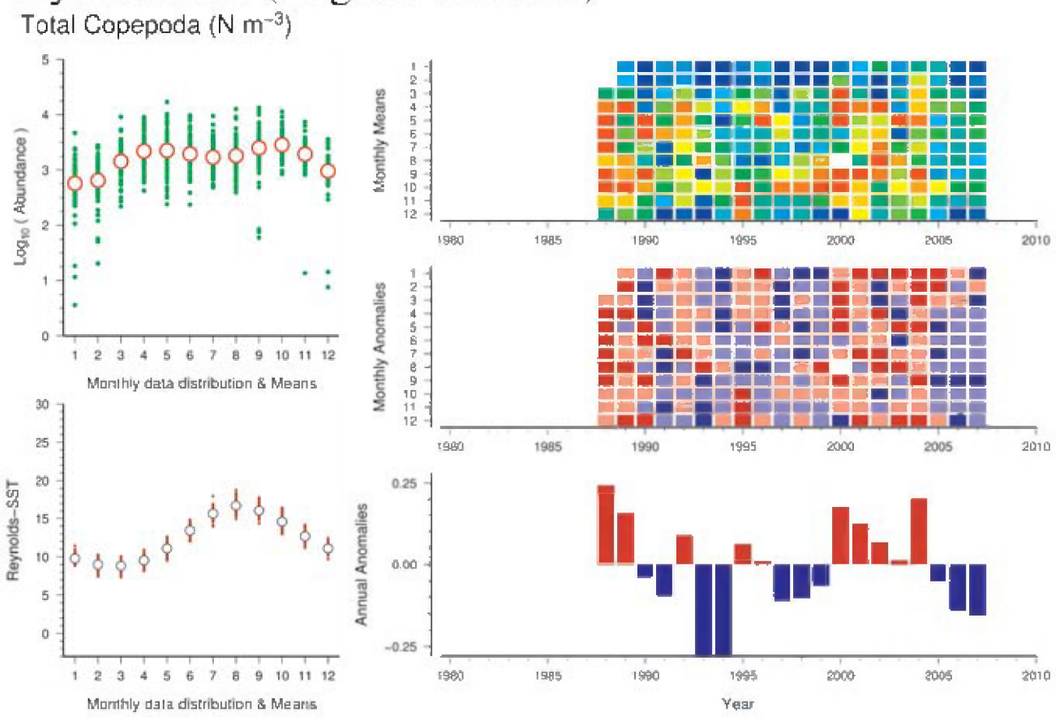

Figure 110.
Standardized WGZE time-series summary plot for copepod abundance at Plymouth L4. (See Section 2.1 for an explanation of the subplots in this figure.)

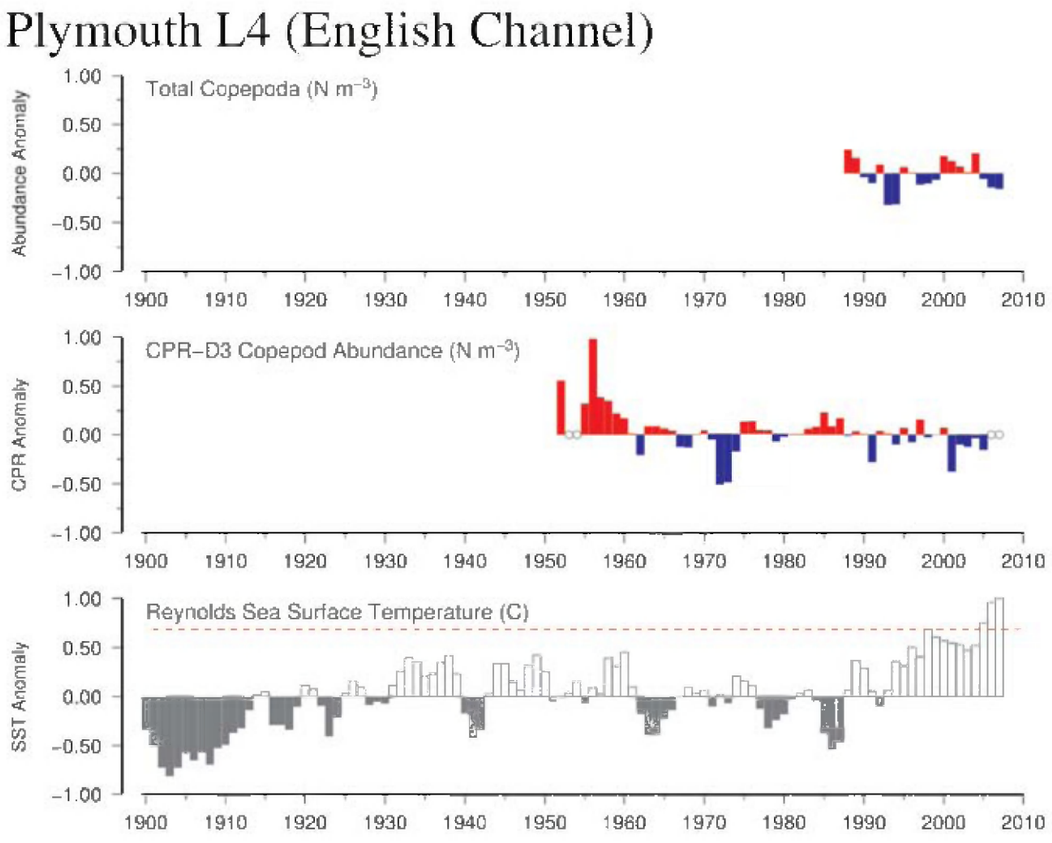

Figure 111.
Long-term comparison of Plymouth L4 copepod abundance with copepod abundance in CPR standard area "D3" and Reynolds sea surface temperatures for the region. (See Section 2.3 for an explanation of the subplots in this figure.)

3.6 Bay of Biscay and Iberian Coast

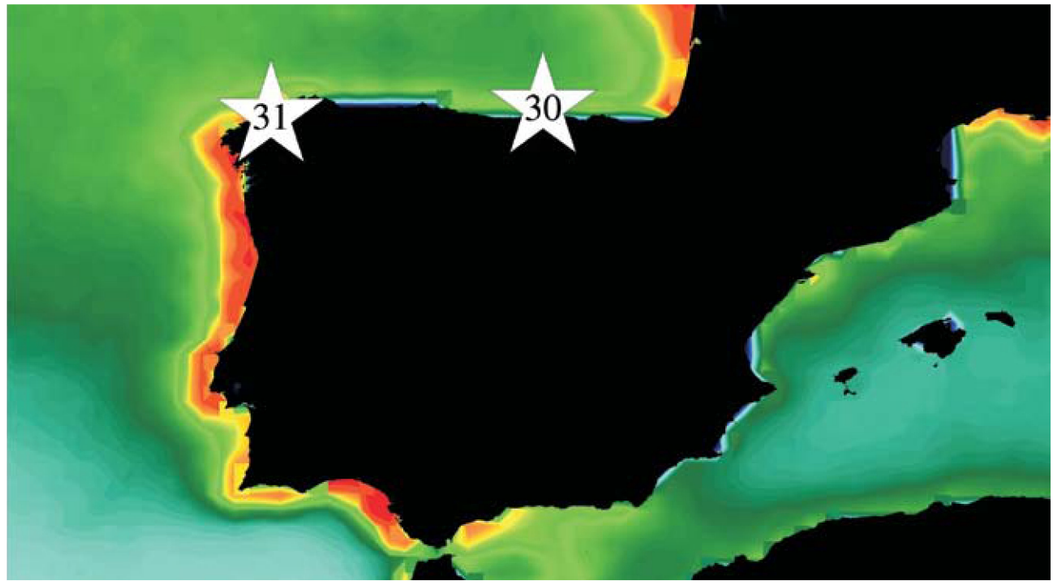

Figure 112.
Locations of Bay of Biscay (Site 30) and Iberian Coast (Site 31) zooplankton time-series, plotted on a map of SeaWiFS average chlorophyll concentrations. Red/orange = high (productive), green/yellow = medium (moderate), blue = low (oligotrophic).

The Bay of Biscay and Iberian Coast (Figure 112) are at the southern limits of Longhurst's Northeast Atlantic Shelf Province (NASP; see Section 3.5). This region is still characterized by the typical seasonal cycle of temperate seas (mixing during winter, spring bloom, summer stratification, and autumn secondary bloom), but upwelling events off Coruña break up the water column during summer. In general, chlorophyll concentrations (and therefore production) are much lower in this region than those observed in the upper NASP (Section 3.5). Nutrient input from upwelling events leads to periodic chlorophyll blooms but, otherwise, summer conditions tend to be oligotrophic. This region is characterized by the presence of pseudo-oceanic copepod species together with an increased presence of warm temperate species (Beaugrand *et al.*, 2002).

Site 30: Santander (Southern Bay of Biscay)

Luis Valdés and Jesús Cabal

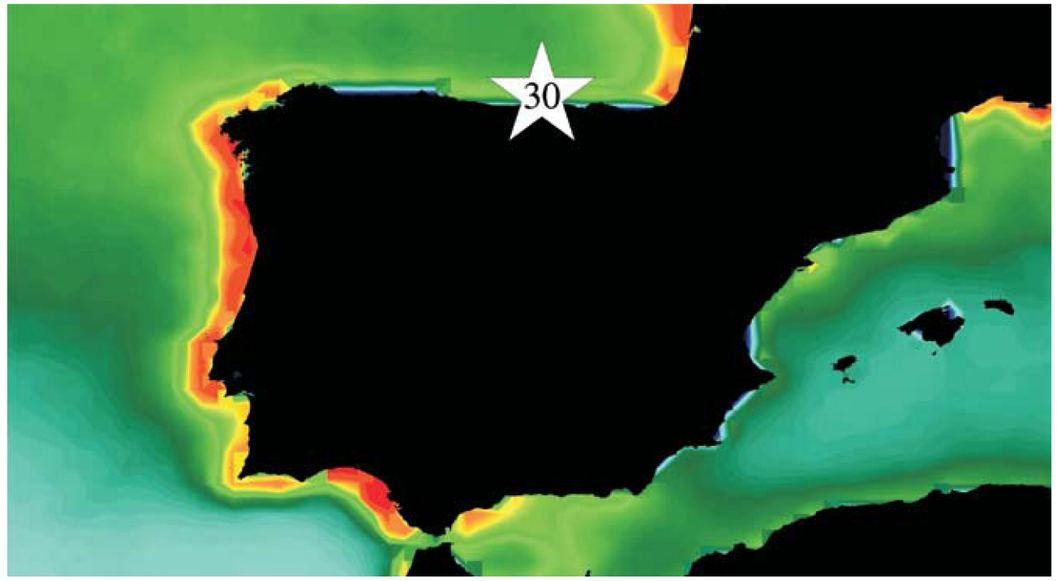

Figure 113.
Location of the Santander survey area (Site 30), plotted on a map of SeaWiFS chlorophyll concentration. Red/orange = high (productive), green/yellow = medium (moderate), blue = low (oligotrophic).

The Santander transect is part of the time-series RADIALES programme (Instituto Español de Oceanografía, www.seriestemporales-ieo.net/). Station 4 of the Santander transect, used for this site summary, is located off the north Iberian coast at 43°34.4′N 3°47.0′W (Figure 113). Zooplankton samples were collected from 50 m to the surface (oblique hauls) on a monthly basis with a Juday–Bogorov net (50 cm diameter, 250 µm mesh). Samples were preserved in 4% formalin in sodium borate-buffered seawater and then examined in the laboratory for identification and counting of mesozooplankton by the rarefaction method (Omori and Ikeda, 1984). Biomass was calculated as dry weight (Lovegrove, 1962) in the laboratory after two months of preservation.

The seasonal cycle of zooplankton abundance and biomass is characterized by a unimodal pattern with sustained high densities from March to September (Figure 114, top left). It is the interannual variability during these months that mainly drives the year-to-year differences in average biomass and abundance. Higher biomass and abundance (Figure 115) were observed at the beginning and end of the time-series, suggesting that there is a low-frequency cycle. Nevertheless, a slightly decreasing trend in zooplankton biomass is observed, even though the past two years have been higher than average.

Both *in situ* temperature and Reynolds SST demonstrate an increasing trend (Figures 115 and 116) over the length of the time-series and since 1900, with the past five years being at or above the highest temperatures seen in the past 100 years (1900–2000). CPR copepod abundance anomalies for the standard area adjacent to Santander (Figure 116) also demonstrate a clear decreasing trend in total copepod abundance. This decrease is in opposition to the upward trend shown by the water column stratification index (Valdés *et al.*, 2007) and SST (Figure 116, bottom). This relationship between zooplankton and environmental conditions highlights the importance that the extended duration of water column stratification could have in limiting the interchange of nutrients from deeper to surface waters and, consequently, limiting the growth of phytoplankton and zooplankton (Valdes and Moral, 1998).

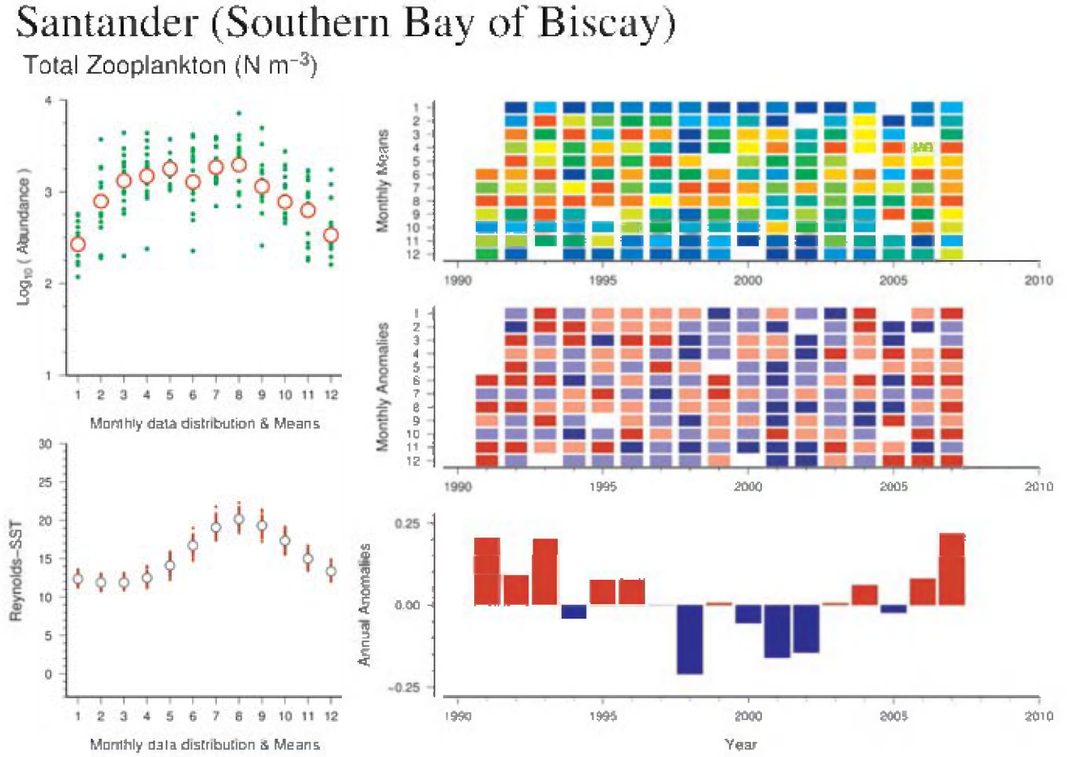

Figure 114.
Standardized WGZE time-series summary plot for zooplankton abundance at Santander. (See Section 2.1 for an explanation of the subplots in this figure.)

Santander (Southern Bay of Biscay)

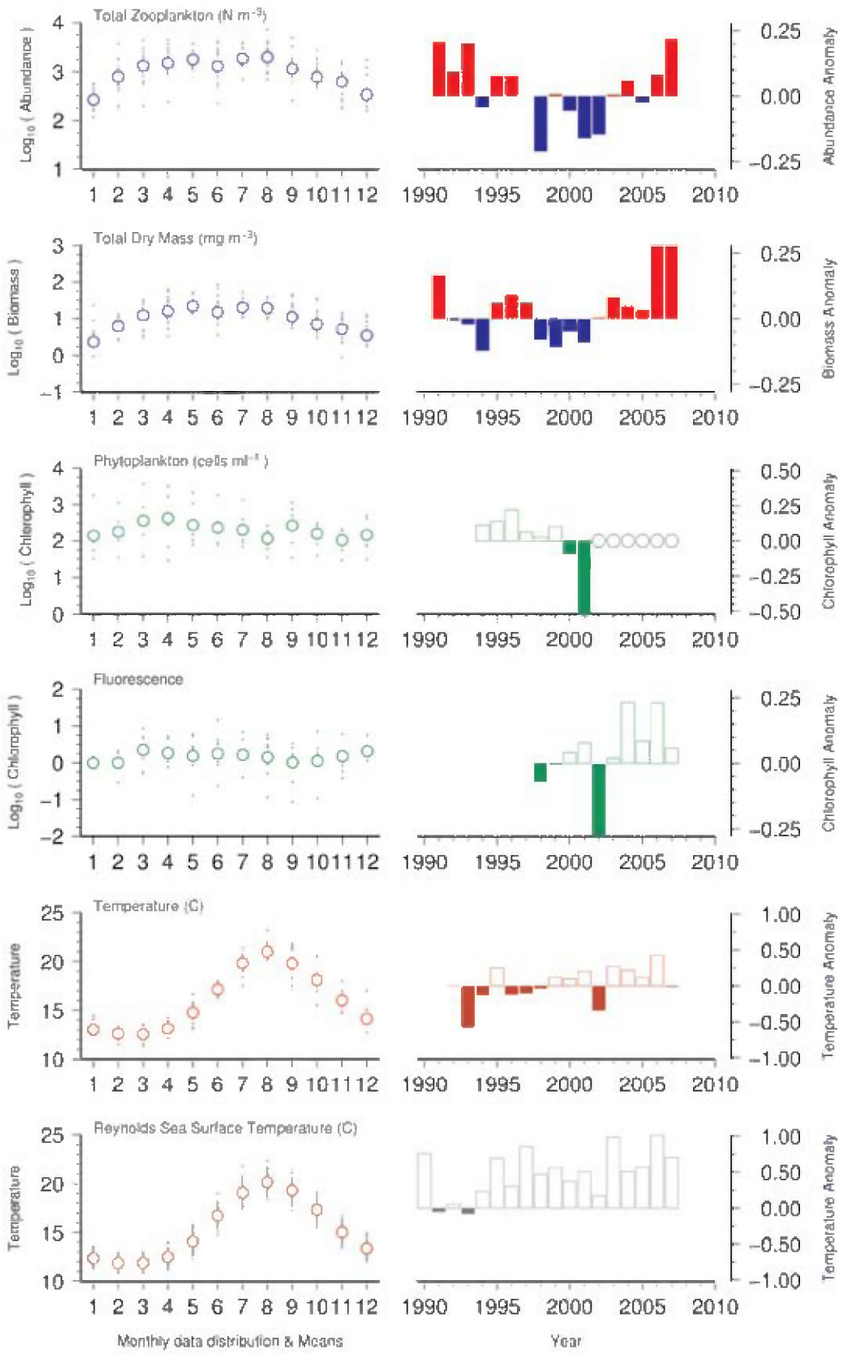

Figure 115.
Seasonal and interannual comparison of co-sampled variables at Santander. (See Section 2.2 for an explanation of the subplots in this figure.)

Santander (Southern Bay of Biscay)

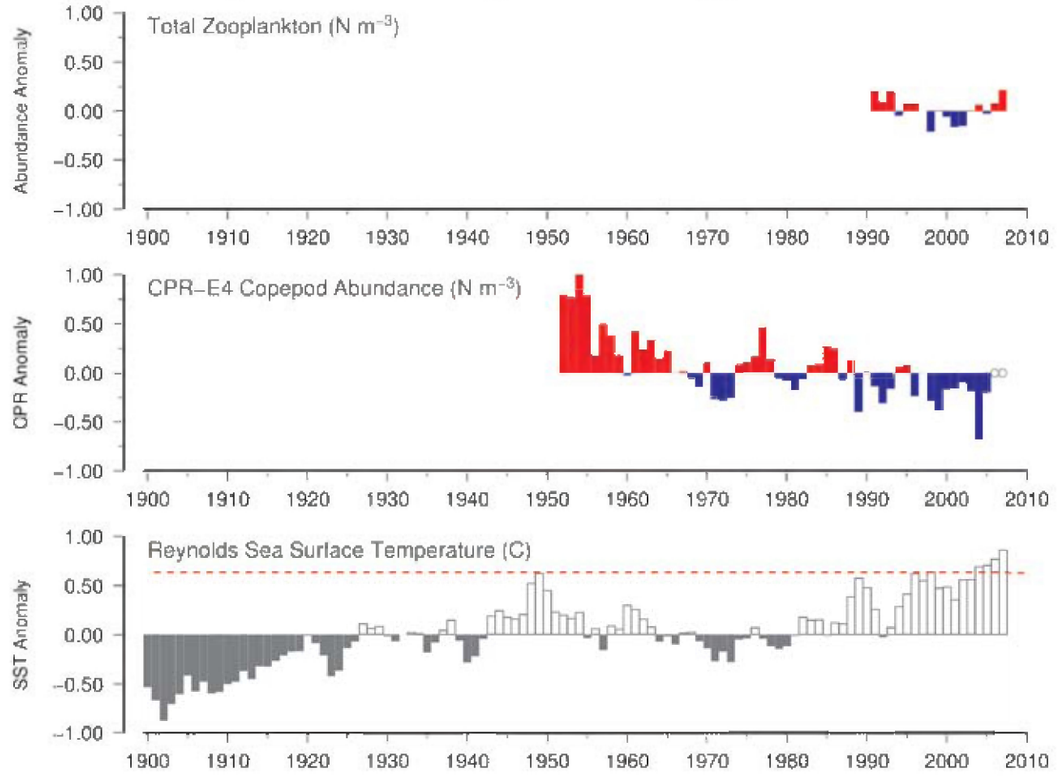

Figure 116.
Long-term comparison of Santander zooplankton abundance with copepod abundance in CPR standard area "E4" and Reynolds sea surface temperatures for the region. (See Section 2.3 for an explanation of the subplots in this figure.)

Site 31: A Coruña (Northwest Iberian Peninsula)

Maite Alvarez-Ossorio

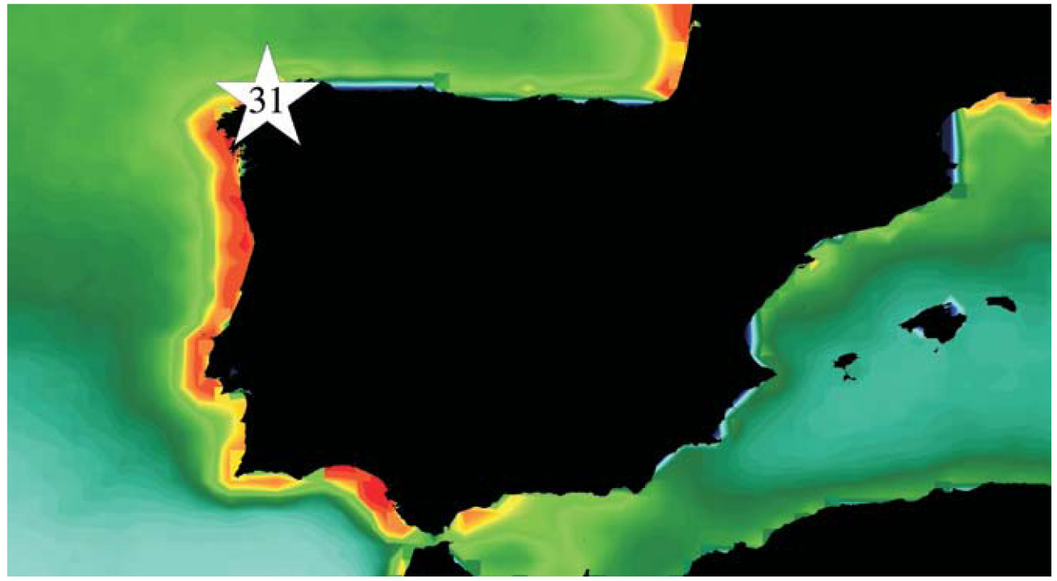

Figure 117.
Location of the A Coruña survey area (Site 31), plotted on a map of SeaWiFS chlorophyll concentration. Red/orange = high (productive), green/yellow = medium (moderate), blue = low (oligotrophic).

The A Coruña section is part of the time-series programme RADIALES (Instituto Español de Oceanografía, www.seriestemporales-ieo.net). Station 2 of the A Coruña section, which was used for this summary, is located off the northwest Iberian coast at 43°25.3′N 8°26.2′W (Figure 117). Zooplankton samples were collected from 65 m to the surface (oblique hauls) on a monthly basis with a Juday–Bogorov net (50 cm diameter, 200 µm mesh). Samples were preserved in 4% formalin in sodium borate-buffered seawater and then examined in the laboratory for identification and counting of mesozooplankton by the rarefaction method (Omori and Ikeda, 1984). Biomass was calculated as dry weight (Lovegrove, 1962) of samples filtered upon arrival at the laboratory.

In the coastal region off Galicia (northwest Spain), the classical pattern of seasonal stratification of the water column in temperate regions is masked by upwelling events from May to September. These upwelling events provide zooplankton populations with favourable conditions for development in summer, which is the opposite of what occurs in other temperate seas in this season of the year. Nevertheless, upwelling is highly variable in intensity and frequency, demonstrating substantial year-to-year variability.

The seasonal cycle of zooplankton biomass is characterized by increased values from April to September, with a slight reduction in biomass from June to August resulting in a relatively bimodal seasonal cycle (Figure 118). Both biomass and abundance demonstrate an overall increasing trend, although a decrease in biomass was observed in 2000–2002 (Figure 119). Surprisingly, this decrease was not paralleled by a decrease in abundance, suggesting an increased prevalence of small organisms during this period.

The abundance and relative fractions of the top ten taxa at A Coruña are shown in Table 14. A comparison of the average composition for 2006 with that of previous years (1994–2005) shows that the relative species compositions both increased (e.g. *Paracalanus parvus*, *Calanus helgolandicus*, *Oithona similis*) and decreased (e.g. *Oncaea media*, *Pseudocalanus elongatus*).

In situ temperature and Reynolds SST reveal an increasing trend of up to 1°C during the 20 years of the time-series (Figure 119). To further investigate both temperature and zooplankton trends at the site, data were compared with long-term data from CPR and Reynolds SST. Although the increasing trend in SST is also evident in the longer record (Figure 120), with SST increasing almost 1°C during the past half-century, the increase in zooplankton abundance recorded at A Coruña during the past 20 years corresponds to a period of low copepod abundance in CPR standard area "F4" (Figure 120). Although the abundance recorded by the CPR during the past ten years in this area features negative anomalies, there is an increasing trend in the CPR data (i.e. moving from negative to positive), suggesting that the increasing trend observed off A Coruña may be a recovery from a period of low abundance.

Table 14.

Rank	Taxa	% of total abundance 1994–2005	% of total zooplankton 2006	(Δ)	Mean abundance (N m^{-3}) 1994–2005	Abundance (N m^{-3}) 2006	(Δ%)
1	*Acartia clausi*	13.6	17.5	(3.9)	411	608	(48)
2	Copepod juveniles	13.1	13.8	(0.7)	384	379	(–1)
3	*Oncaea media*	11.7	2.7	(-9.0)	479	30	(-94)
4	*Paracalanus parvus*	8.6	11.5	(2.9)	255	342	(34)
5	Cirripede nauplii	7.0	4.8	(-2.3)	305	133	(–56)
6	*Clausocalanus* spp.	5.7	3.8	(-1.9)	102	57	(–44)
7	Pseudocalanus elongatus	4.0	0.8	(–3.3)	149	17	(–89)
8	Bivalve larvae	2.7	1.9	(–0.8)	150	103	(–31)
9	*Calanus helgolandicus*	2.5	5.4	(2.9)	92	163	(77)
10	*Oithona similis*	2.5	4.3	(1.9)	72	101	(40)
	"Top ten" totals	**71.4**	**66.5**	**(-4.9)**	**2 399**	**1 932**	**(–19)**
	Total abundance of all zooplankton (N m^{-3})				**3 330**	**2 980**	**(-11)**

Table 14.
Average abundance and relative dominance (percentage of the total zooplankton collected) of the top ten most abundant zooplankton taxa collected at the A Coruña site in previous years (1994–2005) compared with that collected in 2006. Colours in the "Δ" and "Δ%" columns indicate either an increase (red) or decrease (blue) in relative dominance from previous years.

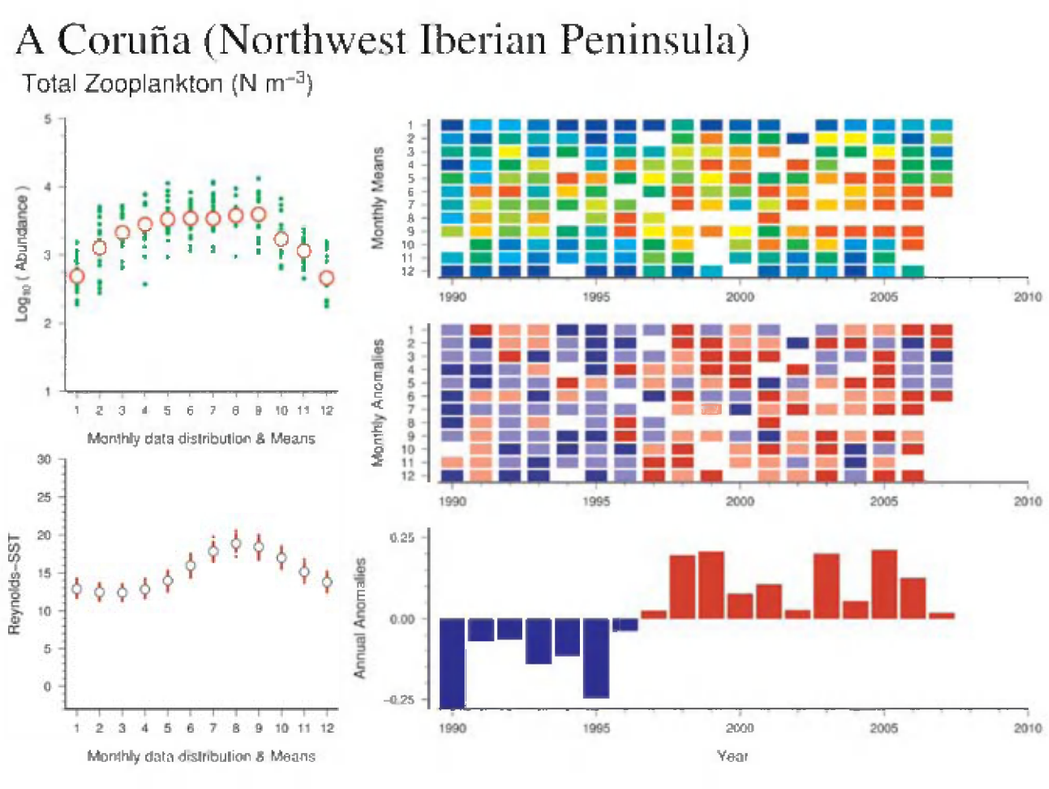

Figure 118.
Standardized WGZE time-series summary plot for zooplankton abundance at A Coruña. (See Section 2.1 for an explanation of the subplots in this figure.)

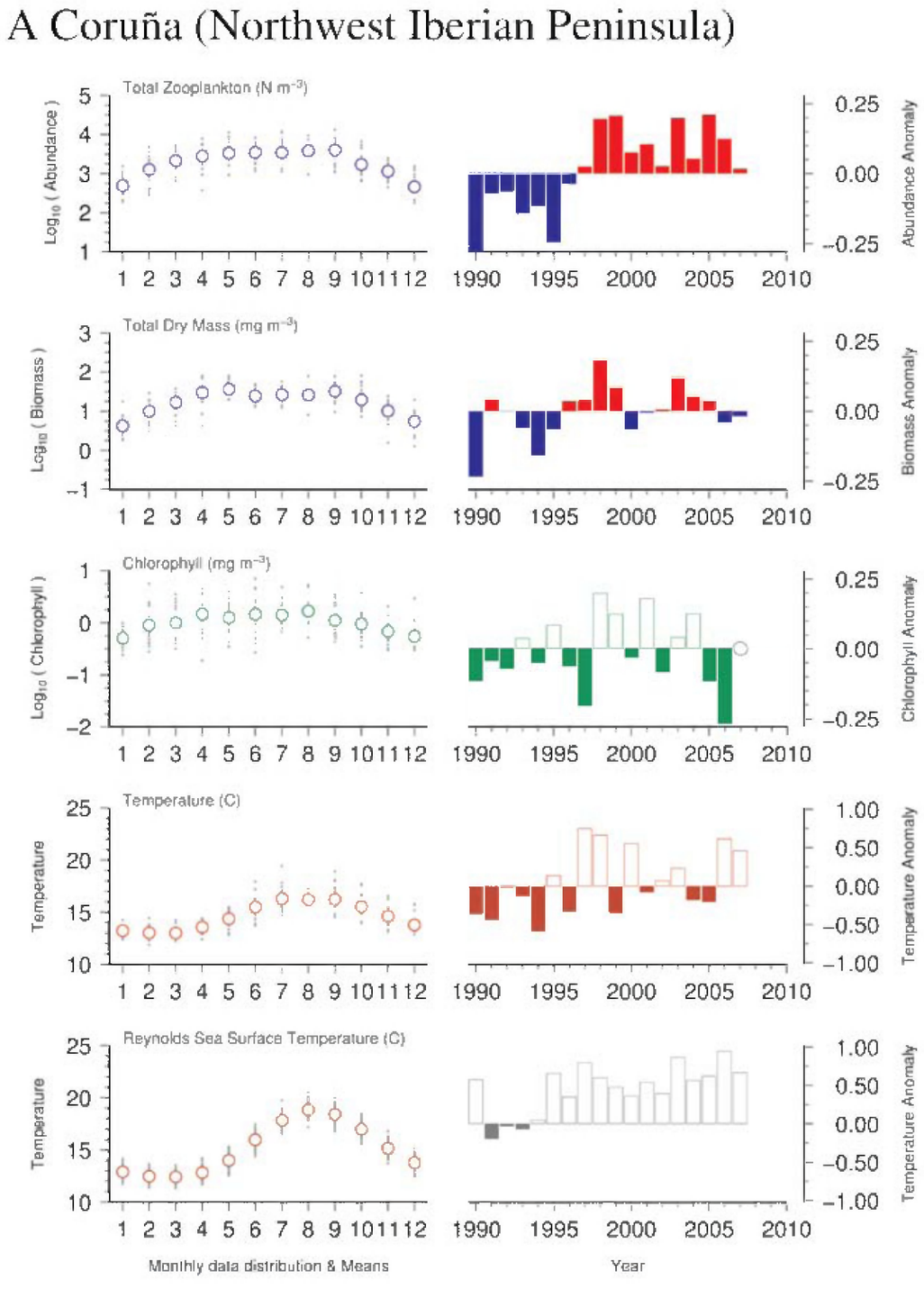

Figure 119.
Seasonal and interannual comparison of co-sampled variables at A Coruña. (See Section 2.2 for an explanation of the subplots in this figure.)

A Coruña (Northwest Iberian Peninsula)

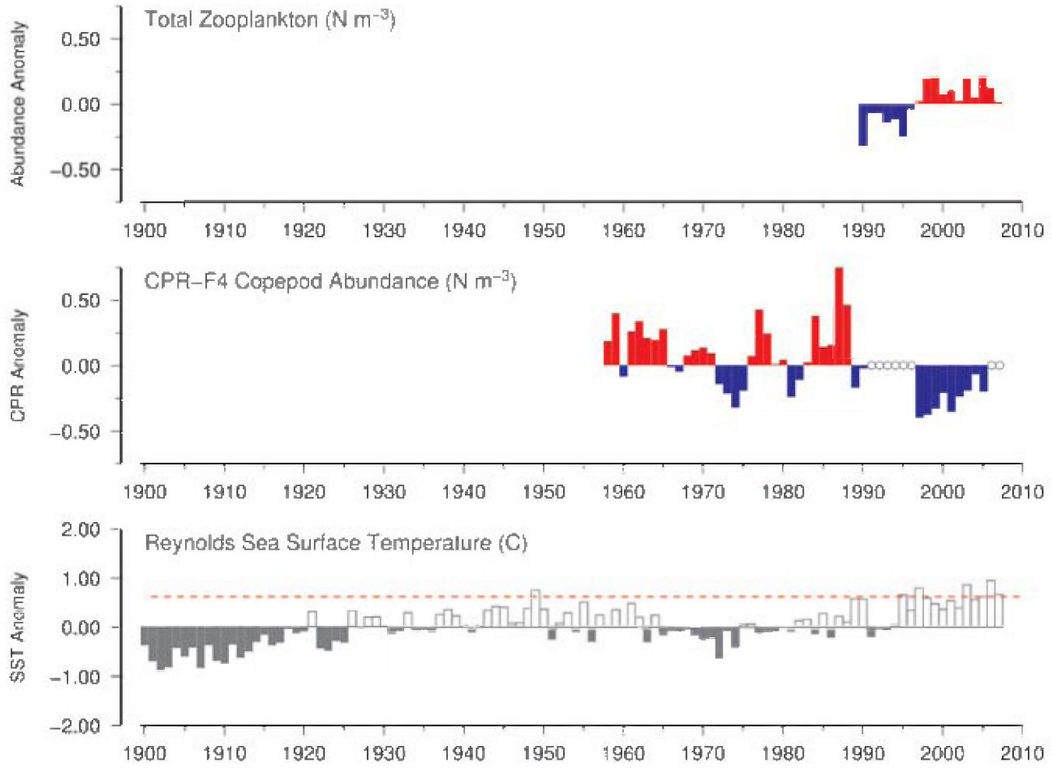

Figure 120.
Long-term comparison of A Coruña zooplankton abundance with copepod abundance in CPR standard area "F4" and Reynolds sea surface temperatures for the region. (See Section 2.3 for an explanation of the subplots in this figure.)

3.7 Mediterranean Sea

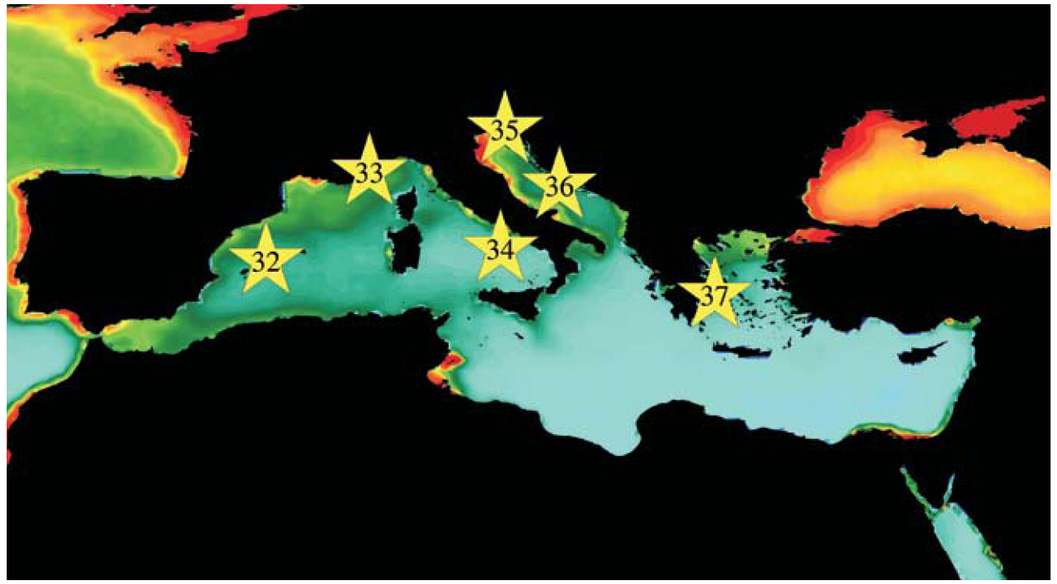

Figure 121.
Locations (Sites 32–37) of Mediterranean zooplankton time-series, plotted on a map of SeaWiFS average chlorophyll concentrations. Red/orange = high (productive), green/yellow = medium (moderate), blue = low (oligotrophic).

In contrast to the North Atlantic, which has several highly productive sea areas around its continental shelf margins, the Mediterranean Sea is oligotrophic, similar to the subtropical part of the North Atlantic. The seasonal cycle of primary and secondary production is more or less similar for both regions, driven by physical processes affecting the stability of the upper layers of the water column and the supply of nutrients from the deeper layers up into the photic zone.

The majority of species in the Mediterranean Sea are of Atlantic origin. Both the North Atlantic Ocean and the Mediterranean Sea have deep oceanic basins that serve as overwintering sites for ontogenetically migrating zooplankton. Dominant species are common in both areas at the same latitude in the epipelagic and mesopelagic layers, whereas the bathypelagic species of the North Atlantic are excluded from the Mediterranean Sea by the Strait of Gibraltar sill. Interestingly, the marginal seas of the North Atlantic and the Mediterranean Sea, such as the Baltic Sea and the Black Sea, have common characteristics (low salinity, anoxic bottom layer, high production) and all face the challenge of exotic/introduced species.

Although the Mediterranean is technically not the North Atlantic or an ICES study area, this year's zooplankton report includes a brief introduction to six Mediterranean zooplankton time-series (see Figure 121) as ICES and the Mediterranean Science Commission (CIESM) prepare for the October 2008 "Joint ICES/CIESM Workshop to Compare Zooplankton Ecology and Methodologies between the Mediterranean and the North Atlantic" (WKZEM; www.wkzem.net).

Site 32: Baleares station (Balearic Sea)

Maria Luz Fernandez de Puelles

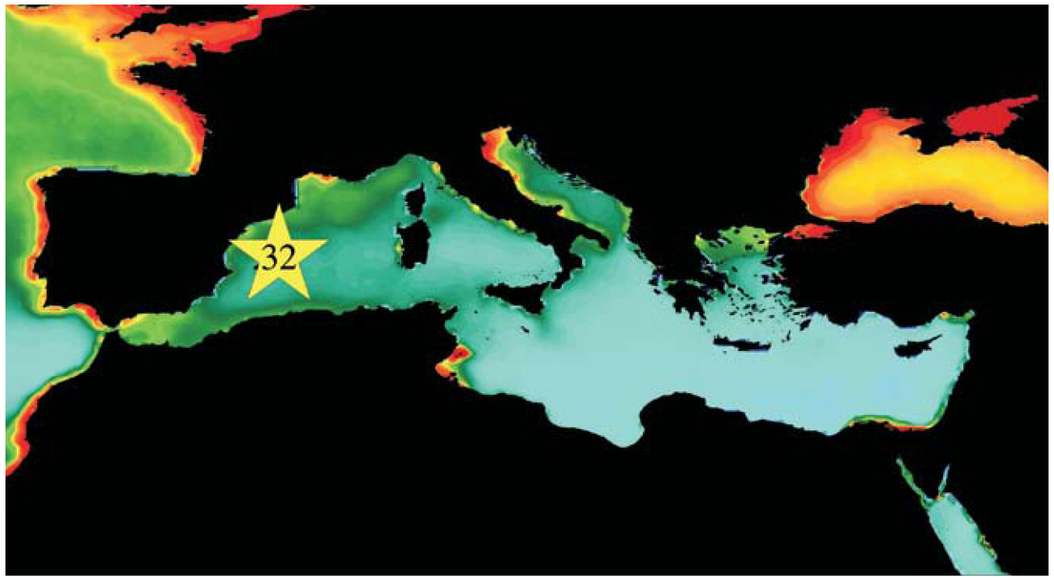

Figure 122.
Location of the Baleares Station survey area (Site 32), plotted on a map of SeaWiFS chlorophyll concentration. Red/orange = high (productive), green/yellow = medium (moderate), blue = low (oligotrophic).

The Baleares station is located southwest off the island of Mallorca, at 39°28′59″N 2°25′63″E, in a boundary area of the Balearic Sea (Figure 122). This area experiences regular influxes of northern Mediterranean and Atlantic waters and their broad range of temperatures and salinities. The seasonal cycle of temperature includes a mixing period during winter followed by a stratified period of more than six months (May–October), which coincides with the period of lowest zooplankton biomass (Figure 123). Phytoplankton blooms generally occur in January and February, and sometimes in late spring. Zooplankton biomass peaks in winter (March), spring (May), and at the end of summer (September), throughout which the dominant zooplankton group is the copepods.

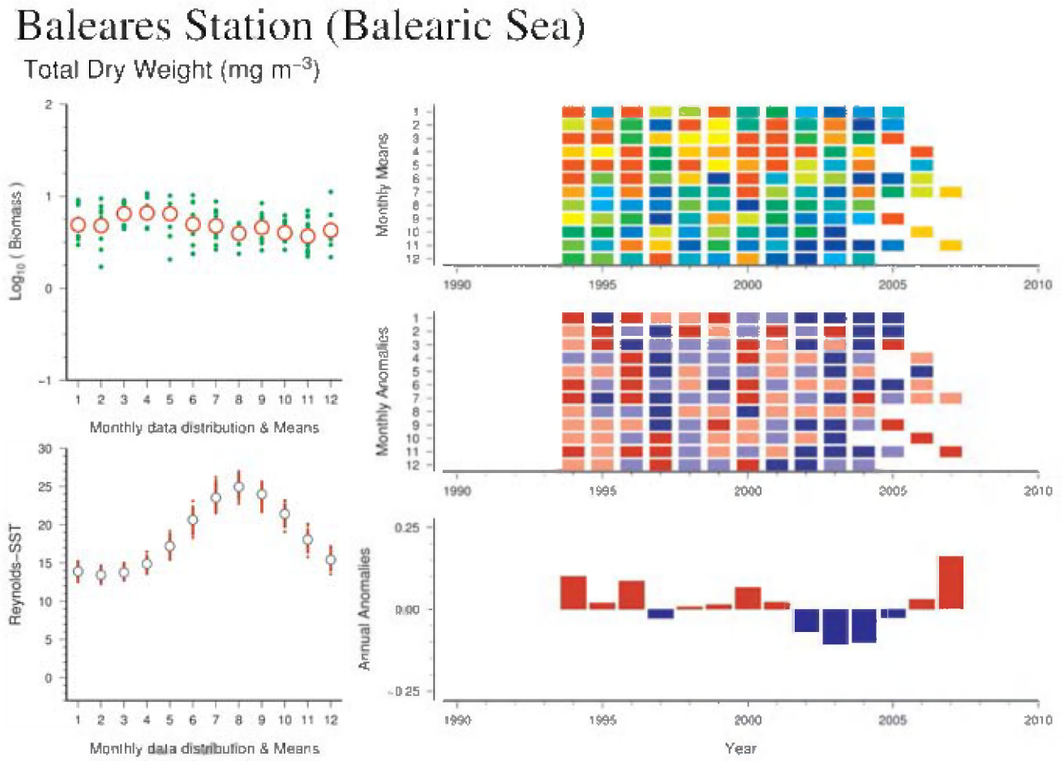

Figure 123.
Standardized WGZE time-series summary plot for total zooplankton dry weight at the Baleares Station. (See Section 2.1 for an explanation of the subplots in this figure.)

Site 33: Villefranche Point B (Côte d'Azur)

Gabriel Gorsky

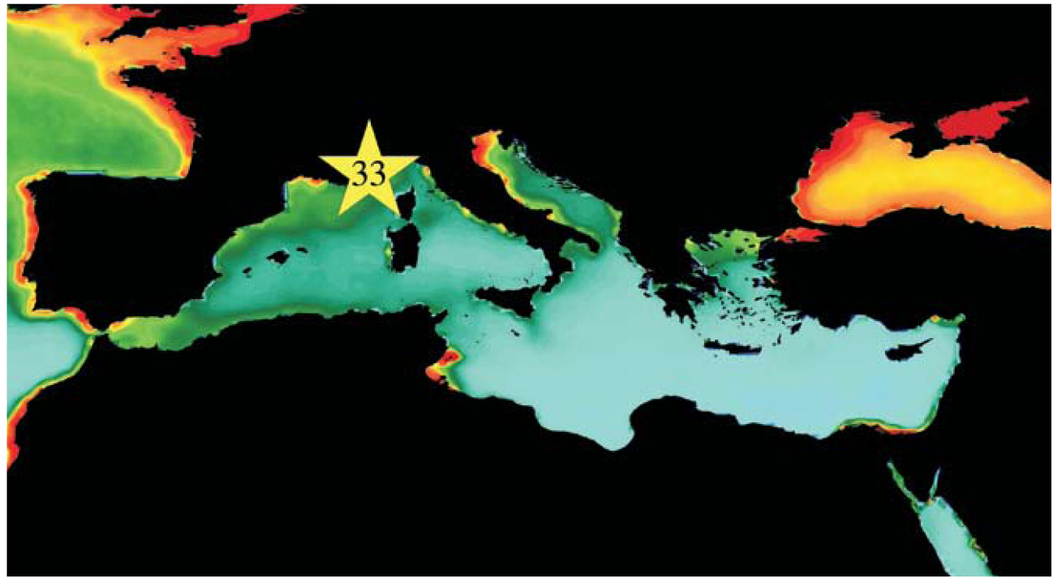

Figure 124.
Location of the Villefranche Point B survey area (Site 33), plotted on a map of SeaWiFS chlorophyll concentration. Red/orange = high (productive), green/yellow = medium (moderate), blue = low (oligotrophic).

The Villefranche Point B dataset consists of more than 30 years of samples collected off Villefranche at 43°41'N 07°19'E (Figure 124). Samples were collected by a vertical tow from bottom to surface (75–0 m), using a Juday–Bogorov net (40 cm diameter, 330 µm mesh). Copepod abundance was counted from ongoing and historical samples using the wet-bed image scanning technique of ZooScan (Grosjean *et al.*, 2004). Copepod abundance was highest during the well-mixed winter period, followed by a general decline, with rising water temperatures and increasing stratification (Figure 125).

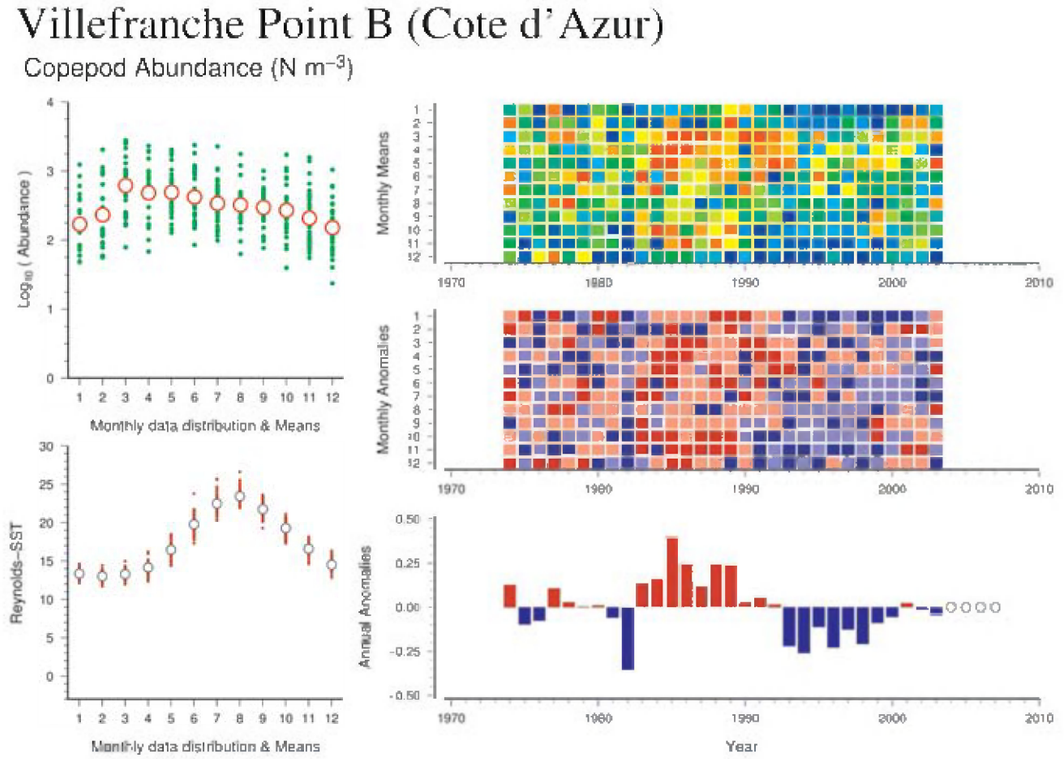

Figure 125.
Standardized WGZE time-series summary plot for copepod abundance at Villefranche Point B. (See Section 2.1 for an explanation of the subplots in this figure.)

Site 34: Gulf of Naples (Tyrrhenian Sea)

Maria Grazia Mazzocchi

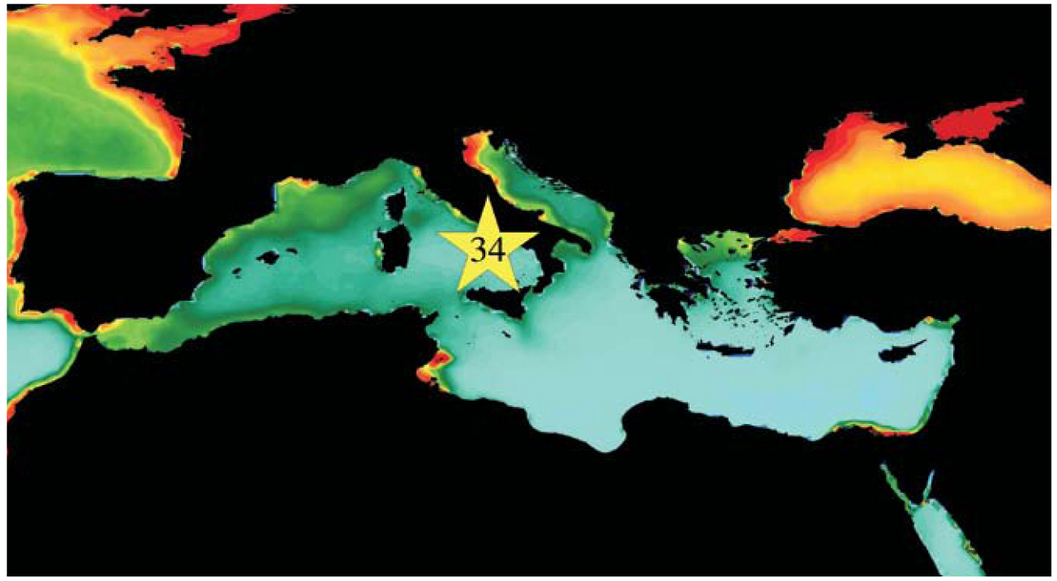

Figure 126.
Location of the Gulf of Naples survey area (Site 34), plotted on a map of SeaWiFS chlorophyll concentration. Red/orange = high (productive), green/yellow = medium (moderate), blue = low (oligotrophic).

The Gulf of Naples zooplankton dataset contains biomass and species composition data collected from the ongoing time-series at Station MC, located at 40°48.5'N 14°15'E in the Tyrrhenian Sea (Figure 126). Zooplankton samples were collected with two successive vertical tows from a depth of 50 m to the surface using a Nansen net (1.13 m diameter, 200 µm mesh). Sampling was regularly conducted from 1984 to 1990 and from 1995 to 2006, although no samples were collected in 1993 and 1994 (Figure 127). Sampling frequency was fortnightly during the first period of the series, and weekly since 1995.

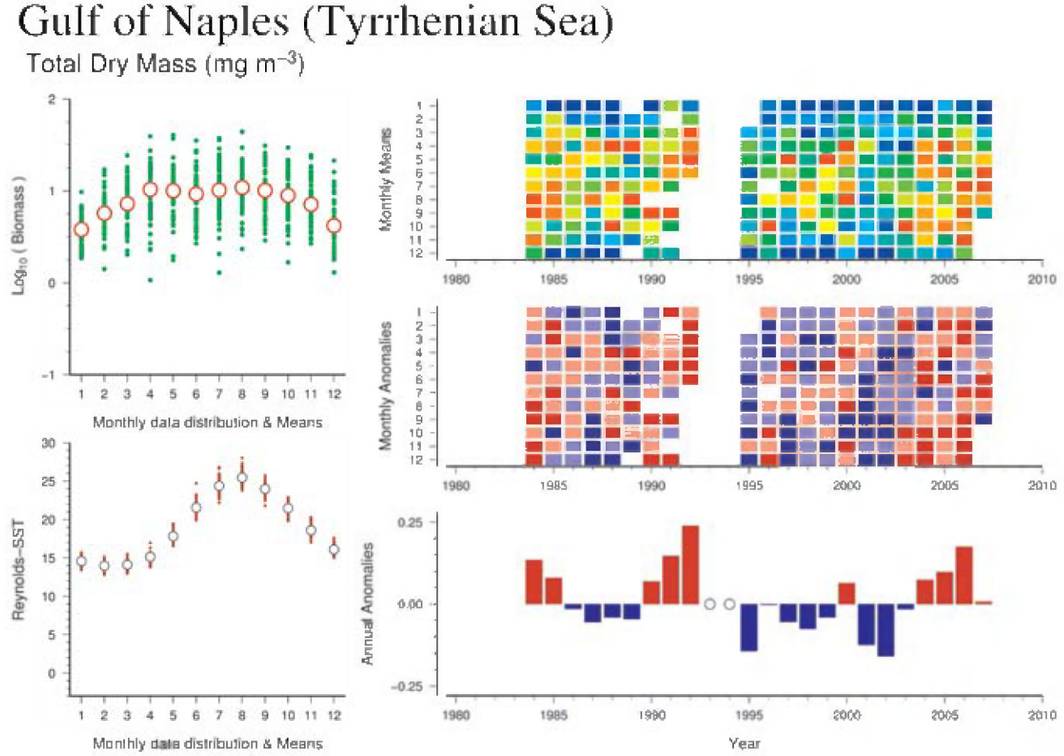

Figure 127.
Standardized WGZE time-series summary plot for total zooplankton dry mass at the Gulf of Naples. (See Section 2.1 for an explanation of the subplots in this figure.)

Site 35: Gulf of Trieste (Northern Adriatic Sea)

Serena Fonda-Umani and Alessandra Conversi

Figure 128.
Location of the Gulf of Trieste survey area (Site 35), plotted on a map of SeaWiFS chlorophyll concentration. Red/orange = high (productive), green/yellow = medium (moderate), blue = low (oligotrophic).

The Gulf of Trieste is the northernmost section of the Adriatic Sea (Figure 128). It is characterized by an overall shallowness, with a maximum depth of around 23 m in the southern part, and by a large and variable fresh-water input. Zooplankton were collected by vertical hauls from bottom (18 m) to surface using a WP-2 net (56 cm diameter, 200 µm mesh).

The mesozooplankton community in the Gulf of Trieste is characterized by a small number (approximately 30) of coastal and estuarine species, which can exhibit high dominance. Copepods dominate in all months except June and July (Figure 129), when cladocerans (especially *Penilia avirostris*) take over. The calanoid copepod *Acartia clausi* is dominant for most of the year, sometimes comprising more than 80% of the total biomass.

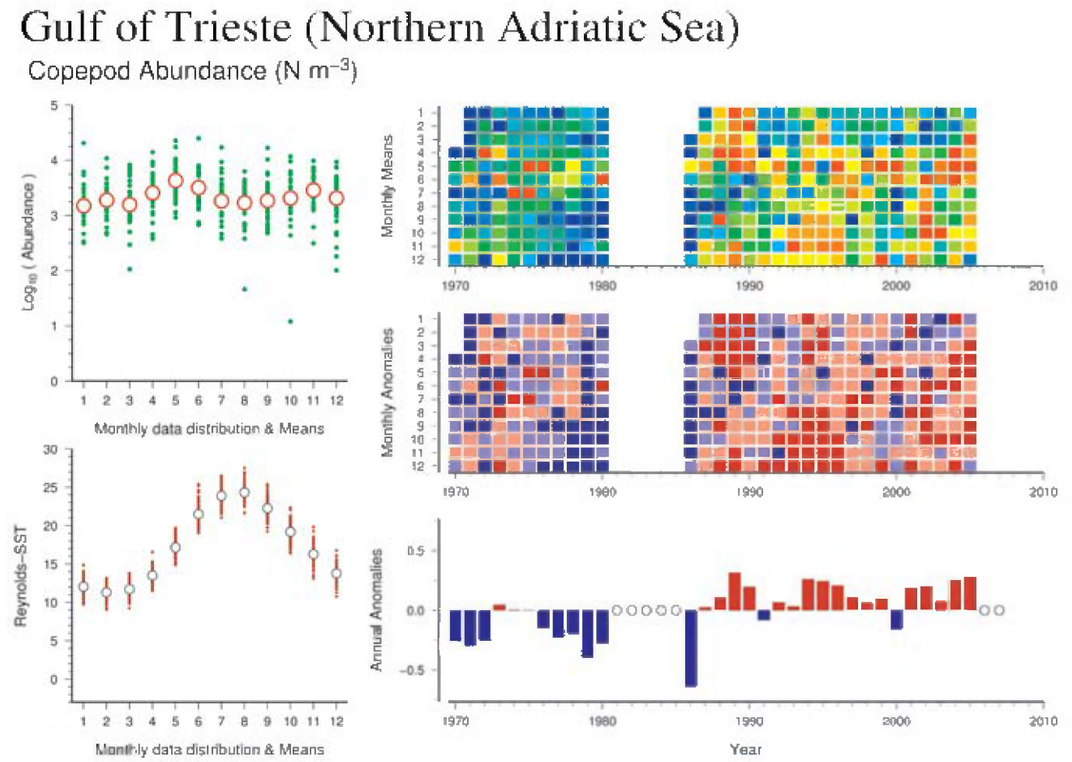

Figure 129.
Standardized WGZE time-series summary plot for copepod abundance in the Gulf of Trieste. (See Section 2.1 for an explanation of the subplots in this figure.)

Site 36: Stončica (Central Adriatic Sea)

Olja Vidjak

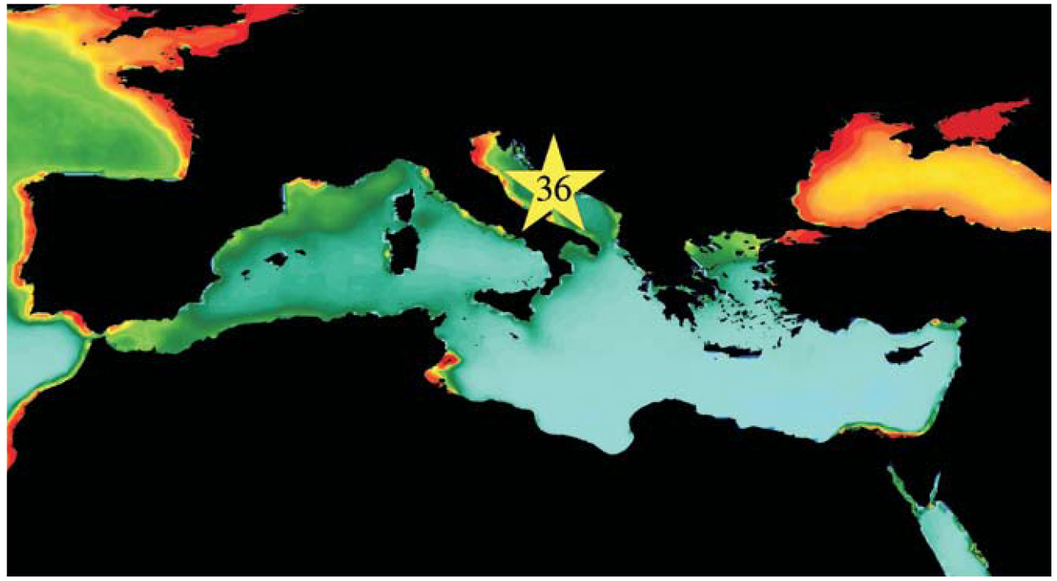

Figure 130.
Location of the Stončica survey area (Site 36), plotted on a map of SeaWiFS chlorophyll concentration. Red/orange = high (productive), green/yellow = medium (moderate), blue = low (oligotrophic).

The offshore station of Stončica is located at 43°2'38"N 16°17'7"E, in the centre of the Adriatic Sea (Figure 130). From 1959 to 1991, mesozooplankton were sampled on an approximately monthly basis, using a Hensen net (0.73 m mouth diameter, 0.419 m^2 mouth area, 330 µm mesh). Sampling was performed by a vertical tow from near-bottom to surface (100–0 m). Group level abundance was counted for the following zooplankton groups: Copepoda, Cladocera, Appendicularia, Chaetognatha, various meroplankton larvae, Pisces ova, Pisces juveniles, and Medusae/Siphonophora.

From 1991 to 1994, the sampling programme was interrupted (Figure 131). In January 1995, the programme was resumed, but the samples have not yet been processed.

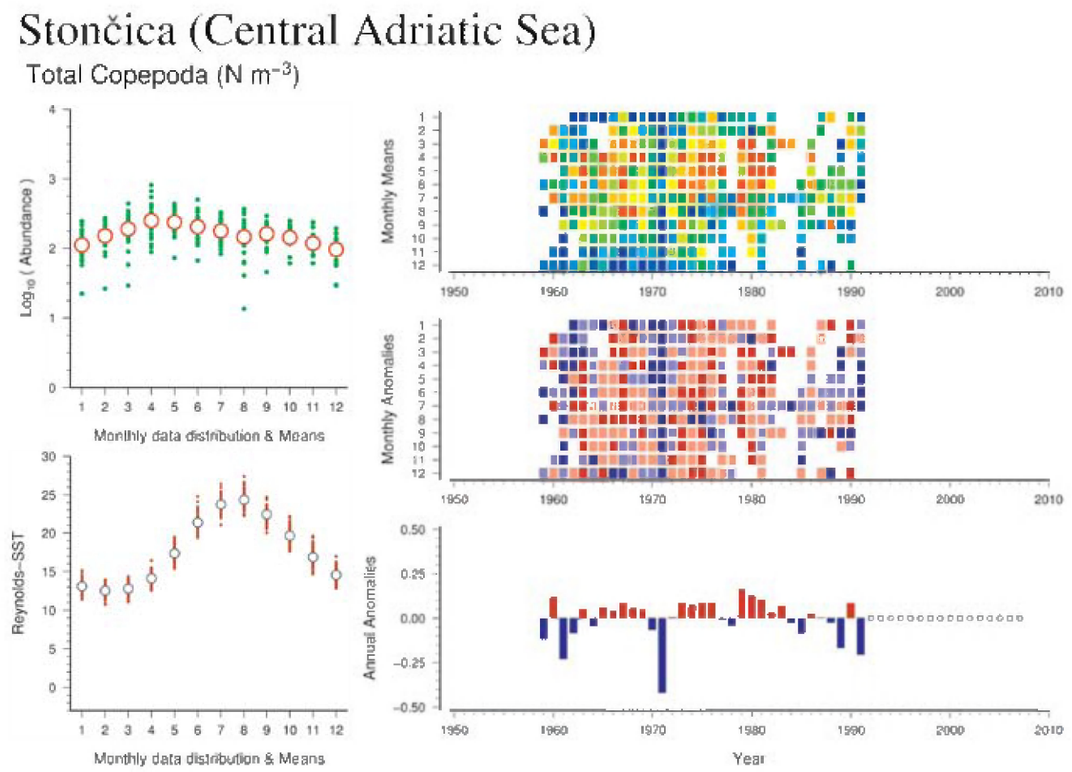

Figure 131.
Standardized WGZE time-series summary plot for copepod abundance at Stončica. (See Section 2.1 for an explanation of the subplots in this figure.)

Site 37: Saronikós–S11 (Aegean Sea)

Ioanna Siokou-Frangou

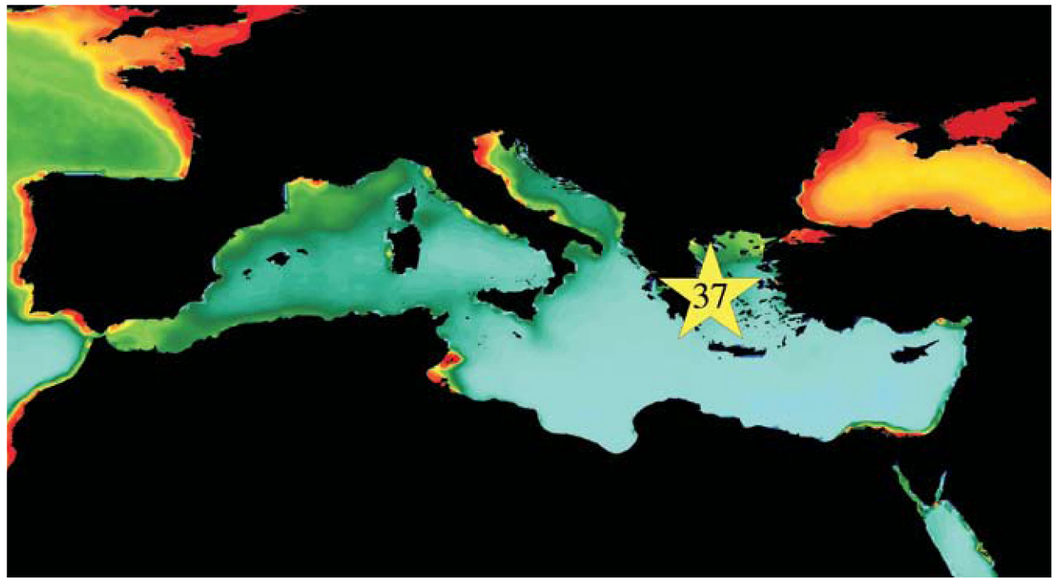

Figure 132.
Location of the Saronikós–S11 survey area (Site 37), plotted on a map of SeaWiFS chlorophyll concentration. Red/orange = high (productive), green/yellow = medium (moderate), blue = low (oligotrophic).

Saronikós Station 11 (S11) is located in the Saronikos Gulf (Figure 132). Zooplankton were sampled with a WP-2 net (56 cm diameter, 200 µm mesh) from 75 m to the surface. Sampling was initially carried out at least four times a year and then increased to monthly sampling since 2000. Zooplankton biomass (as dry mass) was highest during the well-mixed winter period, followed by a general decline with increasing water temperatures and stratification (Figure 133).

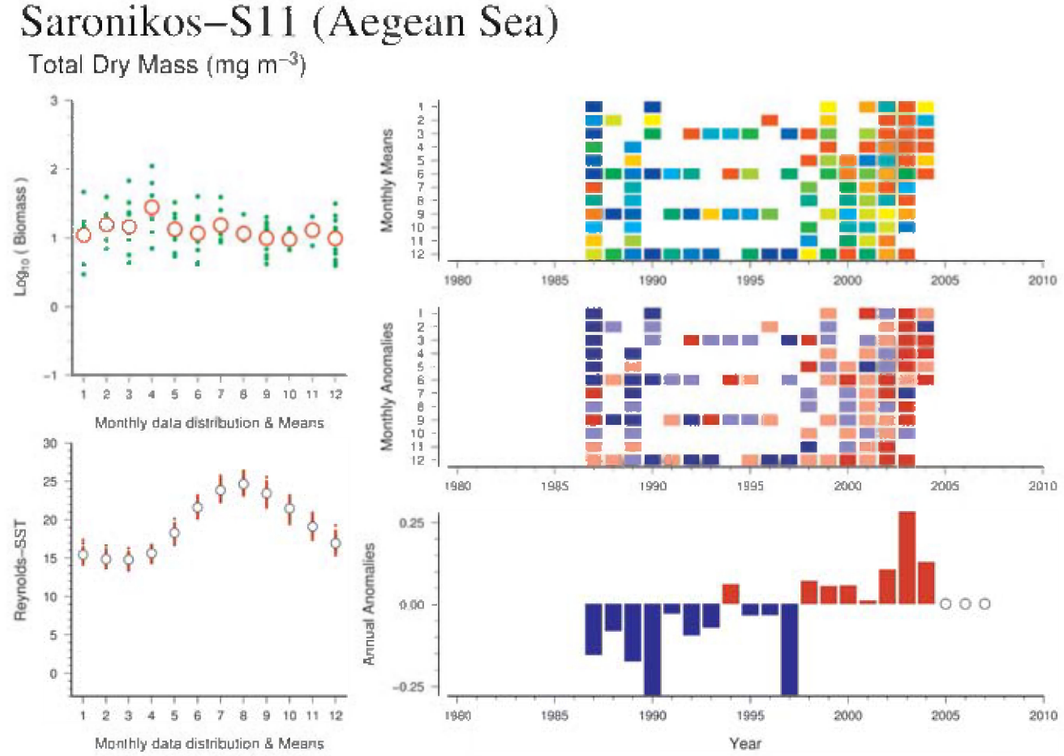

Figure 133.
Standardized WGZE time-series summary plot for total zooplankton dry mass at Saronikós–S11. (See Section 2.1 for an explanation of the subplots in this figure.)

4. DISCUSSION

As evident in the previous time-series and site summaries, zooplankton abundance and biomass vary substantially between years and decades, and are affected both directly and indirectly by the short- and long-term hydrographic and physical conditions of their environment. Local water temperatures, for example, can greatly influence the community structure and production of zooplankton, which, in turn, can lead to large seasonal, annual, and decadal changes in population size and geographic distribution. It is also necessary to look at the phytoplankton, whose species composition and biomass determine both the amount and quality of food available to the zooplankton populations. Zooplankton time-series are thus best studied with a multivariate approach.

4.1 A multivariate overview of the North Atlantic

Priscilla Licandro

The CPR survey has been sampling for more than 70 years, towed at the surface behind volunteer-operated vessels ("ships of opportunity"), and collecting thousands of plankton samples across the North Atlantic and North Sea. From this extensive database, a time-series of total copepod abundance (updated from Edwards *et al.*, 2006, with new data) has been used to look at the status of zooplankton across the entire North Atlantic.

The CPR time-series divides the North Atlantic into 40 geographic regions, known as CPR "standard areas" (Figure 134). In general, the highest data density and temporal coverage are found in areas near land and major shipping lanes, e.g. standard area "C2" (Figure 135). In areas away from major shipping lanes or in the southern central North Atlantic, the available data density and temporal coverage may be less (Figure 136).

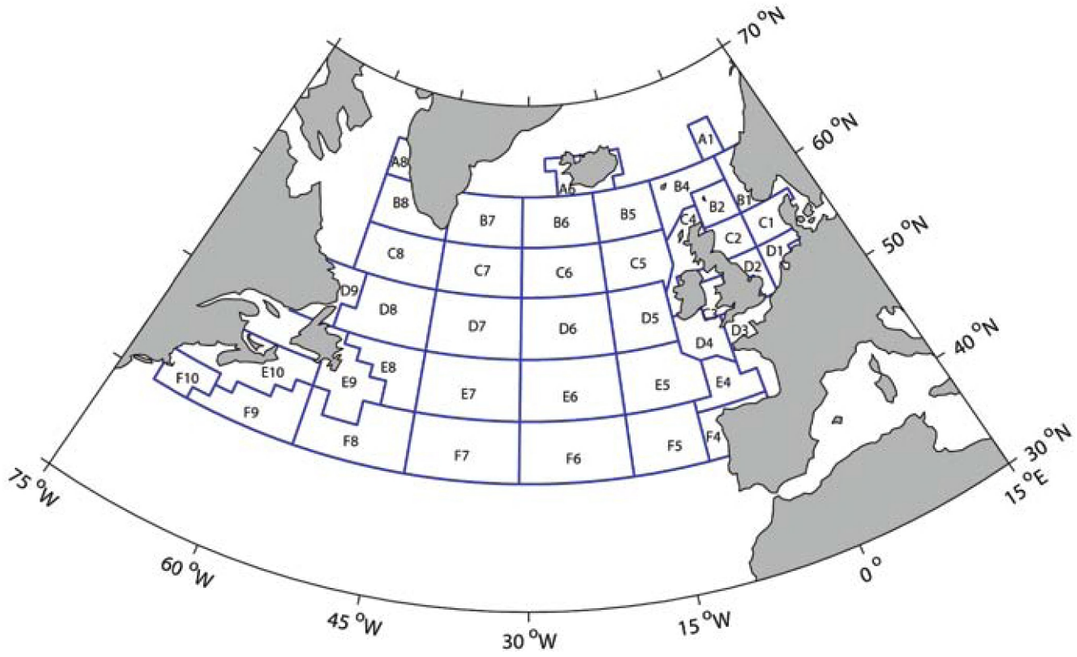

Figure 134.
Map of continuous plankton recorder "standard areas".

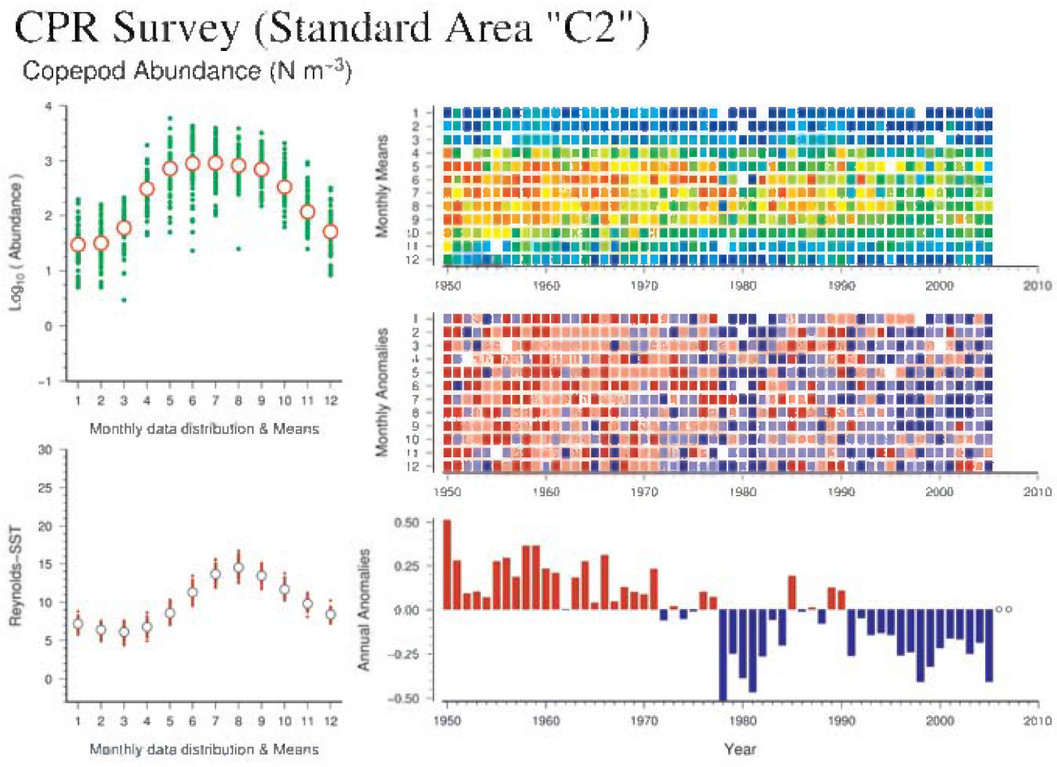

Figure 135.
Standardized WGZE time-series summary plot for copepod abundance at CPR standard area "C2". This is an example of a high data-density CPR standard area, located in the northwestern North Sea. Data from this sampling area were continuous for most years and months. (See Section 2.1 for an explanation of the subplots in this figure.)

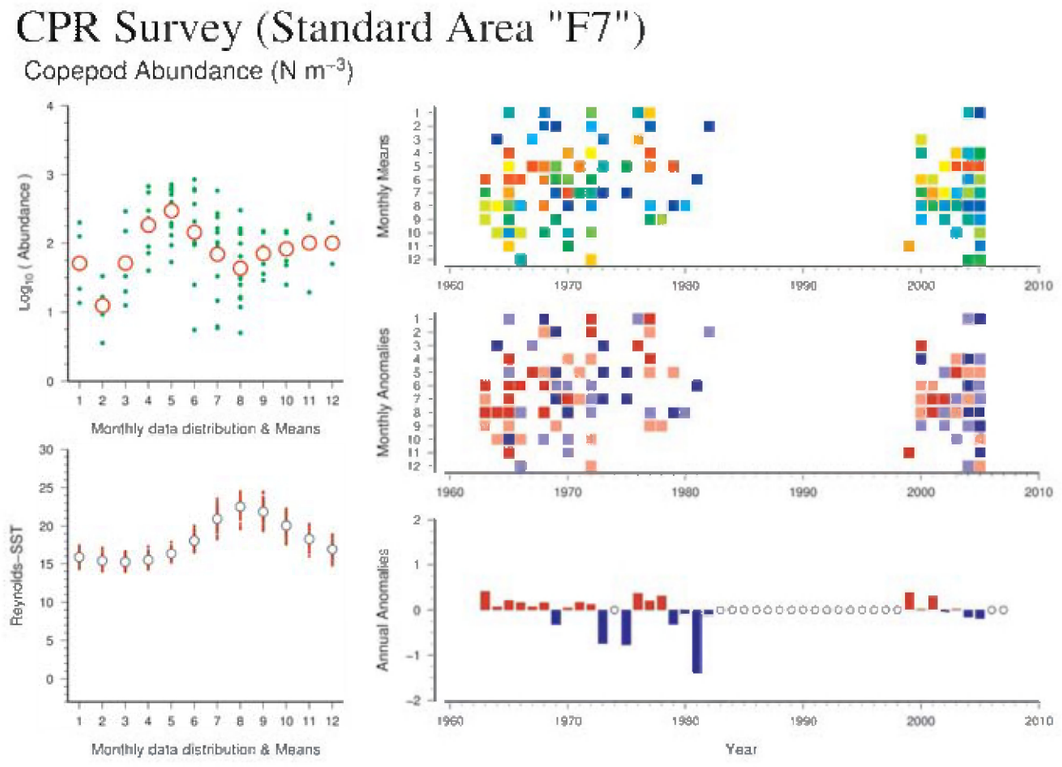

Figure 136.
Standardized WGZE time-series summary plot for copepod abundance in CPR standard area "F7". This is an example of a low data-density CPR standard area, located in the southern central North Atlantic. Data from this sampling area were not continuous for every month and were completely absent for the period 1982–1999. (See Section 2.1 for an explanation of the subplots in this figure.)

A spatial compilation map of the CPR copepod abundance time-series, showing results from each of the CPR standard areas, is shown in Figure 137. The dashed line in each subplot represents the long-term mean abundance in that standard area. The most striking feature of this map is the general long-term decline in copepod abundance in most of the Northeast Atlantic, particularly in the southern North Sea. In contrast, copepod abundance in the western North Atlantic has remained relatively stable or increased slightly since 1946.

To understand long-term changes in zooplankton populations, it is essential to understand the changes occurring in the lower trophic levels. The CPR phytoplankton colour index (PCI) was used to investigate changes in phytoplankton in the North Atlantic. The PCI is the degree of greenness of the CPR silk. It includes the chloroplasts of unbroken and broken cells, as well as small, unarmoured flagellates, which tend to disintegrate on contact with formalin. The phytoplankton colour on the silk is a good index of total chlorophyll content (Hays and Lindley, 1994) and is closely related to phytoplankton biomass estimates from satellite observations (Batten *et al.*, 2003; Raitsos *et al.*, 2005). Long-term interannual values from 1946 to 2006 of phytoplankton colour in CPR standard areas in the North Atlantic are shown in Figure 138. There has been a large increase in phytoplankton colour since the late 1980s in most regions (particularly the Northeast Atlantic and the Newfoundland Shelf).

From the late 1940s to the late 1980s, high phytoplankton biomass was restricted to spring and autumn, when diatoms dominate (data not shown). Since the late 1980s, however, the biomass has increased throughout the seasonal cycle. Biomass generally dropped in 2002, but was still generally higher than the long-term mean. In other parts of the North Atlantic, high increases in biomass were seen off the Newfoundland Shelf (with an increase in winter blooms), the Scotian Shelf, and the Labrador Sea. In the northern North Atlantic and in the Subpolar Gyre, phytoplankton biomass has generally declined since the beginning of sampling, but has increased since 1998.

The drop in phytoplankton biomass recorded by the CPR PCI since 2002 is also apparent in SeaWiFS chlorophyll data (Figure 139). Following McClain *et al.* (2004), the percentage of total SeaWiFS pixels with a chlorophyll value lower than 0.03 mg m^{-3} was calculated for each CPR standard area since 1998. In this calculation, higher values represent prevailing oligotrophic conditions for a given area. For most of the North Atlantic, an increasing trend in this oligotrophy index has been recorded since 1997, except for areas "C5" and "B5" between Ireland and Iceland, which have registered a decreasing trend. Especially for the southeasternmost areas, the increase in areas of low chlorophyll concentration has been remarkable, suggesting a recent recession of the high phytoplankton biomass period recorded by the CPR.

The SST time-series from 1946 to 2006 for CPR standard areas in the North Atlantic increased overall since the early 1970s for the whole North Atlantic (Figure 140). On the other hand, a decreasing trend in SST from the early 1950s until the early 1970s can also be observed in most areas, particularly in the southern part of the central North Atlantic. This decreasing signal in SST is less relevant in the North Sea, where temperatures during this period reveal no clear trend.

This general pattern corresponds well to the hydroclimatic regions proposed by Beaugrand (2003). In this study, it was suggested that the Northeast Atlantic can be divided into three hydroclimatic regions, based on both SST and scalar wind. The first region lies south of the 53°N parallel. North of this region, two additional regions (the Subpolar Gyre and the North Sea) are then defined by their long-term SST properties. Both of these latter northern regions have been characterized by an increasing trend in wind intensity, which is highly positively correlated with monthly North Atlantic Oscillation (NAO) indices, especially in spring and autumn.

In the Subpolar Gyre south of Iceland, phytoplankton biomass has decreased, whereas in the North Sea, phytoplankton biomass has increased (Figure 139; Beaugrand, 2003). This suggests that temperature is an important factor that limits phytoplankton biomass south of Iceland. It is also possible that the decrease in zooplankton abundance in the North Atlantic could be releasing predatory pressure on the phytoplankton, triggering an increase in their biomass and a subsequent increase in the CPR PCI.

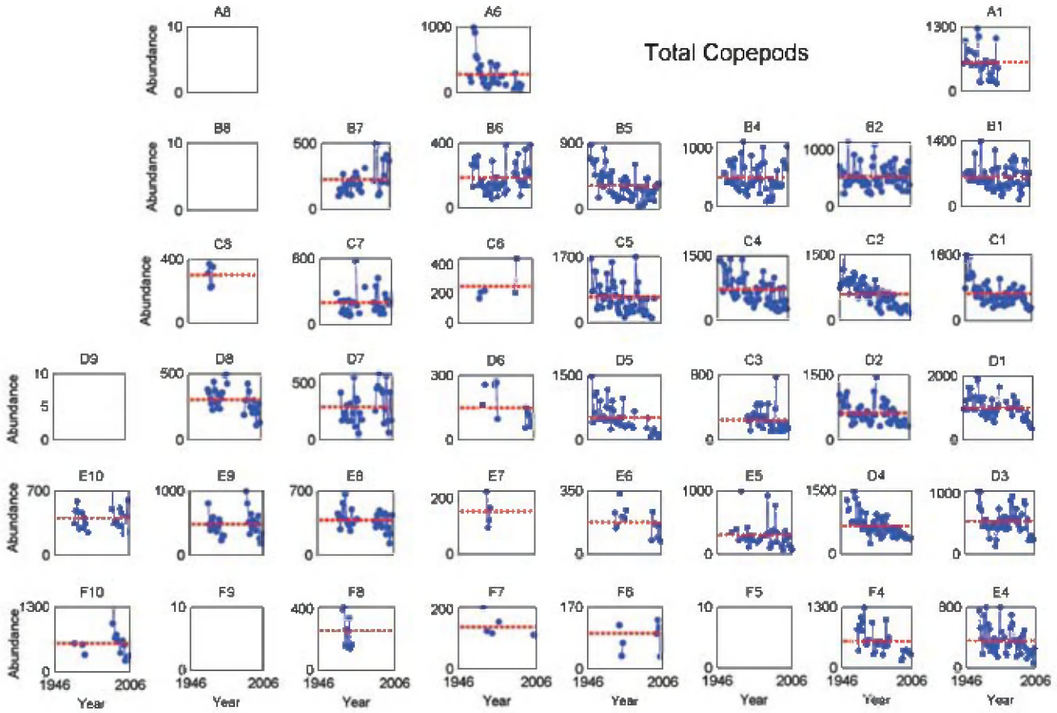

Figure 137.
Time-series from 1946 to 2006 of the total copepod abundance in CPR standard areas in the North Atlantic (see Figure 134 for map).

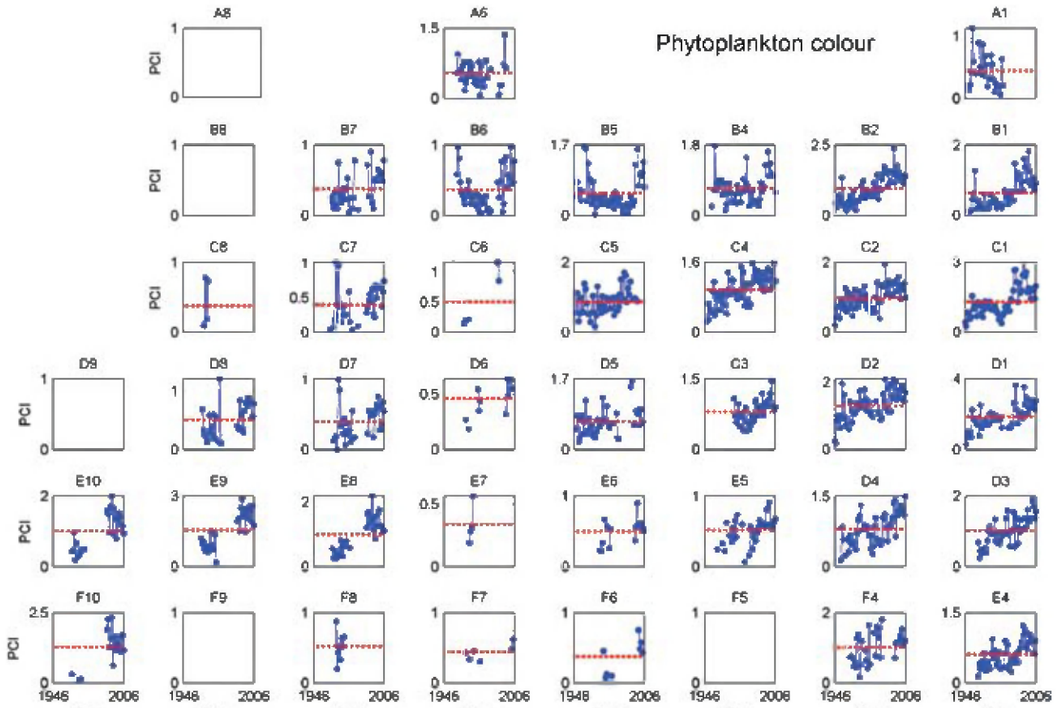

Figure 138.
Time-series from 1946 to 2006 of the phytoplankton colour index in CPR standard areas in the North Atlantic (see Figure 134 for map).

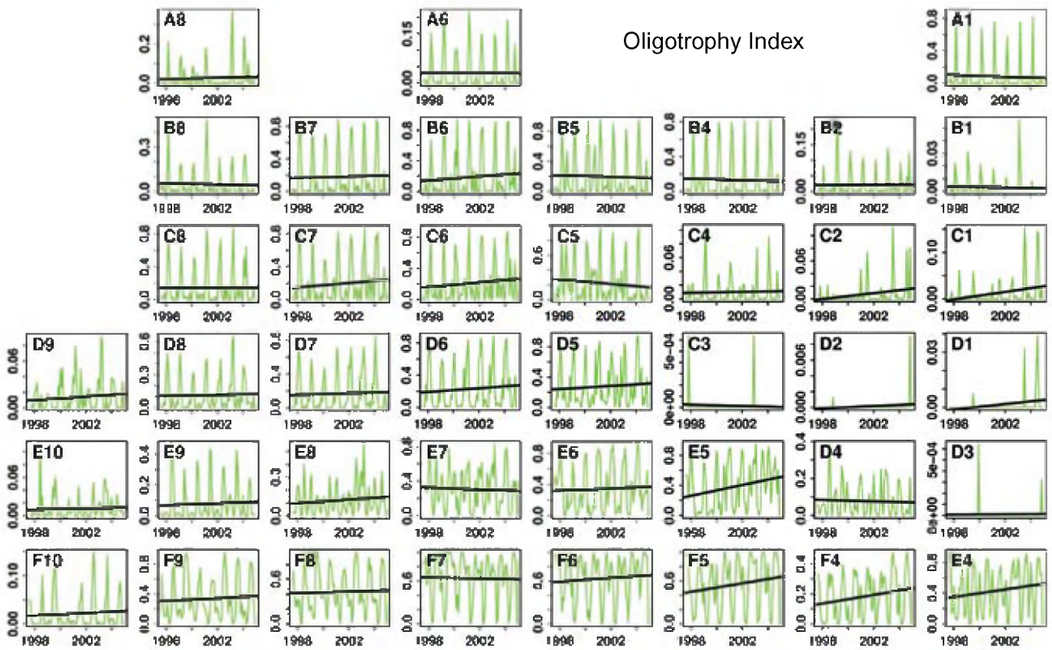

Figure 139.
Time-series from 1997 to 2004 of the oligotrophy index from the SeaWiFS chlorophyll data for each CPR standard area in the North Atlantic (see Figure 134 for map), following McClain et al. *(2004).*

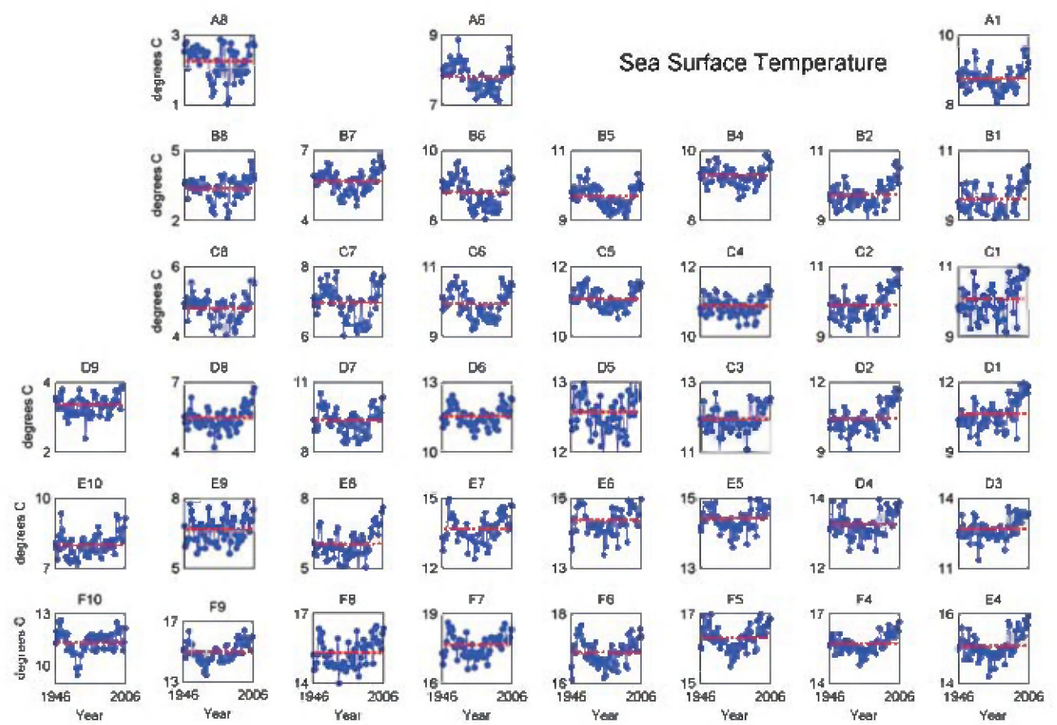

Figure 140.
Time-series from 1946 to 2006 of the sea surface temperature in CPR standard areas in the North Atlantic (see Figure 134 for map).

4.2 Are North Atlantic zooplankton in hot water?

Todd D. O'Brien

This year's zooplankton summary report includes a long-term record of surface water temperatures (i.e. the Reynolds SST) for each monitoring site. As evident in many of the individual sites, as well as the CPR North Atlantic overview, water temperatures in many regions of the North Atlantic have been increasing for the past 30–50 years. These temperatures, at least those before 2001, are still within the normal value ranges of long-term temperature variability of the North Atlantic (Lozier *et al.*, 2008). For example, Figure 141, which goes back to the 1900s, supports this claim, showing a fairly obvious 30–50-year repeating cycle in temperature, and showing that, pre-2001, water temperatures were no higher than those seen in the 1930s.

Unfortunately, Lozier *et al.* (2008) stopped their analysis at the year 2000. A comparison of the maximum water temperatures after 2000 with those from the previous 100 years (1900–2000; Figure 141, red dashed line) shows that the upward temperature trend continues up and above that of the previous 100-year maximum (and may no longer be attributable to natural variability). In addition, the long-term temperature plots from each of the zooplankton sites in this report reveal that most of the eastern North Atlantic sites are currently at or above this maximum, while many of the western North Atlantic sites remain below it.

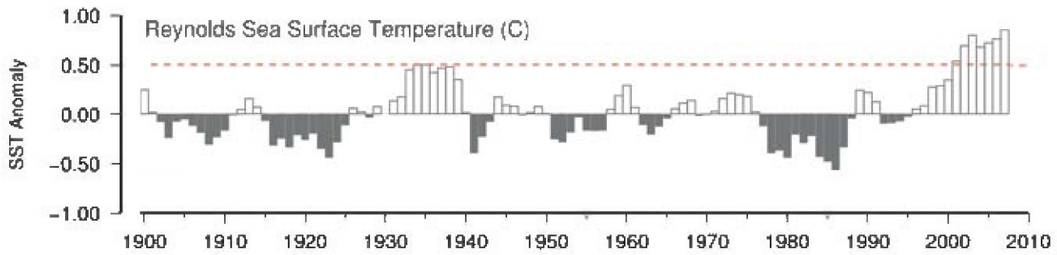

Figure 141.
Annual anomalies of sea surface temperatures in the Norwegian Sea (1900–2007). The red dashed line indicates the maximum anomaly present for the period 1900–2000. In this location, average temperatures have been above this 100-year maximum since 2001.

To investigate this spatial east–west trend in more detail, time-series of annual SST anomalies were calculated for every 2° × 2° Reynolds ERSST grid cell in the North Atlantic (see Section 2.4 for more information on the Reynolds ERSST). Each year in each of these SST time-series was assigned a different colour to represent the relative strength of the anomaly in that year (see Figure 142). Positive anomalies were indicated by either pink or red, where red indicates an anomaly greater than the mean of all other positive anomaly values in the same time-series (Figure 142, light red dashed line). Negative anomalies were indicated by either light blue or dark blue, where dark blue indicates an anomaly less than the mean of all other negative anomaly values (Figure 142, dark blue dashed line). Any anomaly with a value above the 1900–2000 maximum was assigned a dark red colour (Figure 142, heavier red dashed line). For a selected year (e.g. 1985), these assigned colours can then be plotted in each 2° × 2° grid cell of the North Atlantic, giving a spatial view of relative SST anomalies for that year (Figure 143).

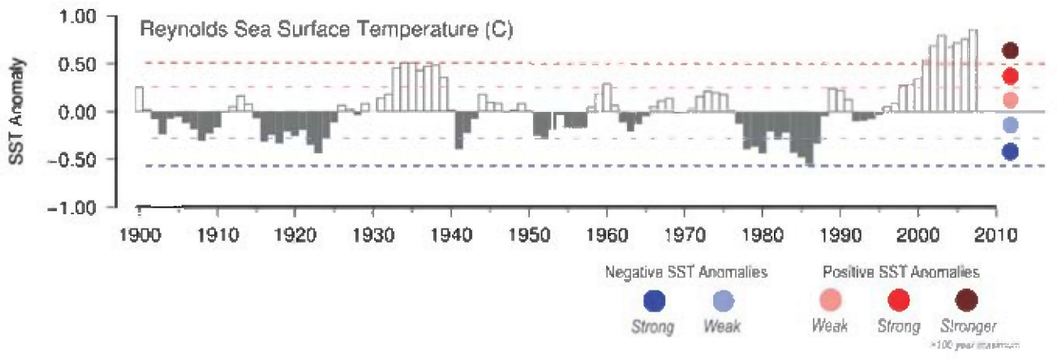

Figure 142.
Illustration of how annual anomaly values were assigned colours. The dark red dashed line indicates the maximum anomaly value for the period 1900–2000. The dark blue dashed line indicates the minimum anomaly value for the period 1900–2000. Light red and light blue dashed lines indicate the mean of all positive (or negative) anomalies. Each year in the time-series was assigned a colour based on these ranges, with values greater than the 1900–2000 maximum assigned a dark red colour.

In order to demonstrate the past 100 years of temperature anomalies in the North Atlantic, five-year averages of relative SST anomalies from 1910 to 2005 are shown in Figure 144. From this series of subplots, it is clear that SST values in the North Atlantic are variable over time and space, with almost every region experiencing extended periods of both above-average and below-average temperatures over the past 100 years. In the early 20th century, the North Atlantic as a whole went from a cool period (1910–1920) to a warm period (1930–1940), returning to a cooler period in the 1970s. These general warming and cooling periods are noted in other North Atlantic temperature analyses (e.g. Polyakov *et al.*, 2005, and Lozier *et al.*, 2008), but the temperature data used in both of these studies ended at or before the year 2000.

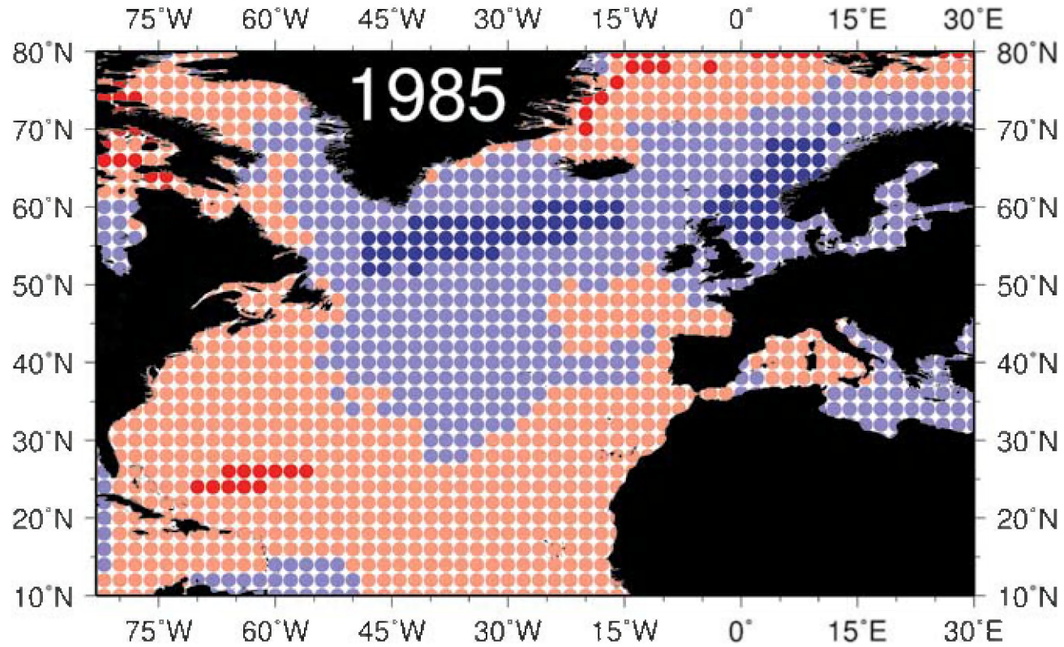

Figure 143.
Map of relative sea surface temperature (SST) anomalies for the year 1985. Each circle represents the 1985 annual anomaly value (per colours specified in Figure 142) from the SST time-series in that Reynolds SST 2° × 2° grid point. In this example, annual average water temperatures in the Norwegian Sea and southwest of Iceland were lower than the long-term (1900–2000) average, whereas much of the southern North Atlantic and Subarctic temperatures were above this long-term average.

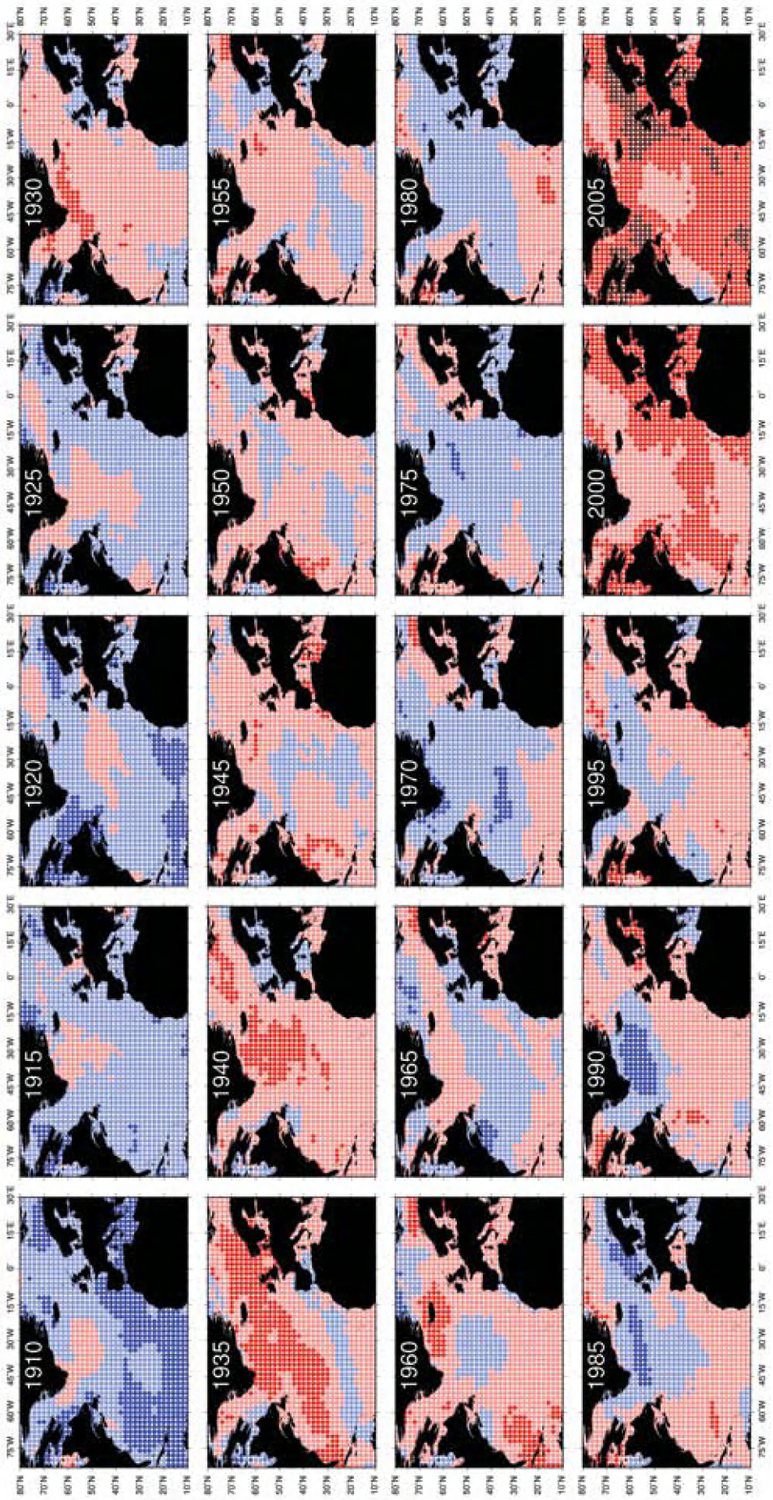

Figure 144.
Relative SST anomalies, plotted as five-year averages from 1910 to 2005. Each subplot represents the average annual anomaly for that year ±2 years (e.g. "1985" is the average of annual anomalies from 1988 to 1992).

Prior to 2000, the warmest period is seen in the 1935 subplot of Figure 144. In the equally warm period of 2000, almost all of the blue dots (indicating below-average temperatures) seen in the 1935 period have been replaced with pink and red dots (indicating above-average temperatures). By 2005, most of these pink dots have been replaced by red dots (indicating a higher level of above-average temperatures). In 2005, there are also extensive regions of dark red dots in the Northeast and Northwest Atlantic, indicating locations where the SST values were greater than any recorded in the previous 100 years.

To continue the series after 2005, relative temperature anomalies for 2006 and 2007 are shown in Figure 145. The regions of dark red dots continued to expand in 2006, covering the entire eastern North Atlantic coastline from Norway to Africa, and then partially receded in 2007. Monitoring reports from UK coastal waters support these results, stating that the average water temperature for 2006 was the second warmest since records began in 1870, and that seven of the ten warmest years in this record have all occurred in the past decade (MCCIP, 2008). To add further to this concern, IPCC (2007) studies find that SST values in the North Atlantic as a whole have been rising faster than the global ocean average for the past 25 years.

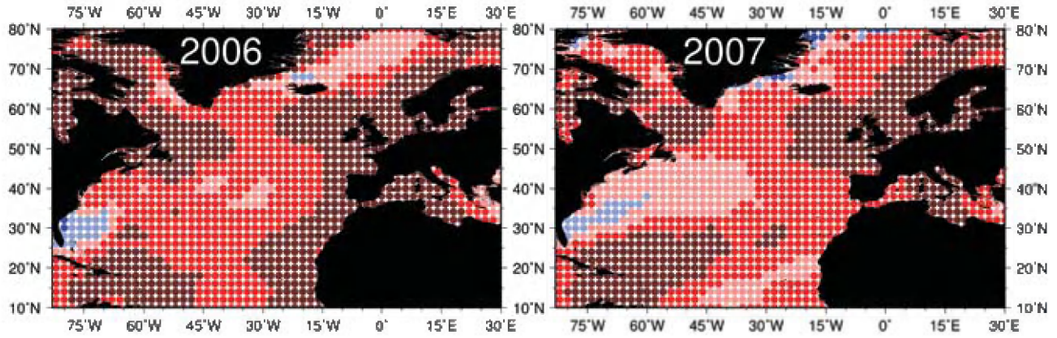

Figure 145.
Map of relative SST anomalies for 2006 and 2007. Each circle represents the annual anomaly value for that year (per colours specified in Figure 142) for the SST time-series in that Reynolds SST 2° × 2° grid.

The "whys" and "hows" of these recent and dramatic temperature increases are left for others to answer. The immediate question, at least to WGZE, is how are the zooplankton reacting to these exceptionally warm water temperatures? The immediate answer is that it is probably too soon to tell, because any zooplankton response may be time-lagged or take multiple seasons to become clearly evident over the natural variability. The basin-wide CPR analysis has already noted a general downward trend in copepod abundance in the eastern side of the North Atlantic, corresponding to many of the regions of highest temperatures. Individual sites within these same regions, however, show a mixed response, with some sites showing a decrease in abundance or biomass, whereas others reveal an increase. Some sites even exhibit both trends, with a decrease in zooplankton abundance paired with an increase in total biomass (usually as a result of anomalous phytoplankton blooms contaminating the zooplankton sample).

The answers to these questions may become clearer as data from further years are added to the zooplankton time-series and, it is hoped, will be addressed in the next WGZE zooplankton summary report. Meanwhile, the finer physical and biological details of each sampling site summarized in this report are best known by the investigators of those sites, and many of those individuals have published focused studies and analyses that go into greater detail than this general summary report. Accordingly, e-mail addresses are provided in the List of Contributors and Metadata Summary table at the end of this report, to enable the reader to contact these investigators directly for more information.

5. REFERENCES

Astthorsson, O. S., and Gislason, A. 1998. Environmental conditions, zooplankton, and capelin in the waters north of Iceland. ICES Journal of Marine Science, 55: 808–810.

Astthorsson, O. S., and Vilhjalmsson, H. 2002. Iceland shelf LME: decadal assessment and resource, pp. 219–243. *In* Large Marine Ecosystems of the North Atlantic. Changing States and Sustainability. Ed. by K. Sherman and H. R. Skjoldal. Elsevier, Amsterdam. 449 pp.

Batten, S. D., Walne, A. W., Edwards, M., and Groom, S. B. 2003. Phytoplankton biomass from continuous plankton recorder data: an assessment of the phytoplankton colour index. Journal of Plankton Research, 25: 697–702.

Beaugrand, G. 2003. Long-term changes in copepod abundance and diversity in the northeast Atlantic in relation to fluctuations in the hydroclimatic environment. Fisheries Oceanography, 12: 270–283.

Beaugrand, G., Ibañez, F., Lindley, J. A., and Reid, P. C. 2002. Diversity of calanoid copepods in the North Atlantic and adjacent seas: species associations and biogeography. Marine Ecology Progress Series, 232: 179–195.

de Lafontaine, Y., Demers, S., and Runge, J. 1991. Pelagic food web interactions and productivity in the Gulf of St Lawrence: a perspective, pp. 99–123. *In* The Gulf of St Lawrence: Small Ocean or Big Estuary? Ed. by J-C. Therriault. Canadian Special Publication of Fisheries and Aquatic Sciences, 113.

Edwards, M., Licandro, P., John, A. W. G., and Johns, D. G. 2006. Ecological Status Report: Results from the CPR Survey 2004/2005. SAHFOS Technical Report No. 3.

Greve, W., Lange, U., Reiners, F., and Nast, J. 2001. Predicting the seasonality of North Sea zooplankton, pp. 263–268. *In* Burning Issues of North Sea Ecology, The 14th International Senckenberg Conference "North Sea 2000", Wilhelmshaven, Germany, 8–12 May 2000. Ed. by I. Kröncke, M. Türkay, and J. Sündermann. Senckenbergiana Maritima, 31(2). 273 pp.

Greve, W., Reiners, F., Nast, J., and Hoffmann, S. 2004. Helgoland Roads time-series meso- and macrozooplankton 1975 to 2004: lessons from 30 years of single spot high frequency sampling at the only offshore island of the North Sea. Helgoland Marine Research, 58: 274–288.

Grosjean, P., Picheral, M., Warembourg, C., and Gorsky, G. 2004. Enumeration, measurement, and identification of net zooplankton samples using the ZOOSCAN digital imaging system. ICES Journal of Marine Science, 61: 518–525.

Hays, G. C., and Lindley, J. A. 1994. Estimating chlorophyll *a* abundance from the "PCI" recorded by the Continuous Plankton Recorder survey: validation with simultaneous fluorometry. Journal of Plankton Research, 16: 23–34.

HELCOM. 1996. Third Periodic Assessment of the State of the Marine Environment of the Baltic Sea, 1989–1993. Baltic Sea Environment Proceedings, 64B. 252 pp.

Heyen, H., Fock, H., and Greve, W. 1998. Detecting relationships between the interannual variability in ecological time-series and climate using a multivariate statistical approach – a case study on Helgoland Roads zooplankton. Climate Research, 10: 179–191.

IPCC. 2007. Climate Change 2007: The Physical Science Basis. Contribution of Working Group I to the Fourth Assessment Report of the Intergovernmental Panel on Climate Change. Ed. by S. Solomon, D. Qin, M. Manning, Z. Chen, M. Marquis, K. B. Averyt, M. Tignor, and H. L. Miller. Cambridge University Press, Cambridge, UK. 996 pp.

Johannsen, S., Lange, U., Reick, C., Backhaus, J-O., Greve, W., and Page, B. 1999. Abschlußbericht des Verbundprojekts: Zooplankton-Analyse und -Prognose gefördert durch das BMBF unter BEO 03 F223. 291 pp.

Kane, J. 2007. Zooplankton abundance trends on Georges Bank, 1977–2004. ICES Journal of Marine Science, 64: 909–919.

Li, W. K. W., Harrison, W. G., and Head, E. J. H. 2006. Multiyear trends in plankton show coherent sign switching. Science, 311: 1157–1160.

Longhurst, A. 1998. Ecological Geography of the Sea. Academic Press, London. 358 pp.

Lovegrove, T. 1962. The effect of various factors on dry weight values. Rapports et Procès-Verbaux des Réunions du Conseil International pour l'Exploration de la Mer, 153: 86–91.

Lozier, M. S., Leadbetter, S., Williams, R. G., Roussenov, V., Reed, M. S. C., and Moore, N. J. 2008. The spatial pattern and mechanisms of heat-content change in the North Atlantic. Science, 319: 800–803.

Mackas, D., Thomson, R. E., and Galbraith, M. 2001. Covariation of zooplankton community changes and oceanographic conditions on the British Columbia continental margin, 1995–1998. Canadian Journal of Fisheries and Aquatic Sciences, 58: 1–18.

Matthäus, W., and Schinke, H. 1999. The influence of river runoff on deep water conditions of the Baltic Sea. Hydrobiologia, 393: 1–10.

MCCIP. 2008. Marine Climate Change Impacts Annual Report Card 2007–2008. Ed. by J. M. Baxter, P. J. Buckley, and C. J. Wallace. Summary Report, MCCIP, Lowestoft. 8 pp.

McClain, C. R., Signorini, S. R., and Christian, J. R. 2004. Subtropical gyre variability observed by ocean-color satellites. Deep Sea Research II, 22: 281–301.

Möllmann, C., Köster, F. W., Kornilovs, G., and Sidrevics, L. 2003. Interannual variability in population dynamics of calanoid copepods in the Central Baltic Sea. ICES Marine Science Symposia, 219: 220–230.

Möllmann, C., Kornilovs, G., Fetter, M., and Köster, F. W. 2005. Climate, zooplankton, and pelagic fish growth in the Central Baltic Sea. ICES Journal of Marine Science, 62: 1270–1280.

Mountain, D. G. 2004. Variability of the water properties in NAFO Subareas 5 and 6 during the 1990s. Journal of Northwest Atlantic Fishery Science, 34: 103–112.

Omori, M., and Ikeda, T. 1984. Methods in Marine Zooplankton Ecology. John Wiley and Sons, Toronto. 332 pp.

Ouellet, M., Petrie, B., and Chassé, J. 2003. Temporal and Spatial Scales of Sea-surface Temperature Variability in Canadian Atlantic Waters. Canadian Technical Report of Hydrography and Ocean Sciences, 228. 30 pp.

Perry, R. I., Batchelder, H. P., Mackas, D. L., Chiba, S., Durbin, E., Greve, W., and Verheye, H. M. 2004. Identifying global synchronies in marine zooplankton populations: issues and opportunities. ICES Journal of Marine Science, 61: 445–456.

Pingree, R. D., and Griffiths, D. K. 1978. Tidal fronts on the shelf seas around the British Isles. Journal of Geophysical Research, 83: 4615–4622.

Polyakov, I. V., Bhatt, U. S., Simmons, H. L., Walsh, D., Walsh, J. E., and Zhang, X. 2005. Multidecadal variability of North Atlantic temperature and salinity during the twentieth century. Journal of Climate, 18: 4562–4580.

Raitsos, D. E., Reid, P. C., Lavender, S. J., Edwards, M., and Richardson, A. J. 2005. Extending the SeaWiFS chlorophyll data set back 50 years in the Northeast Atlantic. Geophysical Research Letters, 32: L06603, doi: 10.1029/2005GL022484.

Roy, S., Silverberg, N., Romero, N., Deibel, D., Klein, B., Savenkoff, C., Vézina, A. F., *et al.* 2000. Importance of mesozooplankton feeding for the downward flux of biogenic carbon in the Gulf of St Lawrence (Canada). Deep Sea Research II, 47: 519–544.

Valdés, L., and Moral, M. 1998. Time-series analysis of copepod diversity and species richness in the southern Bay of Biscay, Santander, Spain, in relation to environmental conditions. ICES Journal of Marine Science, 55: 783–792.

Valdés, L., Lopez-Urrutia, A., Cabal, J., Alvarez-Ossorio, M., Bode, A., Miranda, A., Cabanas, M., *et al.* 2007. A decade of sampling in the Bay of Biscay: what are the zooplankton time series telling us? Progress in Oceanography, 74: 98–114.

Wiltshire, K. H., Malzahn, A. M., Wirtz, K., Greve, W., Janisch, S., Mangelsdorf, P., Manly, B. F. J., *et al.* 2008. Resilience of North Sea phytoplankton spring bloom dynamics: an analysis of long-term data at Helgoland Roads. Limnology and Oceanography, 53: 1294–1302.

6. METADATA: CHARACTERISTICS OF THE COLLECTIONS USED

Ocean region	Western North Atlantic								
Country	USA				Canada				
Sampling/ Monitoring programme	NMFS-NEFSC				AZMP				
WGZE site number	1	2	3	4	5	6	7	7	8
Sampling site name	MAB	SNE	GOM	GB	Prince 5	Halifax Line 2	Gaspé Current	Anticosti Gyre	Station 27
Sampling location	Mid-Atlantic Bight	Southern New England	Gulf of Maine	Georges Bank	Bay of Fundy	Scotian Shelf	Gulf of St. Lawrence	Gulf of St. Lawrence	Newfoundland Shelf
Sampling duration	1977–present	1977–present	1977–present	1977–present	1999–present	1999–present	1999–present	1999–present	1999–present
Sampling frequency	Cross-monthly surveys six times per year				Monthly/Biweekly				
Sampling gear (diameter)	Bongo net				Ringnet (75 cm)				
Sampling mesh (µm)	333 µm				200 µm				
Sampling depth (m)	0–200 (or bottom)				0–bottom				
Contact person	Jon Hare jon.hare@noaa.gov				Erica Head erica.head@dfo-mpo.gc.ca	Michel Harvey michel.harvey@dfo-mpo.gc.ca	Pierre Pepin pierre.pepin@dfo-mpo.gc.ca		

Ocean region	Icelandic–Norwegian Basin					
Country	Iceland		Faroe Islands		Norway	
Sampling/ Monitoring programme	MRI-Iceland		FFI-Faroe Islands		IMR-Bergen	
WGZE site number	9	10	11	12	13	14
Sampling site name	Selvogsbanki Transect	Siglunes Transect	Northern Transect	Faroe Shelf	Svinøy Transect West	Svinøy Transect East
Sampling location	South Iceland	North Iceland	North Faroe Islands	South Faroe Islands	Norwegian Sea	
Sampling duration	1971–present	1961–present	1990–present	1990–present	1996–present	1996–present
Sampling frequency	Annually (May/June)		Annually (late May)		4–6 times per year	
Sampling gear (diameter)	Hensen net (1971–1991); WP-2 net (1992–present)		Hensen net (1990–1991); WP-2 net (1992–present)		WP-2 net (56 cm)	
Sampling mesh (µm)	200 µm		200 µm		180 µm	
Sampling depth (m)	0–50		0–50		0–200	
Contact person	Astthor Gislason astthor@hafro.is		Eilif Gaard eilifg@frs.fo		Webjørn Melle webjorn@imr.no	

Ocean region	Barents Sea			
Country	Norway			
Sampling/ Monitoring programme	IMR-Bergen			
WGZE site number	15	16	17	18
Sampling site name	Fugløya-Bjørnøya Transect North	Fugløya-Bjørnøya Transect South	Vardø-Nord North	Vardø-Nord South
Sampling location	West Barents Sea		East Barents Sea	
Sampling duration	1994–present	1994–present	1994–present	1994–present
Sampling frequency	3–6 times per year		3–4 times per year	
Sampling gear (diameter)	WP-2 net (56 cm)			
Sampling mesh (µm)	180 µm			
Sampling depth (m)	0–100			
Contact person	Webjørn Melle webjorn@imr.no			

Ocean region	Baltic Sea						
Country	Finland		Estonia		Latvia		Germany
Sampling/ Monitoring programme	HELCOM Monitoring				National Monitoring Programme of Latvia	LatFRA Monitoring	IOW
WGZE site number	19	20	21	22	23	24	25
Sampling site name	Bothnian Bay	Bothnian Sea	Tallinn Bay	Pärnu Bay	Station 121	Eastern Gotland Basin	Arkona Basin
Sampling location	Northern Baltic Sea		Gulf of Finland	Gulf of Riga		Central Baltic Sea	Southern Baltic
Sampling duration	1979–present	1979–present	1993–present	1957–present	1993–present	1960–present	1979–present
Sampling frequency	August		Up to ten times per year	Monthly to weekly in non-ice months	At least three times per year	Seasonally	Seasonally
Sampling gear (diameter)	WP-2 net (56 cm)		Juday net (36 cm)		WP-2 net	Juday net (36 cm)	WP-2 net
Sampling mesh (µm)	100 µm		90 µm		100 µm	160 µm	100 µm
Sampling depth (m)	0–bottom		0–bottom		0–50	0–100	0–25
Contact person	Juha Flinkman juha.flinkman@fimr.fi		Arno Põllumäe arno@sea.ee		Anda Ikauniece anda@monit.lu.lv	Solvita Strake, Georgs Kornilovs solvita@hydro.edu.lv	Lutz Postel lutz.postel@io-warnemuende.de

Ocean region	North Sea/English Channel				Bay of Biscay	
Country	Norway	Germany	UK		Spain	
Sampling/ Monitoring programme	IMR	BSH and DZMB	FRS-MLA	L4-PML/UK	IEO-Spain	
WGZE site number	26	27	28	29	30	31
Sampling site name	Arendal Station 2	Helgoland Roads	Stonehaven	Plymouth L4	Santander	A Coruña
Sampling location	Northern Skagerrak	Southeast North Sea	Northwest North Sea	English Channel	Southern Bay of Biscay	Northwest Iberian Peninsula
Sampling duration	1994–present	1975–present	1997–present	1988–present	1991–present	1990–present
Sampling frequency	Twice monthly	Every Monday, Wednesday and Friday	Weekly (52 weeks per year)	Weekly (~40 weeks per year)	Monthly	Monthly
Sampling gear (diameter)	WP-2 net	Hydrobios	Bongo net (40 cm) and Calcofi	WP-2 net	Juday net (50 cm)	Juday net (50 cm)
Sampling mesh (µm)	180 µm	150 µm, 500 µm	200 µm	200 µm	250 µm	250 µm (1976–1996); 200 µm (1996–present)
Sampling depth (m)	0–50	0–bottom	0–50	0–50	0–50	0–50
Contact person	Tone Faulkenhaug tone.falkenhaug@imr.no	Maarten Boersma maarten.boersma@awi.de	Steve Hay s.hay@marlab.ac.uk	Roger Harris rph@ccms.ac.uk	Luis Valdés luis.valdes@gi.ieo.es	Maite Alvarez-Ossorio maite.alvarez@co.ieo.es

Ocean region	Mediterranean						North Atlantic
Country	Spain	France	Italy		Croatia	Greece	UK
Sampling/ Monitoring programme	IEO-Spain	LOV-France	SZN-Italy	UNITS-Italy	IZOR-Croatia	HCMR-Greece	Continuous Plankton Recorder
WGZE site number	32	33	34	35	36	37	CPR
Sampling site name	Baleares Station	Villefranche Point B	Gulf of Naples	Gulf of Trieste	Stončica	Saronikós-S11	CPR Surveys
Sampling location	Balearic Sea	Côte d'Azur	Tyrrhenian Sea	Northern Adriatic	Central Adriatic Sea	Aegean Sea	Continuous Plankton Recorder Surveys
Sampling duration	1994–present	1974–present	1984–present	1970–present	1959–1991; 1995–present (unprocessed)	1987–present	1946–present
Sampling frequency	Monthly (until 2006)	Monthly	Monthly	Monthly	Monthly (with gaps)	Seasonally (1987–1998); monthly after 1999	Monthly (with gaps)
Sampling gear (diameter)	Bongo net (20 cm)	Juday–Bogorov net	Nansen net (113 cm)	WP-2 net	Hensen net (73 cm)	WP-2 net	CPR (1.24 cm)
Sampling mesh (µm)	100/250 µm	330 µm	200 µm	200 µm	330 µm	200 µm	280 µm
Sampling depth (m)	0–100	0–75	0–50	0–18	0–100	0–75	subsurface (7–0 m)
Contact person	Maria Luz Fernandez de Puelles mluz.fernandez@ba.ieo.es	Gabriel Gorsky gorsky@obs-vlfr.fr	Maria Grazia Mazzocchi grazia@szn.it	Serena Fonda-Umani s.fonda@units.it	Olja Vidjak vidjak@izor.hr	Ionna Siokou-Frangou isiokou@ath.hcmr.gr	Priscilla Licandro prli@sahfos.ac.uk

6. LIST OF CONTRIBUTORS

Contributor	Institute
Maite Alvarez-Ossorio (maite.alvarez@co.ieo.es)	Instituto Español de Oceanografía, Spain
Maarten Boersma (Maarten.Boersma@awi.de)	Biologische Anstalt Helgoland/Alfred-Wegener-Institut für Polar- und Meeresforschung, Germany
Jesús Cabal	Instituto Español de Oceanografía, Spain
Cecilie Broms (cecilie.broms.aarnes@imr.no)	Institute of Marine Research, Norway
Alessandra Conversi (a.conversi@ismar.cnr.it)	Consiglio Nazionale delle Richerche Istituto di Scienze Marine, Italy
Tone Falkenhaug (Tone.Falkenhaug@imr.no)	Institute of Marine Research, Norway
Maria Luz Fernandez de Puelles (mluz.fernandez@ba.ieo.es)	Instituto Español de Oceanografía, Spain
Juha Flinkmann (Juha.Flinkman@fimr.fi)	Finnish Institute of Marine Research, Finland
Serena Fonda-Umani (s.fonda@units.it)	University of Trieste, Italy
Eilif Gaard (Eilifg@frs.fo)	Faroese Fisheries Laboratory, Faroe Islands
Astthor Gislason (astthor@hafro.is)	Marine Research Institute, Iceland
Gabriel Gorsky (gorsky@obs-vlfr.fr)	Laboratoire d'Oceanographie de Villefranche, France
Jon Hare (Jon.Hare@noaa.gov)	National Oceanographic and Atmospheric Administration, National Marine Fisheries Service, USA
Roger Harris (RPH@pml.ac.uk)	Plymouth Marine Laboratory, UK
Michel Harvey (Michel.Harvey@dfo-mpo.gc.ca)	Maurice Lamontagne Institute, Canada
Steve Hay (S.Hay@marlab.ac.uk)	Fisheries Research Services, Marine Laboratory, Scotland, UK
Erica Head (Erica.Head@mar.dfo-mpo.gc.ca)	Bedford Institute of Oceanography, Canada
Anda Ikauniece (anda.ikauniece@lhei.lv)	Latvian Institute of Aquatic Ecology, Latvia
Jack Jossi (Jack.Jossi@noaa.gov)	National Oceanographic and Atmospheric Administration, National Marine Fisheries Service, USA
Joe Kane (Joe.Kane@noaa.gov)	National Oceanographic and Atmospheric Administration, National Marine Fisheries Service, USA
Georgs Kornilovs (georgs.kornilovs@lzra.gov.lv)	Latvian Fish Resources Agency, Latvia
Priscilla Licandro (prli@sahfos.ac.uk)	Sir Alister Hardy Foundation for Ocean Science, UK
Angel López-Urrutia (alop@gi.ieo.es)	Instituto Español de Oceanografía, Spain
Maria Grazia Mazzocchi (grazia@szn.it)	Stazione Zoologica Anton Dohrn, Italy
Webjørn Melle (webjoern.melle@imr.no)	Institute of Marine Research, Norway
Todd D. O'Brien (Todd.OBrien@noaa.gov)	National Oceanographic and Atmospheric Administration, National Marine Fisheries Service, USA
Lena Omli	Institute of Marine Research, Norway
Pierre Pepin (Pierre.Pepin@dfo-mpo.gc.ca)	Department of Fisheries and Oceans, Canada
Arno Põllumäe (arno@sea.ee)	Estonian Marine Institute, University of Tartu, Estonia
Maria Polüpüü	Estonian Marine Institute, University of Tartu, Estonia
Lutz Postel (lutz.postel@io-warnemuende.de)	Leibniz Institute of Baltic Sea Research, Germany
Ioanna Siokou-Frangou (isiokou@ath.hcmr.gr)	Hellenic Centre for Marine Research, Greece
Solvita Strake (solvita@hydro.edu.lv)	Latvian Institute of Aquatic Ecology, Latvia
Peter H. Wiebe (pwiebe@whoi.edu)	Woods Hole Oceanographic Institution, USA
Luis Valdés (luis.valdes@gi.ieo.es)	Instituto Español de Oceanografía, Spain
Olja Vidjak (vidjak@izor.hr)	Institute of Oceanography and Fisheries, Croatia